LCH Laboratoire de Constructions Hydrauliques
Laboratory of Hydraulic Constructions

ÉCOLE POLYTECHNIQUE
FÉDÉRALE DE LAUSANNE

Communication 28

Bank protection at the outer side of curved channels by an undulated concrete wall

Alexandre Vela Giró

Editeur : Prof. Dr A. Schleiss

Lausanne, 2007

Communications du Laboratoire de Constructions Hydrauliques ISSN 1661-1179
Ecole Polytechnique Fédérale de Lausanne
Editeur: Prof. Dr A. Schleiss

Preface

In Alpine valleys, rivers often cross urban areas such as villages and cities. The lack of space between the river and the infrastructures requires a protection by walls against flooding and bank erosion. If the surface of these protection walls is smooth, there is a significant danger that its foundation is attacked by scouring of the river bed, especially in bends. After failure of the wall, uncontrolled bank erosion can occur and cause serious damage to buildings and infrastructures. It is known that the risk of scour can considerably decrease if the wall is not smooth but has a high degree of roughness.

In the framework of his Master thesis, Mr. Alexandre Vela Giró systematically studied in a curved flume, of which the outer wall was equipped with an undulated surface, the flow behaviour and the evolution of the scour along the foundation of such undulated walls. He found that the undulations considerably decreased the scour depth. Furthermore, this new type of undulated wall has a higher rigidity and stability and can thus even resist to scouring without overturning. What is more, the architectural integration of an undulated wall is also easier in urban areas.

In the present communication, Mr Alexandre Vela Giró presents the results of his experimental study and gives the practical engineer valuable guidelines and recommendations for the design of undulated protection walls at the outer side of river bends.

We would like to thank Dr. Daniel Hersberger for his advice and support regarding the physical experiments and data processing.

Prof. Dr. Anton J. Schleiss

Abstract

Bank protection at the outer side of curved channels by an undulated concrete wall

In many valleys of the Alps and Pyrenees the lack of space in urban area between the river and the buildings and infrastructures obliges to protect the banks by walls against lateral erosion. Smooth walls are endangered by scouring of their foundation especially at the outer bank in river bends. A possibility to avoid wall's failure is to construct an undulated concrete wall with the purpose to increase the form roughness and reduce the flow velocities as well as depth of scour close to the wall. Such undulated wall can also increase the stability against overturning. Furthermore along an undulated wall a rather rich bed morphology occurs improving conditions for fishes.

In this context experimental tests were performed in a 90° curved 1 m wide channel with an undulated wall at the outer bank. For trapezoidal undulations (0.1 m deep and 0.33 m long), three discharges (150, 180 and 210 l/s) and bed slopes (0.35, 0.5 and 0.7%) with a wide grain size distribution of the bed sediments ($d_m = 8.7$mm) were tested. The following parameters for subcritical flow conditions were studied: bed topography, water level, sediment transport, longitudinal flow velocities and grain sorting across the bend.

Based on the experimental results two scour holes were identified. Compared to the case of a smooth wall without undulations, the depth of the two scour holes was significantly reduced. The reduction was at about 20% at the first hole and 40% (but quite variable) at the second one.

The scour position was also influenced by the undulations. Compared to the smooth wall the two scour holes were shifted 10° downstream (first scour hole was at 45° and the second one at about 1m downstream the bend). The sediment transport was slightly lower with the undulations than without them. The undulated wall also influenced the water surface. With the smooth wall, stationary surface waves of rather high amplitude were observed. With the undulations this waves were replaced by waves of lower amplitude.

Resumen

Protección de la orilla exterior de canales en curva por un muro ondulado de hormigón

En muchos valles de los Alpes y Pirineos la falta de espacio en zonas urbanas entre el río y los edificios e infraestructuras obliga a construir muros de protección contra la erosión lateral. Los muros lisos estan expuestos a la erosión de la cimentacion especialmente en la orilla exterior de las curvas. Una solución para evitar el colapso de estos es construir un muro ondulado de hormigón en la orilla exterior para aumentar la rugosidad de forma y reducir las velocidades de la corriente así como la profundidad de las fosas de erosión cerca del muro. Las ondulaciones del muro aumentan la estabilidad contra vuelco y crean una morfología del lecho del río propicia para el desarrollo de los peces.

En este contexto se ha realizado un estudio experimental en un canal curvo de 90° y 1 m de ancho con un muro ondulado en la orilla exterior. Una geometría de muro trapezoidal (0.1 m de profundidad y 0.33 m de longitud) fue ensayada con tres caudales (150, 180 y 210 l/s), tres pendientes longitudinales (0.35, 0.5 y 0.7%) y una granulometría de sedimentos extendida ($d_m = 8.7$mm).

Los parámetros estudiados en condiciones subcríticas son los siguientes: la topografía del lecho, el relieve de la superficie del agua, el transporte sólido, las velocidades longitudinales y la granulometría de la capa de armado.

En base a los resultados experimentales obtenidos, se observa la formación de dos fosas de erosió. Con respecto a ensayos tipo sin la pared ondulada, la profundidad de estas fosas se reduce considerablemente (entorno a un 20% la primera y un 40% en la segunda).

La localización de las fosas de erosión está también influenciada por las ondulaciones. Comparado con el muro liso, las dos fosas de erosión estan desplazadas unos 10° aguas abajo (la primera fosa está a unos 45° y la segunda a 1 m aguas abajo del final de la curba). El transporte sólido se reduce ligeramente con respecto al muro liso. La superfície del agua también se ve influenciada por las ondulaciones. Las ondas estacionarias de amplitud importante observadas durante los ensayos sin ondulaciones son sustituidas por pequeñas ondas de choque generadas aguas arriba de las ondulaciones.

Contents

Chapter 1

Introduction

1.1 Context

In valleys of the Alps and Pyrenees rivers often pass through the villages and cities. The lack of space between the river and the infrastructures requires protection by walls against floods and bank erosion. Due to bend effects, bend scour occurs near the outer bank.

An extreme flood can erode the bank foundations and results in wall failure. Subsequently an uncontrolled erosion can propagate behind the failed wall causing serious damages at buildings and infrastructures.

The construction of an undulated concrete wall along the outer bank of a bend has the following advantages:

1. The undulations can reduce considerably the scour depth along the foundations of the wall.

2. The undulations increase the rigidity and stability of the wall. Even if there is scouring along the foundation, the wall undulations increase resistance against overturning by earth pressure.

3. The top slab of the wall can be used as a public space for example as a part of a street or a sidewalk. Therefore without reducing the width of the river, the undulated wall can increase space for public uses.

This diploma project is in the live of the research of *Hersberger* [1] and *Chèvre* [2] about the local scouring protection in curved channels. *Hersberger*[1] studied the effects on flow and scouring of roughness elements on vertical walls at the outer side wall of a bend. *Chèvre*[2] studied the influence of an undulated rip rap protection on local scouring and bed load sediment transport in curved flows.

1.2 Objectives

Foregoing research has shown that an increase of the roughness at the outer bank of a bend reduces the local scour depth (*Hersberger* [1], *Chèvre* [2]). The main goal of this research is to study the influence of the undulated concrete wall at the outer bank of a bend scour and sediment transport.

The principal steps to carry out in this research are:

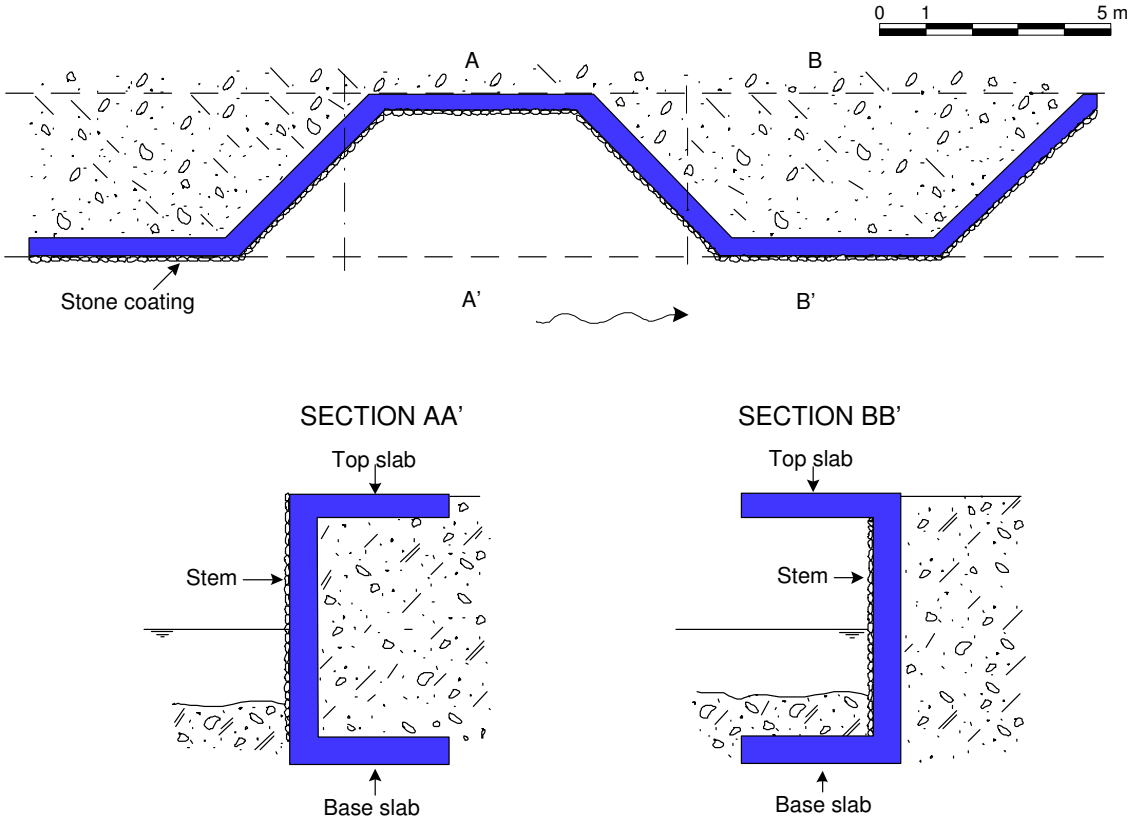

Figure 1.1: Undulated wall with stone coating

- To perform systematic test with the undulated wall in a physical model changing the longitudinal bed slope and the discharge.
- To study the bed topography after the test and compare with reference test without wall undulations (smooth wall).
- To establish a formula for the estimation of the scour depth.
- To study the influence of the undulations of the wall on the flow and solid transport.
- To analyse the stability of the wall against overturning and sliding.

Chapter 2

Review of previous studies

2.1 Flow in bends

A bend in a channel results in a change of the flow direction. A raise in water surface at the outer bank is created by the acceleration forces towards the outer side of the bend. This difference in pressure induces a secondary flow towards the inner bank at the bottom of the channel and towards the outer bank near the water surface. The secondary flow in transversal direction and the longitudinal flow create an spiral flow along the bend.

Flow in open channel bends has been investigated by *Shukry* [3], *Garbrecht* [4], *Rozowskii* [5], *de Vriend* [6], *Blanckaert&de Vriend* who developed a numerical model for the bend flow. The head losses at the bend were studied by *Onishi et al.*[7]. *Bathurst et al.*[8] measured the secondary flow and the boundary shear stresses. *Blanckaert* [9] performed experiments in a 120° bend. He observed a weaker and secondary cell at the outer bank close to the water surface. The turbulence is strongly reduced and therefore the erosion capacity at the outer bank is less important. The same observations where made by *Hersberger* [1] with vertical walls with macro-roughness

2.2 Scour in bends

In general, bend scour depends on the nature of the bend (curvature, capacity of the bank erosion, grain size distribution) but also on characteristics of the flow and upstream conditions (depth, solid transport, redistribution of the flow). No theory can describe precisely this complex scour phenomenon but many approximations have been presented.

Many formulas are based on the equilibrium of the grain of the bed sediments and have the following structure:

$$\sin\beta = k \cdot \frac{h_s}{r} \tag{2.1}$$

The approach $sin\beta \approx \frac{dh}{dr}$ allows to do the integration and to find the bed level profile at the cross section.

$$h_s = h_m \cdot \left(\frac{r}{R_c}\right)^k \tag{2.2}$$

A good overview of the existing scour formulas in bends is given by *Hersberger*[1].

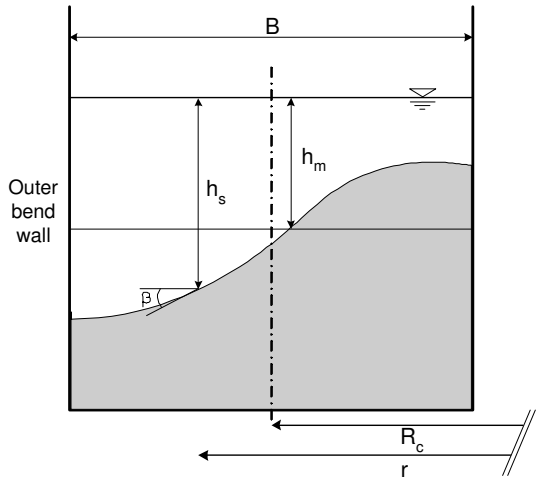

Figure 2.1: Parameters for the estimation of the scour in bends

Farge [10] was one of the first to establish a scour formula for river bends. He presented 6 laws derived on momentum considerations. Later, *Williams*[11] based a theory on *Fargue*'s laws which allows not only calculating the scour depth but also the position of the scour holes.

Van Bendegom[12] established an equation based on the equilibrium of the grains on an inclined plan affected by three forces: the weight, the buoyancy and the dynamic stream force.

Engelund[13] also established his formula based on the equilibrium of the grains. He assumed that the dynamic lift force acts vertically and the grains slips on the bed. He obtained a constant factor of proportionality k=7.

$$\tan\beta = 7 \cdot \frac{h_s}{r} \cdot \tan\phi \tag{2.3}$$

Bridge [14] based on the model of *Rozowskii* [5] gave a formula very similar to *Engelund*'s one.

$$\tan\beta = 11 \cdot \frac{h_s}{r} \cdot \tan\phi \tag{2.4}$$

Kikkawa, Ikeda & Kitagawa [1] assumed a constant eddy viscosity and a logarithmic velocity distribution. The component of the stream force were calculated with the relative flow velocity (flow velocity-grain velocity). Based on the equilibrium of the grains (assuming that the grain slips on the surface) they found the equation:

$$\frac{h_s}{h_m} = exp\Big(\frac{A}{2} \cdot \Big(\frac{r^2}{R^2} - 1\Big)\Big) \tag{2.5}$$

where

$$A = \Big(1.8955 - 3.0023 \cdot \frac{V^*}{V}\Big) Fr_d^2 \tag{2.6}$$

Falkon & Kennedy [15] used du *Boys* approach of sediment transport in layers. They considered at the equilibrium state a vertical control volume in the armoring layer and a

vertical distribution of velocities. The equation they found was a function of the porosity, the particle Froude number and the dimensionless shear stress.

Odgaard [16] based on the equation of *Falcon & Kennedy* [15] established an equation as a function of densimetric Froude number and the dimensionless shear stress.

$$sin\beta \approx \frac{dh}{dr} = 4.8 \cdot \sqrt{\theta} \cdot Fr_d \cdot \frac{h_s}{r} \tag{2.7}$$

Peter [17] established his formula on a dimensional analysis of his experimental data.

$$\frac{h_{s,max}}{h_m} = 5.23 - 13.0 \cdot \frac{h_m}{B} - 0.379 \cdot \sigma + 68.4 \cdot S_e \tag{2.8}$$

It is important to say that this formula does not consider neither the characteristics of the bend $\left(\frac{R_c}{B}\right)$ nor the diameter of the sediments.

Reindl[18] considered the equilibrium of the forces on a grain to establish a formula similar to *Kikkawa et al.* He took into account his test in a double bend of 60°. The mean diameter of the grains utilized was from 2 mm to 8 mm. His formula not only depends on Fr_d and V/V^*, but also on the sediment saturation $Q_b/Q_{b,satt}$.

Thorne[19] base his equation on prototype and flume experiments in which the diameter varied from 0.3 to 63 mm.

$$\frac{h_s - h_m}{h_m} = 1.07 - log(R/B - 2) \qquad for \quad 2 < \frac{R}{B} < 22 \tag{2.9}$$

Hersberger[1] took into account a large number of his own test and the test of *Peter* [17] to obtain the following formula

$$h_s = h_m + \tan\phi \cdot c \cdot \left[6.23B - \frac{(r - R_c - 8.8B)^3}{260 \cdot B^2} + (r - R_c - 8.8B)\right] \tag{2.10}$$

and

$$h_{s,max} = h_m + \tan\phi \cdot c \cdot [0.129 \cdot B] \tag{2.11}$$

where

$$c = 290 \cdot \left(1 - 3.2 \cdot \frac{h_m}{B}\right) \cdot \frac{V \cdot R_h}{\sqrt{g \cdot B^3}} \tag{2.12}$$

This formula was obtained as an approach of a polynomial function of third degree to the cross-section in the scour holes.

Hersberger also proposed a modified formula of *Bridge* for the computation of the maximum scour depth without macro roughness.

$$\sin\beta = 0.394 \cdot \left(11 - 23 \cdot \frac{h_m}{B}\right) \cdot \frac{R_c}{B} \tan\phi \cdot \frac{h_s}{r} \tag{2.13}$$

This formula gives a better prediction for the field data than the Eq. 2.10.

In the presence of vertical ribs, *Hersberger* [1] recommended the Eq. 2.14.

$$\frac{h_{s,max}}{h_m} = 7.7 \cdot \frac{e_s}{R_h} \cdot Fr \cdot (0.001 + (\theta - \theta_{cr})^2) + 1.7 \tag{2.14}$$

where $\theta > \theta_{cr}$ and e_s [m] is the spacing between the macro roughness (from axis to axis).

Chapter 3

Experimental work

3.1 Description of experimental installation

The experimental facility has been described in detail by *Hersberger*[1]

3.1.1 Channel geometry

The channel is composed of one inlet reach of 7.5 m long, followed by 90 ° bend of 6 m centerline radius and an outlet reach of 6 m. The channel width is 1 m. A water supply pipe connected to a pump at the inlet reach allows a discharge up to 250 *l/s* in the model.

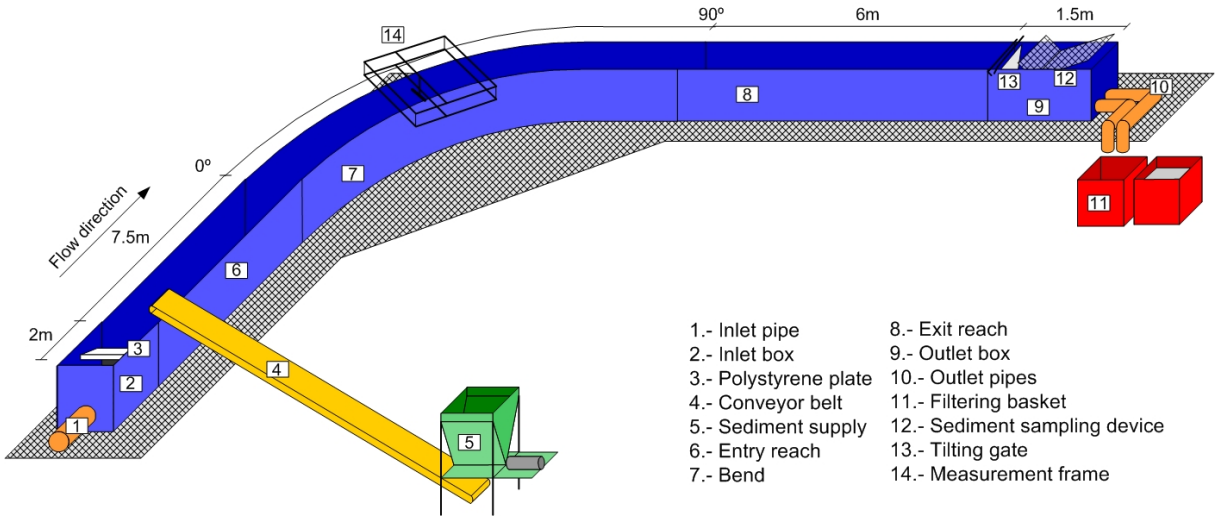

Figure 3.1: Experimental installation

3.1.2 Sediment supply

To obtain an automatic and continuous sediment supply, a conic tank stores half a cubic meter of sediments. At the bottom of the tank there is a cylinder with a longitudinal slide.

The rate of sediments introduced in the channel is controlled by the rotation velocity of the cylinder. The sediments were transported into the channel by a 10 m long conveyor belt.

3.1.3 Inlet box

At the beginning of the channel the water supply pipe ($\emptyset 40\, cm$) is connected to a 80 cm long perforated cylinder. A floating polystyrene plate is placed to calm the water surface at the entry of the channel.

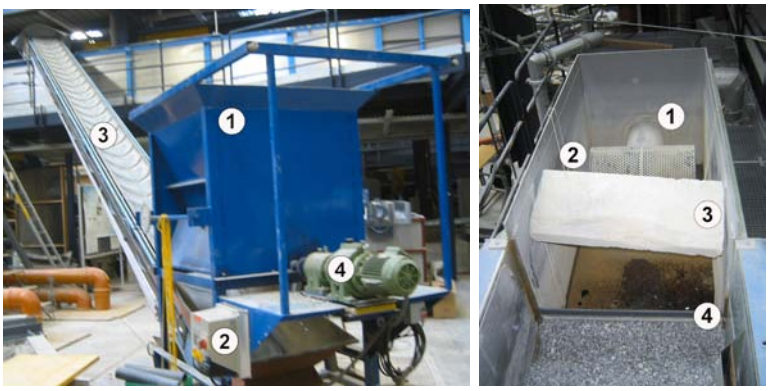

Figure 3.2: LEFT: Sediment supply (1. Conic reservoir, 2. Discharge controller, 3. Conveyor belt and 4. Electric motor) RIGHT: Inlet box (1. Inlet pipe, 2. Perforated cylinder, 3. Polystyrene plate, 4. Over fall)

3.1.4 Outlet box

The outlet box is composed by:

- An overfall that controls the bed level.
- A tilting gate that allows a smooth filling and emptying of the channel.
- A sediment sampling device.
- Two outlet pipes.

Figure 3.3: LEFT: Outlet pipes (top), tilting gate (center), sediment sampling device (bottom), RIGHT: general view of the outlet box

3.1.5 Sediment recover

At the end of the channel, the water and sediments are collected by two outlet pipes and guided into a filtering basket which retains the sediments. The basket has a dimension of $1 \times 1 \times 1\, m$ and the walls and the bottom are covered by a double metallic grid. The bottom of the basket can be tilted to facilitate the recover of the sediments.

Two identical baskets were used. When one basket was full the change could be done without interruption of the test.

Figure 3.4: LEFT: Outlet pipes and filtering baskets with the skirts against splashing, RIGHT: filtering basket with the sediments (top), double grid, closing mechanism, wheel and rails (bottom)

3.1.6 Characteristics of the sediment mixture

A granulometry of the sediments was chosen similar to the grain size distribution used by *Hersberger*[1]. This coarse sediment mixture was selected similar to typical granulometry of alpine rivers.The minimum diameter was 2 mm to allow the correct sampling and the recovery of all the sediments at the filtering basket (the smaller sediments would pass through the sampling grid and the grid of the filtering basket).

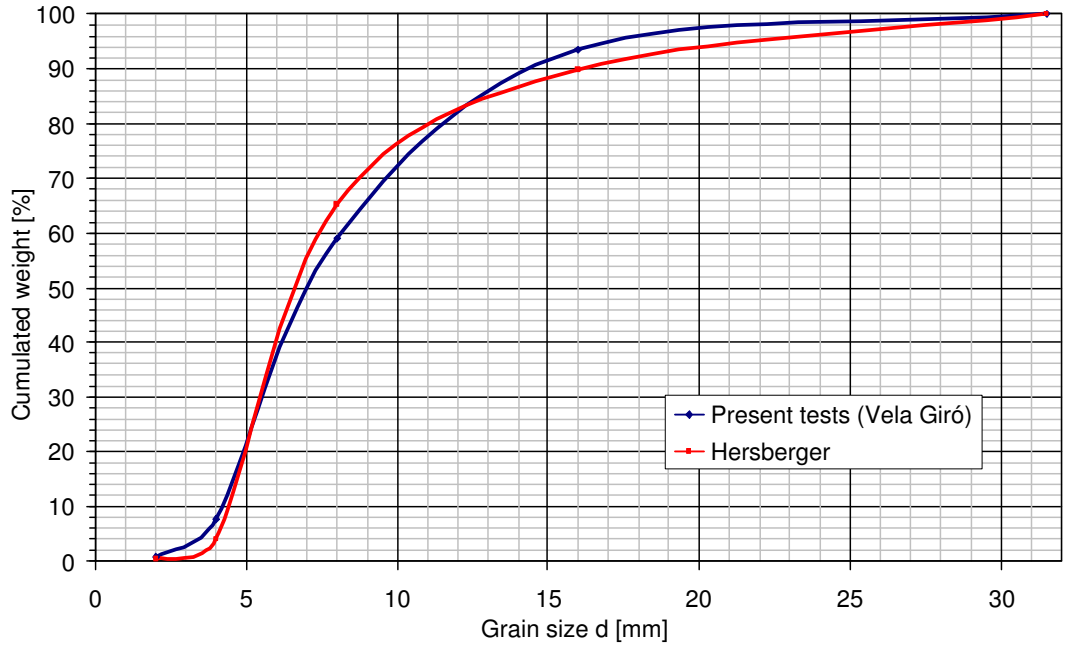

Figure 3.5: Grain size distribution used by *Hersberger* and the sediment mixture used in the present tests

3.2 Parameters of the experiments

3.2.1 Bed slope

Three bed slopes were chosen for the tests, namely 0.35, 0.5 and 0.7%, similar to *Hersberger*[1]. 0.7% was the maximum value to maintain subcritical flow conditions whereas 0.35% was the minimum slope to get significant sediment transport.

3.2.2 Discharge

The experiments were performed with five different discharges. 70 l/s was used to create the initial armoring layer. The test with the slopes 0.5% and 0.7% were carried out with 150, 180, 210 l/s. For the tests with a slope of 0.35% the discharges were 150, 170, 190 and 210 l/s. For the slope of 0.35% with 150 l/s the solid transport was very low therefore one discharge was added between 150 and 210 l/s to guarantee that for 3 of the 4 tests the scour phenomenon was fully developed.

3.2.3 Wall geometry

The geometry of the wall was created by trapezoidal ribs of steel sheet placed vertically along the outer side of the channel. A stiffener is placed inside the ribs to avoid the deformation due to the sediments and water pressure.

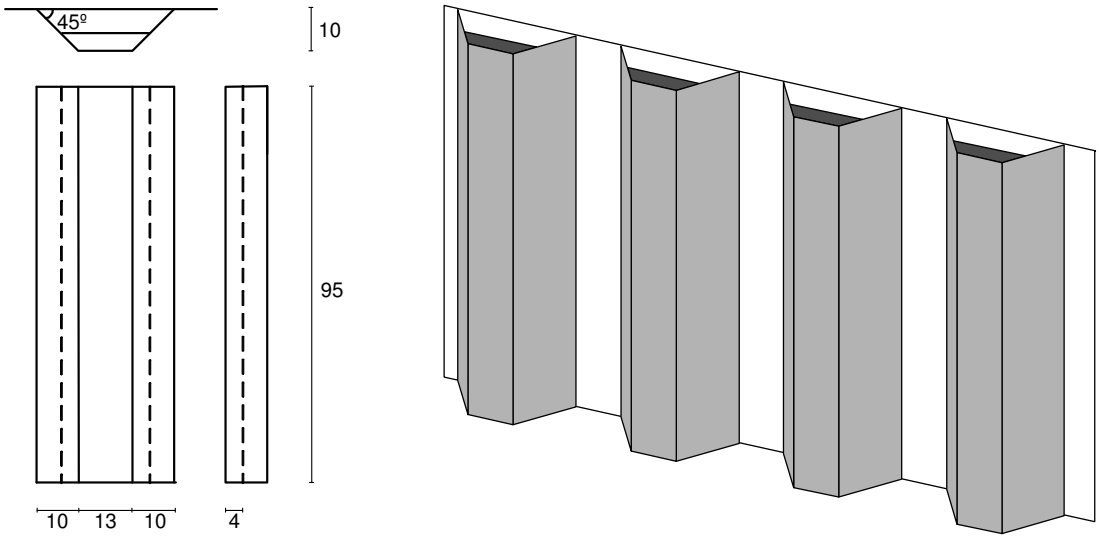

Figure 3.6: Wall ribs (units in cm) fixed at the outer vertical wall of the flume

3.2.4 Sediment transport

The test were performed at the equilibrium conditions to maintain the longitudinal slope at the inlet reach constant during the test. The solid transport was estimated according *Smart&Jaëggi* [20] formula. In order to fit at the beginning of the test the sediment supply device. The sediment supply had to be changed during the test as a function of the water and bed levels to obtain the equilibrium conditions. The most important problem during the test was the regulation of the sediment supply. The quantity of sediments dropped on the conveyor belt was not always constant. It depends on the sediments humidity and the size of the grains (a big stone can bloc the motor and stop the supply), the quantity of sediments inside the reservoir and the velocity of the motor. According to *Hersberger*[1] the precision of the time-average sediment supply is estimated to be at about 10% to 15%.

To calculate the sediment transport capacity of the flume the following assumptions have to be made.

- The velocity is constant over the section in the inlet reach.
- The channel width is 0.9 m which corresponds to the shortest distance between the inner flume wall to the undulated wall.
- The bed roughness is calculated as the average of the formulas of *Meyer-Peter & Müller* and *Strickler* [21]:

$$K_s = \frac{21.1}{d_m^{\frac{1}{6}}} \qquad (3.1) \qquad\qquad K_s = \frac{26}{d_{90}^{\frac{1}{6}}} \qquad (3.2)$$

The wall roughness is considered 100 $m^{\frac{1}{3}}s^{-1}$ for the inner wall and 50 $m^{\frac{1}{3}}s^{-1}$ (first estimation) for the outer wall.

- The equivalent coefficient of friction for a composite roughness section was computed according to the hypothesis that the total friction force is the summation of all the resistance sub-forces [22].

$$K_s = P^{\frac{1}{2}}\left[\sum_{i=1}^{n}\left(\frac{P_i}{K_{si}^2}\right)\right]^{\frac{-1}{2}} \qquad (3.3)$$

- The water depth was calculated with the formula of *Manning*:

$$Q = K_s R_h^{2/3} S_0^{1/2} A \qquad (3.4)$$

- The *Smart&Jaeggi* formula [20] is:

$$q_s = \frac{4}{s-1}\cdot\left(\frac{d_{90}}{d_{30}}\right)^{0.2}\cdot q\cdot S^{1.6}\cdot\left(1-\frac{\tau_{cr}\cdot(s-1)\cdot d_m}{h_m\cdot s}\right) \qquad (3.5)$$

S_o *initial* [%]	**Qw** [l/s]	**Qs** [g/min]	**Water depth** [m]
0.7	150	8181	0.151
	180	11600	0.170
	210	15102	0.187
0.5	150	2906	0.168
	180	4782	0.189
	210	6716	0.208
0.35	150	225	0.187
	170	882	0.204
	190	1567	0.219
	210	2274	0.233

Table 3.1: Calculated sediment discharge and water depth with the formulas 3.5 and 3.4

3.2.5 Test nomenclature

The data treatment and analysis was partially based on procedures developed by *Hersberger*[1]. That needs the utilization of a standard nomenclature to identified the test. The following nomenclature composed by four characters is adopted:

- The first character designates the slope B=0.5%, C=0,7% and D=0.35%
- The number designates the geometry of the wall: 01 smooth wall and 02 undulated wall
- The last character designates the discharge a=70 l/s, b=150 l/s, c=180 l/s and d=210 l/s. For the test with the slope of 0.35% a=70 l/s, b=150 l/s, c=170 l/s e=190 l/s and d=210 l/s

Example: C02d: Test with initial slope of 0,7% an undulated wall and a discharge of 210 l/s

3.2.6 Boundary conditions

At the beginning of the inlet reach, the bed level was controlled by a sill. Water surface perturbations were attenuated at the inlet box by a floating polystyrene plate. The sediments were added 70 cm downstream the beginning of the channel. At the end of the exit reach the bed level was controlled by a sill at the outlet box. Over the sill, critical flow conditions occurred that created a backwater curve in the exit reach. In some cases it reached the bend. The level of the sills can be adjusted to define the initial longitudinal slope.

The backwater curve has a moderate influence when the Froude number is close to one. But the influence increases for the flat slopes (see Figure 3.7). For the highest slope the difference between the uniform flow depth and the backwater depth is less than 1 mm at the end of the bend. For the lowest slope the difference is about 15 mm for a discharge of 150 l/s (8% of the flow depth) and 23 mm for 210 l/s (10% of the flow depth). This differences can have a certain influence on the second scour hole.

3.3 Description of the data acquisition

3.3.1 Automatic data acquisition

Level acquisition unit

The acquisition data frame was positioned over the channel. It was moved manually to 8 fixed positions (every 15°) from 2 m upstream of the bend to 2 m downstream. In each frame position the frame recorded automatically the level data. The measurements took about 4h to record about 1000 points over the entire channel.

The level acquisition was done with 3 ultrasonic probes (UNAM 30I9001) mounted on a probe support. The support prove was moved by 3 motors into the wished frame coordinates (X,Y,Z). The precision of ultrasonic probe is less than 0.3 mm.

3.3.2 Manual data acquisition

Bed level at the inlet and outlet reach

The automatic measurements were complemented with manual level recordings in the straight reaches. The measurements were done from 1.5 to 5.5 m in the inlet and from

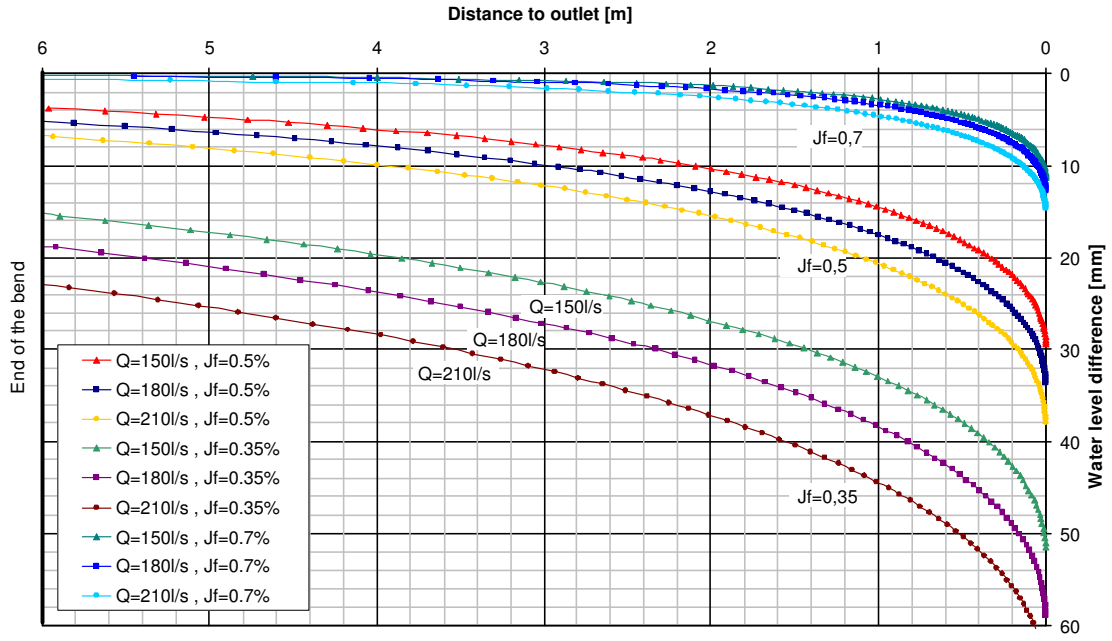

Figure 3.7: Computed backwater curve in the exit reach of the flume

2.0 to 5.0 m at the outlet reach every 1 m. Over the cross section the measurements were taken every 10 cm. The precision of this measurements is 1 mm.

Water and bed level evolution at the outer bank

The water and bed levels were measured at the outer bank of the channel. This wall was transparent but partially covered by the vertical ribs introduced for the test. The measures were taken between the vertical ribs (approximately every 30 cm). The measures were done every 40 minutes at the beginning. Towards the end of the test the frequency was reduced because the changes in water and bed levels became smaller.

Velocity acquisition

The longitudinal velocity was measured manually with the electromagnetic flow sensor NAUTILUS C 2000 in six cross-sections along the channel. At the inlet reach: -2.85 m and -2 m, bend: 46° and 72° and outlet reach: 1 m and 2.40 m, (see Fig. 3.8 left) The longitudinal velocities were recorded for all the points on a 10 cm width × 2.5 cm depth grid over the entire cross section (see Fig. 3.8 right).

The velocity measurement device consist of a metallic profile put on top of the channel. The NAUTILUS was supported by a vertical metallic bar maintained by a metallic profile. A PVC plate put on the metallic profile allows to adjust the level of the NAUTILUS (see Fig. 3.9)

It was not possible to record the tangential velocities with the electronic flow sensor because the flow velocity measurer has to be placed orthogonally to the flow. As the NAUTILUS is not streamline in this direction, the turbulence created around the device

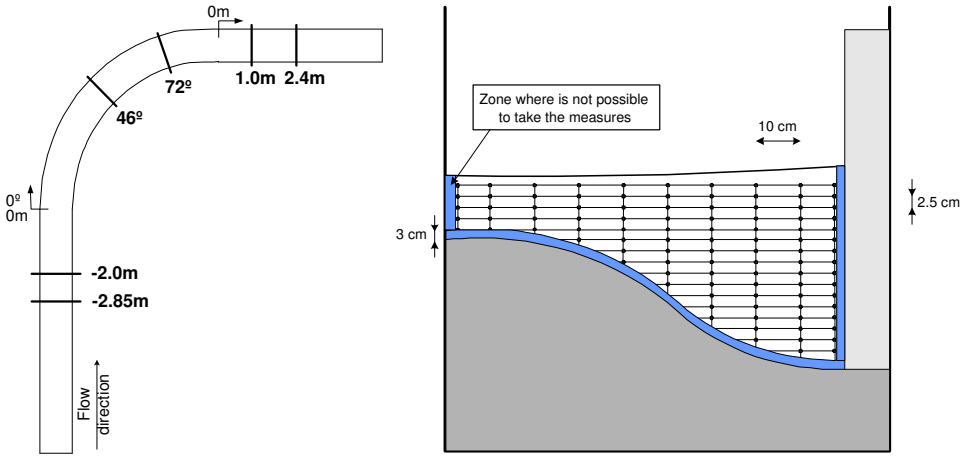

Figure 3.8: LEFT:The 6 sections where the velocities were measured. RIGHT: Grid of the velocity cross-section measurements

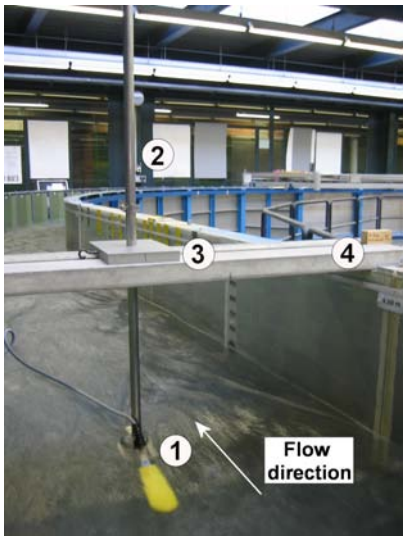

Figure 3.9: Velocity measurer device: 1. Flow sensor NAUTILUS, 2. Metallic bar, 3. PVC plate, 4. Metallic profile

hinders the measurements.

Sediment sampling at the outlet box

During the test some samples of the transported sediment where taken at the outlet box. The samples were taken every 40min. at the beginning of the test. The sampling frequency was reduced towards the end of the test because sediment transport became more stable. The sediments were taken out with a sieve introduced in the stream during 3 to 5 min (see Section 3.1.4). Later the samples were dried and weighted. In some tests one sample taken at the end of the test was also sieved.

Sediment weight at the filtering basket

At the end of each test the sediments accumulated in the filtering basket were weighted.

Sediment sampling of the armour layer

After each test, samples of the armor layer were taken at 45° and 90° near the inner and the outer side of the bend. To extract the sample of the armor a zone of 10×30 cm was painted with a spray, then colored the stones were manually taken out. Later the samples were sieved.

Photos

During the test, photos were taken of different parts of the channel.

3.4 Test procedure

The tests were performed with the procedure as described hereafter.

3.4.1 Test preparation

1. Sediments were leveled to the initial bed slope (S_0=0.7, 0.5 and 0.35%)
2. A discharge of 70 l/s was run during 5 to 6 hours in order to armor the bed.
3. Automatic and manual bed level measurements were performed.
4. The channel was filled slowly (Q=10 l/s) with the tilting gate lifted.
5. The discharge was increased gradually and the tilting gate was lowered.
6. The sediment feeding was started with a solid discharge as calculated in Section 3.2.4

3.4.2 During the test

Before the stabilization of the scour in the bend

1. The bed and water level at the outer side wall were measured (every 40 min.)
2. Sediment samples were taken at the outlet of the channel every 40 min.
3. Sediment and water discharge was controled frequently.
4. The sediment feeding was adapted to maintain the water level constant at the inlet reach.

Criteria of a stable situation

The situation was considered stable when there were no changes at the water level on the outer side wall of the bend and the solid transport at the outlet was approximately equal to the sediment feeding into the flume.

After the stabilization

1. The water level measurements with the ultrasonic probe were performed. The measurements needed about 4 hours to be completed (30 min for each position of the frame)

2. Water velocities were measured while water levels were automatically recorded.

3. Bed and water level at the outer side wall were measured (every hour)

4. Some sediment samples were taken at the outlet box.

5. Some photos of the flow were taken.

6. The filtering basket was changed and the sediment feeding reservoir was filled if it was necessary.

7. After the measurements, the tilting gate was lifted, the water and sediment supply were stopped and the channel was emptied gradually.

3.4.3 After the test

1. The final bed topography was recorded (automatically and manually).

2. Systematic photos of the bed were taken every 15° from one meter upstream to one meter downstream of the bend (see Appendix H).

3. Sediment samples of the armor were taken at 45° et 90° near the inner and the outer side of the banks.

Chapter 4

Analysis of the test results

4.1 Description of the Appendix

Test results are summarized in the Appendix of the present report. The present section gives an overview of the contents of Appendixes.

A Principal parameters and hydraulic results of the test.

B Final bed topography compared to the initial bed level.

C Final water surface compared to an horizontal surface (average of all the points)

D Longitudinal profiles of the water and bed surfaces. Every plot shows the average, minimum and maximum bed and water levels.

E Bed and water levels at the cross section every 15° from $1m$ upstream the bend to $1m$ downstream. The bed and water mean level and the initial bed level are also plotted.

F Water reference level calculated according to the different hypothesis.

G Pictures of the water surface of every test. They are taken approximately at 15° from the beginning of the bend, 1.8m over the water surface and 1.5m from the axe of the channel at the left and downstream direction.

H Pictures of the armoring layer taken vertically every 15° from 0° to 90°. They show the evolution of the grain size distribution at the cross section along the bend.

I The grain size distribution of the armoring layer after the test. The samples were taken at 45° and 90° near the inner and the outer side of the bend..

J Kinetic energy and total energy (kinetic energy + specific energy) of every cross section along the whole channel (see Section 4.6).

K Measured longitudinal velocities at six cross sections along the channel (see Section 4.7).

L Required minimum thickness of the undulated wall to guarantee the stability against overturning, sliding and overstress foundation (see Chapter 5).

4.2 Analysis of bed topography

4.2.1 Definition of a reference water surface

The scour depth obtained by the scour formulas is frequently calculated related to a water surface. Before doing an analysis of the bed topography it's important to define a reference water surface. The scour depth related to the real water surface could have some centimeters of error due to the existence of the shock and/or stationary waves. To avoid this problem a mean reference water level is calculated for each test and the scour depth is calculated related to this reference water level.

The the channel is divided in a grid of 1×1 cm.

- The $H_w(i,j)$ is the water level at the point (i,j) where i are the different cross sections and j the different longitudinal profiles (see Fig. 4.1). The water level is related to a reference level situated approximately 0.5 m below the channel bottom.
- The $H_w(i)$ is the average water level over the cross section i

$$H_w(i) = \sum_{j=1}^{101} \frac{H_w(i,j)}{101} \tag{4.1}$$

- The $\overline{H_w}(i)$ corresponds to the reference water level (see Fig. 4.2).

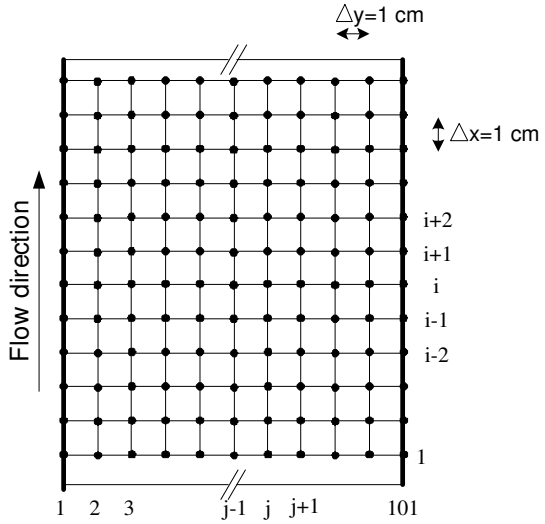

Figure 4.1: Schema of the channel grid

Four water reference levels are analysed to calculate the scour depth. The selected reference level is described here below the other reference levels are described at the Appendix F.

This reference water surface is proposed to minimize the difference between the measured water level and the reference water level. This surface is constant over the cross section. The surface in the bend is the regression line of the two variables $H_w(i)$ and i,

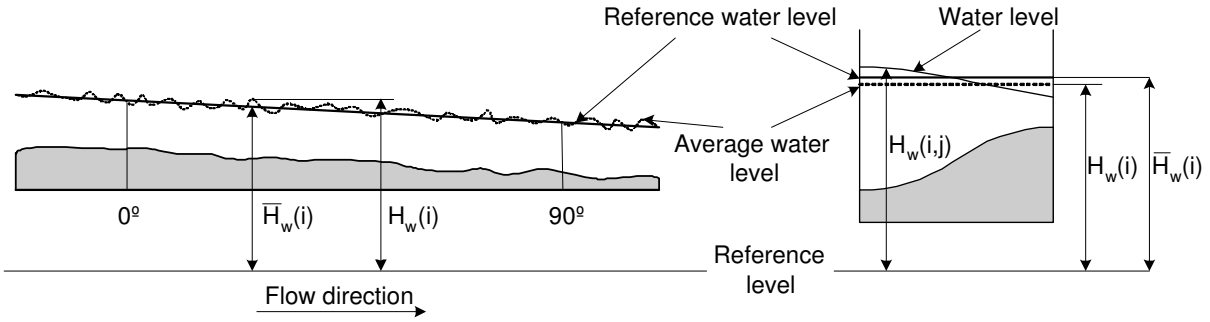

Figure 4.2: LEFT: Schema of the longitudinal profile at the axe of the channel RIGHT: Schema of the cross section

$\forall i$ inside the bend. The criterion for the best fit used is the "least squares criterion" and consist to minimize the sum of squared deviations.

The reference water level at the sections -4m upstream (A) and 3m downstream (B) of the bend are the same as the case R1:

$$H_{wA} = \sum_{i=A-10}^{A+10} \frac{H_w(i)}{21}$$

and

$$H_{wB} = \sum_{i=B-10}^{B+10} \frac{H_w(i)}{21}$$

The reference level between -4m and the beginning of the bend is straight line that connects H_{wA} with the level of the regression line at the section 0°. The reference level at the outlet reach is the straight line between the level of the regression line at 90° and H_{wB} (see Fig. 4.3).

The reference water level equation is:

$$\overline{H_{1w}}(i) = H_{wA} - \frac{H_{wA} - \overline{H_{2w}}(l_1)}{l_1} \cdot i\Delta x \tag{4.2}$$

from -4 m to 0°

$$\overline{H_{2w}}(x) = a + b \cdot x \tag{4.3}$$

from 0° to 90°

where a and b where obtained according the least squares criterion.

$$\overline{H_{3w}}(i) = \overline{H_{2w}}(l_1 + l_2) - \frac{\overline{H_{2w}}(l_1 + l_2) - H_{wB}}{l_3} \cdot (i\Delta x - l_1 - l_2) \tag{4.4}$$

from 90° to 3 m

where $l_1 = 4$, $l_2 = \frac{2 \cdot \Pi \cdot R}{4}$, $l_1 = 3$, $R_c = 6m$ and $\Delta x = 0.01m$

This method to obtain the reference water surface was selected for the following reasons:

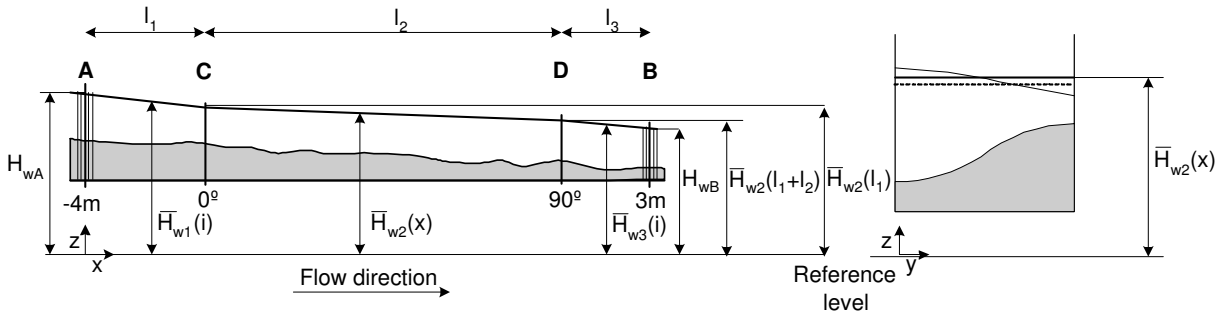

Figure 4.3: Schema of the reference water level R4; LEFT:longitudinal profile; RIGHT: Cross section

Advantages

- All the scour formulas consider that the water level is constant over the cross section. This reference water surface has a constant level over the cross section.
- At the bend there is the maximum scour depth, where the reference water surface fits best with the measured water level.

Disadvantages

- The calculation procedure differs in the bend from straight reaches in order to guarantee the continuity of the reference water surface.

4.2.2 Depth of the scour holes

By the analysis of the final bed topography, it can be observed that two scour holes in the bend are formed during the test.

The discharge and the bed slope are two parameters that influences the maximum scour depth [1]. The Figure 4.4 shows that with the increase of the discharge, the relative scour depth $\frac{h_{max}}{h_m}$is reduced for the two scour holes. This can be explained in the following way. By increasing the discharge the increase of the mean water depth is more important than the maximum scour depth therefore the relative scour depth is reduced.

The first scour hole is always deeper than the second one. The two regression lines are quite parallel but correlation coefficient of the first scour erosion is a little better. The discharge influence is more important in the first scour hole than in the second one.

The Figure 4.5 shows that an increase of the bed slope in the stream direction causes an increase of the relative scour depth.

It's important to note that the correlation coefficients in the two Figures are very low. Nevertheless the above mentioned tendencies are quite clear.

An other interesting parameter to analyze is the velocity. In the case of a smooth wall the relative hole depth increases if the densimetric Froude number $\left(\frac{V}{\sqrt{(s-1)g \cdot d}}\right)$ is increased. For the undulated wall the relative hole depth is not a function of Fr_d. In

[1]The scour depth is defined as the distance between the reference water surface and final bed topography

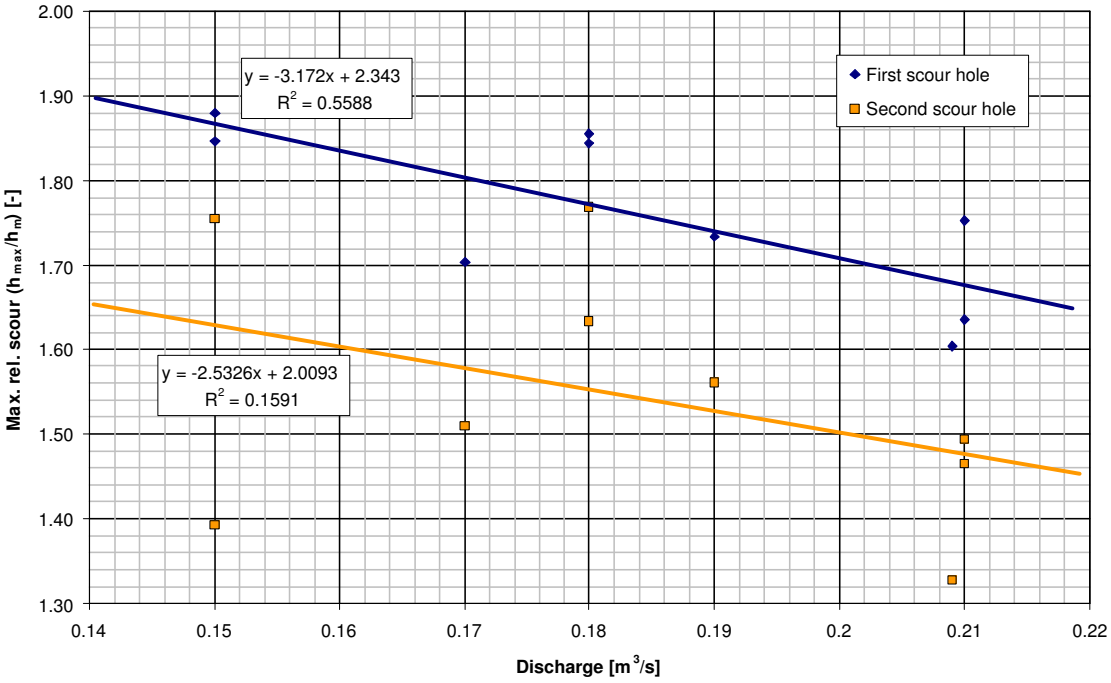

Figure 4.4: Maximum relative scour depth $\frac{h_{max}}{h_m}$ as a function of the discharge

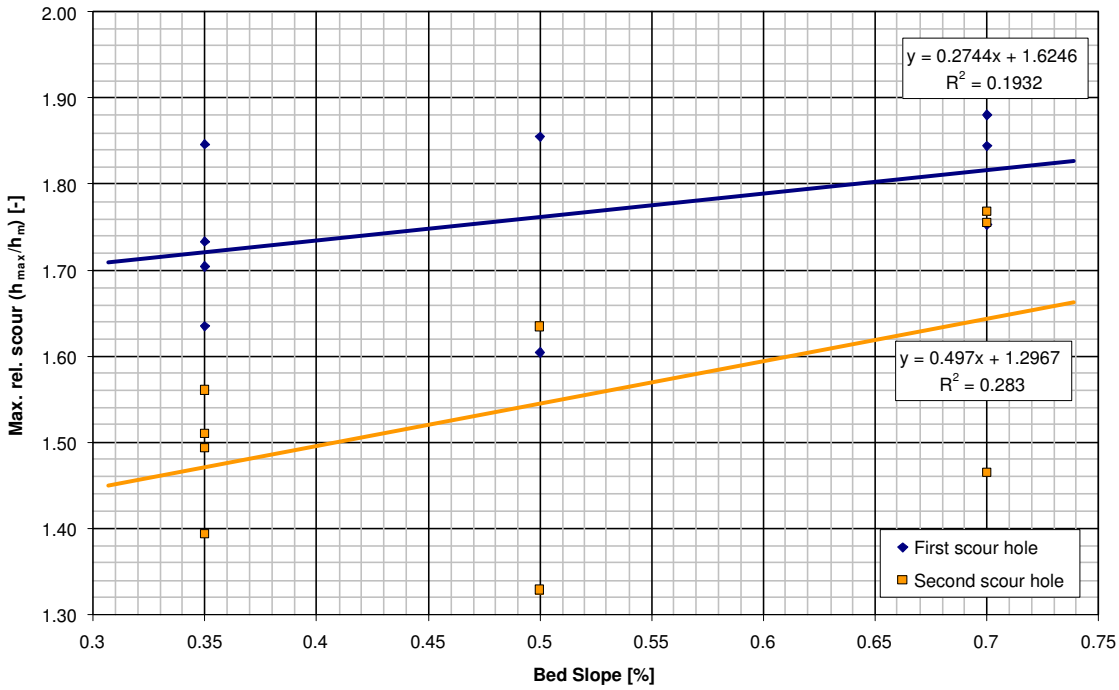

Figure 4.5: Maximum relative scour depth $\frac{h_{max}}{h_m}$ as a function of the bed slope

the tests of the present study, the sediment density coefficient and the granulometry are constants therefore the relative scour depth is independent of the velocity.

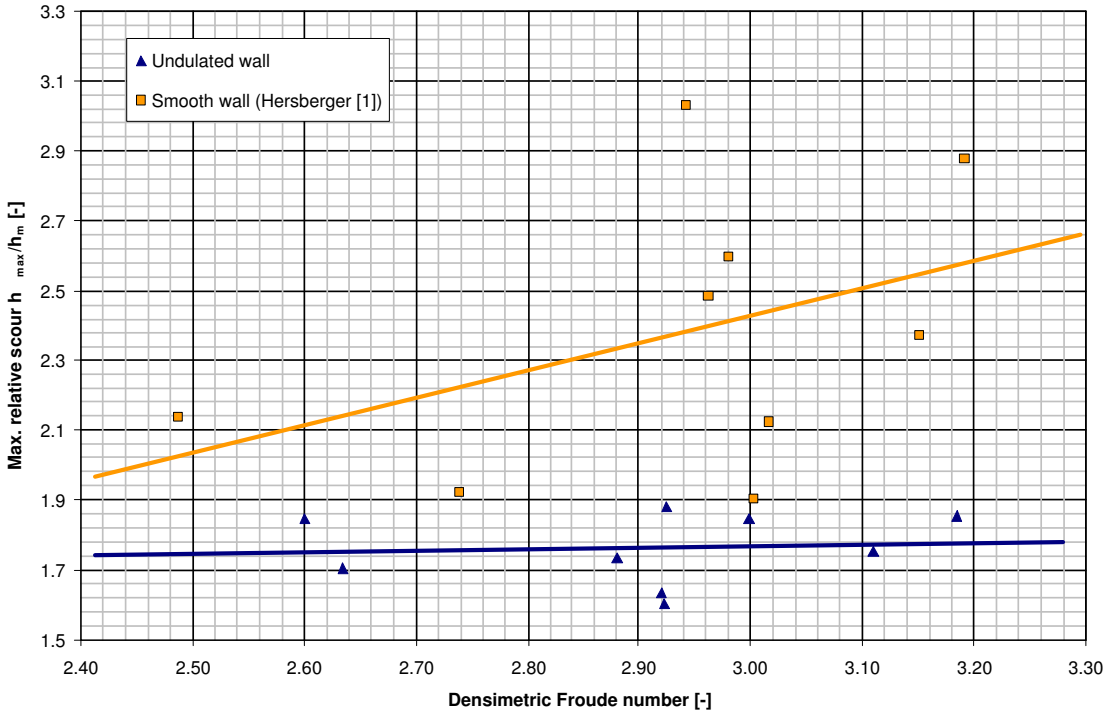

Figure 4.6: Maximum relative scour depth $\frac{h_{max}}{h_m}$ as a function of densimetric Froude number F_{rd}

Compared to a smooth wall, the undulated wall reduces significantly the scour depth, especially in the second scour hole. For the first hole, the scour depth is reduced [2] between 5 to 35% (mean value 17%) and 0 to 60% (mean value 39%) for the second hole (see Fig. 4.7). This results can be compared with the results obtained by Hersberger [1] with macro roughness [3] . The test with the macro roughness have a scour reduction between 10 and 60% (mean value 37%)for the first hole and between 35 to 85% (mean value 60%) for the second one compared to a smooth wall.

Despite the good results with the undulated wall, the reduction of the scour depth with macro roughness is, in general, more important.

The Fig. 4.8 shows that with the same mean water depth the maximum hole depth is in average 1.5 deeper with the smooth wall than with the undulated wall. The upper curve represents the modified formula of Bridge Eq.4.5 (Hersberger [1]) that takes into account the bend geometry (R_c, B) the flow conditions (h_m) and the bed characteristics ($tan\phi$). The local lateral bed slope is given by

$$sin\beta = 0.394\Big(11 - 23\frac{h_m}{B}\Big)\frac{R_c}{B}tan\phi \cdot \frac{h_s}{r} \tag{4.5}$$

[2]The scour depth reduction is defined as $\frac{(h_{max}-h_m)_{smooth}-(h_{max}-h_m)_{und.}}{(h_{max}-h_m)_{und.}} \cdot 100$ [%]

[3]Hersberger [1] obtained the best results with a macro roughness separation of 4°. The comparation will be done with those test

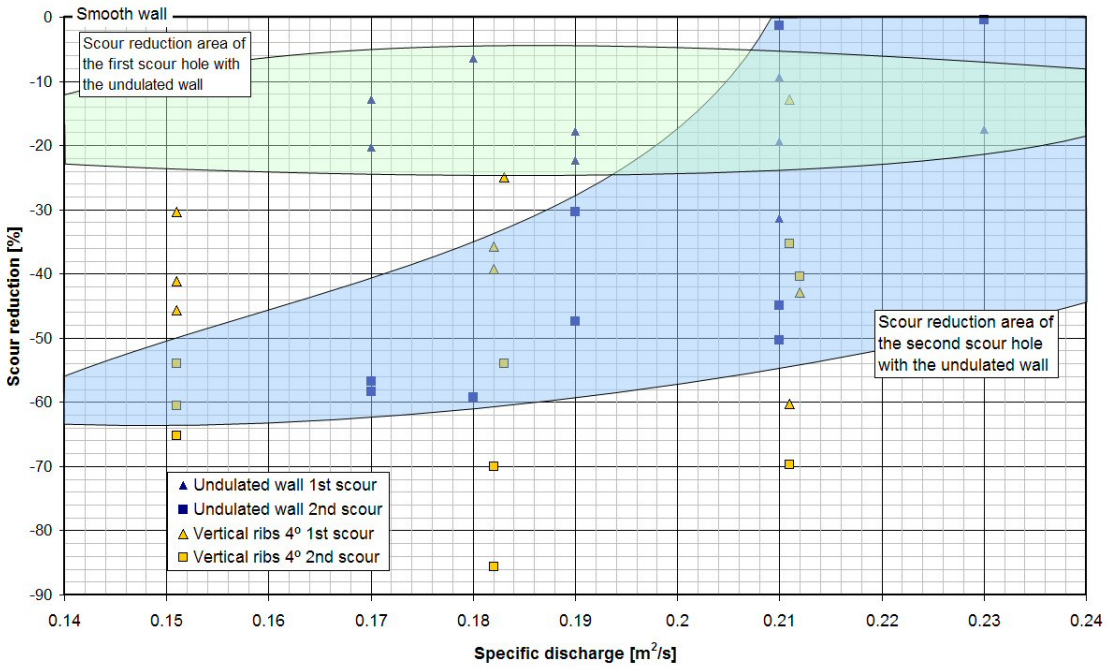

Figure 4.7: Reduction of the scour depth by the undulated wall and with vertical ribs spaced 4° compared to a smooth wall

The inferior curve shows the modified formula of *Bridge* adapted to the undulated wall in the present study:

$$sin\beta = 0.3\Big(11 - 21\frac{h_m}{B}\Big)\frac{R_c}{B}tan\phi \cdot \frac{h_s}{r} \tag{4.6}$$

The correlation coefficient R^2 between the observed data and the calculated with Eq.4.6 is quite good $R^2 = 0.924$. On the other hand R^2 obtained with the Eq. 4.5 for the smooth wall is very low $R^2 = 0.16$ (see Fig. 4.9). Some other formulas have been tried (*Hersberger*[1] Eq. 2.11 $R^2 = 0.61$, *Kikawa*[1] Eq. 2.5 $R^2 = 0.25$, *Bridge*2.4 Eq. 2.4 $R^2 = 0.13$) only the *Hersberger*'s formula have good results for the smooth wall.

The first scour hole is probably due to the reflection of the flow at the outer wall of the bend. The flow plunges down towards the bottom of the channel causing the hole and increasing the secondary flow. Then the flow is directed towards the second hole.The scour reduction is more significant at the second hole because the effect of the undulations is produced after the first hole (inside the bend). The flow in the first scour hole arrives directly from the inlet reach with almost no effect of the bend. At the beginning of the bend the effect of the undulations is not as important as in the second hole, where the flow has passed all the bend.

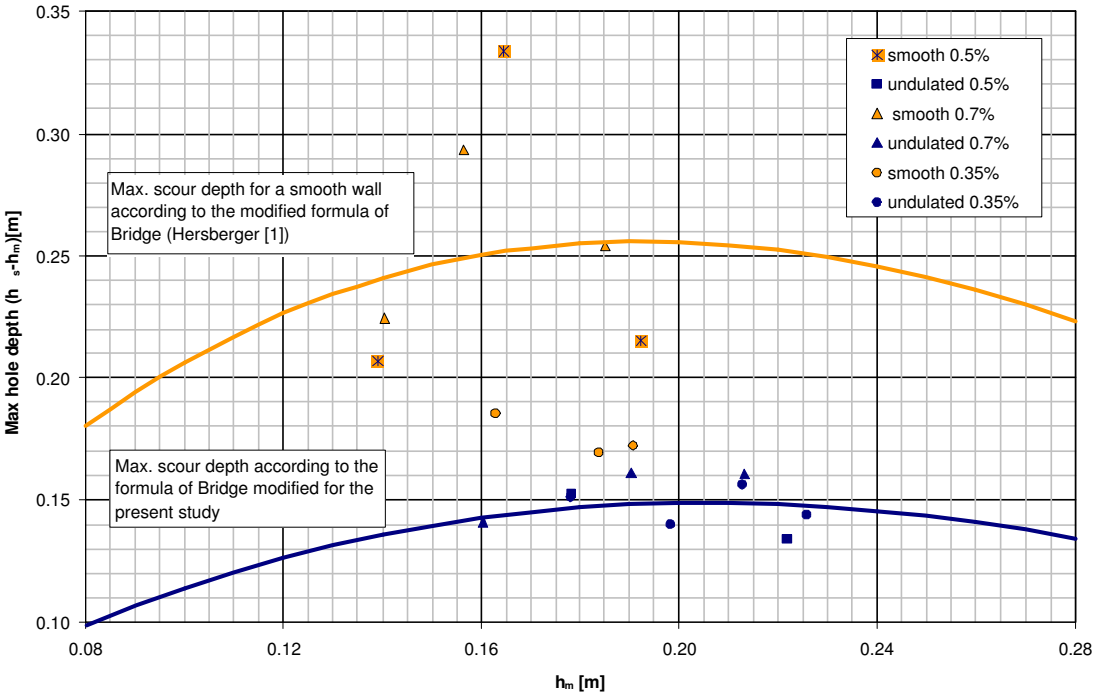

Figure 4.8: Maximum hole depth below mean bed level $h_s - h_m$ as a function of the mean water depth h_m

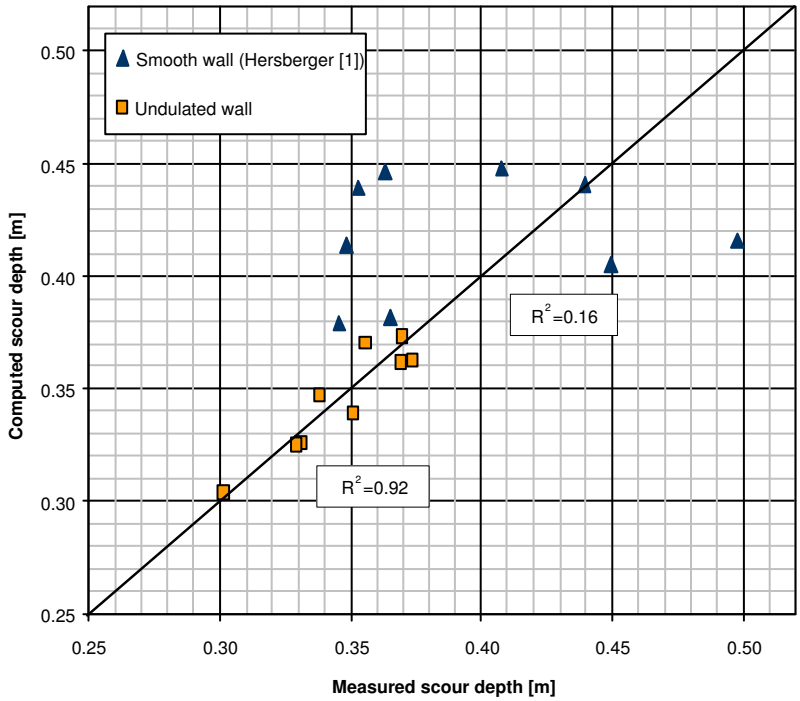

Figure 4.9: Comparison of maximum scour depth between measured data and computed with the equations 4.5 (for the tests with the smooth wall) and 4.6 (for the tests with the undulated wall)

4.2.3 Location of the scour holes in the bend

Analyzing the thalweg of the tests with the smooth wall it can be observed that the first scour starts at about 10° and it reaches the maximum at 30°. The first scour ends at about 60°. The second hole begins at 70° and reaches the maximum depth at about 90°. The thalweg comes up at about 2.2 m after the bend. In the case of an undulated wall the two scour holes are displaced about 10° in downstream direction(see Appendix D and Table 4.2.3).

		Smooth wall	**Undulated wall**
	Start erosion	10°	20°
1st scour	Max. depth	30°	45°
	Min. Thalweg	60°	70°...75°
	Start erosion	70°	80°
2nd scour	Max. depth	90°	0.8m
	Min. Thalweg	2...2.5m	3...4m

Table 4.1: Description of scour locations

The location of the first scour seems not to be a function of the discharge. An increase of the discharge causes a slight displacement of the second hole in downstream direction for the smooth wall and in upstream direction for the undulated wall (see Fig. 4.10)

Peter [17] developed a formulae to estimate the position of the scour holes in the bend. This formula is based on the standard deviation $\sigma = \sqrt{\frac{d_{84}}{d_{16}}}$ of the grain size distribution:

upstream scour

$$\alpha_1 = 26.3\sqrt{\sigma} + 11 \tag{4.7}$$

downstream scour

$$\alpha_2 = 104 + 5.66\sigma \tag{4.8}$$

For the tests with a smooth wall ($\sigma = 1.82$) the first scour should be developed at 46° and the second at 114°. For the tests with an undulated wall ($\sigma = 1.65$) the first scour it would be at 45° and the second one at 113°. The formula of Peter fits better for the undulated than for the smooth wall. It's important to note that both equations have a rather low correlation coefficient.

The formulas proposed by *Hersberger* [1] to estimate the location of the scour for the smooth wall are:

$$\alpha_1 = \sigma \cdot \left(0.58 \cdot \frac{B}{h_m} + 12.7\frac{S_e}{\sigma - Fr_d}\right) + 1.4 \cdot Fr_d \cdot \frac{V}{V^*} - 6.6, R^2 = 0.829 \tag{4.9}$$

$$\alpha_2 = 12.6 \cdot Fr_d - 0.9\left(\frac{R_c}{B}\right)^2 + 91.6, R^2 = 0.602 \tag{4.10}$$

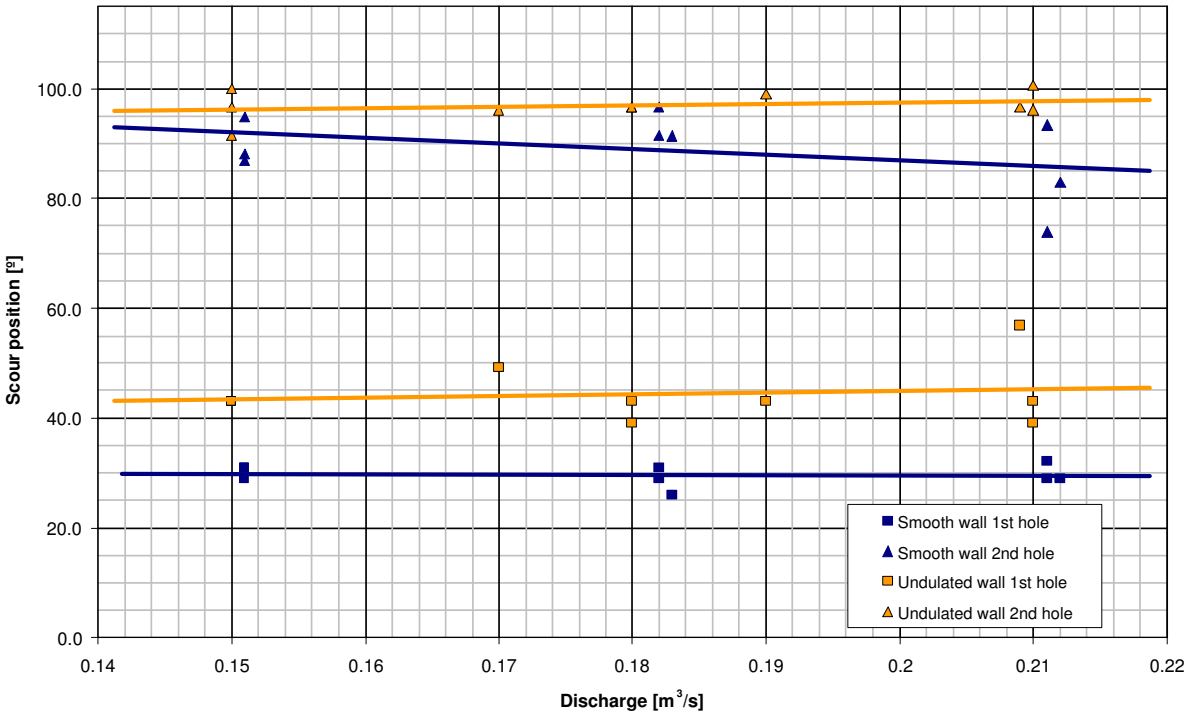

Figure 4.10: Location of scour as a function of discharge.

	Smooth wall		Undulated wall	
Scour	**Measured**	**Computed Peter**	**Measured**	**Computed Peter**
1^{st}	$\simeq 30°$	$46°$	$\simeq 45°$	$45°$
2^{nd}	$\simeq 90°$	$114°$	$\simeq 100°$	$113°$

Table 4.2: Comparison of the mean scour position between the measurements and the results computed with the Eq. 4.7 and 4.8

Good agreement is obtained for the first scour with the smooth wall and somewhat less good for the second scour. The results with the undulated wall are in quite good agreement for the second scour hole but not for the first (see Fig. 4.11).

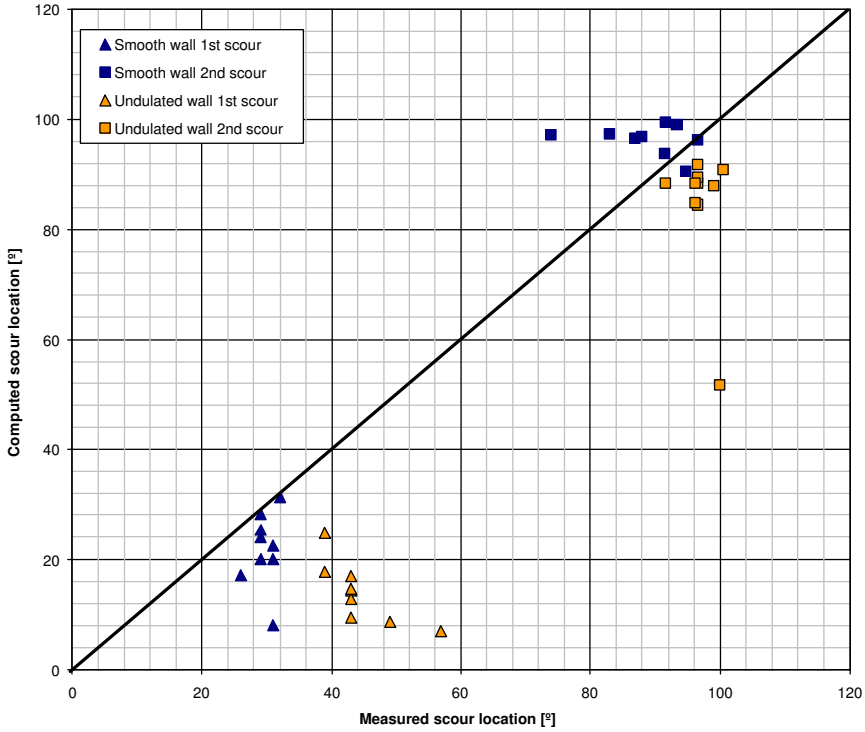

Figure 4.11: Comparison between scour location computed with *Hersberger* formula and measured data

It is interesting to observe that with the smooth wall the first scour hole is always located before the point bar. In the case of the undulated wall, in general, it is displaced downstream of the point bar (see Appendix D).

4.2.4 Position of the point bars

Analyzing the maximum bed elevation at the point bars for the smooth wall it can be observed that the deposits starts at 20° and it reaches the maximum at about 40°. The second point bar starts somewhere between 60° and 80° depending on the tests and it reaches the maximum at about 90°. Adding the undulated wall at the outer side of the channel, the maximum point bars are shifted by about 10° downstream.

Point bar	**Smooth wall**	**Undulated wall**
1^{st}	41°	50°
2^{nd}	89°	$\simeq 1m$

Table 4.3: Mean location of the point bars

4.2.5 Evolution of the scour holes

The evolution of the scour with the undulated wall was observed during the test, along the outer side wall.

The erosion for the tests with $S_0 = 0.5\%$ starts at the end of the bend (2^{nd} hole). The formation of the scour hole is quite fast (from 1h to 1.5h).

The formation of the first scour hole begins when the second one is almost at the maximum depth, at about 1 hour after the beginning of the test. The formation of the first scour hole is slower than the second one.

During the erosion of the first scour hole the second one is filled up a height of 1.5 d_{max}. A possible explanation could be that the transport capacity at the first hole is more important than in the second hole (see Section 4.4). The sediments eroded at the first hole are transported along the bend and deposited in the second hole.

The scour evolution in the tests with a bed slope of 0.7% is similar as in the tests with a slope of 0.5%. The only difference observed is that the second hole is filled up a height of d_{max}. For tests with $S_0 = 0.35\%$ the two scour holes have developed at the same time and no filling up of the second hole was observed.

It was interesting to observe that during the development of the scour holes some sediments were blocked between the undulations of the wall. This results in a displacement of the maximum scour depth from the outer wall by 10 to 15 cm towards the channel axis. This phenomenon was also observed with the smooth wall.

4.3 Analysis of sediment transport

4.3.1 Solid discharge

The sediment transport was calculated as the ratio between the weight of all sediments collected in the filtering baskets and the total test duration. Some assumptions have to be accepted to be able to compare all the tests:

1. The bed slope is constant during the test.
2. The sediment feeding is constant during the test and equal to the sediment transport capacity.
3. The volume of sediments eroded at the beginning of the test to form the final bed morphology in the bend is included at the calculus of the sediment transport.

Analyzing Fig. 4.13 it can be observed that the relation between solid discharge and liquid discharge is linear with a good correlation factor. The initial bed slope has an important influence on the sediment transport: an increase of the bed slope causes an increase of the linear regression slope. The wall undulations have also an influence on the solid discharge. For the initial bed slopes of 0.7 and 0.5%, the regression line slope is more inclined for the smooth wall than for the undulated wall. For the slope of 0.35% is the opposite.

It can be notice, that depending on the initial bed slope and the water discharge, the solid discharge is sometimes higher with the undulated wall and sometimes with the smooth wall. A possible explanation to this phenomenon is that the solid transport is a result of combination of two effects:

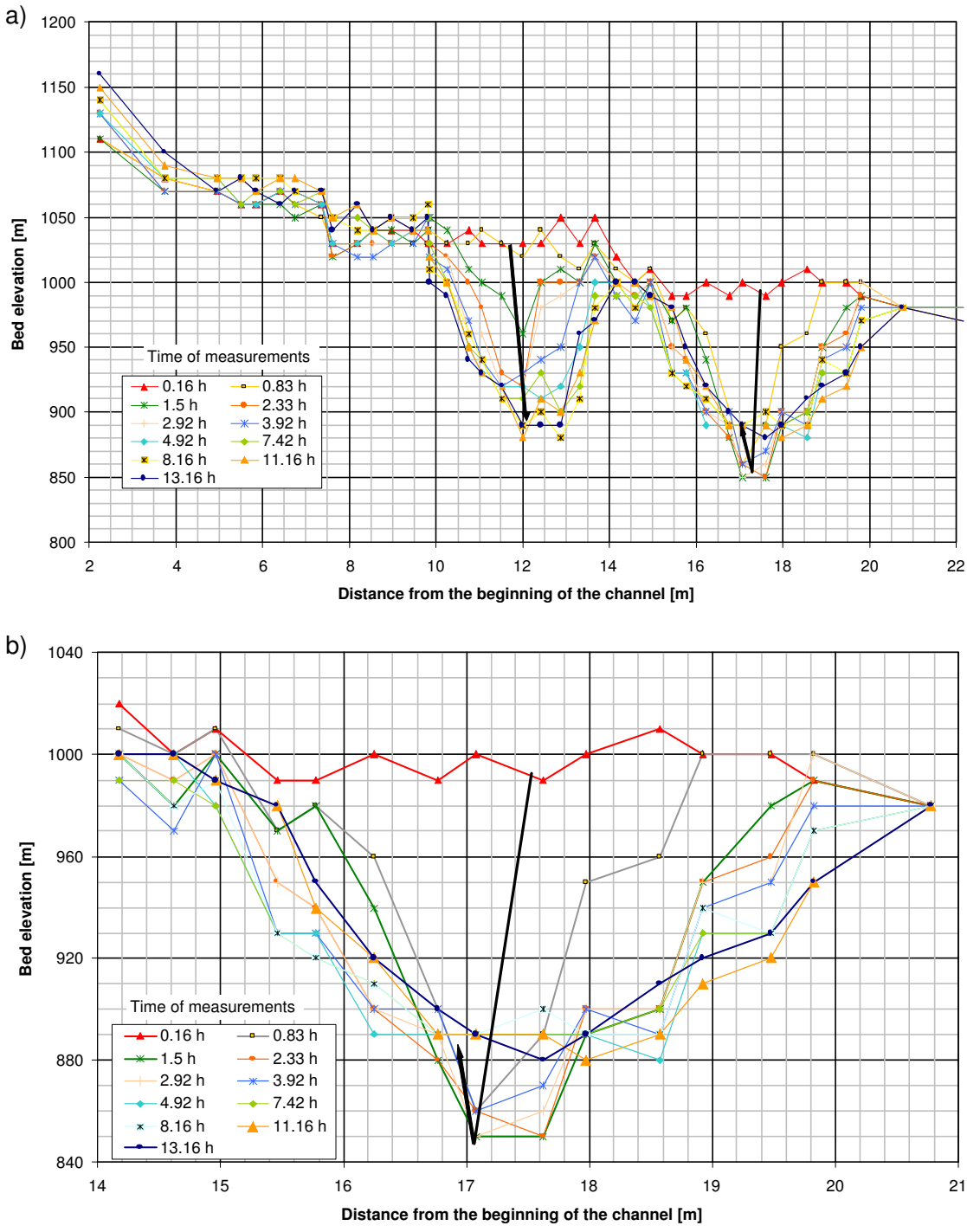

Figure 4.12: Evolution of the erosion of the channel bed along the outer wall for the tests with $S_0 = 0.5\%$. Along the whole channel (a), detail near second scour hole (b)

1. The undulations causes an increase of the water depth, and therefore of the shear stress at the channel bed and consequently an increase of the sediment discharge.

2. The undulations produce additional roughness and turbulence (return flows) that probably decrease the solid transport.

Depending on which effect is more important the solid transport is higher with the undulated or the smooth wall.

Despite the poor correlation coefficients, Fig. 4.14 shows that an increase of the densimetric Froude number causes an increase of the dimensionless solid discharge. When the densimetric Froude number Fr_d is higher than 2.6, the dimensionless solid discharge $\left(\frac{q_s}{q_w \cdot \rho_s}\right)$is higher with the smooth wall than with the undulations.

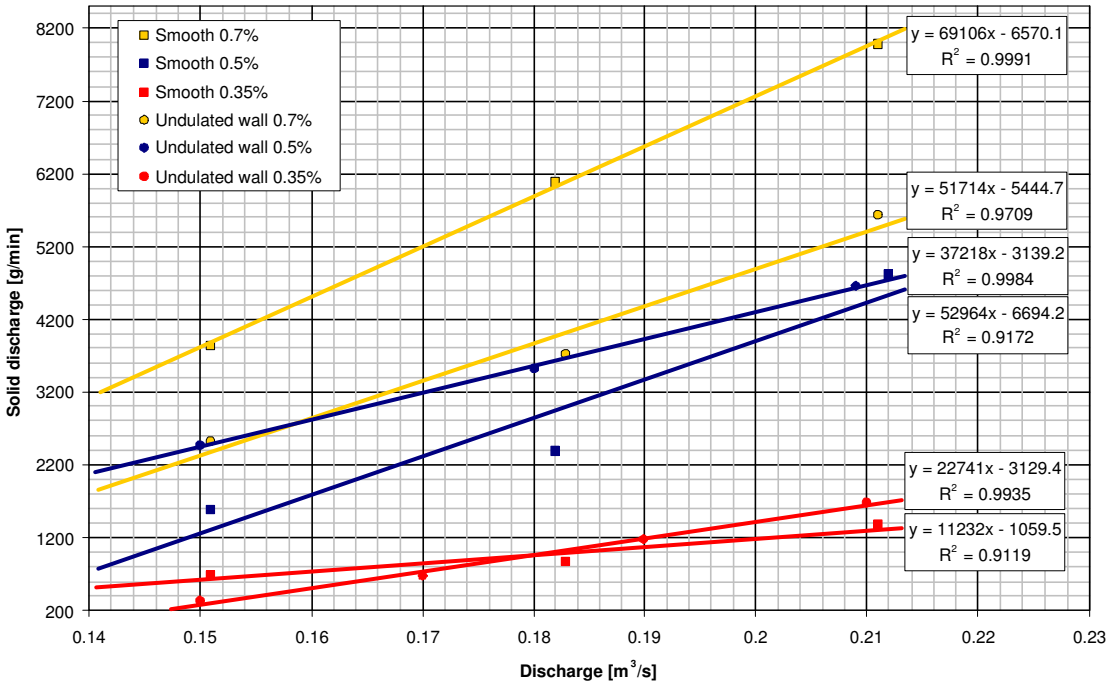

Figure 4.13: Sediment discharge as a function of water discharge

The solid discharge has been determined by the *Smart & Jäggi* [20] formula (see section 3.2.4). The correlation between the calculated and measured solid discharge is very good for the low but not for the high discharges (see Fig. 4.15).

The correlation factor is $R^2 = 0.98$ for the smooth wall and $R^2 = 0.86$ for the undulated one (see Fig. 4.15). The calculated solid transport is always higher for the undulated wall because only the reduction of the section is considered but not the roughness and turbulence effects due to the undulations.

4.3.2 Evolution of sediment transport

The present section describes the solid transport measured at the outlet of the channel during the test. At the beginning of the test there is a high solid discharge due to scour formation in the bend. Then the solid transport has the tendency to stabilize. Despite the

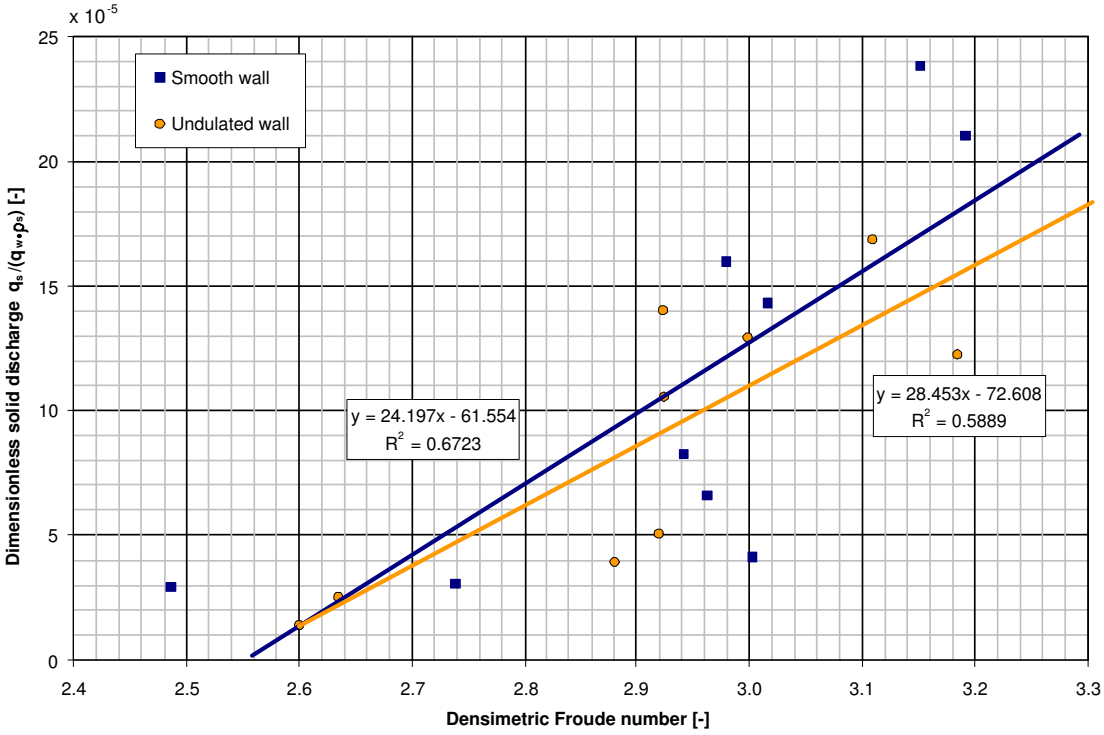

Figure 4.14: Dimensionless sediment discharge as a function of the densimetric Froude number

low correlation, an exponential function [4] represents best the sediment transport evolution In Fig. 4.16 it's possible to see that the instantaneous solid discharges don't fit well with such an exponential function. This can be explained by the fact that the solid transport is not continous but, occurs by waves of sediments.

A more accurate study of the sediment transport evolution could be done if more samples would have be taken during the test. Due to time constraints this was not possible.

4.3.3 Granulometry of solid discharge

At the end of some tests, one big sample of the sediment transport was taken at the outlet of the channel to analyze the grain size distribution. Not many differences can be observed between the different tests. For d_{50} there is less than $1.5mm$ of difference between the coarsest granulometry and the finest one. For d_{90} the difference is $1.6mm$ (see Fig. 4.17).

[4] Hersberger [1] used also an exponential function but his correlation factors were better, probably because he had much more samples

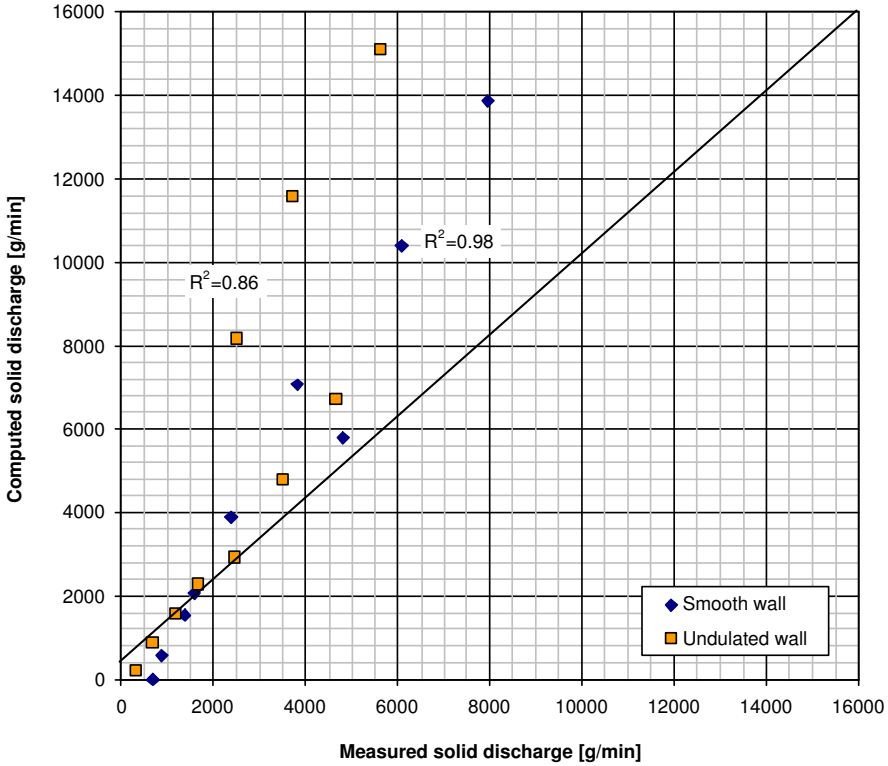

Figure 4.15: Comparison of sediment discharge between values computed according *Smart&Jäggi* [20] formula and measured data

Discharge	**Q=150 l/s**	**Q=180 l/s**			**Q=210 l/s**
Slope	0.5%	0.35%	0.5%	0.7%	0.5%
d_{50}	8.6	8.9	7.8	9.1	8.3
d_{90}	14.8	15.2	14.6	16.2	15.2

Table 4.4: Characteristic grain size diameter of solid discharge at the flume outlet for different test discharges (units in mm)

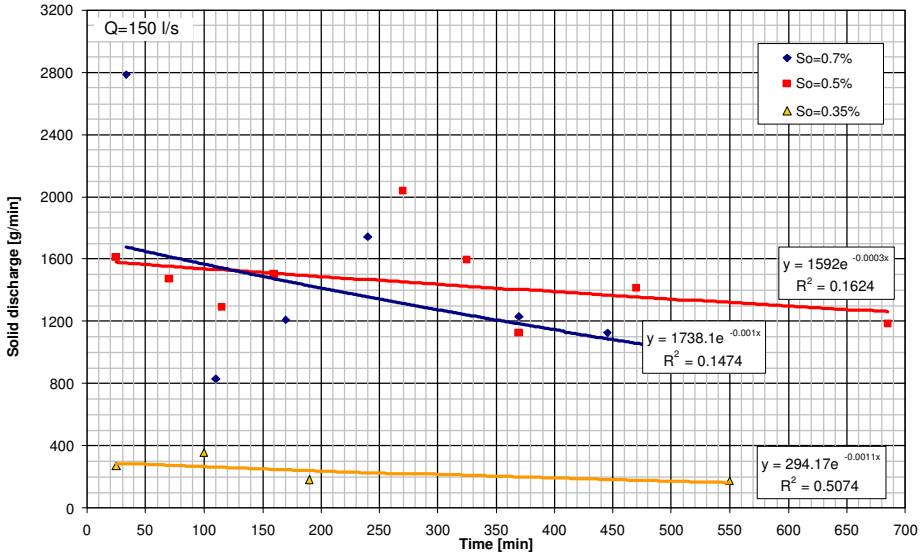

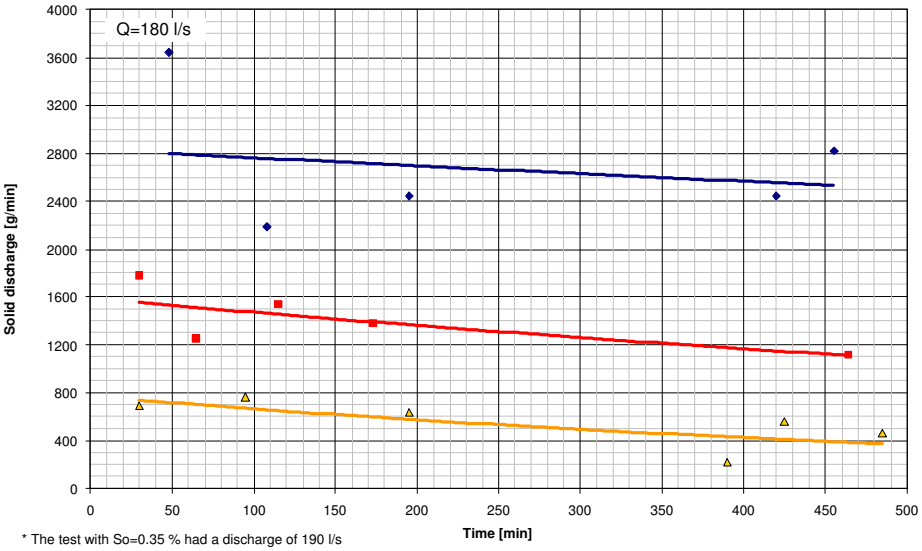

* The test with So=0.35 % had a discharge of 190 l/s

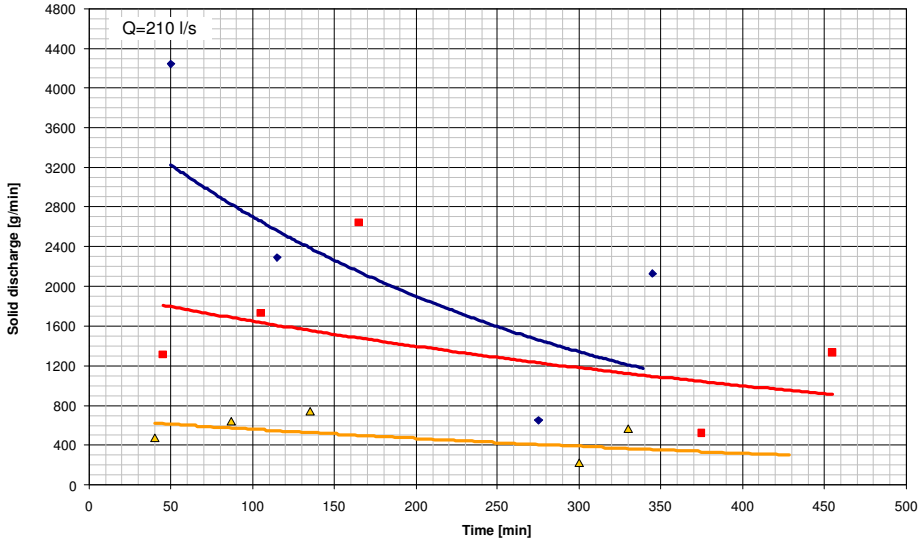

Figure 4.16: Evolution of the solid transport during the test

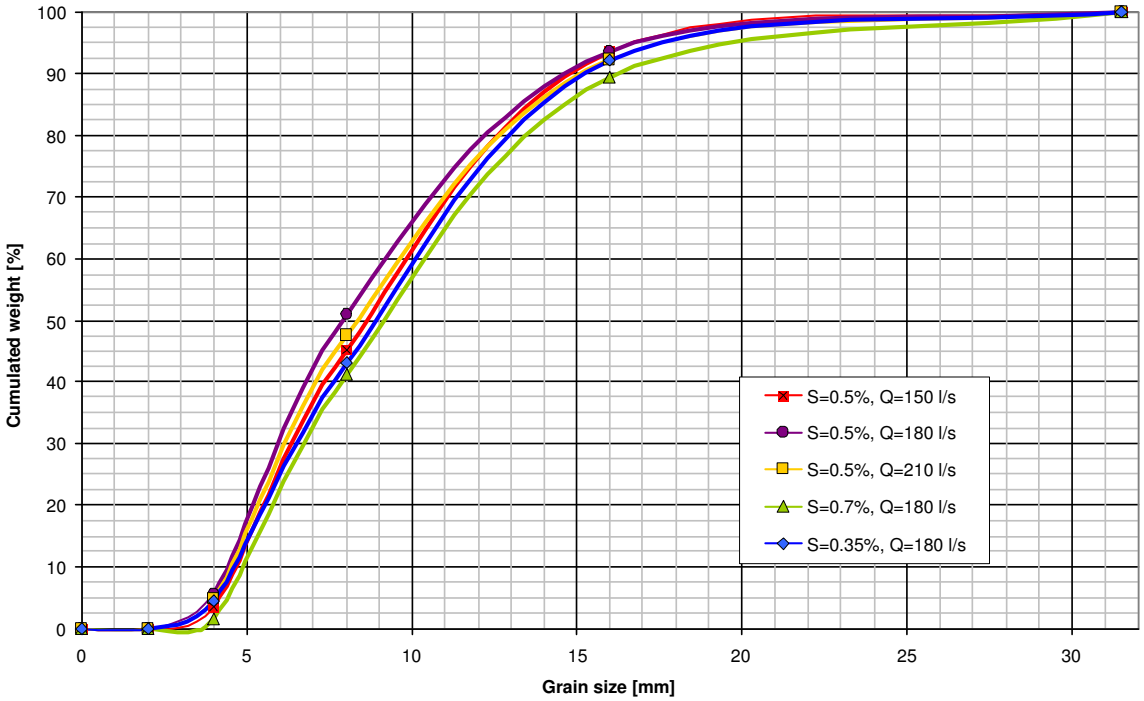

Figure 4.17: Grain size distribution of the solid discharge

4.4 Analysis of the granulometry of the armoring layer

For some of the tests 4 samples were taken of the armouring layer across the section(see Section 3.3.2). The analysis of the grain size distribution of this samples shows that as expected the grains are much bigger at the outer than at the inner bank (see appendix H and I). The difference of the d_m between the outer and the inner bank is 14 mm (1.6 d_m) at 45° and 11.3 mm (1.3 d_m) at 90°.

At the outer bank the grain size is always coarser at 45° (see Fig. 4.18).

As we have seen in Section 4.2.2 the first scour hole is deeper than the second. According Section 4.2.5 the grains eroded in the first hole are transported and deposited in the second hole. Furthermore as mentioned the grains are coarser in the first than in the second hole. This means that at 45° the sediment transport and the scour capacity is more important than at the second hole.

At the inner bank the smallest grains are observed at 45° where the transport capacity is lower due to the shallow water depth.

If the tests are compared, the finest grains at the outer wall can be found for the test with $S_0 = 0.35\%$ Q=150 l/s at 90° and the coarsest grains are for $S_0 = 0.35\%$ and $S_0 = 0.50\%$ with Q=210 l/s at 45°. Curiously the coarsest grains are not found at the tests with the highest slope as could logically be expected.

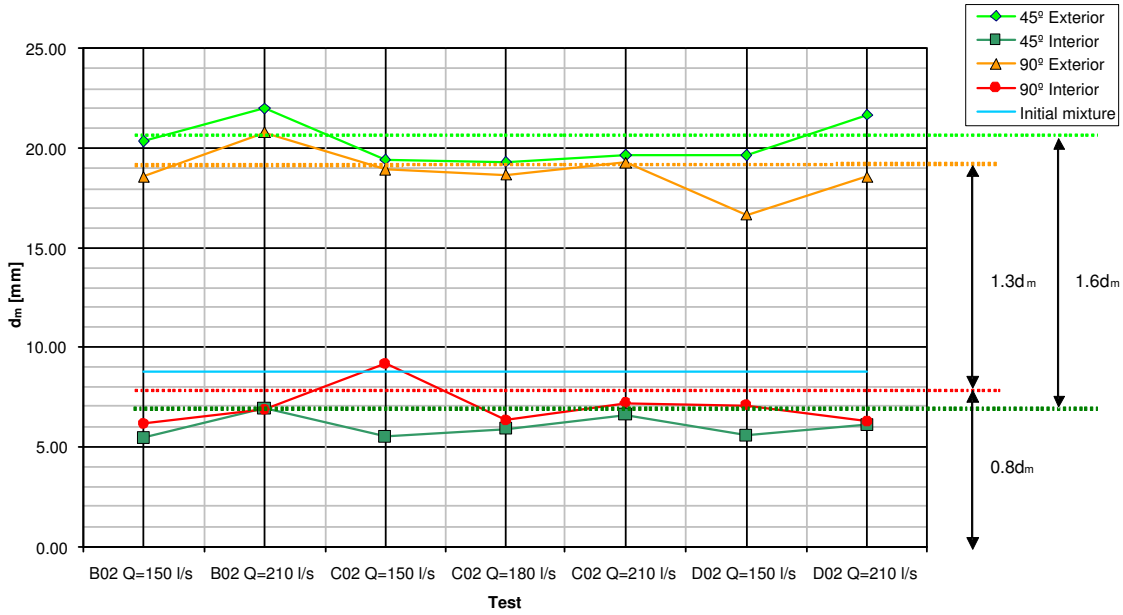

Figure 4.18: Mean diameter of the armouring layer for different tests with the undulated wall

4.5 Analysis of water surface

Hersberger [1] observed in his experiments without wall undulations that stationary surface waves are formed at the outer wall. They have an amplitude of $10\,cm$ and a length of $60\,cm$ to $1\,m$. With the undulated wall, a kind of shock waves are formed at the outer side of the channel by the undulations. They are directed towards the center of the channel and they are mainly over the outer half of the channel (see Fig. 4.19). The effect of the wall undulations on the water surface is very similar to the ribs used by *Hersberger* [1].

The water surface is much less wary along the channel with the undulated wall than with the smooth wall (see Appendix D and G). With the undulations there are no high stationary waves. But shock waves with much lower amplitudes.

The raise in the water surface observed due to the acceleration forces at the outer side wall is between 2 to 4 cm, which is similar to the observations without wall undulations.

Figure 4.19: Water surface waves with the smooth wall (left) (picture taken from *Hersberger* [1]) and the undulated wall (right)[1]

4.6 Analysis of the energy profile

4.6.1 Kinetic energy head

The calculation of the kinetic energy over a section along the channel are based on the following assumptions:

- Radial and vertical components are much smaller than the longitudinal so that they can be neglected.
- The channel width is 0.9 m for the test with the undulated wall and 1 m for the smooth wall.
- The mean velocity for the section "i" is:

$$V(i) = \frac{Q}{h_m(i) \cdot B} \tag{4.11}$$

- The kinetic energy head for the section "i" is

$$E_k(i) = \frac{V^2(i)}{2 \cdot g} \tag{4.12}$$

Analyzing the Appendix J.1 it can be observed that for the tests with smooth walls, at the inlet reach E_k has, in general, a growing tendency. This means that the water

[1]The pictures are taken in downstream direction.

is accelerated before the bend. From 0° to 1m after the bend the E_k has a decreasing tendency due to the head losses of the bend. One meter downstream of the bend, E_k starts to increase. On the other hand in almost all the test with smooth walls, there are two rapid changes in the kinetic energy profile. The first is at about 45° (it's not the case in all tests) and the second at about 0.5 m downstream the bend (for all the tests and much more important than the first one). These sudden decreases of the velocity are due to the scour holes, the increase of the h_m (increase of the cross section area) causes the reduction of the longitudinal velocity. In reality, the velocity is not reduced at the scour holes. But there are turbulence and return flows caused by the holes that are not considered in the mean velocity calculated with the Eq. 4.11.

The kinetic energy at the tests with an undulated wall has an increasing tendency at the inlet reach for the tests for the highest discharges (*D02*, Q=170l/s, has also this increasing tendency).

For the tests with the undulated wall there is only significant change of E_k located at about 60°.

4.6.2 Energy level

Appendix J.2 gives the longitudinal energy profiles from 2 m upstream the beginning of the bend and 2 m downstream of the end of the bend.

The energy of each section of the channel is calculated as:

$$E(i) = H_w(i) + E_k(i) = H_w(i) + \frac{V^2(i)}{2 \cdot g} \tag{4.13}$$

For the smooth wall, it can be observed that for the tests with the same S_0 in the inlet reach and in the bend, the energy lines are approximately parallel. This, means that the energy slope is more or less the same with equal S_0 and the different discharges.

At the outlet reach the energy lines are not parallel, especially for the tests *B01* and *C01*. Here the head losses are more important for high discharges than for small ones. A possible explanation could be the influences of the backwater curve. Nevertheless this hypothesis is not probable since at the tests *D01*, where the backwater curve has the most important influence, the energy lines are quite parallel. Moreover at the tests *C01*, where the backwater curve has almost no influence, the energy lines are not parallels.

There is not a significant change of the slope between the inlet reach and the bend. On the other hand there is a change of the energy slope (S_e) between the bend and the inlet reach in almost all the tests.

For the tests with an undulated wall, the energy slope (at the inlet, bend and outlet reach) is also approximately the same for the tests with the same S_0 different discharges. In general, the head losses at the inlet reach are less important than at the bend but the energy slope is higher at the outlet reach than at the bend. These head losses may be caused by the turbulence at the second scour hole.

The undulations at the outer wall also causes more head loses than in the case of the smooth wall.

4.7 Analysis of measured longitudinal velocities

As described in Section 3.3.2, longitudinal velocity measurements were made in six sections of the channel. The mean velocity was calculated at every section. The Fig. 4.20 shows the evolution of the mean velocity at the six different sections along the channel. There is a significant decrease of the longitudinal velocity at the scour holes (at about 46° and 1 m after the bend). Two reasons can be identified. On one hand there is a head loss due to the impact of the flow towards the wall. On the other hand, as a result of the impact, the velocity changes its direction. The longitudinal component is reduced to increase the vertical and the radial components.

In all the tests the highest velocities at the inlet reach are at the inner bank due to the high friction effect of the outer wall. In the bend and 1 m after the bend the velocities are higher at the outer wall. At 2.4 m after the bend the flow with the highest velocities is in the center of the channel (see Figures in Appendix K).

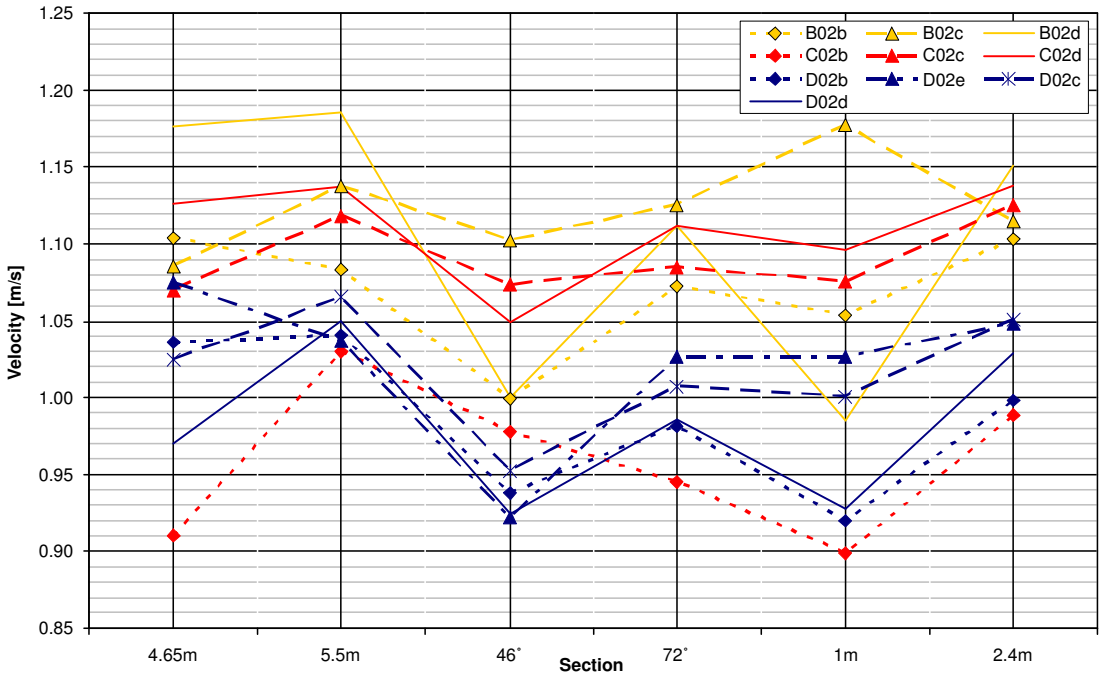

Figure 4.20: Evolution of the longitudinal mean velocities measured along the channel

It is interesting to compare the measured with the calculated velocities at the inlet reach. The following assumptions are made:

- The average water depth at the inlet reach was calculated between -2.85 m to -2 m (upstream of the bend) (h_m).
- The average velocity is:

$$V_c = \frac{Q}{h_m \cdot B}$$

where B=0.9 m

- The mean velocity measured at the inlet reach is the average of the measured velocities in the two sections in the entry reach.

The measured velocities are from +10% to -10% different of the calculated ones (see Fig. 4.21). Two possible reasons of these differences can be given.

- At one hand the calculated velocities are based on a channel width of 0.9 m. The effective width of the channel could be from 0.9 to 1 m. A change on the width affects considerably the calculated velocity.

- On the other hand due to the limitations of the flow sensor, the measurements close to the channel bed, water surface and channel walls were not possible. There was about 3 cm between the wet perimeter and the first point of measurement (see Fig. 3.8). In this region the velocities are much lower than in the center. Therefore the average of the measured velocities is higher than the real mean velocity.

Therefore the real mean velocity in the inlet reach is somewhere between the measured and the calculated one.

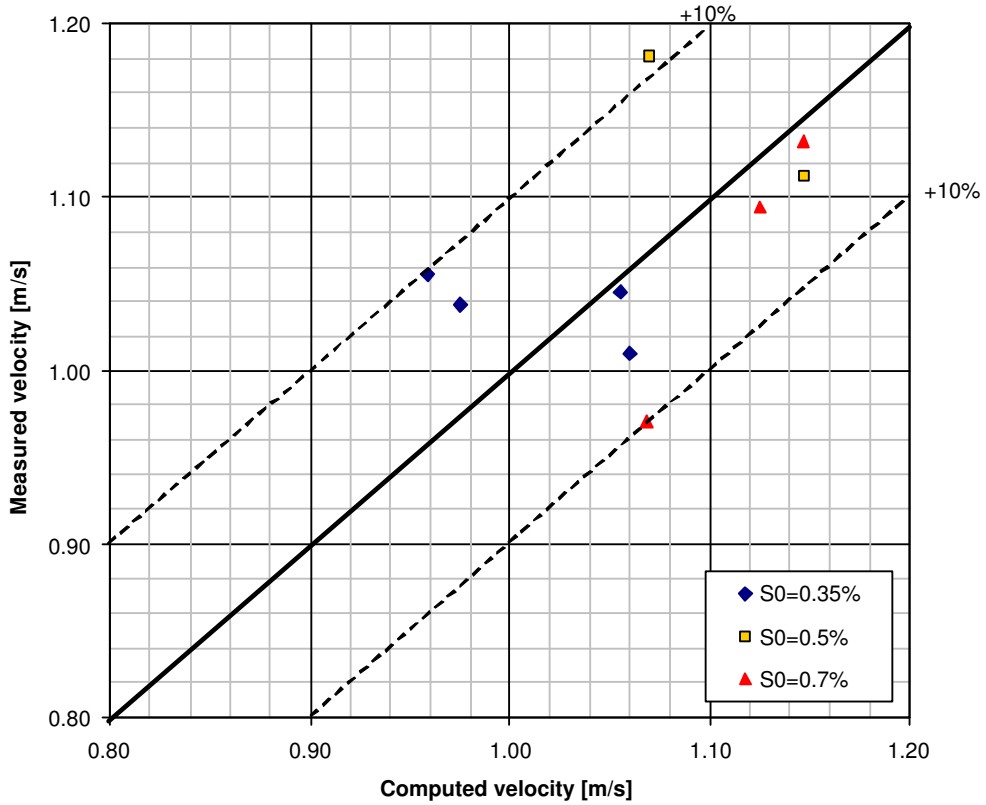

Figure 4.21: Comparison between the measured and the computed mean velocities at the inlet reach

		B02b	B02c	B02d	C02b	C02c	C02d	D02b	D02e	D02c	D02d
Entry	**-2.85m**	1.10	1.09	1.18	0.91	1.07	1.13	1.04	1.08	1.02	0.97
	-2m	1.08	1.14	1.19	1.03	1.12	1.14	1.04	1.04	1.07	1.05
Bend	**46°**	1.00	1.10	1.00	0.98	1.07	1.05	0.94	0.92	0.95	0.92
	72°	1.07	1.13	1.11	0.94	1.09	1.11	0.98	1.03	1.01	0.99
Exit	**1m**	1.05	1.18	0.98	0.90	1.08	1.10	0.92	1.03	1.00	0.93
	2.4m	1.10	1.11	1.15	0.99	1.13	1.14	1.00	1.05	1.05	1.03

Table 4.5: Mean velocities measured[m/s]

4.8 Equivalent roughness of the undulated wall

A roughness coefficient of *Strickler* for the undulated wall was determined based on the following assumptions and procedure:

- The roughness coefficient is only valid for the wall geometry used in the tests of the present study.
- The considered channel width was B=1 m
- The roughness was determined at the inlet reach between two sections -4 m and -1 m upstream of the beginning of the bend.
- The wet perimeter of the cross section was divided in 3 sub-perimeters according to the different roughness. The channel bed had a roughness of K_1, the interior wall K_2 and the undulated wall K_3.
- The zone where the roughness was calculated was covered by an armoring layer so that the *Strickler*'s coefficient of the channel bed was calculated with the formula proposed by Eq. 3.2.
- $K_1 = 53\frac{m^{1/3}}{s}$ and K_2 is considered $100\frac{m^{1/3}}{s}$
- The composite roughness is calculated according to Eq. 3.3
- Q is the water discharge measured at the tests and Q_c is the discharge calculated with Eq. 3.4

- The combination of Eq. 3.3 and Eq. 3.4 is

$$K_3 = \sqrt{\frac{h}{\left(\frac{S_0^{\frac{1}{2}} \cdot R_h^{\frac{2}{3}} \cdot b \cdot h\sqrt{2h+b}}{Q}\right)^2 - \frac{b}{K_1^2} - \frac{h}{K_2^2}}} \tag{4.14}$$

Figure 4.22 represents K_3 as a function of $h_m^{2/3} \cdot S_0^{1/2}$. Despite the low correlation coefficient it can be seen that an increase of h_m or S_0 causes an increase of the roughness.

$$K_3 = -2823.48 \cdot h_m^{\frac{2}{3}} \cdot S_0^{\frac{1}{2}} + 102.87 \tag{4.15}$$

ID	**Q** $[\frac{m^3}{s}]$	S_0 [%]	h_m [m]	R_h [m]	K $[\frac{m^{\frac{1}{3}}}{s}]$	K_1 $[\frac{m^{\frac{1}{3}}}{s}]$	K_2 $[\frac{m^{\frac{1}{3}}}{s}]$	$\mathbf{K}_3$ $[\frac{m^{\frac{1}{3}}}{s}]$
B02c	**0.18**	0.5	0.178	0.131	55.2	53	100	**51**
B02d	**0.209**	0.5	0.222	0.154	46.3	53	100	**28**
C02b	**0.15**	0.7	0.16	0.121	46.1	53	100	**25**
C02c	**0.18**	0.7	0.19	0.138	42.6	53	100	**22**
C02d	**0.21**	0.7	0.213	0.149	42.0	53	100	**22**
D02b	**0.15**	0.35	0.178	0.131	55.0	53	100	**50**
D02e	**0.17**	0.35	0.198	0.142	53.2	53	100	**42**
D02c	**0.19**	0.35	0.213	0.149	53.4	53	100	**42**
D02d	**0.21**	0.35	0.226	0.156	54.2	53	100	**45**

Table 4.6: Summary of the calculated and measured parameters to find the equivalent *Strickler*'s roughness coefficient of the undulated wall (K_3)

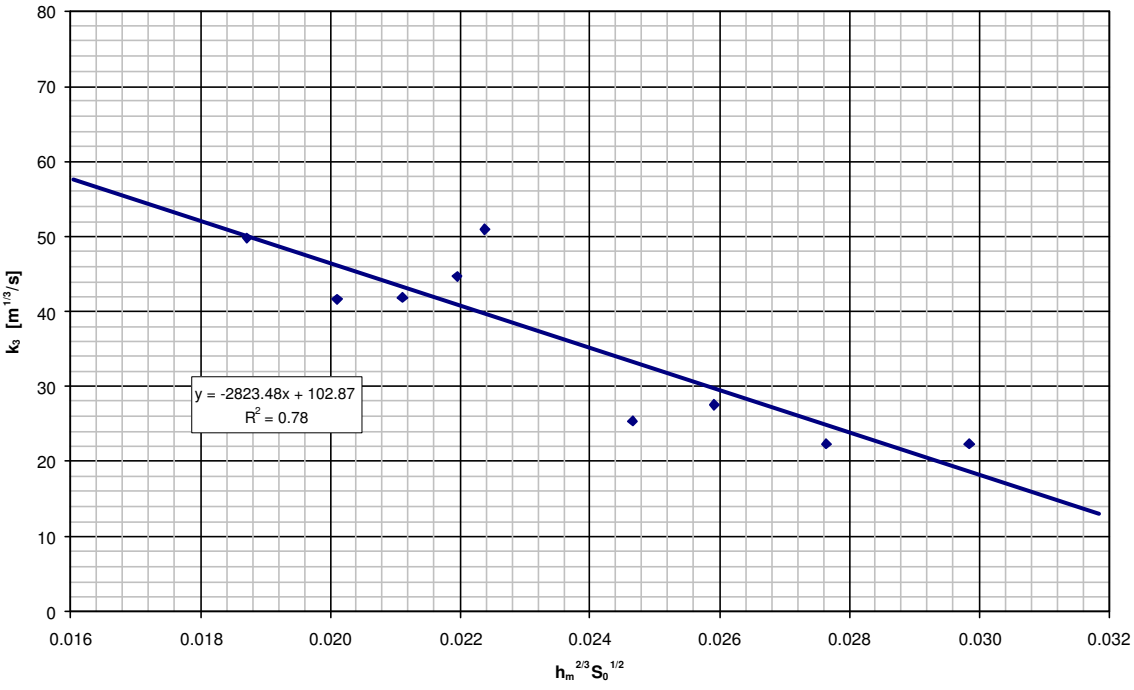

Figure 4.22: *Strickler* roughness coefficient of the undulated wall as a function of $h_m^{\frac{2}{3}} \cdot S_0^{\frac{1}{2}}$

Chapter 5

Stability analysis of the protection wall

A properly designed retaining wall or abutment must satisfy different independent requirements. On the one hand, to make the structure safe against failure, the structural security verification must be done. On the other hand the aptitude of service have to be verified.

The codes SIA define four types of limit state to verify the structural security.

- Type 1: Failure by overturning (sliding along its base or floating by the pressure of the water).
- Type 2: Resistance of the structure or one of his elements (the failure of the structure or excessive deformations)
- Type 3: Resistance of the foundations (the foundation failure, sliding along failure plans in the soil)
- Type 4: Resistance by fatigue of the structure.

The major problem in the design of earth retaining structures is the determination of the magnitude and distribution of the forces produced by the soil. These forces are either induced by the sole action of the gravity effects (the body forces) or are the result of the combined action of the body forces and other effects such as temperature or volume changes or dynamic loading, e.g. earthquakes. The knowledge of these forces will enable to design the structure and to check their overall stability and hence their safety against all possible modes of failure.
In this chapter some practical ideas and values are given to design the undulated wall. The analysis is not exhaustive and all the results, have to be taken carefully since every site and every wall is different.

5.1 Undulated wall description

The undulated wall is formed by three parts:

- The base is a slab of width L_D and thickness L_G.

- The undulated vertical wall (stem) has a thickness of L_G and a height of $L_H - 2L_G$
- The top slab has a thickness of L_G and a width of L_D

The wall could have water on both sides: h_{w2} is the water height at the river side and h_{w1} is the water height at the soil side.

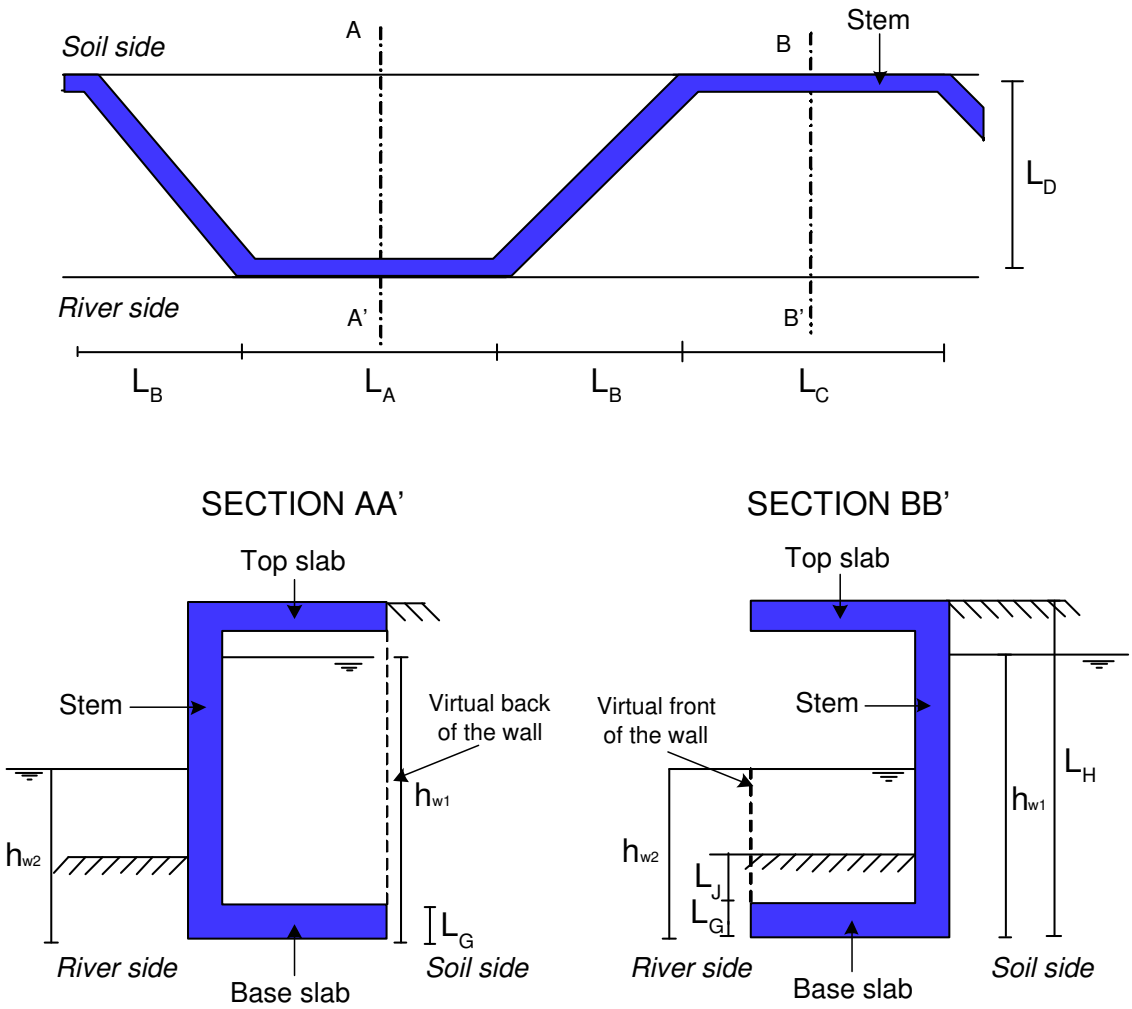

Figure 5.1: Schema of the undulated wall

5.2 Acting forces

5.2.1 Earth pressure (E_{ah}, E_{ph})

The size, the direction and the distribution of the earth pressure depends on the movement of the retaining wall. It causes a deformation of the soil behind the wall and a mobilization of the shear strength of the ground.
In the case of a horizontal ground surface or a wall that is not allowed to move, the horizontal and vertical stress is the earth pressure at rest:

$$\sigma_{0z} = \gamma_s z \tag{5.1}$$

$$\sigma_{0x} = K_0 \cdot \sigma_{0z} = K_0 \cdot \gamma_s z \tag{5.2}$$

where K_0 is known as the *coefficient of earth pressure at rest.*

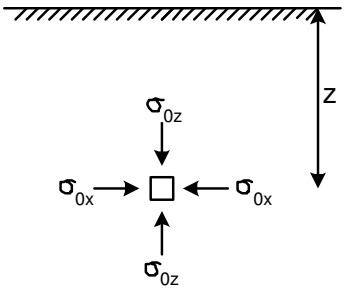

Figure 5.2: Vertical and horizontal stresses in the soil

If we consider that the undulated wall is free to move away of the mass of soil, the soil is hence to expand laterally. The lateral expansion of the soil against the wall does not affect the vertical stress but it decreases the lateral stress σ_{0x} to some new value σ_{ex}. If the dilatation continues it will result in a rupture of the ground by shearing. The prism of soil will slip towards the wall. In this state the earth pressure is minimum σ_{ax} and it is called *active stress* and it corresponds to one of the states of limiting equilibrium of Rankine (K_a).
On the other hand if the action of an external horizontal force pushes the wall into the soil, then the soil is compressed laterally and the initial earth stress at rest σ_{0x} increases to some new value σ_{cx}. If the compression proceeds further a state of stress will eventually be reached. The further lateral compression takes place at a constant lateral stress σ_{px}, which is maximum [23]. The soil is again in the state of limiting equilibrium (K_p).
According to the theory of Rankine, there is a simple way to calculate the earth pressure. This theory is based on five hypothesis:

1. The soil is in the state of limiting equilibrium rupture of Mohr-Coulomb.
2. There is a flat state of deformation.
3. There is not any friction between the back side of the wall and the soil.
4. The back side of the wall is vertical.
5. The surface of the soil behind the wall is horizontal.

According [23] the active and passive earth pressure are:

- Active earth pressure

$$\sigma_{ah} = \gamma_s z \cdot K_a - 2c \cdot \sqrt{K_a} \tag{5.3}$$

  where $K_a = \tan^2(45° - \varphi/2)$ is the coefficient of lateral active stress,

- Passive earth pressure

$$\sigma_{ph} = \gamma_s z \cdot K_p + 2c \cdot \sqrt{K_p} \tag{5.4}$$

where $K_p = \tan^2(45° + \varphi/2)$ is the coefficient of lateral passive stress.

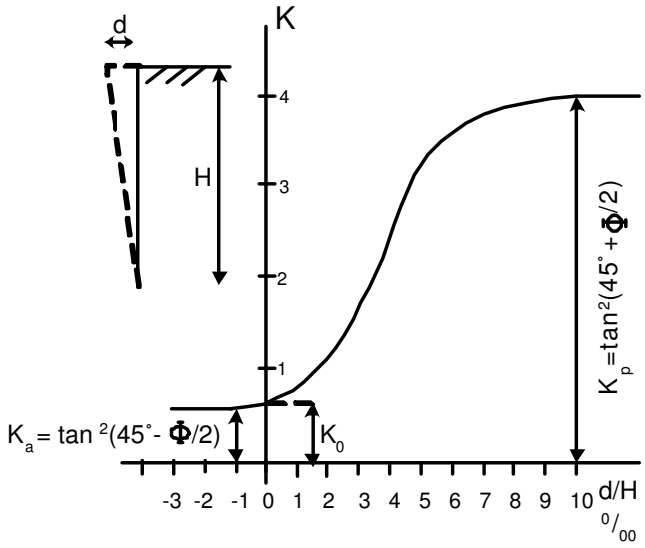

Figure 5.3: Influence of the relative movement of the wall to the coefficient of earth pressure

According to Eq. 5.3 and 5.4, the earth pressure increases proportionally to the depth below the surface.
The above formulas do not include the effects of the pore-water pressure. The Archimedes pressure acting to the grains of soil reduce the effective stress σ'. To find the effective stress γ, specific weight must be replaced by apparent specific weight $\gamma' = (\gamma_{sat} - \gamma_w)$. The layer which is not immersed acts like a vertical load.

$$\sigma'_{ah} = [\gamma'_s z + \gamma_s (H - h_w)] \cdot K_a - 2c \cdot \sqrt{K_a} \tag{5.5}$$

$$\sigma'_{ph} = [\gamma'_s z + \gamma_s (H - h_w)] \cdot K_p + 2c \cdot \sqrt{K_p} \tag{5.6}$$

5.2.2 Hydrostatic water pressure (W_{ah}, W_{ph}, W_v)

The hydrostatic water pressure is added to the effective stress to obtain the total stress. It is also important to consider the vertical water pressure. This force acts between the soil and the base slab and has a destabilizing effect.
The water level on the two sides of the wall is different. The unbalanced water level on both sides produces a flow under the wall. This flow creates a water pressure which is smaller than hydrostatic pressure. However, to consider the hydrostatic force pushing outwards, would be to simplify the problem in a conservatory way. In addition the force pushing from the wall towards the soil is not dangerous for the wall's stability.

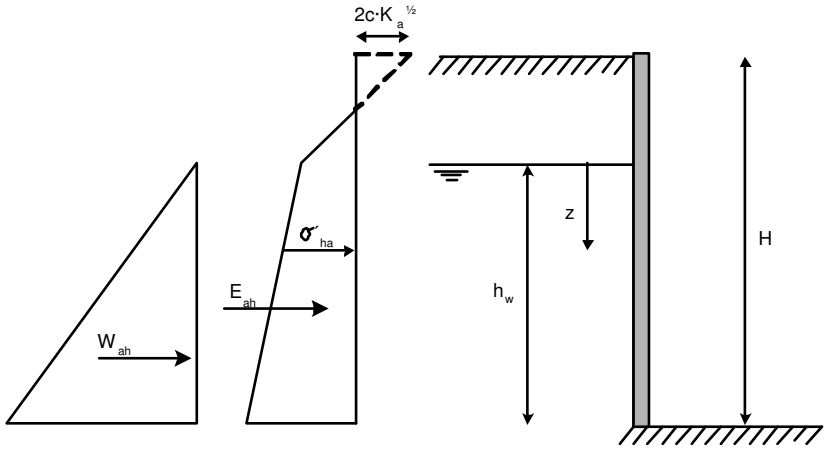

Figure 5.4: Schema of the active stress and forces in a vertical wall

5.2.3 Weight of the structure (G_s, G_c, G_w)

The weight of the structure (base slab, top slab and stem) is an important parameter to help stabilizing the structure. The weight of the water and the soil on the base slab between the stem and the virtual back or virtual front also adds to the structure's stabilization (see Fig 5.1).

5.2.4 Shear force between the soil and the inner side of the wall (E_{av}, E_{pv})

When the wall moves outward, there is also a relative vertical movement between the soil and the interior side of the wall. The shear resistance E_v along the wall is given by the formula of Mohr-Coulomb.

$$E_v = c_a + \sigma \tan \delta \tag{5.7}$$

To calculate the vertical stress on the undulated wall two cases can be considered:

1. Smooth wall: $c_a = 0$; $\delta = 0$
2. Rough wall: $c_a = 0$; $\delta = \frac{2}{3}\varphi$

5.2.5 Shear force between the soil and the base slab (E_{ah}, E_{ph})

The shear force between the soil and the base slab of the structure is strongly influenced by the character of the soil. If the surface of contact between the concrete and the soil is rough, the maximum shearing strength of the soil could be considered. The maximum friction force is calculated according to the Mohr-Coulomb formula:

$$S_s = c_a + F_v \tan \delta \tag{5.8}$$

where F_v is the normal force that acts on the soil. For in situ concreted foundations, we consider the cohesion c_a equal to zero and the angle of shearing resistance δ equal to the angle of shearing resistance of the soil.

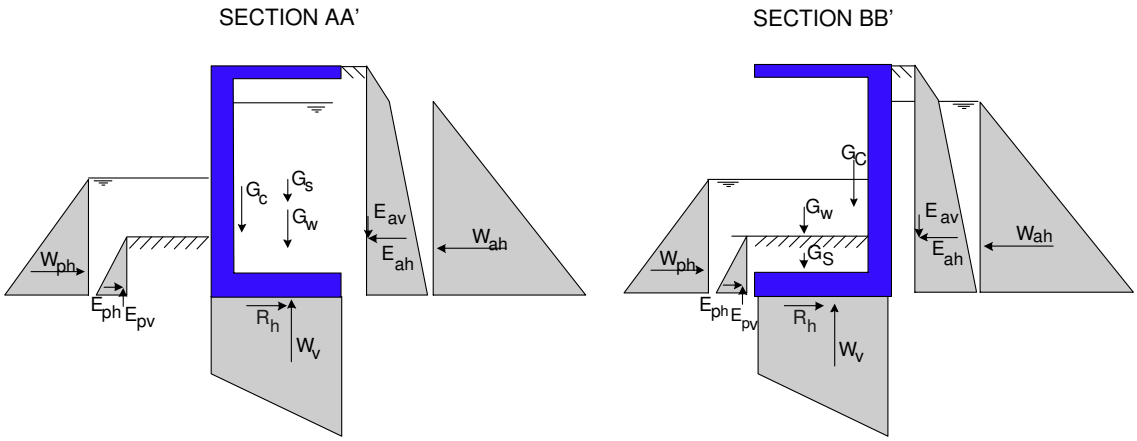

Figure 5.5: Schema of all the forces acting on the undulated wall

5.3 Safety factors

5.3.1 Safety against overturning

The overturning is defined as the ratio between the stabilizing moments and the destabilizing ones. The ratio should be not less than 1.5.

$$SF = \frac{M_{stab}}{M_{unstab}} \geq 1.5 \tag{5.9}$$

The stabilizing forces are:

- Weight of the wall, the soil and the water, G_c, G_s, G_w.
- Vertical active soil pressure, E_{av}.
- Horizontal passive soil pressure, E_{ph}.
- Water pressure at the river side.

and the destabilizing forces are:

- Horizontal active soil pressure, E_{ah}.
- Vertical water pressure, W_v.
- Vertical passive soil pressure, E_{pv}.
- Water pressure at the river side, W_{ph}.

5.3.2 Safety against sliding

Both, the horizontal component of the active earth pressure and the hydrostatic force, have the tendency to move the wall towards the river side. These forces have to be equilibrated by the horizontal component of the passive earth pressure and the shear

between the soil and the base slab. The ratio between the stabilizing and the destabilizing forces is:

$$SF = \frac{F_{stab}}{F_{unstab}} \geq 1.5 \tag{5.10}$$

Where the stabilizer forces are:

- Horizontal passive earth pressure, E_{ph}.
- Water pressure at the river side, W_{ph}.
- Shear between the soil and the base slab, R_h.

and the destabilizing forces are:

- Horizontal active earth pressure, E_{ah}.
- Water pressure at the soil side, W_{ah}.

The factor of safety must be more than 1.5.

5.3.3 Overstress of foundation

The factor safety against the bearing failure is defined as the ratio between the vertical force per unit length of wall at failure and the applied vertical force per unit length. Due to the difficulties to predict the bearing capacity of the soil, the required minimum factor of safety is 2.0.
To calculate the vertical force of a wall at failure, the following hypotheses must be adopted [24]:

- The contact between the soil and the base slab is rough.
- The length of the foundation is infinite.
- The soil is compact($\gamma_s \geq 20KN/m^3$), homogeneous and isotope.

The failure mechanism considers that:
The load failure is the addition of three terms:

- The cohesion resistance between the surface CDE.
- The total vertical resistance due to the lateral load P_0 at the foundation level.
- The resistance due to the weight of soil BCDE.

Correction factors (f_i) must be applied because the loading of the foundation is neither vertical nor central. The vertical load capacity of a strip foundation is [25]:

$$q_{ult} = c' N_c f_{ci} + P_0 N_q f_{qi} + 0.5b \cdot \gamma' N_\gamma f_{\gamma i} \tag{5.11}$$

where

$$N_q = e^{\pi \tan \varphi'} \tan^2(45 + \varphi'/2) \qquad N_c = (N_q - 1)\cot \varphi' \qquad N_\gamma = 2(N_q + 1)\tan \varphi'$$

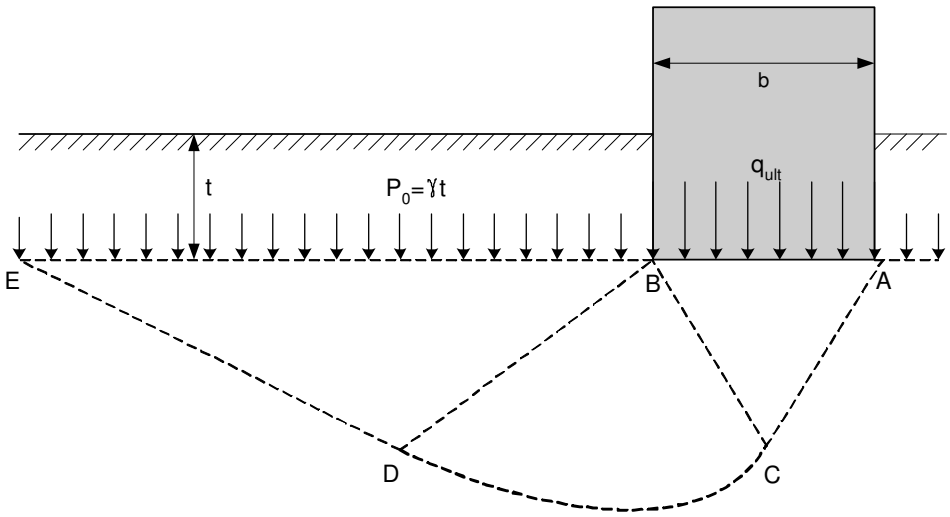

Figure 5.6: Bearing capacity of a shallow foundation

and

$$f_{qi} = \left[1 - \frac{F_h}{(F_v + b' \cdot c' \cdot \cot \varphi')}\right]^2 \qquad f_{ci} = f_{qi} - \frac{1 - f_{qi}}{N_c \cdot \tan \varphi'} \qquad f_{\gamma i} = f_{qi}^{3/2}$$

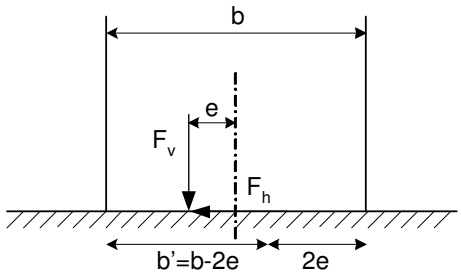

Figure 5.7: Bearing capacity for inclined eccentrically load. Effective width b'

5.4 Calculation procedure

The figures of in Appendix L give the required wall thickness of the undulated wall as a function of the wall's height, width, water depth (at the river side and at the soil side) and the angle of the soil friction.
The wall thickness obtained guarantees a SF higher than 1.5 for the overturning and sliding and a SF higher than 2 for the bearing failure.
The stability of the wall has been calculated adopting the following hypotheses:

- The undulated wall is not rigid. It can have a light outward movement due to the active earth pressure.

- The active and passive earth pressures have been calculated according to the Rankine's theory.
- There is no overload on the wall.
- There is no groundwater stream below the wall.
- The soil cohesion (c') is neglected.
- The cohesion and the friction angle between the back of the wall and the soil (c_a, δ) are neglected.
- The soil weight is $\gamma_s = 19kN/m^3$.

The wall can have different loadings depending on the water levels and the erosion in the foundations. Considering these facts, two load cases have been considered:

During a flood the water level is high and often the same on both sides of the wall. Due to the scouring, the sediments at the outward foundations could disappear. Hence there is no passive resistance. The hypotheses adopted for this case are:

- $h_{w1} = h_{w2} \neq 0$
- $E_p = 0$

After the flood the water level on the river side is low. If the drainage is not suffitient the water level at the inner side could be high. After the flood the scour holes are usually filled up. Therefore the sediment's level at the river side is the initial one. The hypotheses adopted are:

- $h_{w1} = 0$
- $h_{w2} \neq 0$
- $E_p \neq 0$

The wall dimensions and the water and soil levels are shown in the figures of the appendix L

Chapter 6

Conclusions

6.1 Conclusions

The main aim of this work was to study the influence of the undulated wall on the local scouring. The undulated wall geometry tested in the experiments revealed the following:

1. The tests demonstrated that the undulated wall affects the bed topography, the water surface, the flow velocities and the solid transport.

2. Compared to the smooth wall, with the same specific discharge and bed slope, the undulated wall reduces the scour depth by 5 to 35% (mean value 17%) at the first hole and by 0 to 65% (mean value 39%) at the second one . The most important reductions are for the more pronounced slopes.

3. The modified formula of Bridge proposed by Hersberger[1] for the scour depth computations with the smooth wall was modified to fit the data of the undulated wall. This scour formula shows a quite good correlation with the data of undulated wall:

$$sin\beta = 0.3\Big(11 - 21\frac{h_m}{B}\Big)\frac{R_c}{B}tan\phi \cdot \frac{h_s}{r} \qquad\qquad R^2 = 0.92$$

4. With the wall undulations the position of the scour holes and the point bars were shifted by about 10° in downstream direction.

5. Shock waves are created at the water surface by the undulated wall. Nevertheless no high stationary waves were observed during the tests as for a smooth wall. The increase of the water surface towards the outer bank is approximately similar to that with a smooth wall undulations.

6. Despite a poor correlation of the data it seems that for the same densimetric *Froude* number, the capacity of sediment transport is higher in the case of the smooth wall.

7. The transversal grain sorting process at the bend is quite significant. At the outer bank the mean diameter is at about $2.5d_m$ and at the inner bank is about $0.8d_m$.

8. An estimation of the roughness coefficient of *Strickler* is proposed for the used wall geometry.

$$K = -2823 \cdot h_m^{2/3} \cdot S_0^{1/2} + 103 \qquad R^2 = 0.78$$

6.2 Further research

Further research can comprise:

- Systematic tests with changed geometry of the undulated wall. The aim would be finding an optimal geometry of the wall undulations in order to reduce the scour depth.
- Velocity measurements with UVP probes. The knowledge of the field velocities in the channel would allow to better understand the effects of the undulated wall on the flow.

Notation

Variables and constants

β	$[^\circ]$	Lateral bed slope
Δx	$[m]$	Distance between two cross-sections
δ	$[^\circ]$	Friction angle between the concrete and the soil
γ_s	$[\frac{N}{m^3}]$	Weight
ν	$[\frac{m^2}{s}]$	Cinematic water viscosity
ϕ	$[^\circ]$	Dynamic friction angle
φ	$[^\circ]$	Static friction angle
σ_0	$[\frac{N}{m^2}]$	Stress of the earth pressure at rest
σ_a	$[\frac{N}{m^2}]$	Active stress
σ_p	$[\frac{N}{m^2}]$	Passive stress
σ	[-]	Width of the grain size distribution
τ	$[\frac{N}{m^2}]$	Shear stress
τ_{cr}	$[\frac{N}{m^2}]$	Critical shear stress
θ	[-]	Dimensionless shear stress
A	$[m^2]$	Cross-section area
B	$[m]$	Width of the channel
b	$[m]$	Width foundations
b'	$[m]$	Effective width foundations b'=b-2e
c	$[\frac{N}{m^2}]$	Soil cohesion
c_a	$[\frac{N}{m^2}]$	Cohesion between the concrete and the soil
d	$[m]$	Characteristic diameter of a grain sample
d_{30}	$[m]$	Diameter of grain, equal to 30% in the granulometric curve
d_{90}	$[m]$	Diameter of grain, equal to 90% in the granulometric curve
d_m	$[m]$	Grain size mean diameter
d_{max}	$[m]$	Grain size maximum diameter
e	$[m]$	Eccentricity of the vertical load at the founding level
E	$[m]$	Total energy
E_a	$[\frac{N}{m}]$	Active earth pressure
E_p	$[\frac{N}{m}]$	Passive earth pressure
E_k	$[m]$	Kinetic energy

F	$[N]$	Force
Fr	[-]	*Froude* number $Fr = \frac{V}{\sqrt{g \cdot h}}$
Fr_d	[-]	Densimetric *Froude* number $Fr_d = \frac{V*}{\sqrt{(s-1) \cdot g \cdot h}}$
g	$[\frac{m}{s^2}]$	Gravity acceleration
G_c	$[\frac{N}{m^3}]$	Wall weight
G_s	$[\frac{N}{m^3}]$	Soil weight inside the undulations of the wall
G_w	$[\frac{N}{m^3}]$	Water weight inside the undulations of the wall
h_1	$[m]$	Flow depth at the first hole
h_2	$[m]$	Flow depth at the second hole
h_m	$[m]$	Mean water depth above mean bed level
h_{max}	$[m]$	Maximum flow depth
h_s	$[m]$	Local water depth
H_w	$[m]$	Water level
$\overline{H_w}$	$[m]$	Reference water level
k	[-]	Constant
K_a	[-]	Lateral active stress coefficient
K_p	[-]	Lateral passive stress coefficient
K_s	$[\frac{m^{1/3}}{s}]$	Roughness coefficient of *Strickler*
L	$[m]$	Wall dimensions
P	$[m]$	Wetted perimeter
P_0	$[\frac{N}{m}]$	Total vertical stress in the soil adjacent to the foundation, at the founding level
q	$[\frac{m^2}{s}]$	Unit discharge
Q	$[\frac{m^3}{s}]$	Discharge
q_s	$[\frac{m^2}{s}]$	Solid specific discharge
q_{ult}	$[\frac{N}{m}]$	Ultimate bearing capacity
r	$[m]$	Radius of curvature
R_c	$[m]$	Radius of curvature at the axe
R_h	$[m]$	Hydraulic radius
Re	[-]	*Reynolds* number $Re = V \cdot 4R_h/\nu$
$Re*$	[-]	Shear *Reynolds* number $Re^* = V^* \cdot d/\nu$
S	[-]	Longitudinal slope
s	[-]	Sediment density coefficient
S_0	[-]	Initial longitudinal bed slope at the axe of the channel
S_e	[-]	Longitudinal energy slope
Sc_{LOC1}	[°]	First hole position
Sc_{LOC2}	[°]	Second hole position

SF	[-]	Security Factor
V	$[\frac{m}{s}]$	Longitudinal velocity
V^*	$[\frac{m}{s}]$	Shear velocity
V_m	$[\frac{m}{s}]$	Mean longitudinal velocity
W_a	$[\frac{N}{m}]$	Active water pressure
W_p	$[\frac{N}{m}]$	Passive water pressure

Subscripts and exponents

x	x direction
y	y direction
z	z direction
v	Vertical direction
h	Horizontal direction
$'$	Effective

Abbreviations

LCH	Laboratoire de Constructions Hydrauliques
EPFL	École polytechnique fédérale de Lausanne
ETSECCPB	Escola Tècnica Superior d'Enginyers de Camins, Canals i Ports de Barcelona
UW	Undulated wall
SW	Smooth wall

Acknowledgements

En primer lloc m'agradaria donar les gràcies a la meva família per la seva ajuda comprensió i paciència durant tots els estudis. Sense ells mai hagués estat el que sóc. Moltes gràcies.
I would like to thank Prof. A. Schleiss who provided me with all the facilities to carry out this work. Our progress meetings made me review and plan my work periodically so we were able to achieve our goals.
I am also grateful to Prof. A. Bateman for his interesting suggestions. Many thanks to M. Mayaud, D. Hersberger and K. Blanckaert for their helpful advices, suggestions and corrections.
I also wish to thank Louis Schneiter and Marc-Eric Pantillon for their efficiency in the technical support.
Special thanks to the enthusiastic group of LCH specially Pedro Manso, Marcelo Leite, Farid Boushaba, Fréderic Jordan and Philipe Heller who have answered me hundreds of questions during this year.
Many friends have contributed with suggestions, corrections and remarks. Thank you very much to all of them. Special mention to Annigna and Roger.

Bibliography

[1] Hersberger D. *Wall roughness effects on flow and scouring in curved channels with gravel bed.* PhD thesis No. 2632, École Polytechnique Fédérale de Lausanne, 2002 and Comunication No. 14 of Laboratory of Hydraulic Constructions (LCH), École Polytechnique Fédérale de Lausanne, 2002.

[2] Chèvre P. *Influence de la macro-rugosite d'un enrochement sur le charriage et l'érosion en courbe.* Comunication No. 19, Laboratoire de Constructions Hydrauliques (LCH), École Polytechnique Fédérale de Lausanne, 2004.

[3] Shukry A. Flow around bends in an open flume. *Transactions, ASCE*, 115,751-779, 1950.

[4] Garbrecht G. *Wasserabfluss in gekrümmten Gerinnen*, volume 44(2+3),29-35,66-71. Wasserwirtschaft, 1953.

[5] Rozovskii L.L. *Flow af water in bends of open channels.* PhD thesis, Academy of Sciences of the Ukrainian SSR, Kiew, 1957.

[6] de Vriend H.J. A mathematical model of steady flow in curved shallow channels. *Journal of Hydraulic Research, IAHR*, 15(1),37-54, 1976.

[7] Onishi, Subhash C.J., and Kennedy J.F. Effects of meandering in alluvial streams. *Journal of the Hydraulics Division, ASCE*, Vol. 102 (7), July 1976.

[8] Bathurst J.C., Thorne C.R., and Hey R.D. Secondary flow and shear stress at river bends. *Journal of the Hydraulics Division, ASCE*, Vol. 105 (10), Octobre 1979.

[9] Blanckaert K. *Flow and turbulence in sharp open-channel bends.* PhD thesis No. 2545, École Polytechnique Fédérale de Lausanne, 2003.

[10] Hager W.H. Fargue, founder of experimental river engineering. *Journal of Hydraulic Research, IAHR*, Vol. 41, No. 3, pp. 227233, 2003.

[11] Williams R. *Flussbefestigungen erläutert an einer Flusstrecke der weissen Elster sowie Beispiele zur Nachprüfung der Fargue'schen Gesetze mit Hilfe der Stossflächen.* Verlag Wilhelm Engelmann, Leipzig, 1899.

[12] van Bendegom L. Eenige beschouwingen over riviermorphologie en rivierbetering. *De Ingenieur*, 59(4),1-11, 1947.

[13] Engelund F. Flow and bed topography in channel bends. *Journal of the Hydraulics Division, ASCE*, Vol. 100 (11), November 1974.

[14] Bridge J.S. *Bed topography and grain size in open channel bends*, volume 23. Sedimentology, Int. Association of Sedimentologist, 1976.

[15] Falcon A.M and Kennedy J.F. Flow in alluvial-river curves. *Journal of Fluid Mechanics*, 133, 1-16, 1983.

[16] Odgaard A.J. Flow and bed topography in alluvial channel bend. *Journal of Hydraulic Engineering, ASCE*, Vol. 110, No. 4, 1984.

[17] Peter W. *Kurvenkolk-Untersuchungen über Soblenausbildung in Flusskrümmungen.* PhD thesis, Mitteilung 85 der Versuchsanstalt für Wassebau, Hydrologie und Glaziologie (VAW), Eidgenössische Technische Hochschule (ETHZ), Zürich,CH, 1986.

[18] Reindl R. *Sohl-und Strömungsusbildung in einer Bodenfolge mit und ohne Rückstaueinfluss.* PhD thesis, Institut für Wasserbau, Leopold-Franzens-Universitt, Innsbruck, 1994.

[19] Hoffmans G.J.C.M. and Verheij H.J. *Scour Manual.* A.A. Balkema, Rotterdam, Netherlands, 1997.

[20] Graeme M. Smart; Martin N.R. Jaeggi. *Sediment Transport on Steep Slopes.* Mitteilungen der Versuchsanstalt fr Wasserbau, Hydrologie und Glaziologie, Zürich,CH, 1983.

[21] Strickler A. *Beiträge zur Frage der Geschwindigkeitformeln.* Mitteilung No. 16; Amt f. Wasserwirtschaft, Bern, Switzerland, 1923.

[22] Sinniger R.O. and Hager W.H. *Constructions Hydrauliques.* Traité de génie civil No.15. Presses Polytechniques et universitaires romandes.

[23] Ralph B. Peck, Walter E. Handson, and Thomas H. Thornburn. *Foundation Engineering.* John Wiley and Sons, Inc., USA, 1953.

[24] Labiouse V. *Fondations.* Polycopié de École polytechnique fédérale de Lausanne, Laboratoire mecanique des roches, Lausanne, Switzerland, 1999.

[25] Clayton CRI and Milititsky J. *Earth pressure and earth retaining structures.* Surrey University Press, Glasgow and London, 1986.

[26] Chin lien Yen, Fellow, ASCE, and Kwan Tun Lee. Bed topography and sediment sorting in channel bend with unsteady flow. *Journal of Hydraulic Engineering, ASCE*, 121 No. 8, 1995.

[27] Graf W.H. *Hydraulique fluviale.* Traité de génie civil No.16. Presses Polytechniques et universitaires romandes.

[28] Graf W.H. *Hydrodinamique.* Traité de génie civil No. 14. Presses Polytechniques et universitaires romandes.

[29] Schleiss A. *Aménagements de cours d'eau.* Polycopié de École polytechnique fédérale de Lausanne, Lausanne, Switzerland, 2003.

[30] Schleiss A. *Aménagements hydrauliques.* Polycopié École polytechnique fédérale de Lausanne, Lausanne, Switzerland, 2002.

[31] Recordon. *Mécanique des sols.* Polycopié de École polytechnique fédérale de Lausanne, Laboratoire mécanique des sols, Lausanne, Switzerland, 1999.

Appendix A

Overview of the tests

This appendix gives of the principal test parameters.

- The mean water depth h_m was computed at the inlet reach between -1m and -4m.
- The variables R_h, V_m, V*, ζ, θ, Fr_d, Fr, Fr*, Re and Re* were calculated from h_m, B, d_{90}, g, etc.
- Q_w is the mean discharge measured during the test.
- S_0 is the initial longitudinal bed slope at the axe of the channel.
- h_1, h_2, h_{max} are the maximum depth at the first scour hole, at the second and the maximum of them.
- Sc_{Loc} is the position of the scour holes.
- $S_{e,bend}$, $S_{e,all}$ are the energy slope at the bend (from 0° to 90°) and at the whole channel (from -2m to 2m)

A.1 Table of tests parameters and measurements performed

ID	S_o [%]	Q_w $[m^3/s]$	Q_s [g/min]	Duration of test [h:min]	Measurements			Sed. Sampling	
					Water Level	Bed Level	Velocity	Armor.	Outlet
B02b	0.5	0.15	2468	13:40		X	X	X	X
B02c	0.5	0.18	3509	7:55	X	X	X		X
B02d	0.5	0.209	4665	10:00	X	X	X	X	X
C02b	0.7	0.15	2509	8:25	X	X	X	X	
C02c	0.7	0.18	3709	7:50	X	X	X	X	X
C02d	0.7	0.21	5632	6:10	X	X	X	X	
D02b	0.35	0.15	327	10:15	X	X	X	X	
D02c	0.35	0.17	677	8:55	X	X	X		
D02d	0.35	0.19	1176	7:52	X	X	X		X
D02d	0.35	0.21	1676	5:40	X	X	X	X	

A.2 Table of tests results

ID	Q_w $[m^3/s]$	S_o [%]	h_m [m]	R_h [m]	h_1 [m]	h_2 [m]	h_{max} [m]	Sc $_{Loc1}$ [°]	Sc $_{Loc2}$ [°]	$S_{e,bend}$ [%]	$S_{e,all}$ [%]
B02b	**0.15**	0.5	-	-	-	-	-	43	100	-	-
B02c	**0.18**	0.5	0.178	0.128	0.331	0.292	0.331	39	97	0.93	0.96
B02d	**0.209**	0.5	0.222	0.149	0.356	0.295	0.356	57	97	1.04	1.04
C02b	**0.15**	0.7	0.160	0.118	0.301	0.281	0.301	43	92	0.95	1.03
C02c	**0.18**	0.7	0.190	0.134	0.351	0.337	0.351	43	97	0.99	1.05
C02d	**0.21**	0.7	0.213	0.145	0.374	0.312	0.374	39	101	0.94	1.03
D02b	**0.15**	0.35	0.178	0.128	0.329	0.248	0.329	43	97	0.73	0.77
D02c	**0.17**	0.35	0.198	0.138	0.338	0.299	0.338	49	96	0.74	0.84
D02d	**0.19**	0.35	0.213	0.144	0.369	0.332	0.369	43	99	0.85	0.81
D02d	**0.21**	0.35	0.226	0.150	0.369	0.337	0.369	43	96	0.81	0.84

ID	V_m [m/s]	V* [m/s]	ζ $[kN/m^2]$	θ [-]	Fr_d [-]	Fr [-]	Fr* [-]	Re [-]	Re* [-]
B02b	-	-	-	-	-	-	-	-	-
B02c	1.153	0.128	16.3	0.141	3.184	0.871	0.376	491051	766
B02d	1.059	0.150	22.5	0.195	2.923	0.717	0.442	524314	901
C02b	1.059	0.122	14.9	0.129	2.925	0.845	0.359	417191	732
C02c	1.086	0.136	18.4	0.160	2.999	0.795	0.400	484243	815
C02d	1.126	0.140	19.6	0.170	3.110	0.779	0.412	543045	840
D02b	0.942	0.113	12.8	0.111	2.600	0.712	0.333	400619	678
D02c	0.954	0.120	14.3	0.124	2.635	0.684	0.352	437785	719
D02d	1.043	0.133	17.7	0.153	2.880	0.722	0.392	502270	798
D02d	1.058	0.134	17.9	0.155	2.921	0.710	0.394	530147	802

Appendix B

Bed topography compared to initial bed level

This Appendix gives the bed topography measured at the end of the test compared to the initial bed level. More information can be found in the Section 4.2.2.

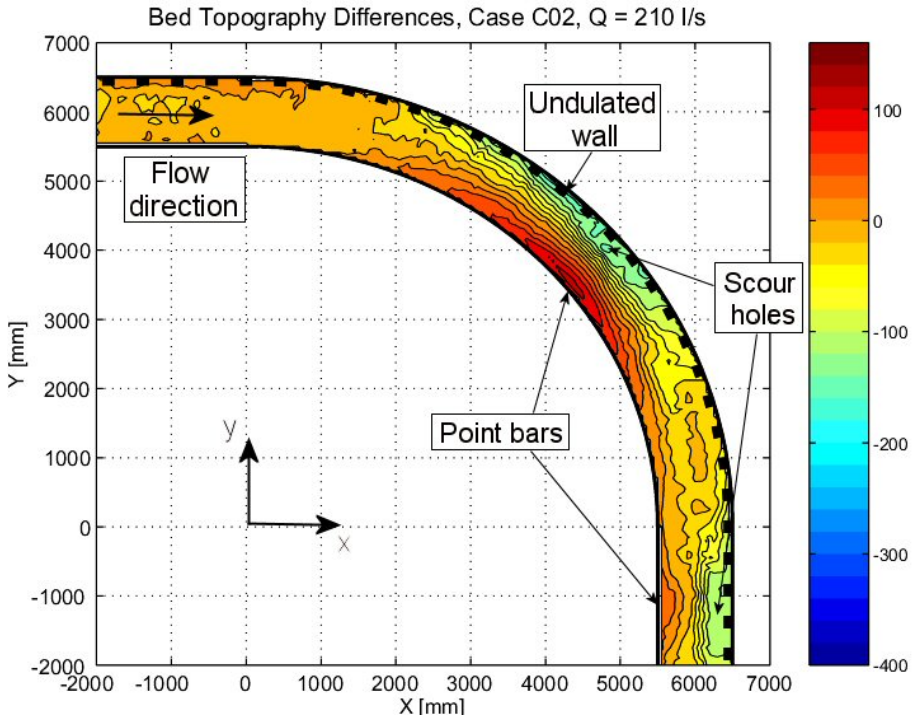

B.1 Channel slope $S_0 = 0.5\%$

Smooth wall (Hersberger)	Undulated wall

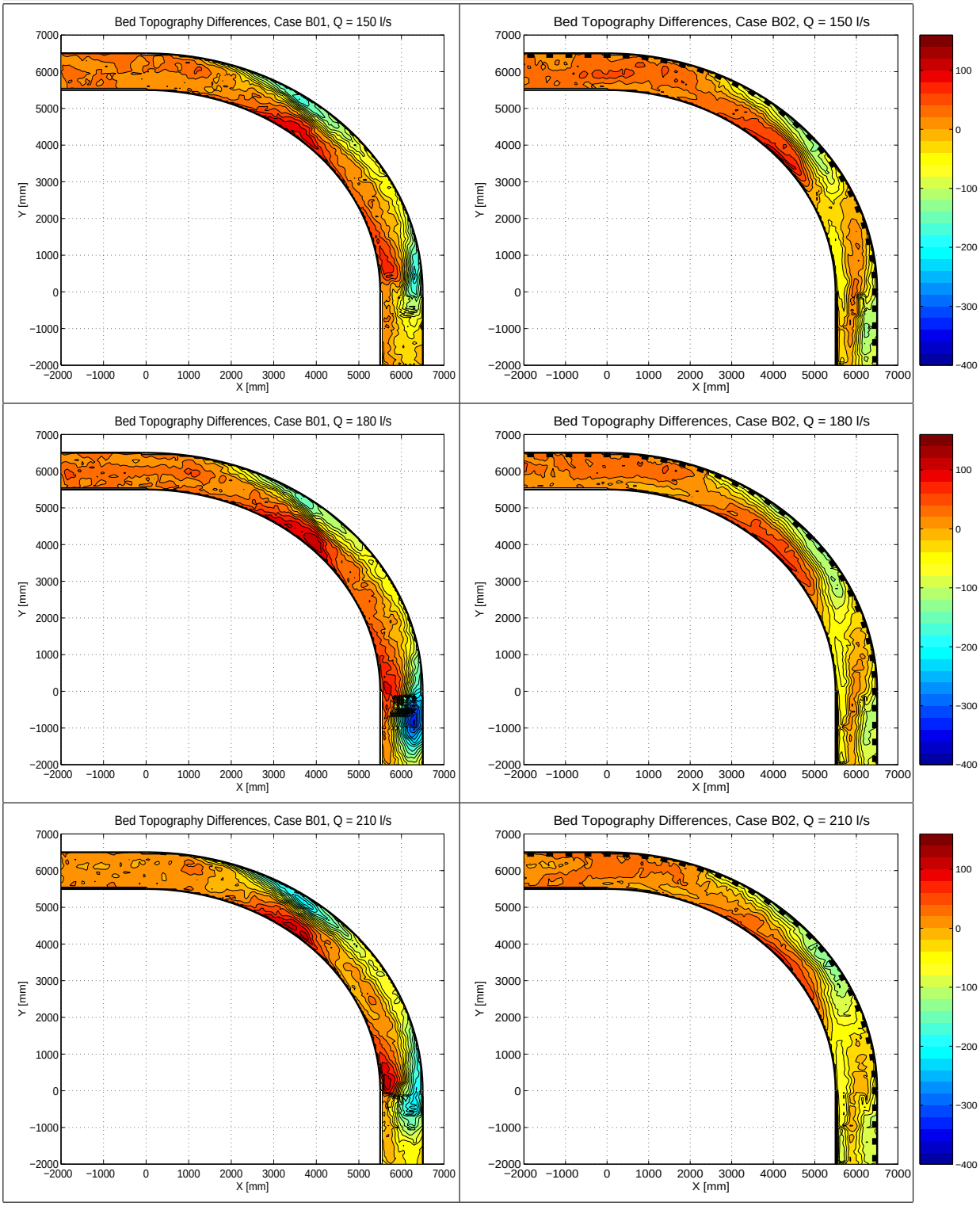

B.2 Channel slope $S_0 = 0.7\%$

Smooth wall (Hersberger)	Undulated wall
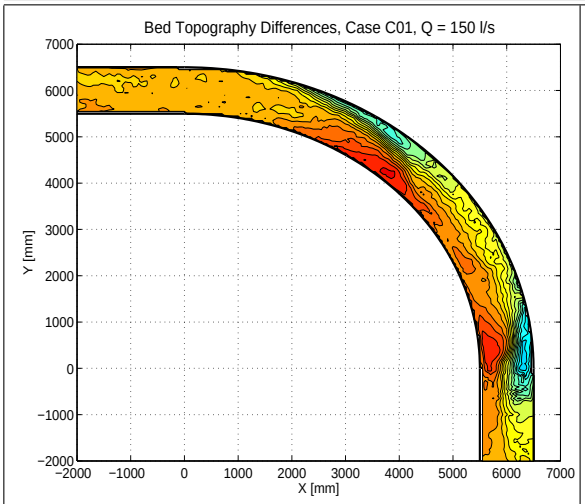	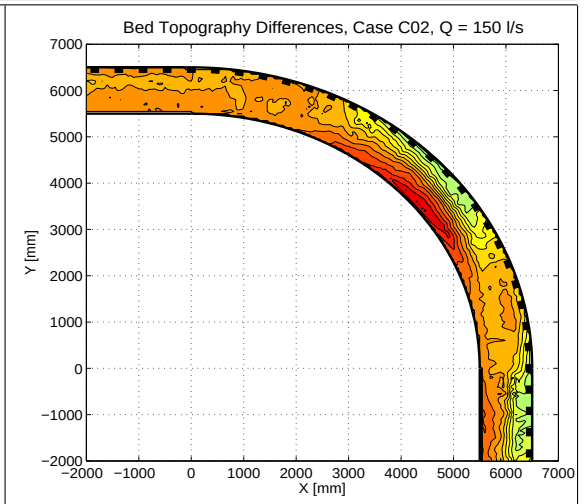
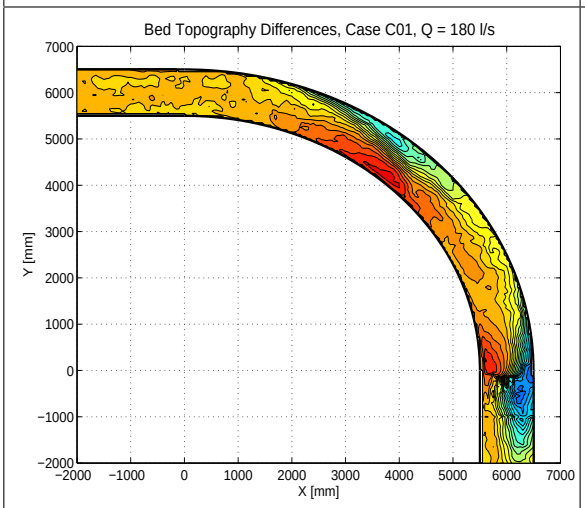	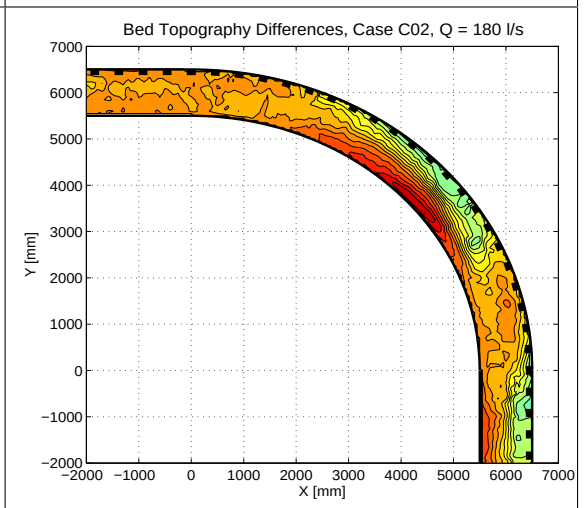
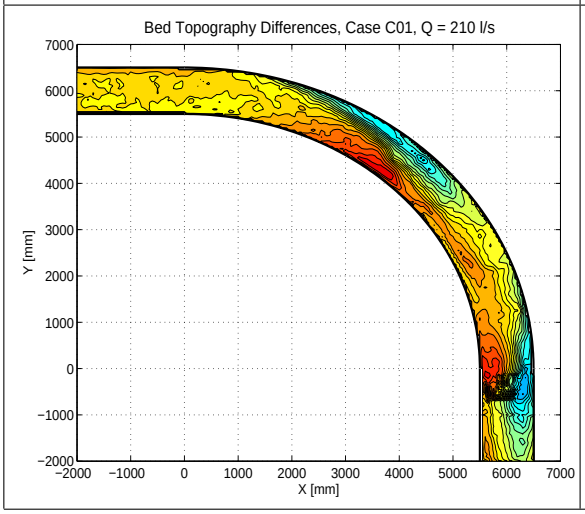	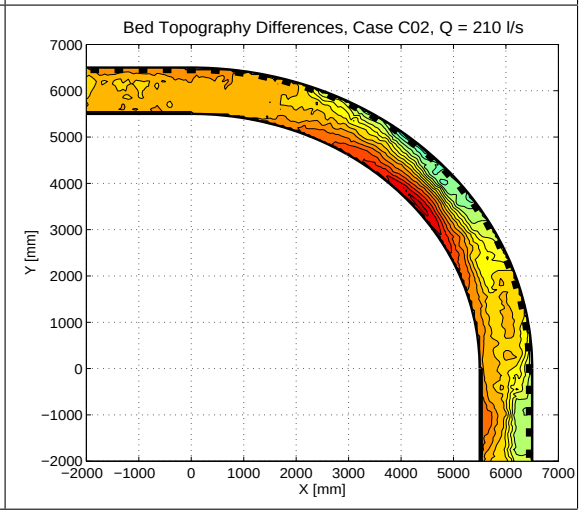

B.3 Channel slope $S_0 = 0.35\%$

Smooth wall (Hersberger)	Undulated wall

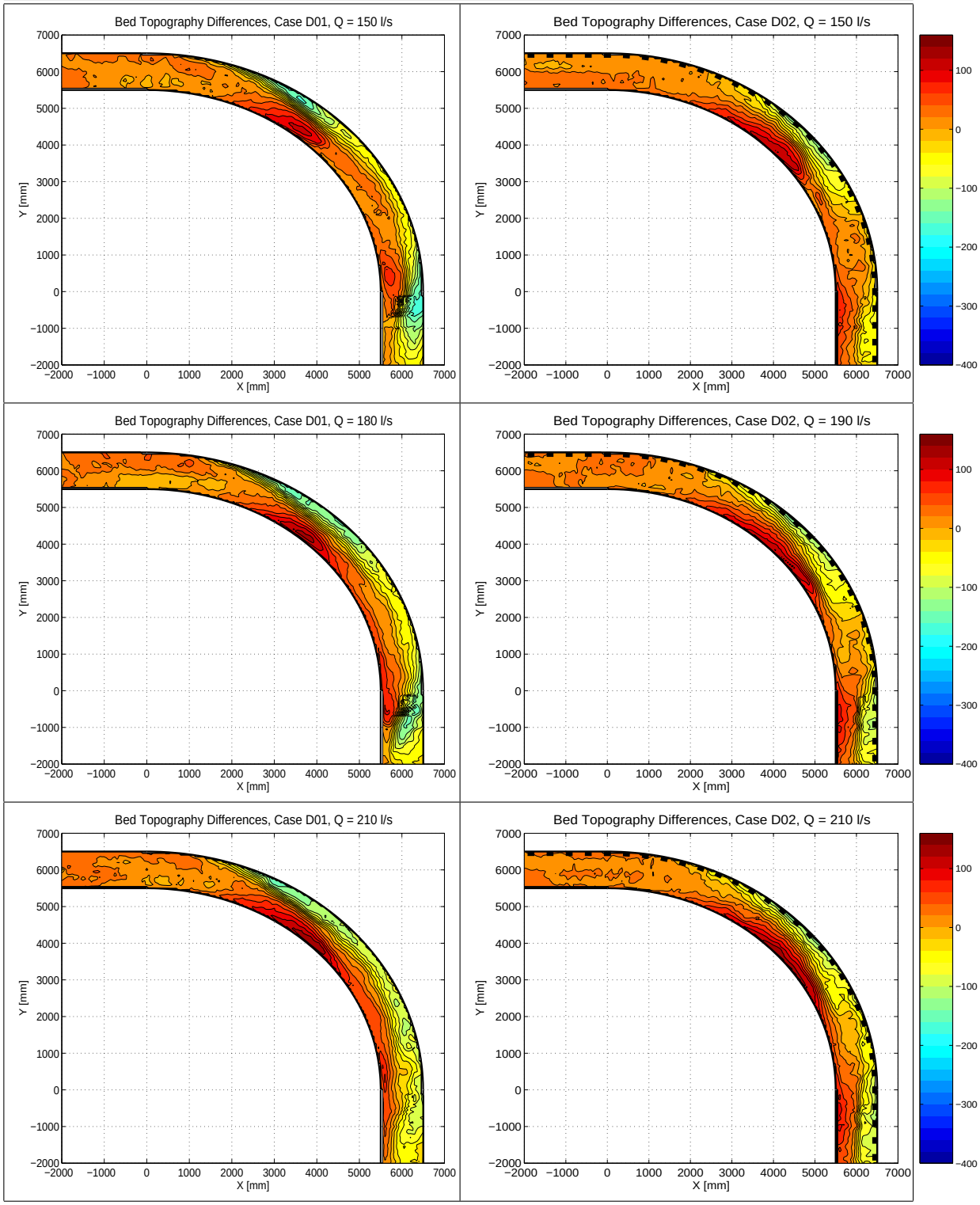

Appendix C

Water surface compared to horizontal surface

This Appendix gives the measured water level compared to an horizontal surface. This surface is the average of the water level over the channel. More information can be found at the Section 4.5.

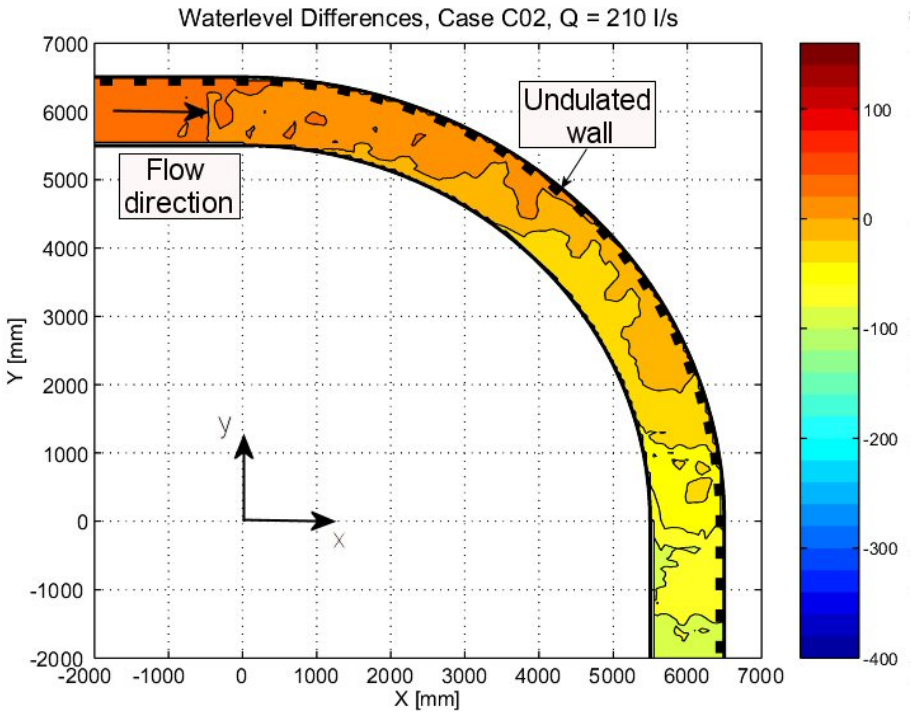

C.1 Channel slope $S_0 = 0.5\%$

Smooth wall (Hersberger)	Undulated wall
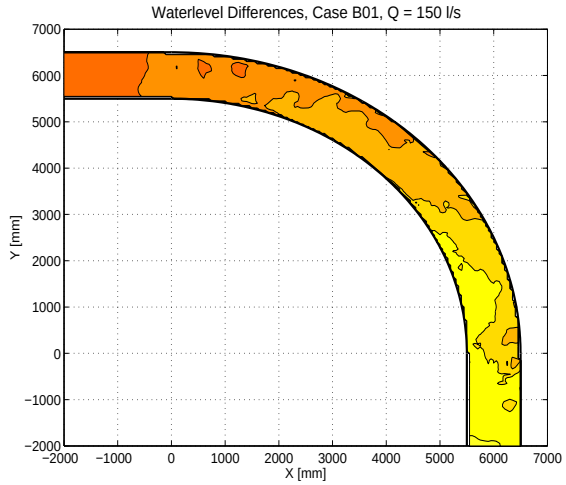	Measures unavailable
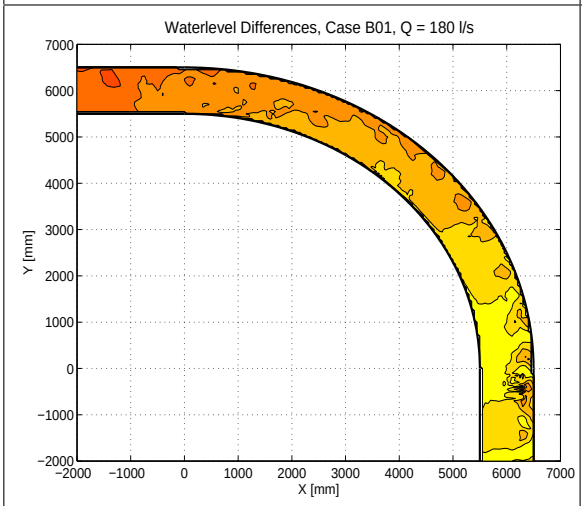	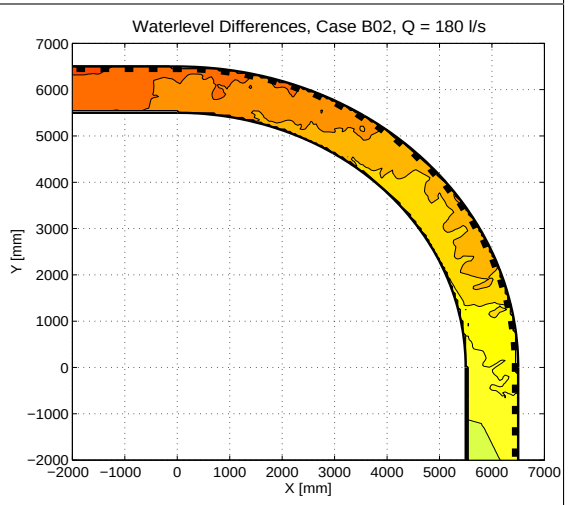
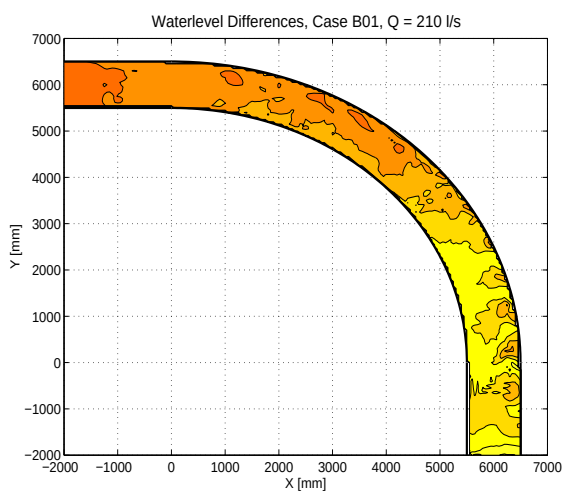	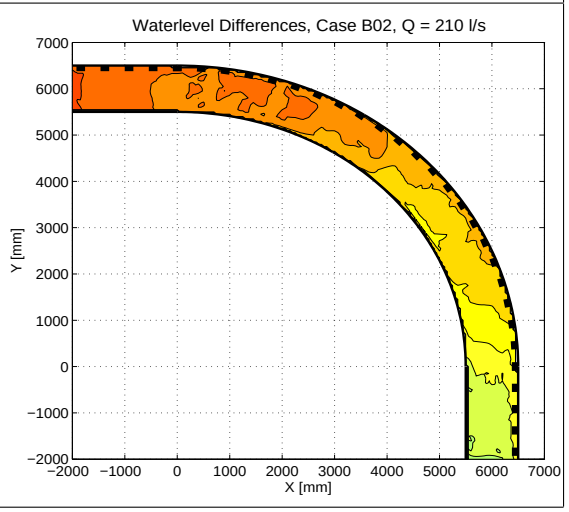

C.2 Channel slope $S_0 = 0.7\%$

Smooth wall (Hersberger)	Undulated wall

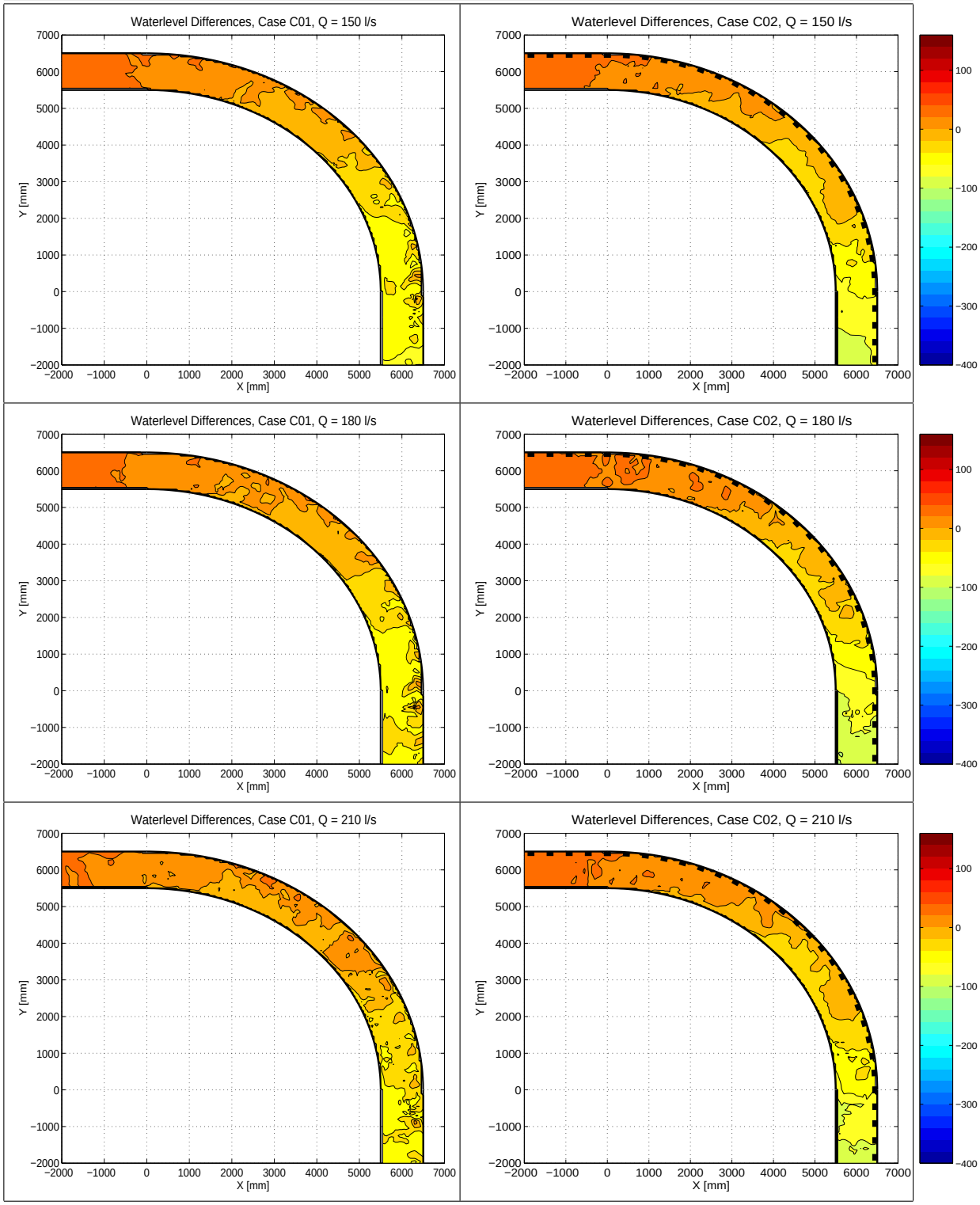

C.3 Channel slope $S_0 = 0.35\%$

Smooth wall (Hersberger)	Undulated wall

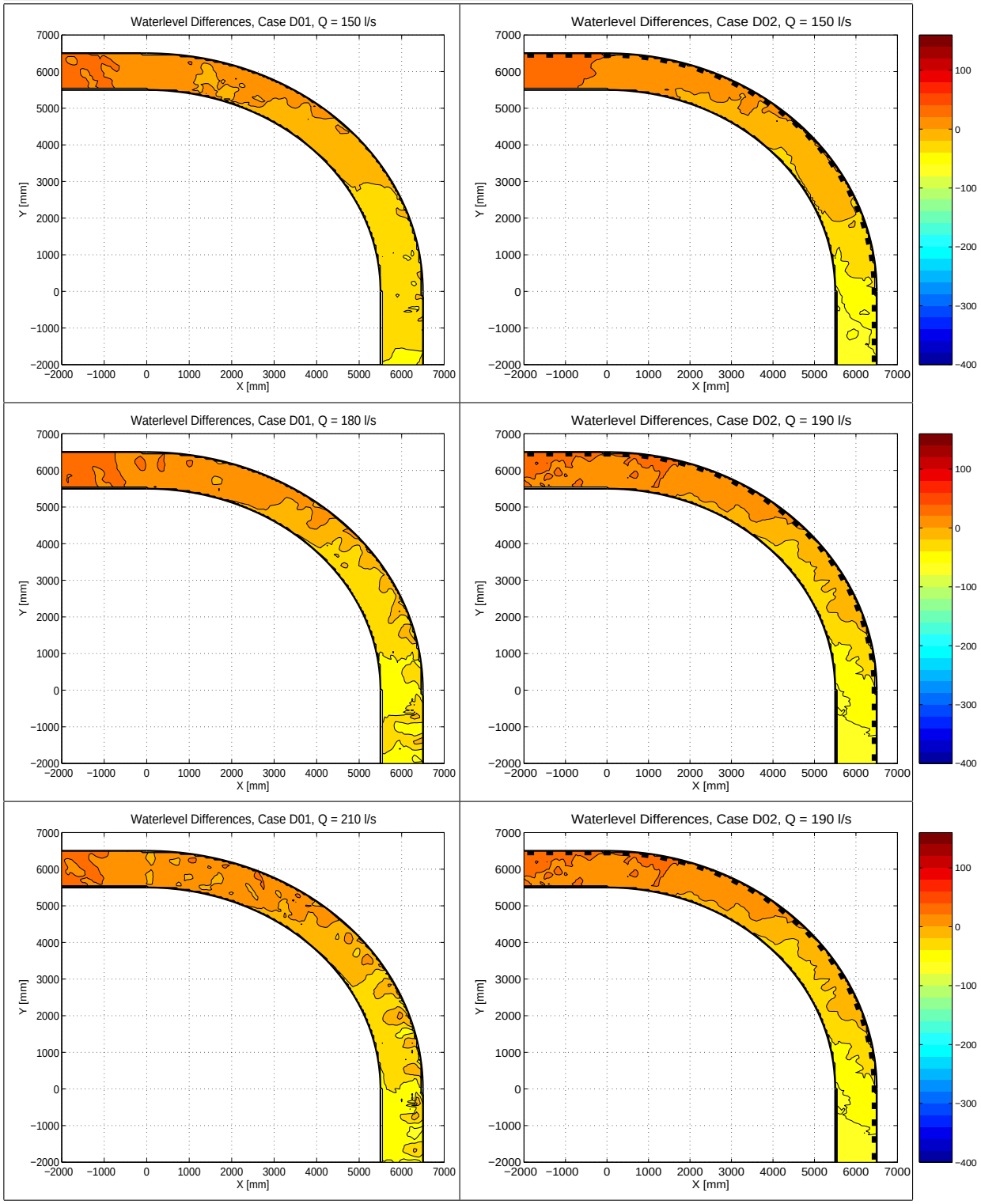

Appendix D

Longitudinal mean, min. and max bed and water profiles

This Appendix gives the maximum, minimum and the mean longitudinal water level and the initial, maximum, minimum and mean longitudinal bed level. More information can be found at the Section 4.2.2 and 4.2.3.

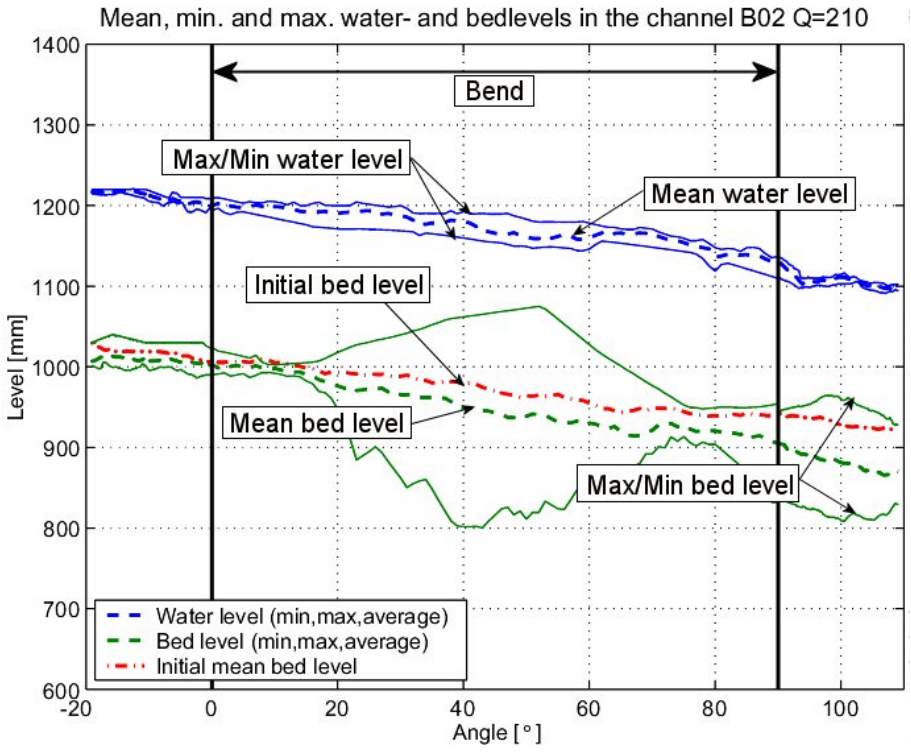

D.1 Channel slope $S_0 = 0.5\%$

Smooth wall (Hersberger)	Undulated wall[1]
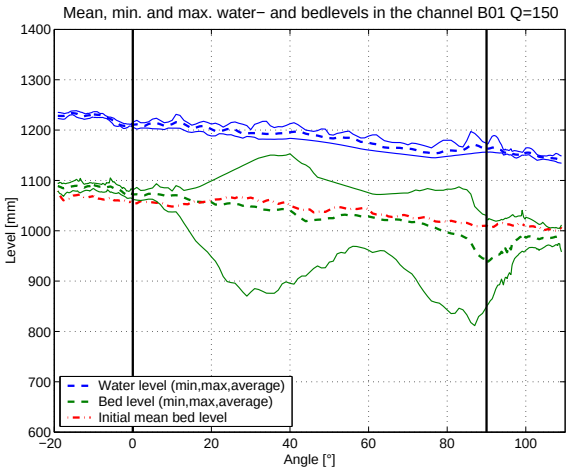	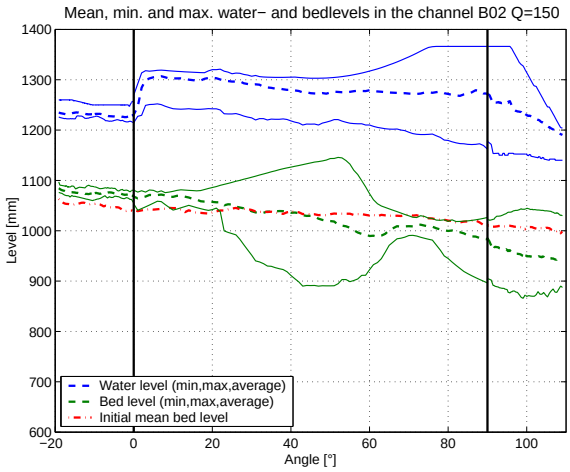
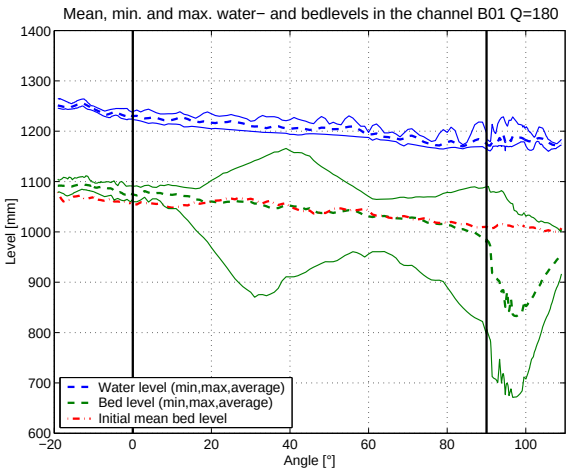	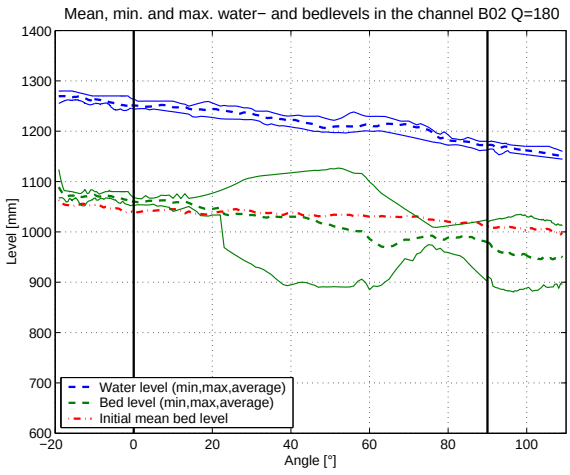
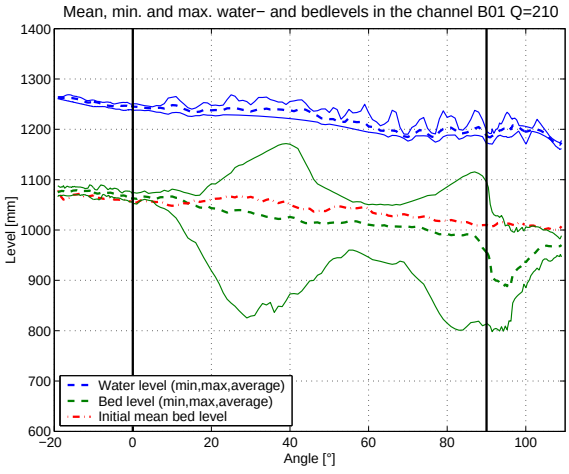	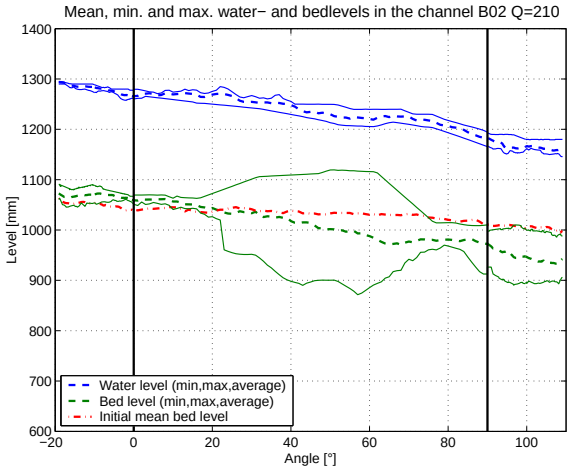

[1] At the test B02 with 150 l/s the water measurements are not correct

D.2 Channel slope $S_0 = 0.7\%$

Smooth wall (Hersberger)	Undulated wall
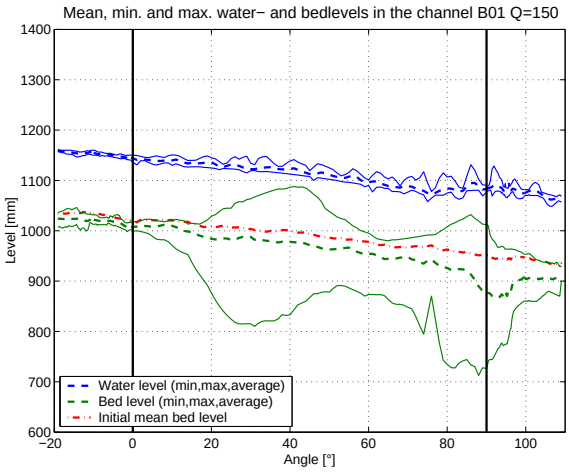	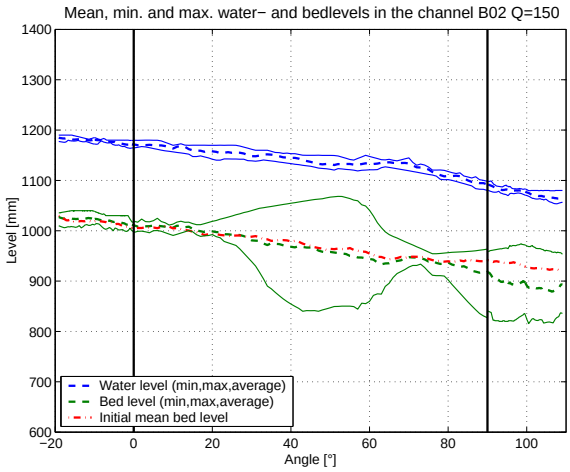
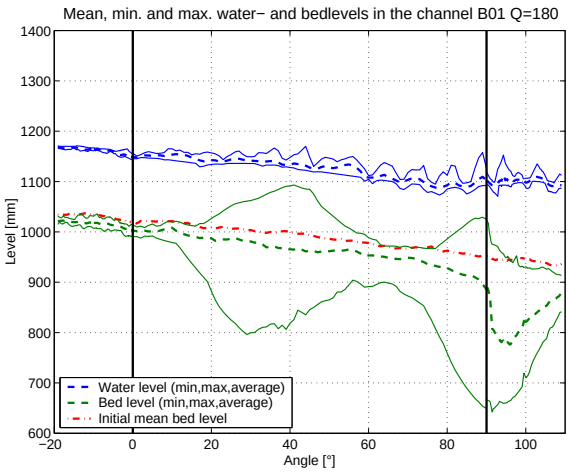	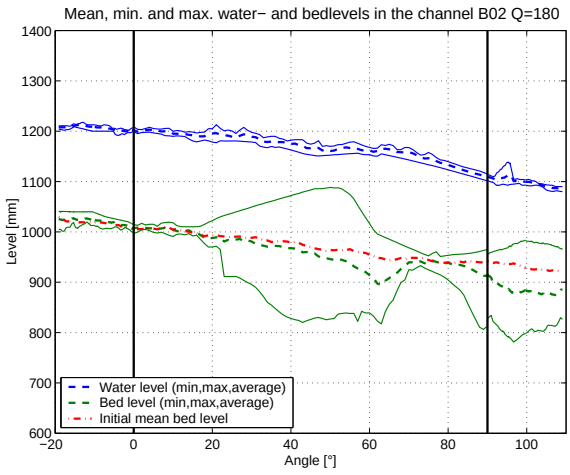
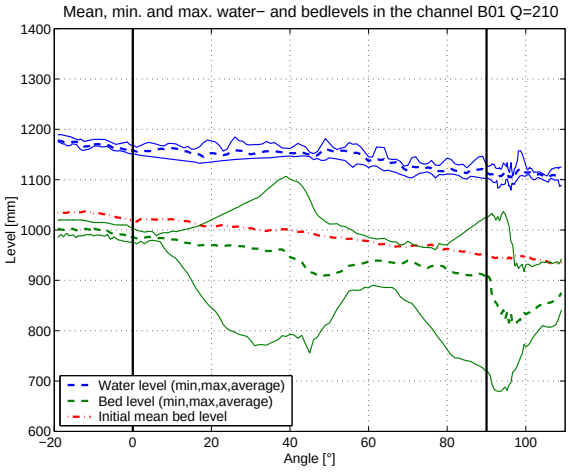	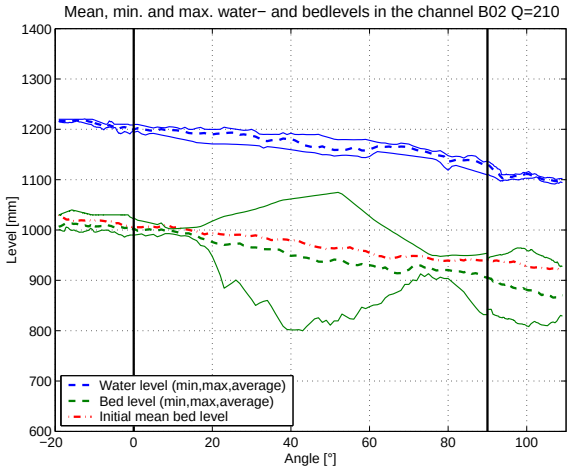

D.3 Channel slope $S_0 = 0.35\%$

Smooth wall (Hersberger)	Undulated wall
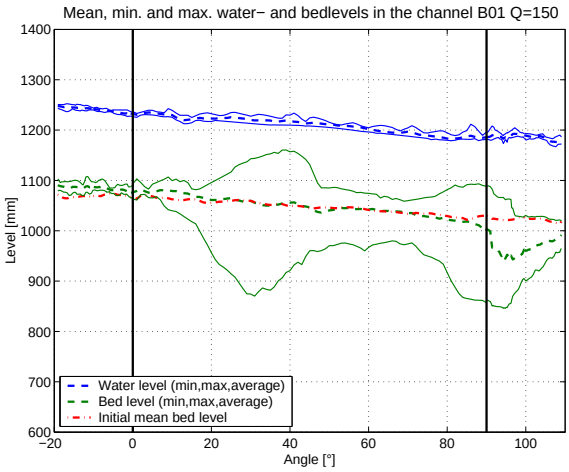	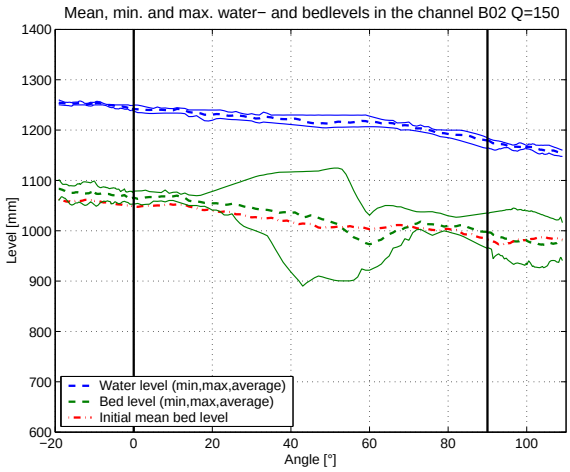
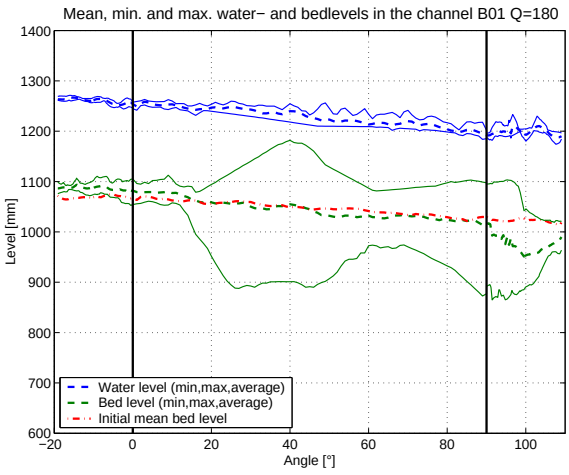	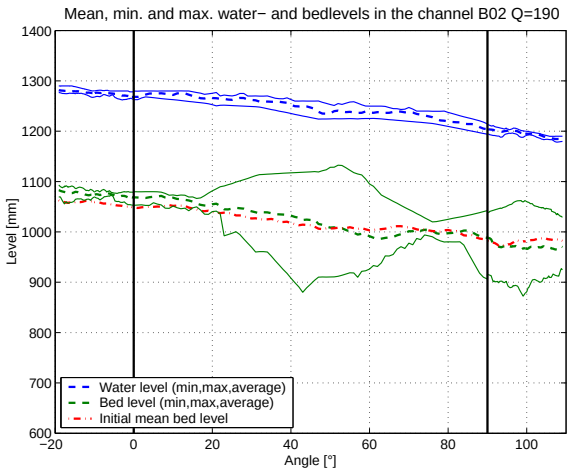
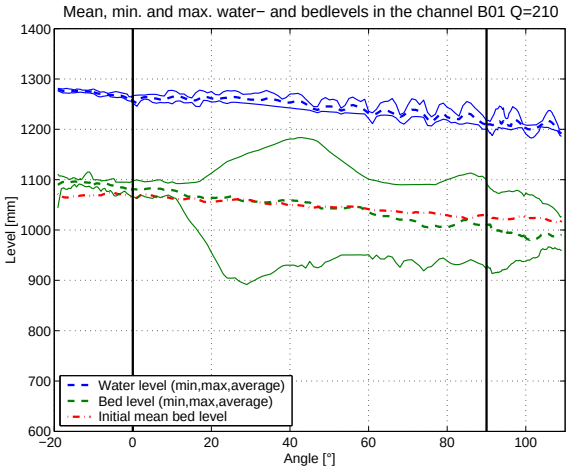	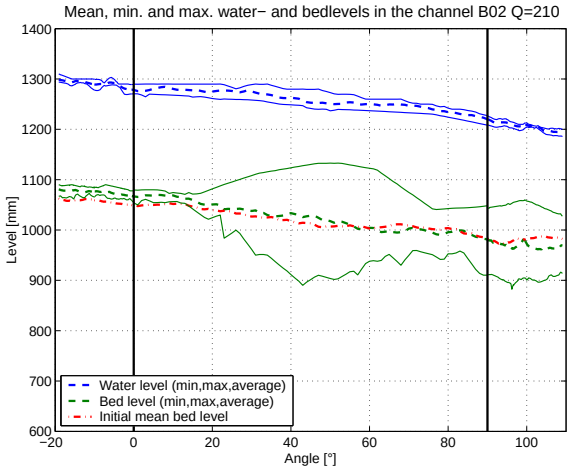

Appendix E

Bed and water levels in cross section

This Appendix gives the water level, the mean water level, the final, the initial and the mean bed levels in 8 cross sections along the channel. More information can be found at the Section 4.2.2 and 4.2.3.

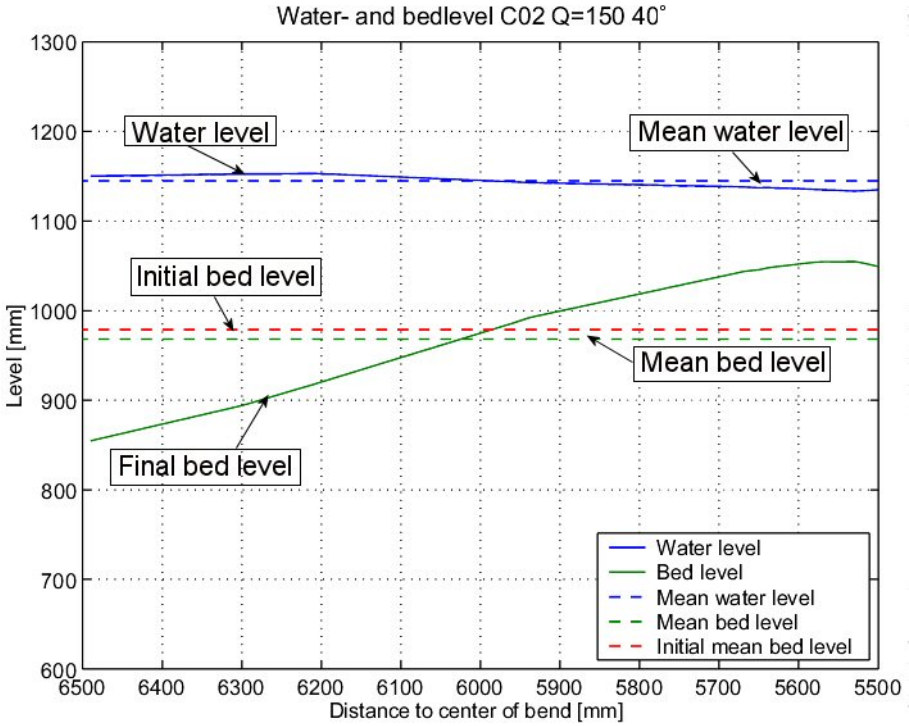

E.1 Cross section at $S_0 = 0.5\%$ and $Q = 150l/s$

Pos.	Smooth wall (Hersberger)	Undulated wall[1]
-1m	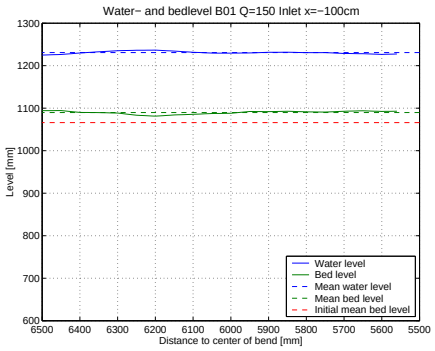	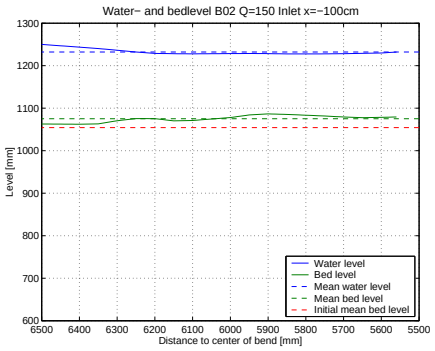
10 °	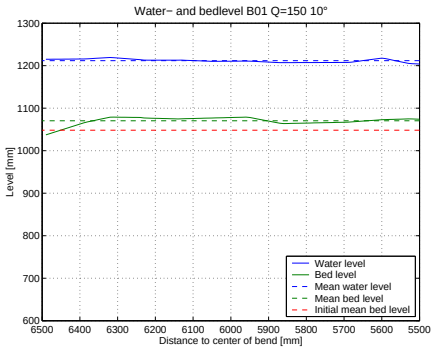	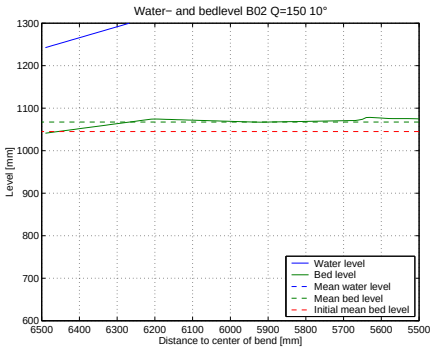
25 °	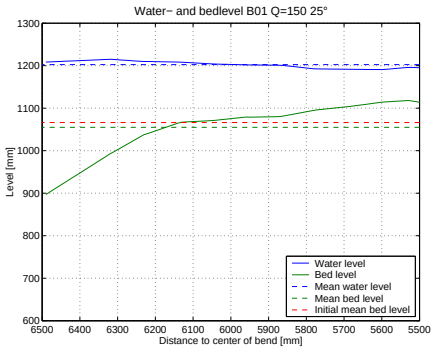	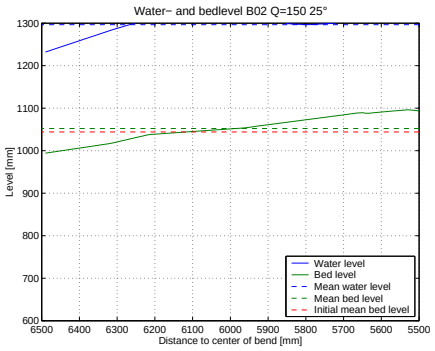
40 °	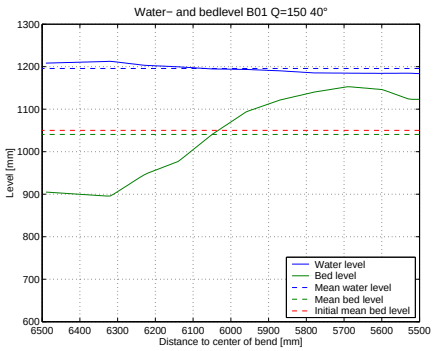	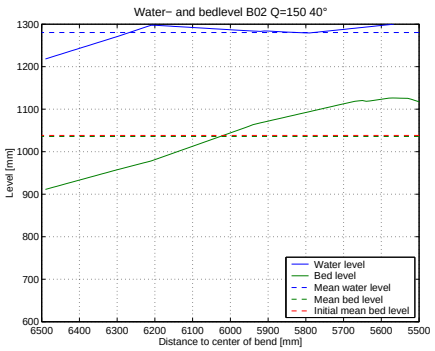

[1] At the test with undulated wall with $S_0 = 0.5\%$ and 150 l/s the water level and the mean water level are not correct

Pos.	Smooth wall (Hersberger)	Undulated wall
55 °	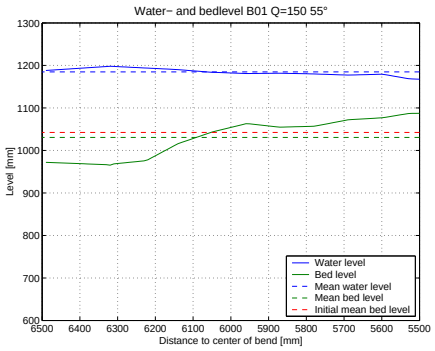	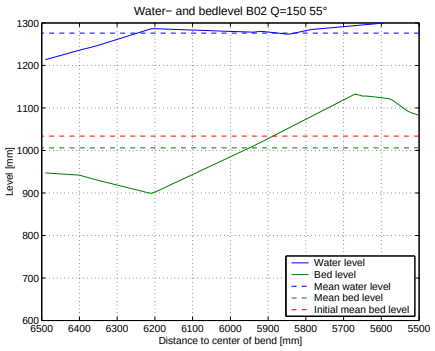
70 °	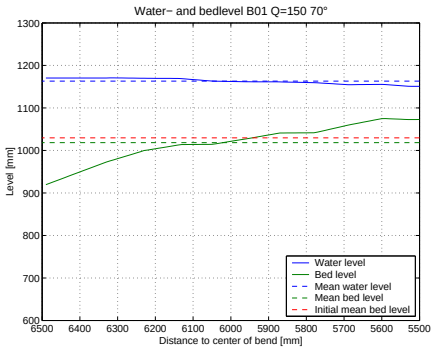	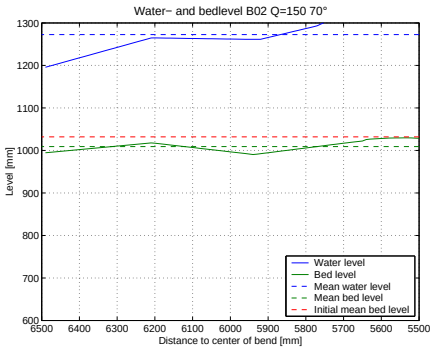
85 °	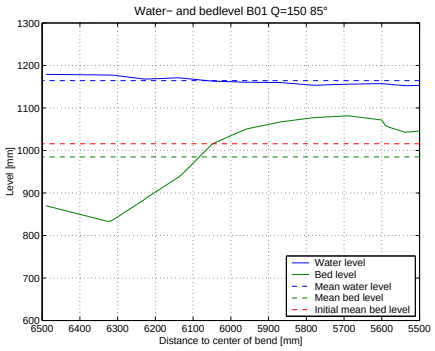	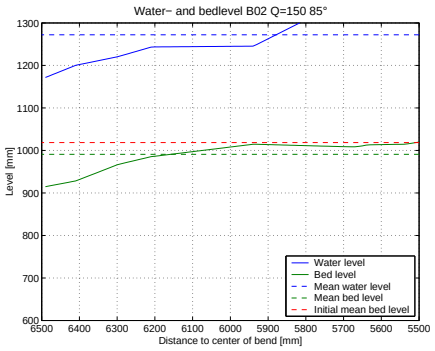
1m	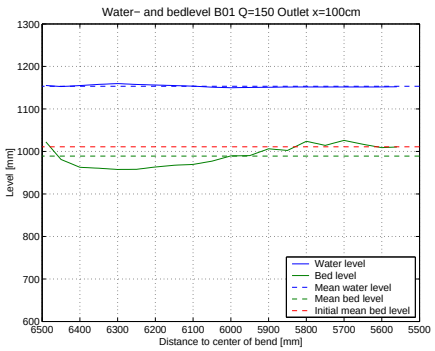	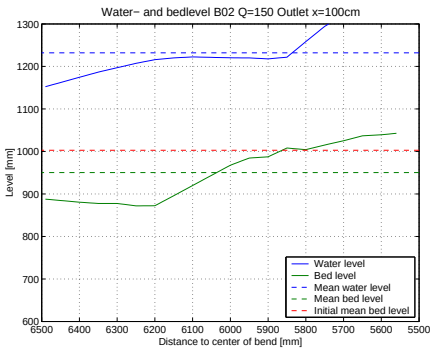

E.2 Cross section at $S_0 = 0.5\%$ and $Q = 180l/s$

Pos.	Smooth wall (Hersberger)	Undulated wall
-1m	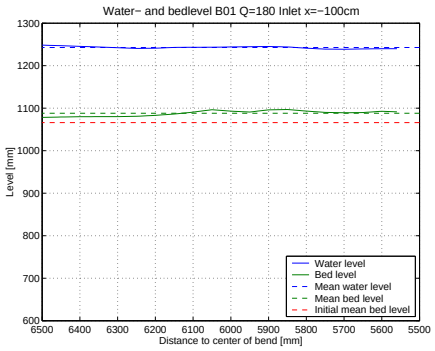	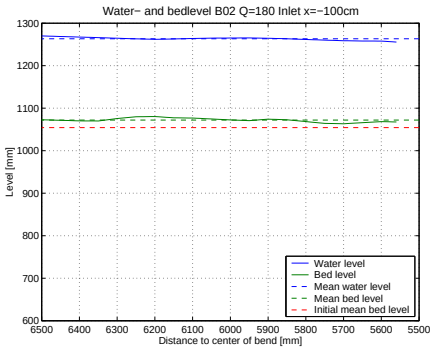
10 °	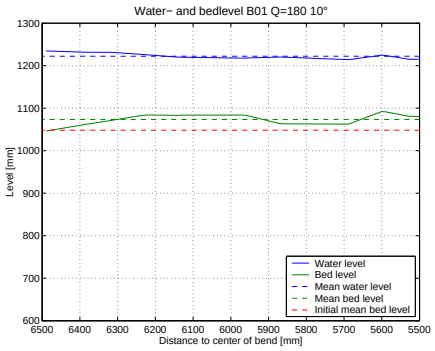	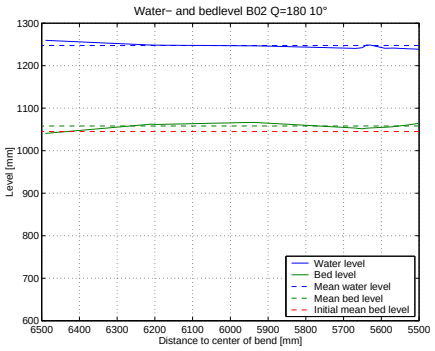
25 °	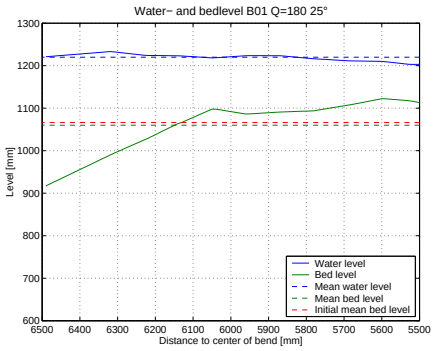	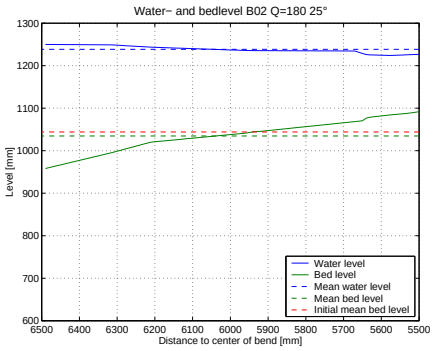
40 °	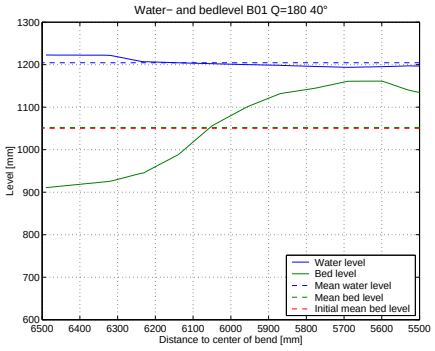	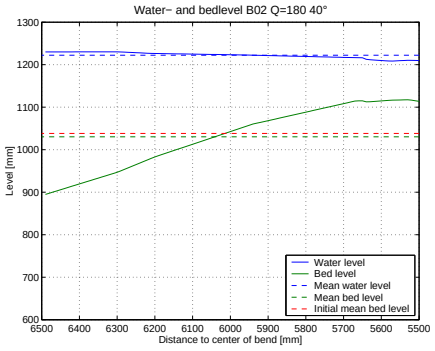

Pos.	Smooth wall (Hersberger)	Undulated wall
55 °	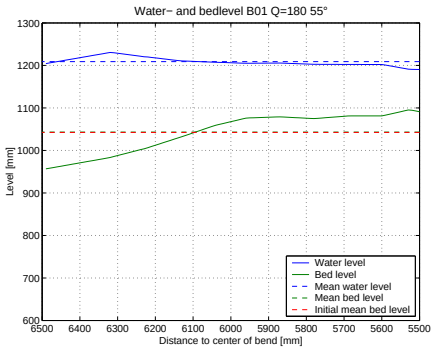	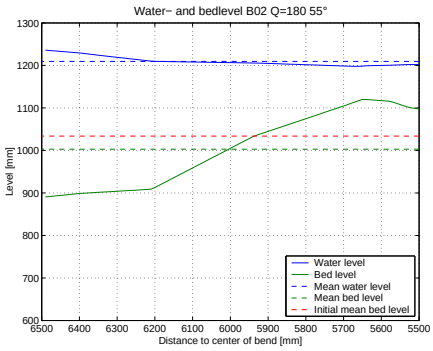
70 °	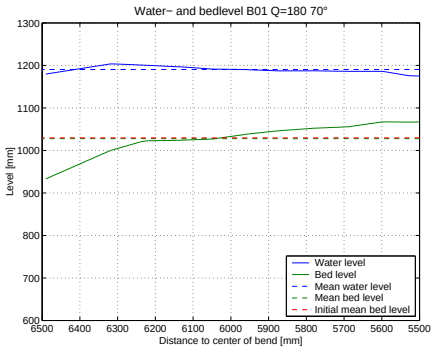	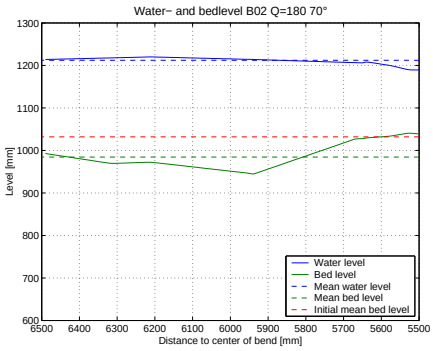
85 °	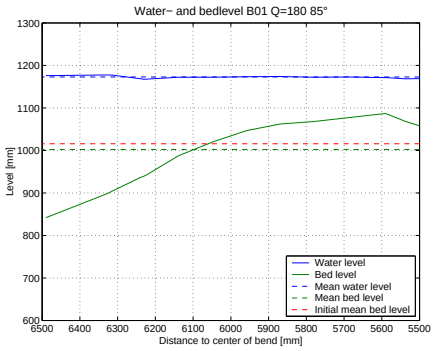	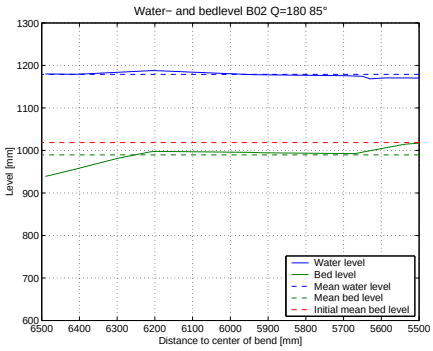
1m	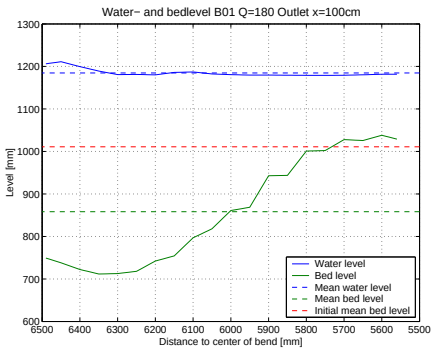	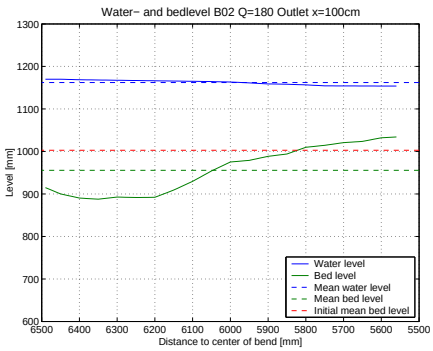

E.3 Cross section at $S_0 = 0.5\%$ and $Q = 210 l/s$

Pos.	Smooth wall (Hersberger)	Undulated wall
-1m	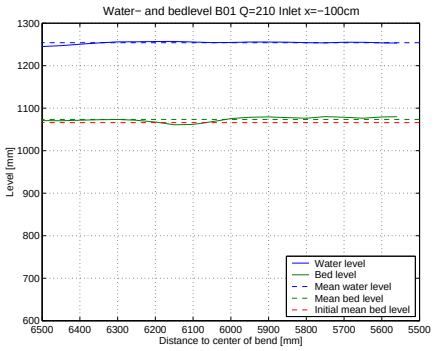	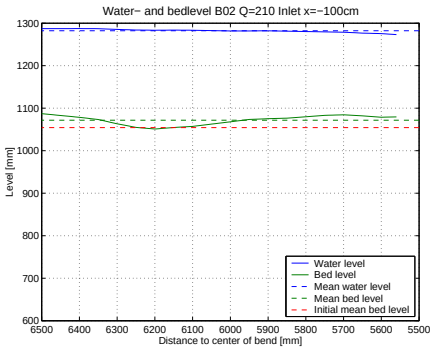
10 °	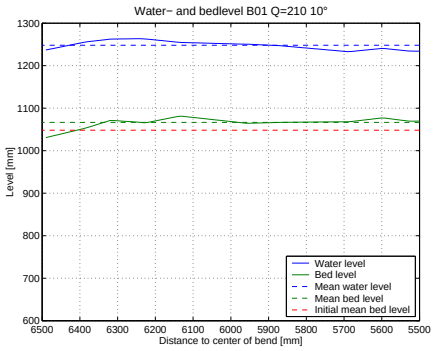	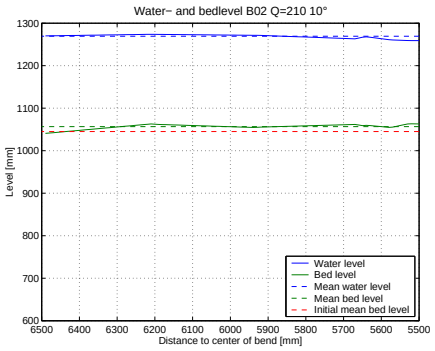
25 °	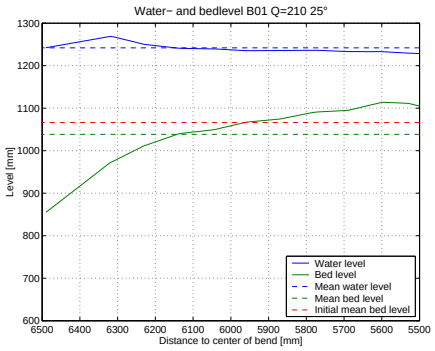	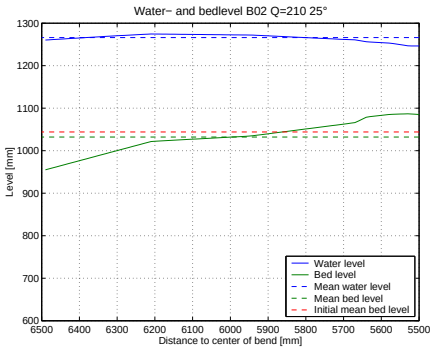
40 °	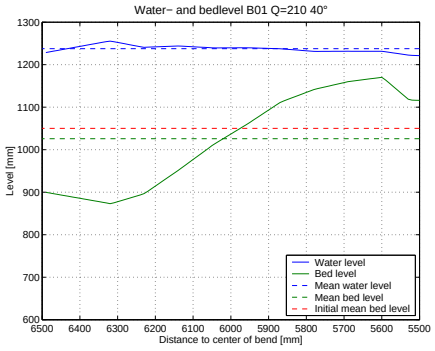	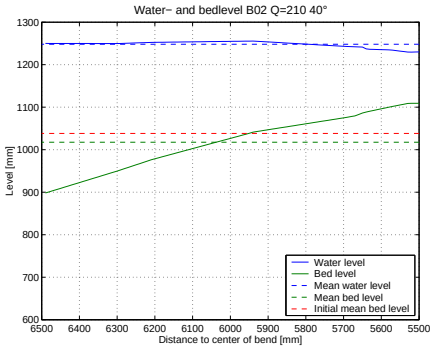

Pos.	Smooth wall (Hersberger)	Undulated wall
55 °	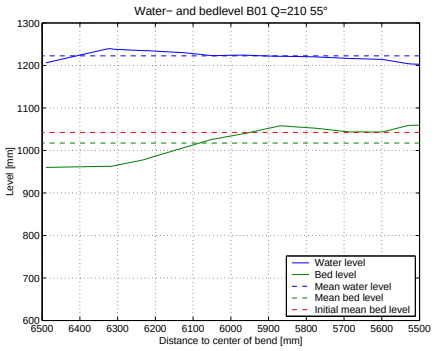	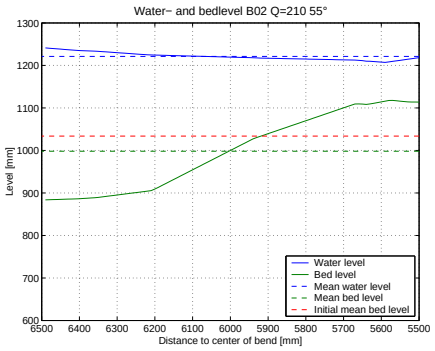
70 °	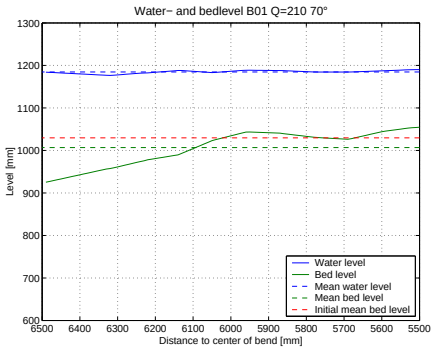	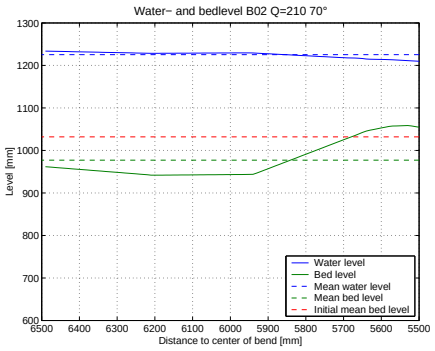
85 °	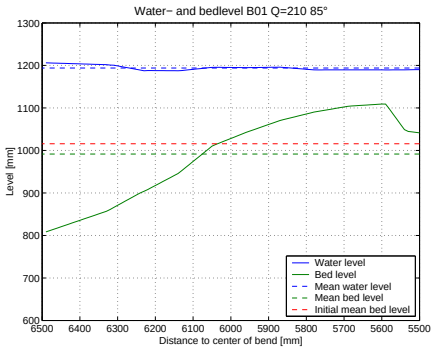	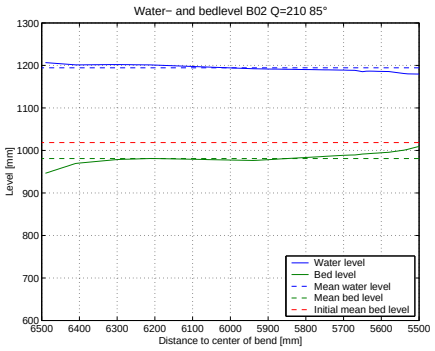
1m	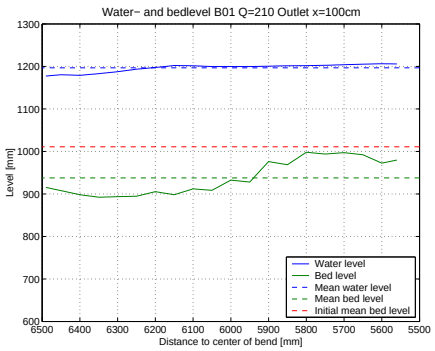	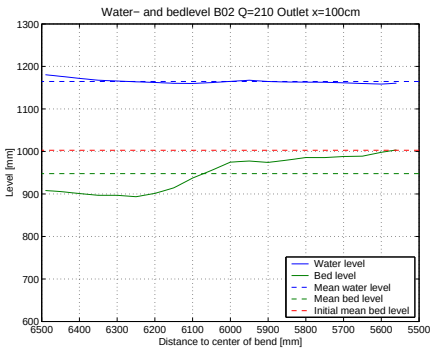

E.4 Cross section at $S_0 = 0.7\%$ and $Q = 150l/s$

Pos.	Smooth wall (Hersberger)	Undulated wall
-1m	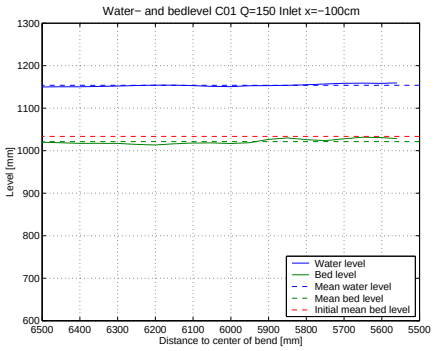	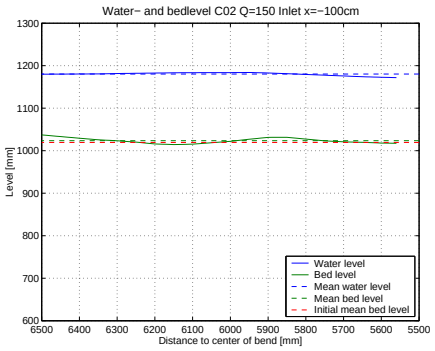
10 °	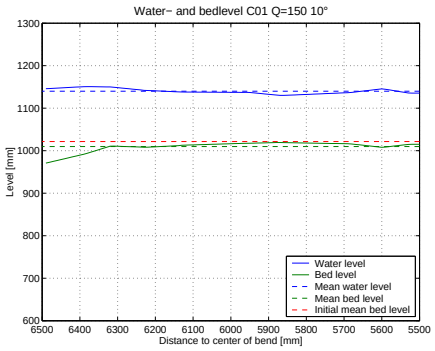	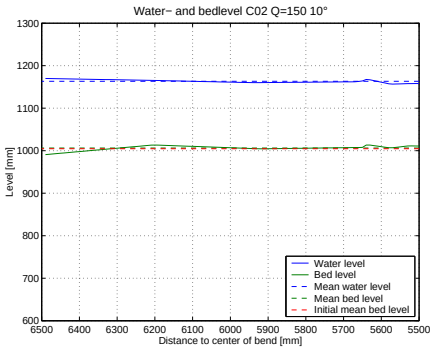
25 °	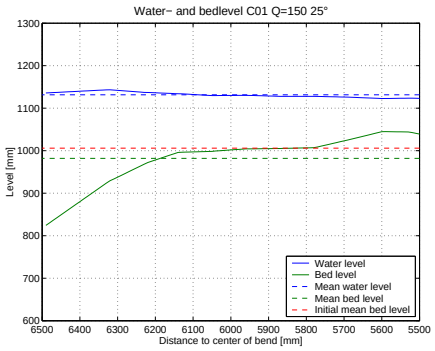	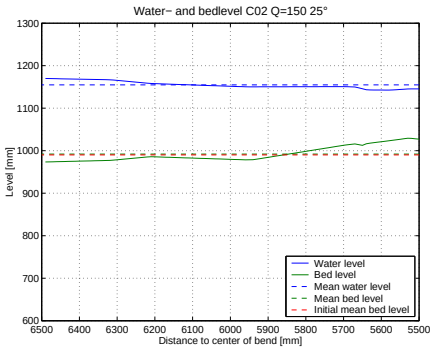
40 °	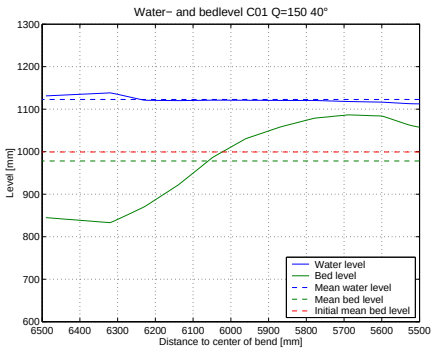	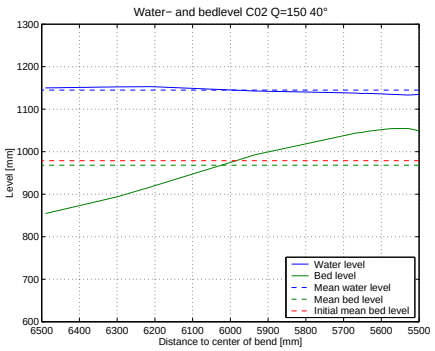

Pos.	Smooth wall (Hersberger)	Undulated wall
55 °	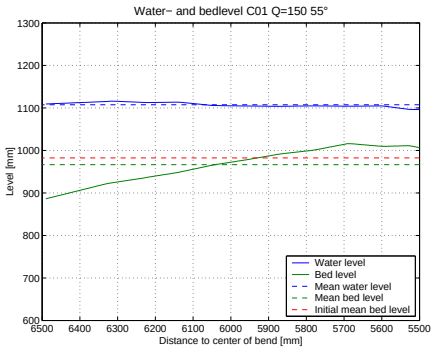	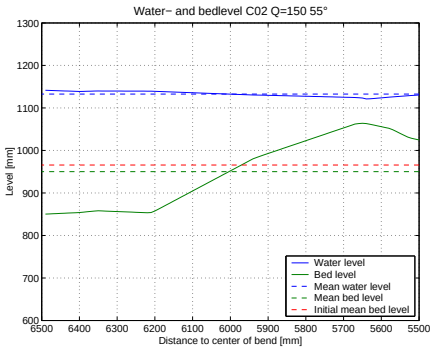
70 °	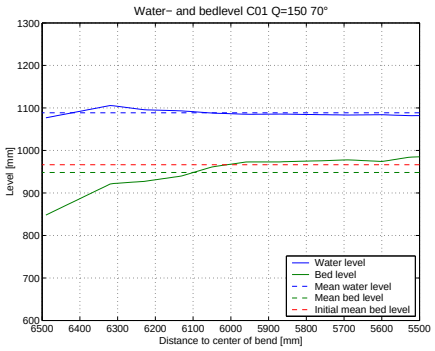	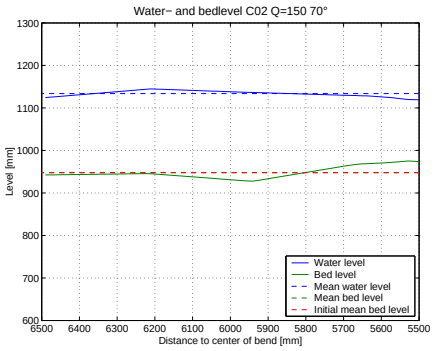
85 °	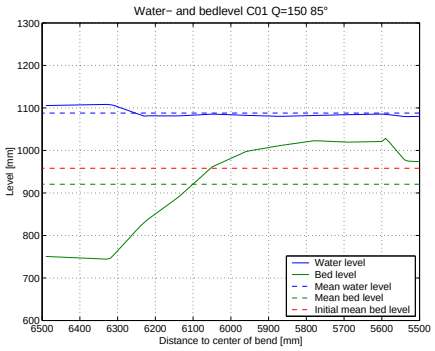	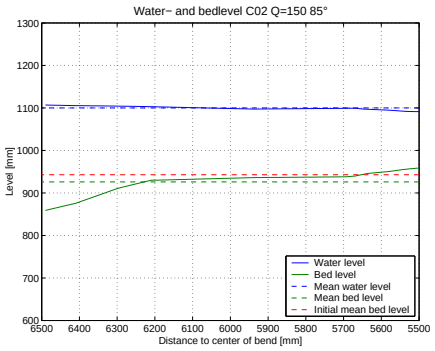
1m	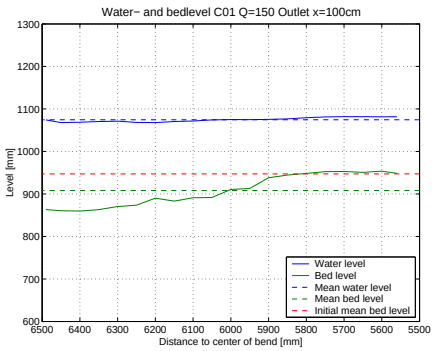	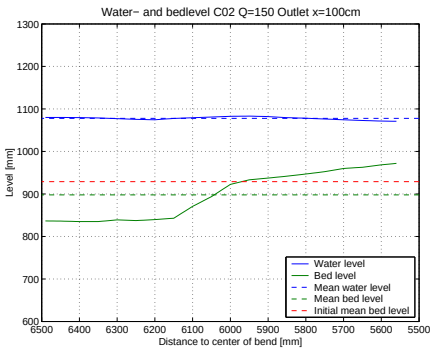

E.5 Cross section at $S_0 = 0.7\%$ and $Q = 180l/s$

Pos.	Smooth wall (Hersberger)	Undulated wall
-1m	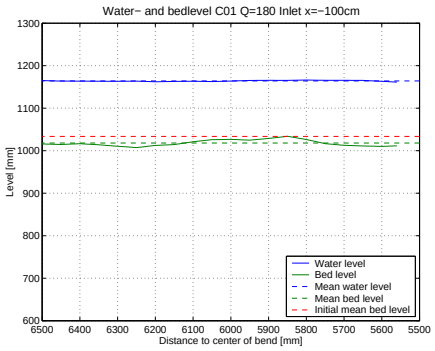	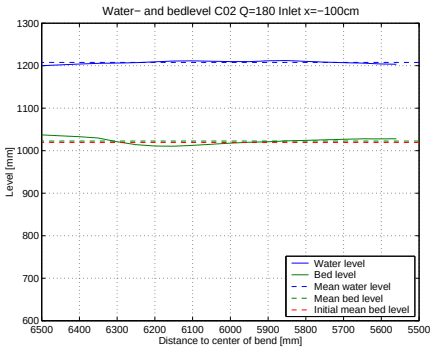
10 °	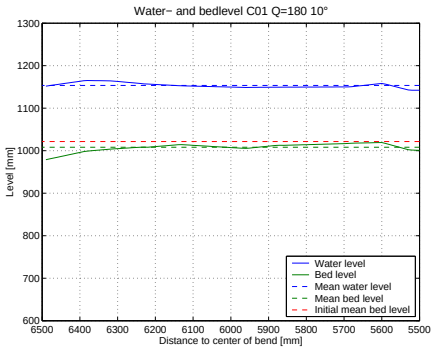	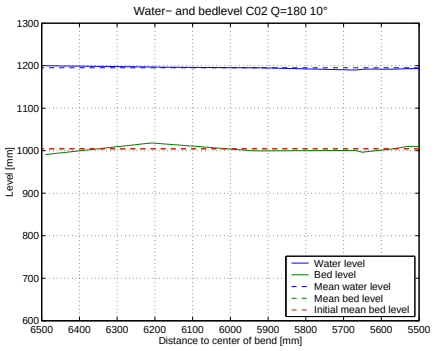
25 °	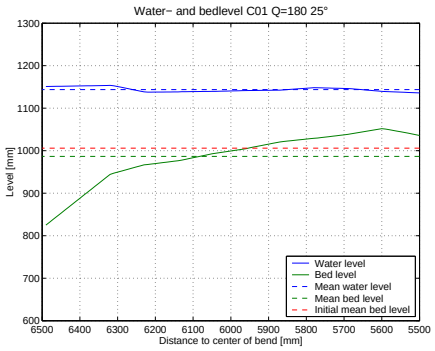	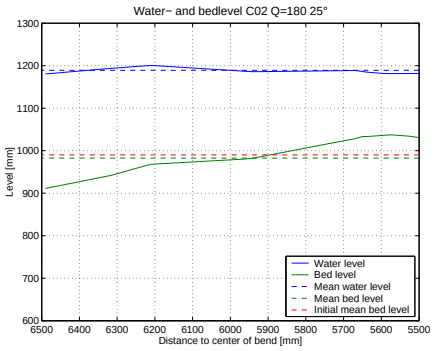
40 °	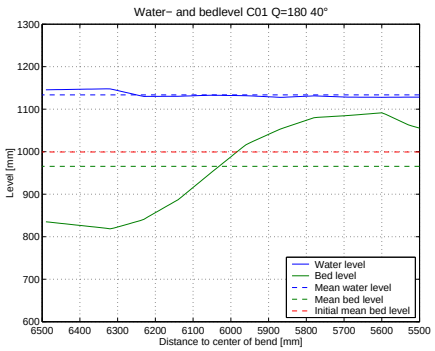	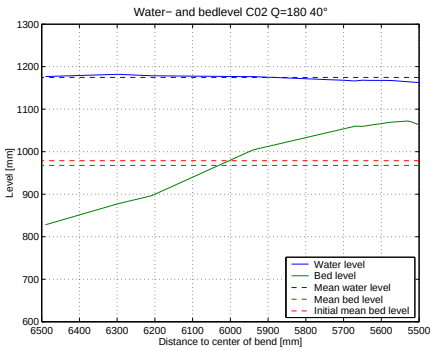

Pos.	Smooth wall (Hersberger)	Undulated wall
55 °	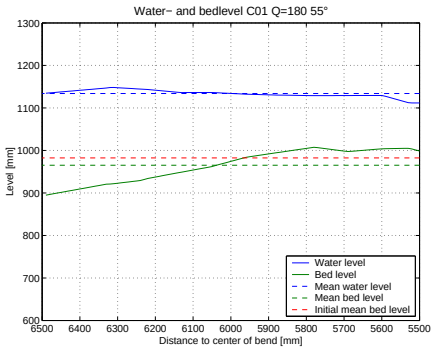	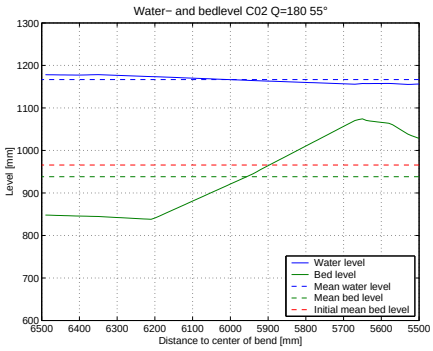
70 °	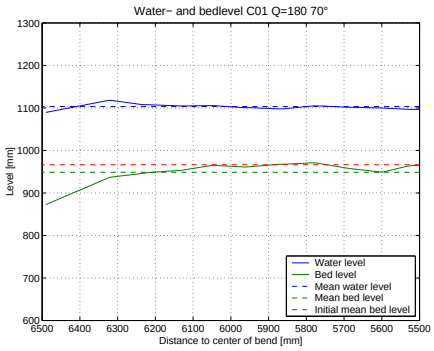	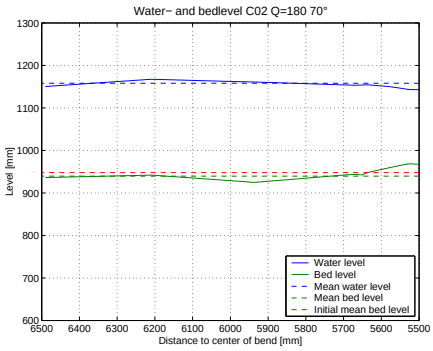
85 °	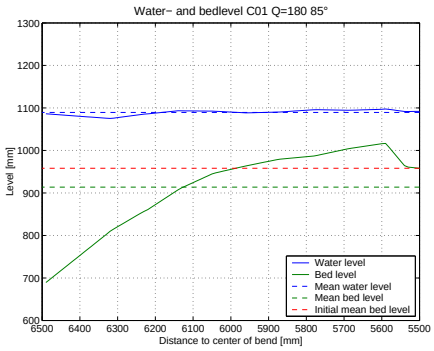	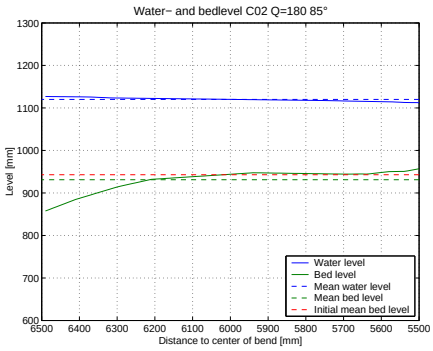
1m	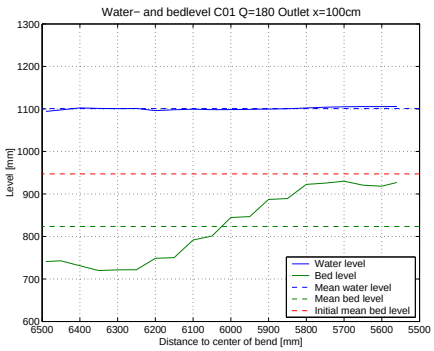	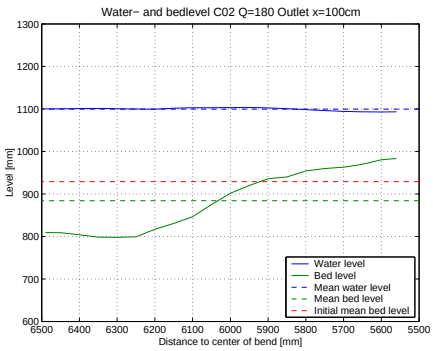

E.6 Cross section at $S_0 = 0.7\%$ and $Q = 210 l/s$

Pos.	Smooth wall (Hersberger)	Undulated wall
-1m	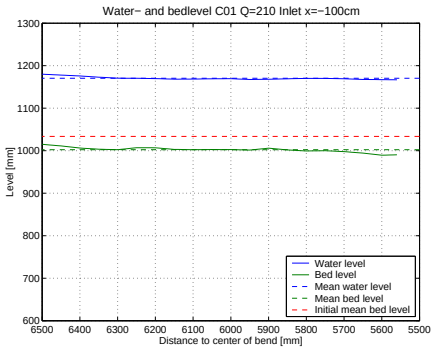	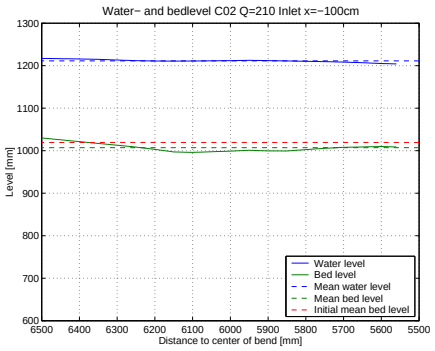
10 °	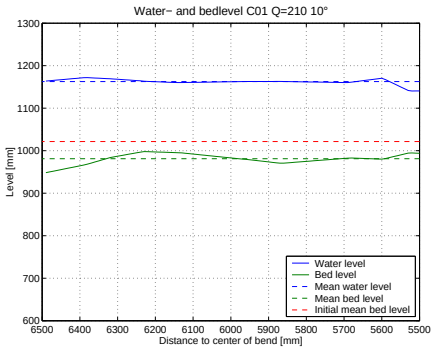	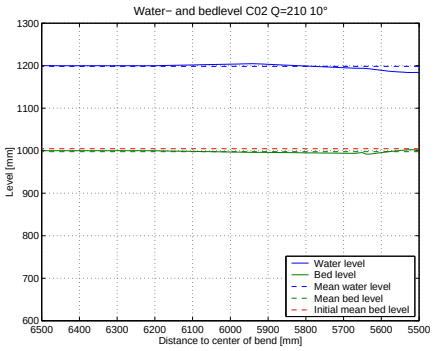
25 °	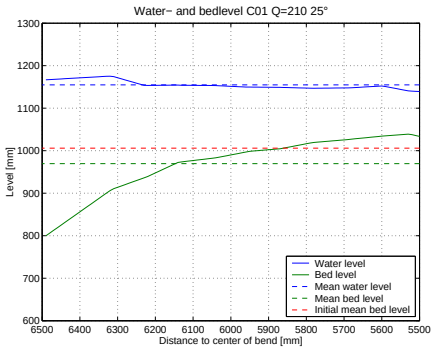	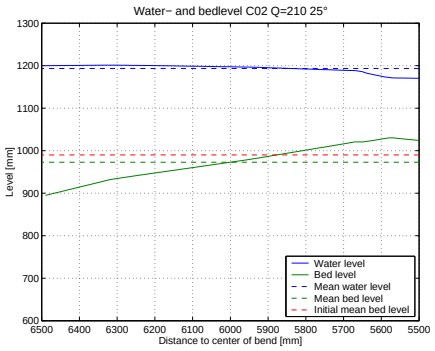
40 °	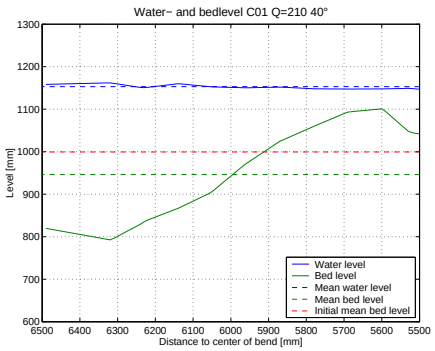	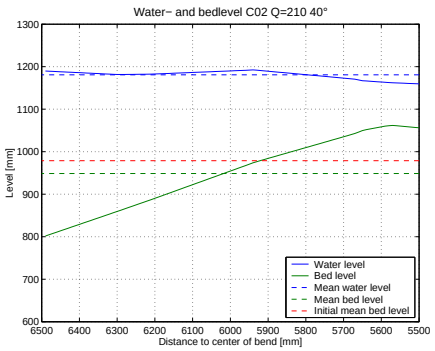

Pos.	Smooth wall (Hersberger)	Undulated wall
55 °	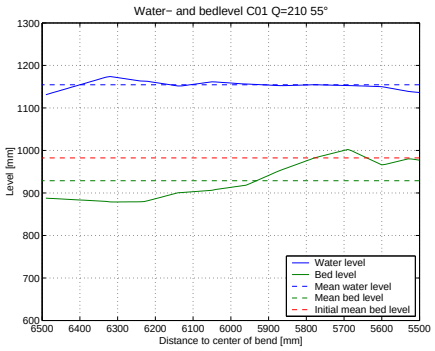	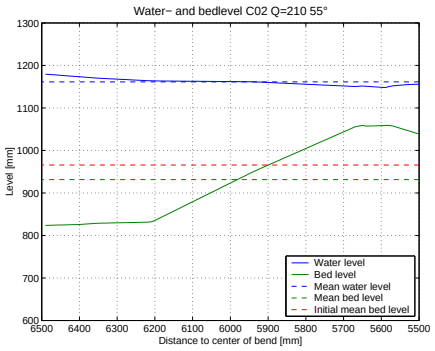
70 °	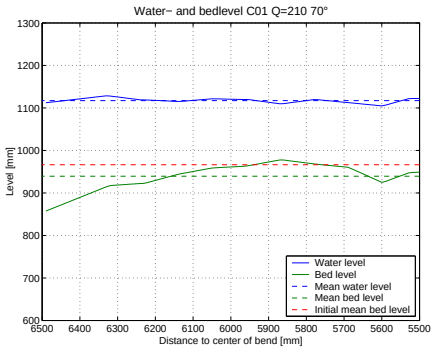	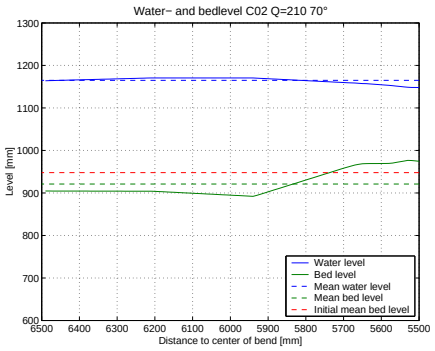
85 °	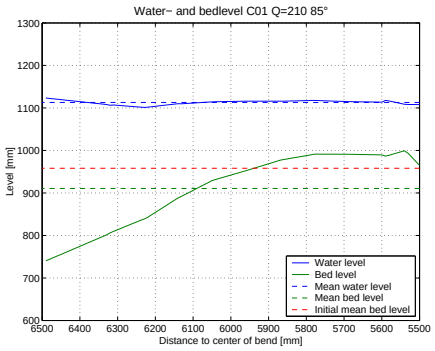	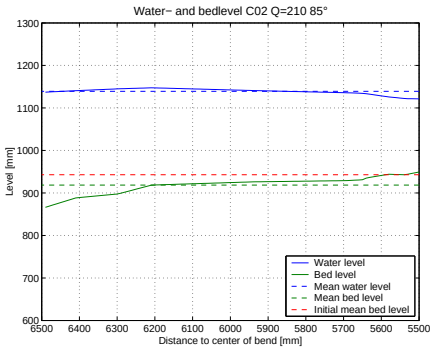
1m	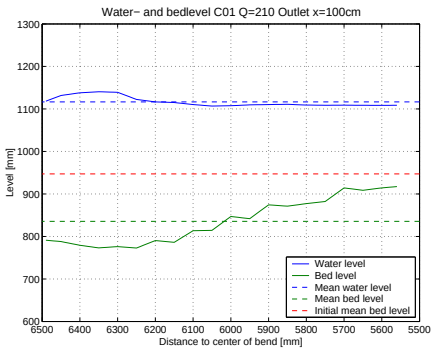	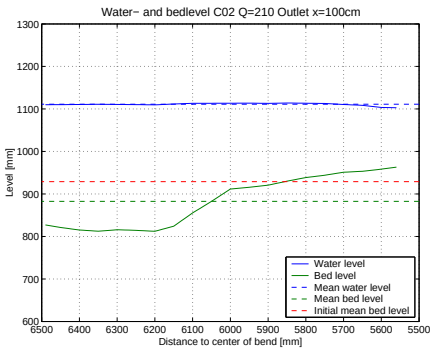

E.7 Cross section at $S_0 = 0.35\%$ and $Q = 150l/s$

Pos.	Smooth wall (Hersberger)	Undulated wall
-1m	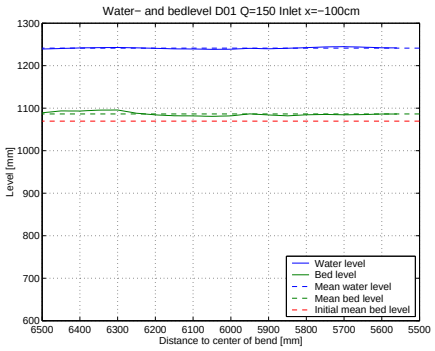	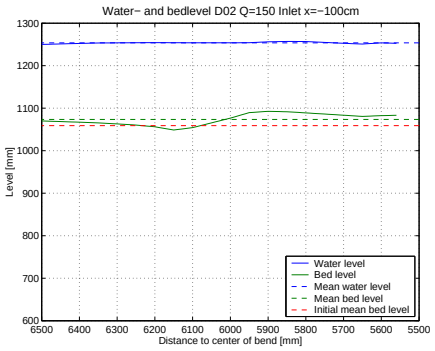
10 °	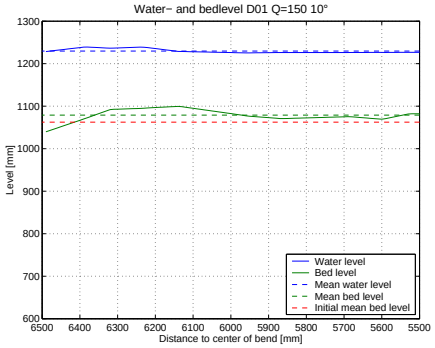	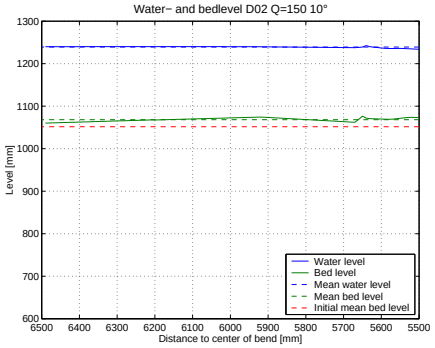
25 °	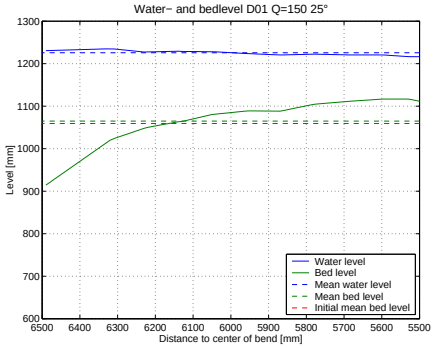	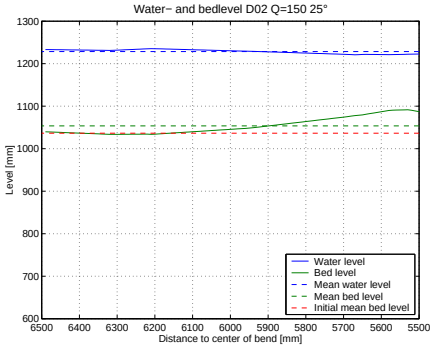
40 °	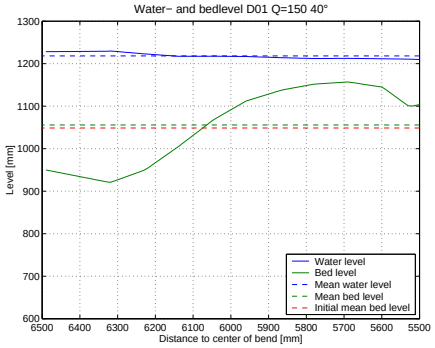	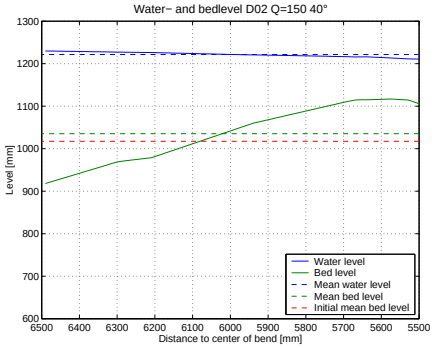

Pos.	Smooth wall (Hersberger)	Undulated wall
55 °	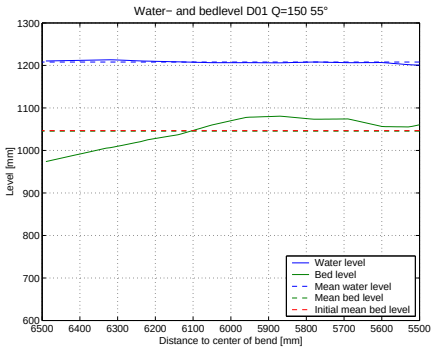	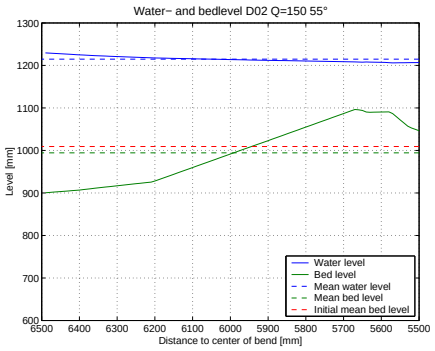
70 °	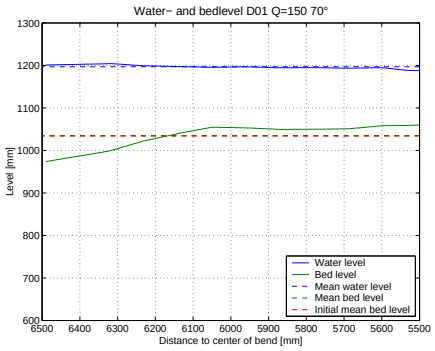	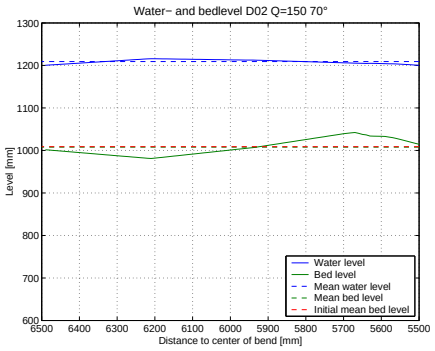
85 °	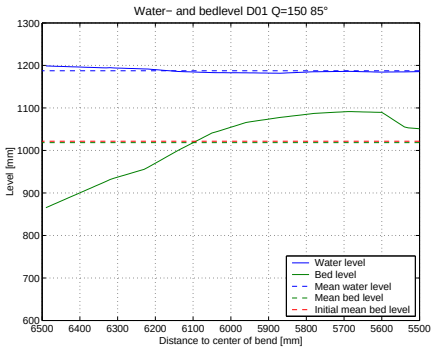	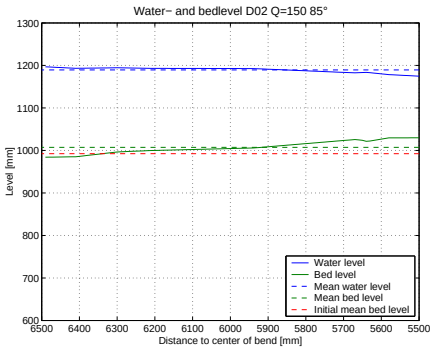
1m	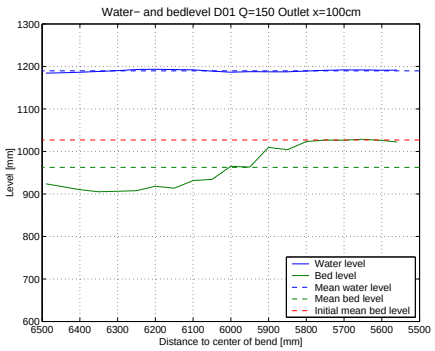	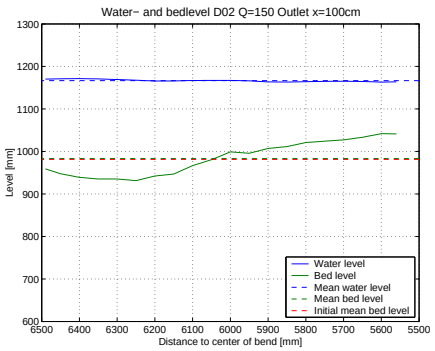

E.8 Cross section at $S_0 = 0.35\%$ and $Q = 180l/s$ or $Q = 190l/s$

Pos.	Smooth wall (Hersberger)	Undulated wall
-1m	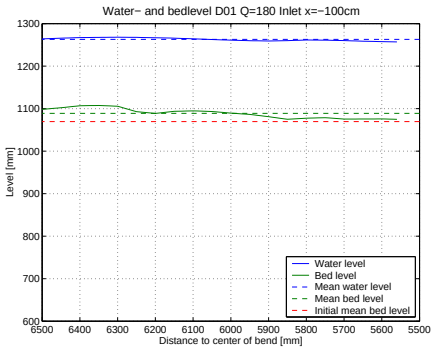	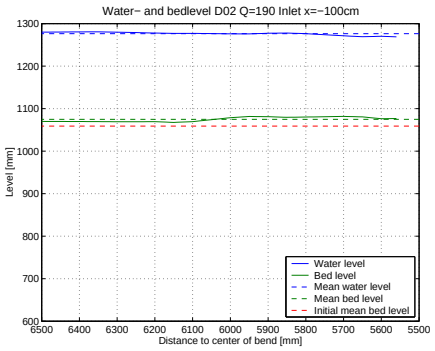
10 °	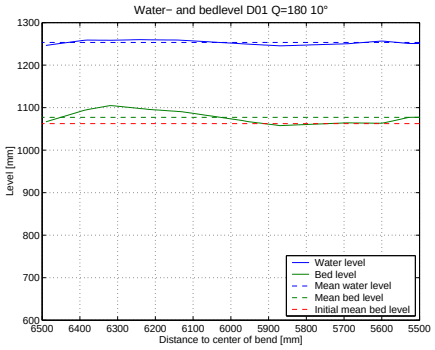	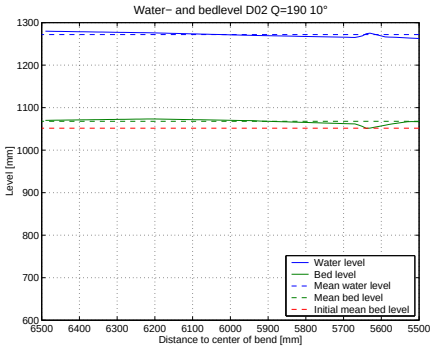
25 °	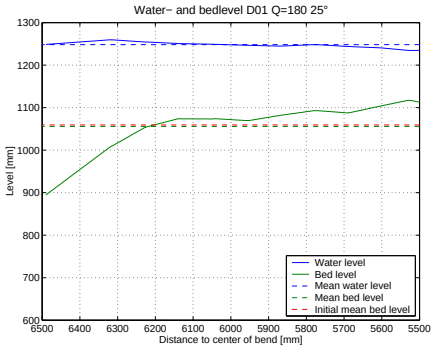	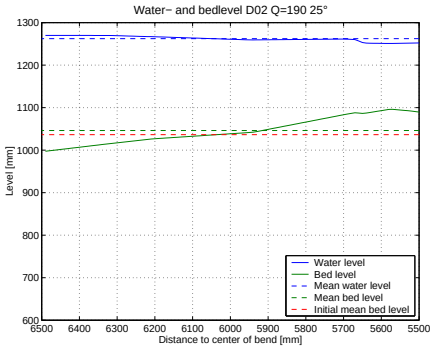
40 °	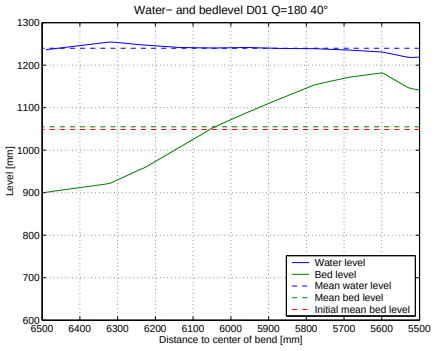	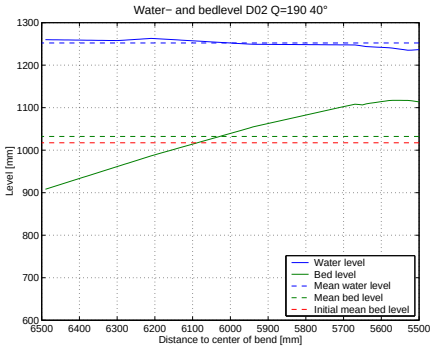

Pos.	Smooth wall (Hersberger)	Undulated wall
55 °	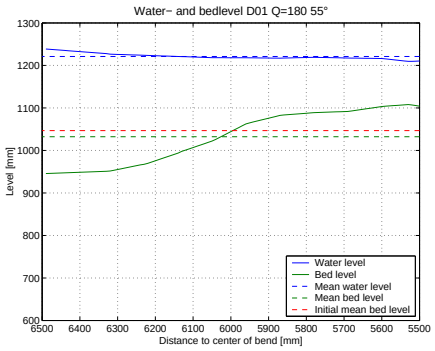	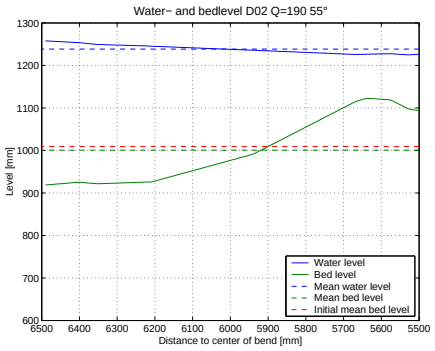
70 °	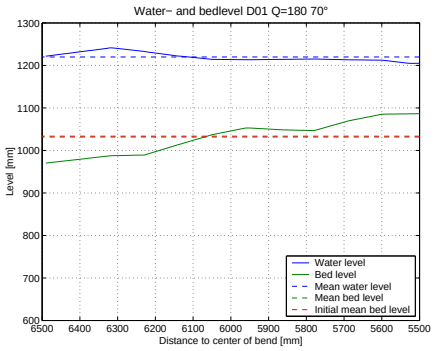	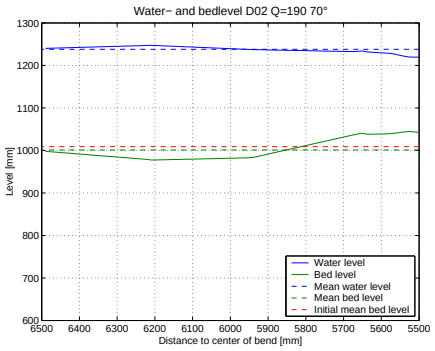
85 °	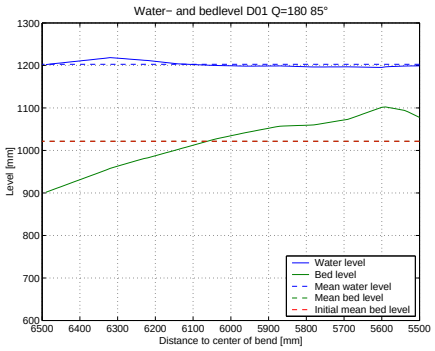	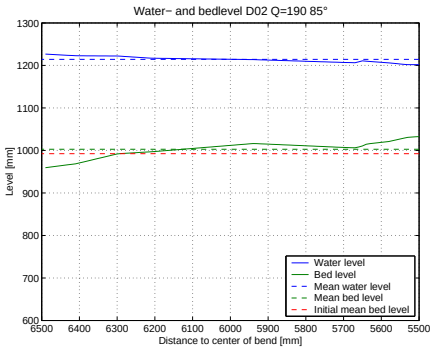
1m	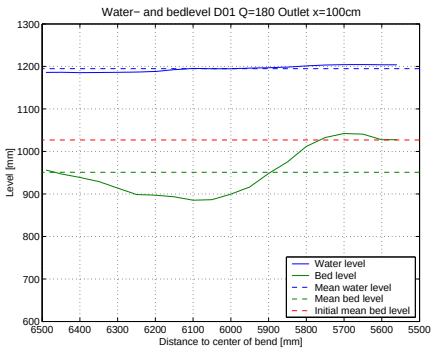	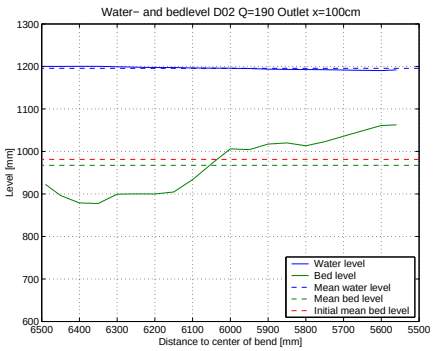

E.9 Cross section at $S_0 = 0.35\%$ and $Q = 210l/s$

Pos.	Smooth wall (Hersberger)	Undulated wall
-1m	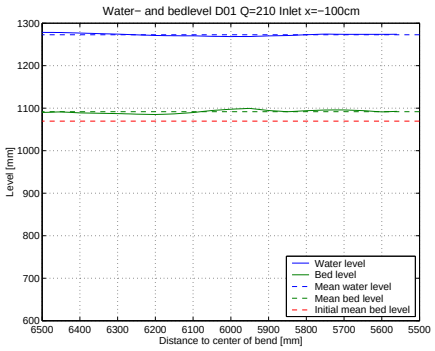	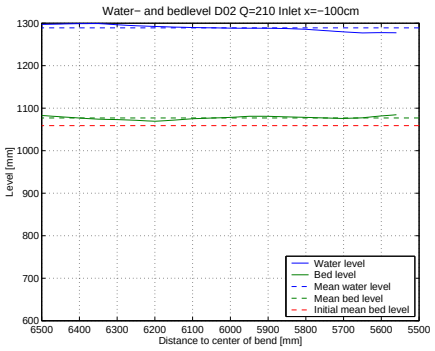
10 °	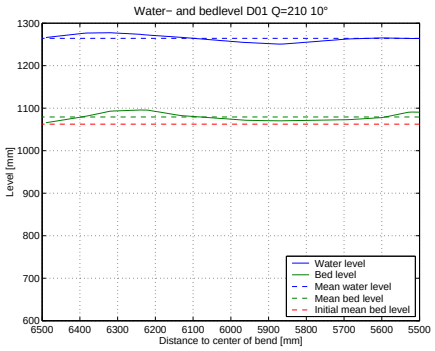	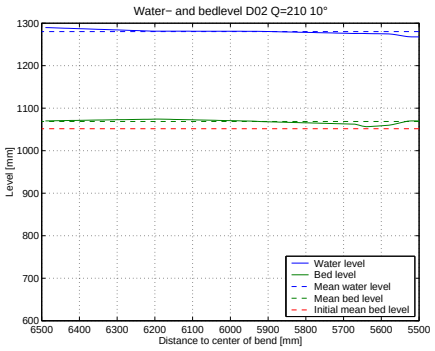
25 °	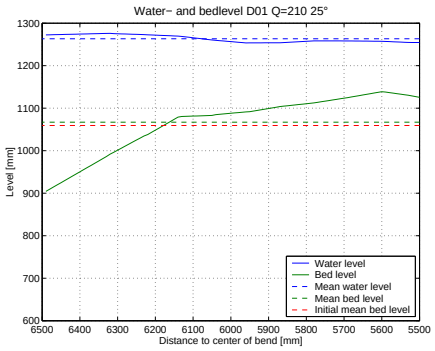	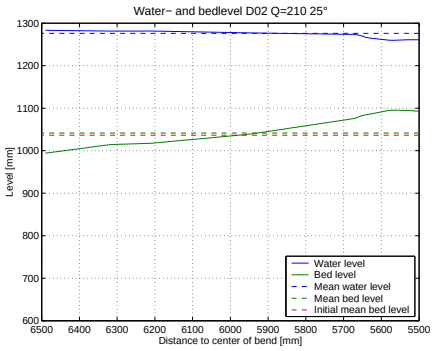
40 °	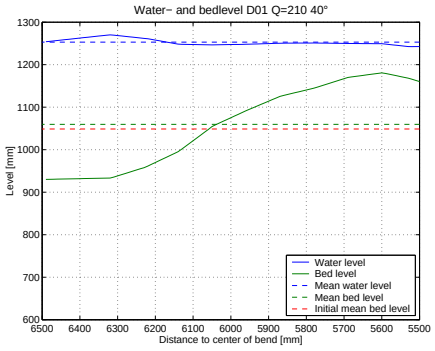	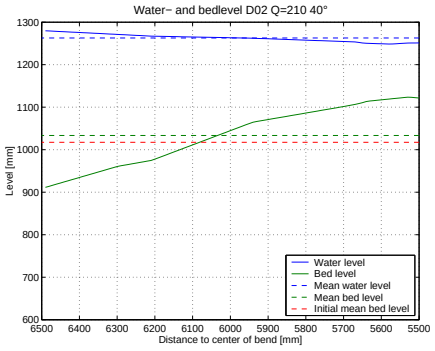

Pos.	Smooth wall (Hersberger)	Undulated wall
55 °	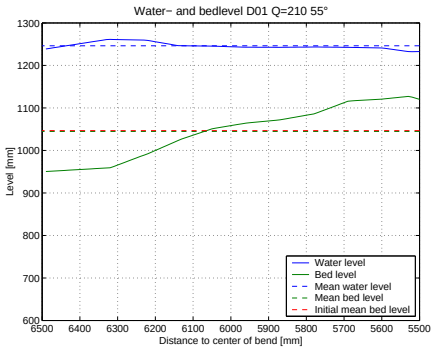	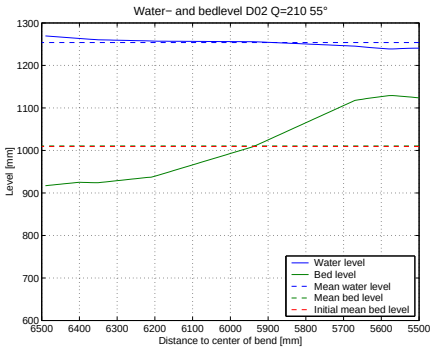
70 °	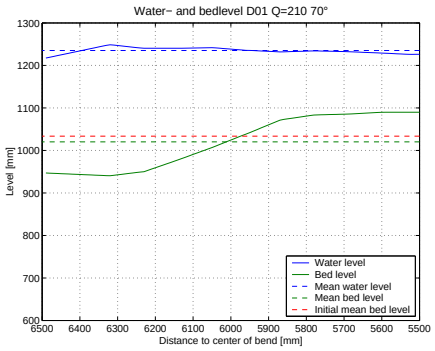	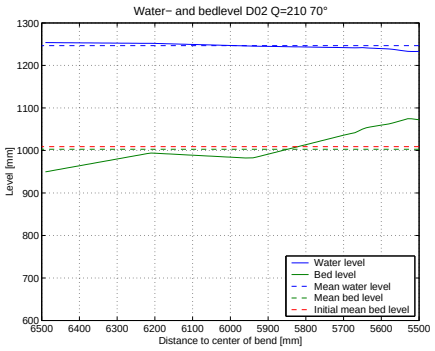
85 °	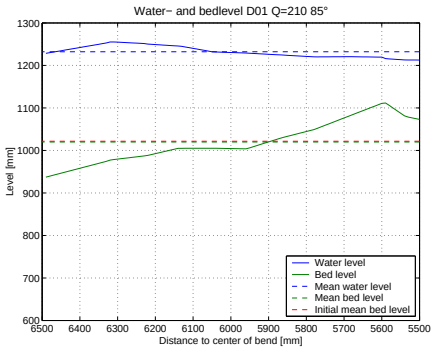	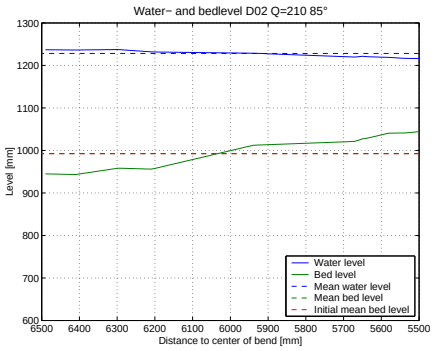
1m	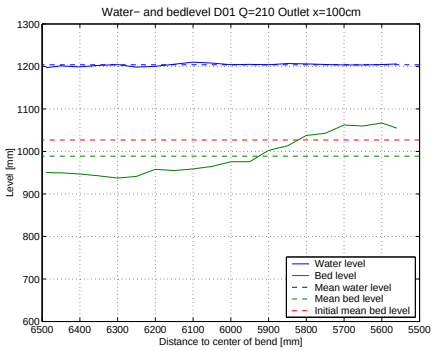	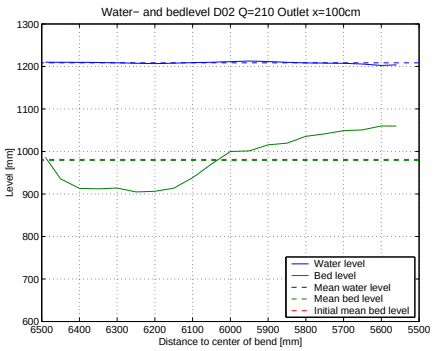

Appendix F

Reference water level

This Appendix gives the description of the reference water level proposed (except the selected one) and the graphic representation of the mean water level by section along the channel, the reference water surface and the difference between them (the right axis). More information can be found at the Section 4.2.1.

R1 Reference water surface has a constant slope from -4 m upstream (section A) to 3 m downstream the bend (section B). The water reference level over the cross section is constant (see Fig. F.1).

The elevation of the section A and B is the average of $H_w(i)$ of 21 sections around the section. The sections A and B were not taken near the extremities of the channel to avoid the influence of the boundary conditions.

$$H_{wA} = \sum_{i=A-10}^{A+10} \frac{H_w(i)}{21}$$

and

$$H_{wB} = \sum_{i=B-10}^{B+10} \frac{H_w(i)}{21}$$

The equation of the water reference level is:

$\forall i = 1, n$

$$\overline{H_w}(i) = H_{wA} - \frac{H_{wA} - H_{wB}}{l} \cdot i\Delta x \tag{F.1}$$

where $l = 4 + \frac{2 \cdot \Pi \cdot R}{4} + 3$, $R_c = 6m$ and $\Delta x = 0.01m$

R2 Reference water level corresponds to three planes with constant slope from -4 m upstream of the bend to 0°, from 0° to 90° and from 90° to 3 m downstream of the bend. The reference water level at the sections A and B were calculated as for case R1. The level at the sections C and D is the average of $H_w(i)$ of three sections around C and D. The water level at the cross section is constant (see Fig. F.2)

$$H_{wA} = \sum_{i=A-10}^{A+10} \frac{H_w(i)}{21} \qquad H_{wC} = \sum_{i=C-1}^{C+1} \frac{H_w(i)}{3}$$

$$H_{wD} = \sum_{i=D-1}^{D+1} \frac{H_w(i)}{3} \qquad H_{wB} = \sum_{i=B-10}^{B+10} \frac{H_w(i)}{21}$$

The reference water level equation is:

$$\overline{H_{1w}}(i) = H_{wA} - \frac{H_{wA} - H_{wC}}{l_1} \cdot i\Delta x \tag{F.2}$$

from -4 m to 0°

$$\overline{H_{2w}}(i) = H_{wC} - \frac{H_{wC} - H_{wD}}{l_2} \cdot (i\Delta x - l_1) \tag{F.3}$$

from 0° to 90°

$$\overline{H_{3w}}(i) = H_{wD} - \frac{H_{wD} - H_{wB}}{l_3} \cdot (i\Delta x - l_1 - l_2) \tag{F.4}$$

from 90° to 3 m

where $l_1 = 4$, $l_2 = \frac{2 \cdot \Pi \cdot R}{4}$, $l_1 = 3$, $R_c = 6m$ and $\Delta x = 0.01m$

R3 The reference water level is formed by straight lines from -4m upstream the bend to 3m downstream the bend. The level at the cross section is not constant, it's a function of y (see Fig.F.3).

$\forall j = 1, m$

$$H_{wA}(j) = \sum_{j=A-10}^{A+10} \frac{H_w(i,j)}{21} \qquad H_{wB}(j) = \sum_{j=B-10}^{B+10} \frac{H_w(i,j)}{21}$$

The reference water level equation is:

$\forall i = 1, n \; \forall j = 1, 101$

$$\overline{H_w}(i,j) = H_{wA}(j) - \frac{H_{wA}(j) - H_{wB}(j)}{l} \cdot i\Delta x \tag{F.5}$$

where $l = 4 + \frac{2 \cdot \Pi \cdot R}{4} + 3$, $R_c = 6m$ and $\Delta x = 0.01m$

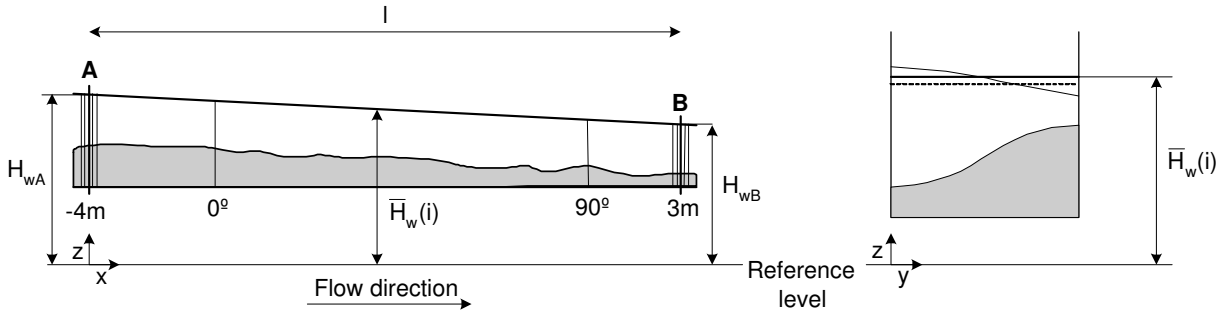

Figure F.1: Schema of the reference water level R1, LEFT: longitudinal profile at the axe of the channel, RIGHT: Cross section i

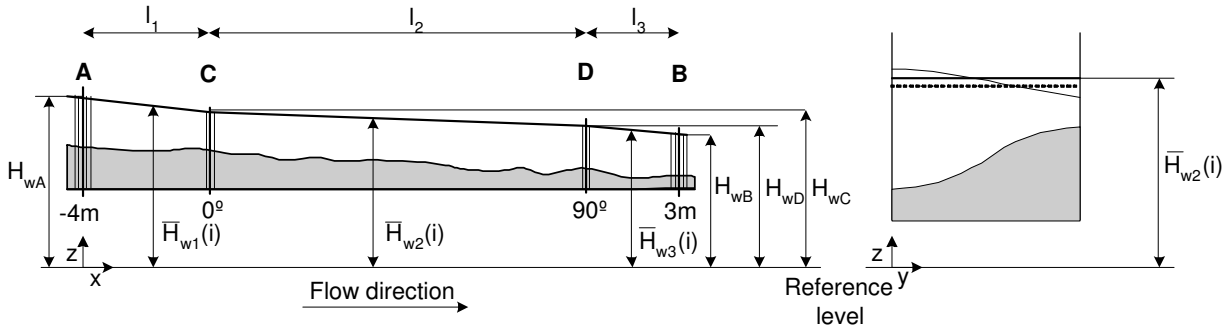

Figure F.2: Schema of the reference water level R2, LEFT: longitudinal profile at the axe of the channel, RIGHT: Cross section i

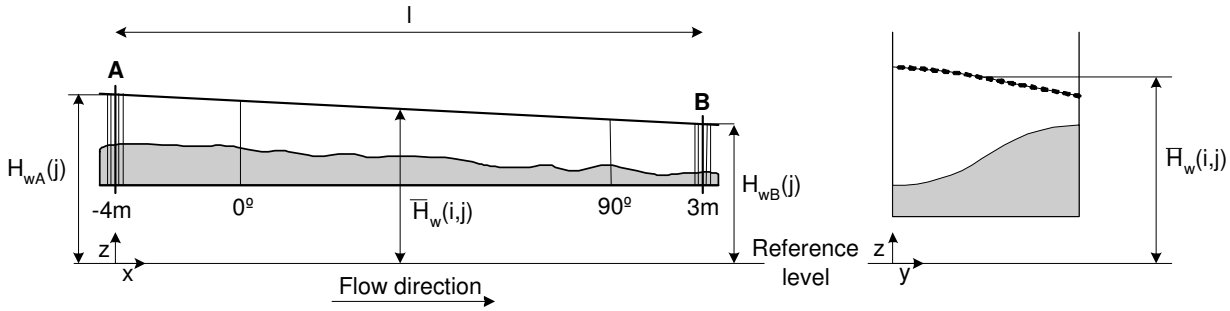

Figure F.3: Schema of the water reference level R3, LEFT: longitudinal profile j, RIGHT: Cross section i

Graphic representation of reference water surface

Description of the graphic representation of the mean water levels, the reference water surface and the difference between them.

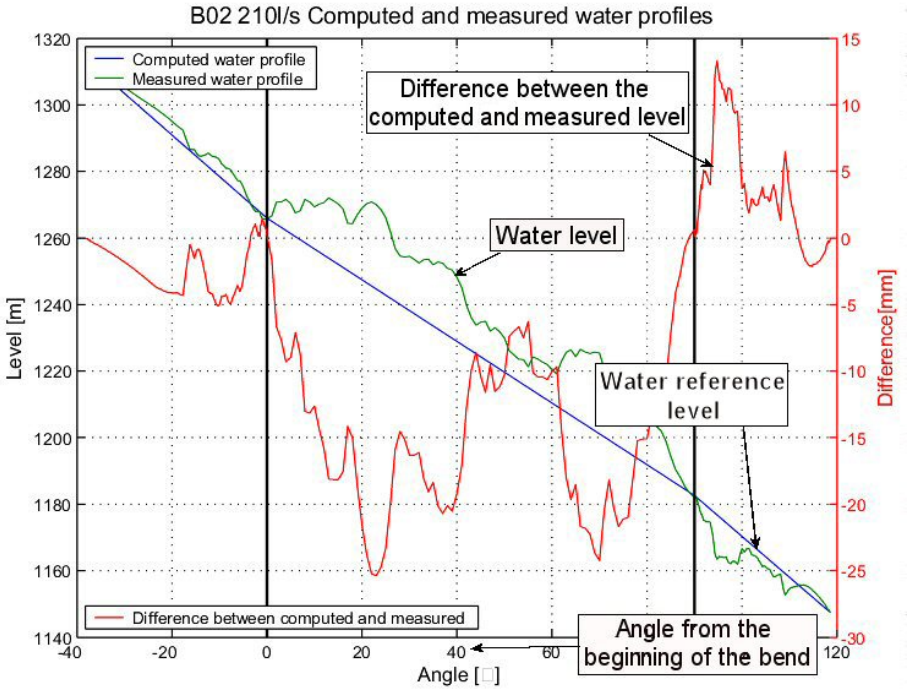

F.1 Water reference level R1

Smooth wall (Hersberger)	Undulated wall
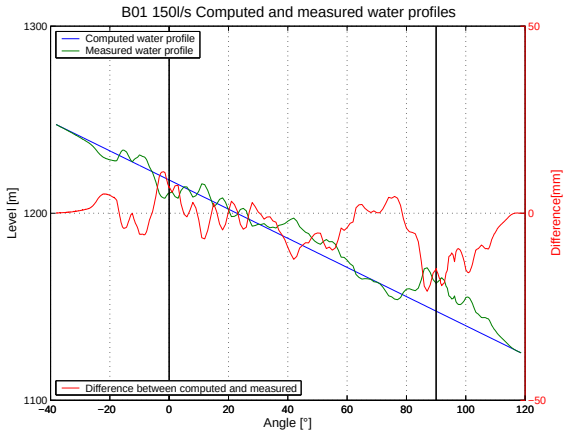	Data non available
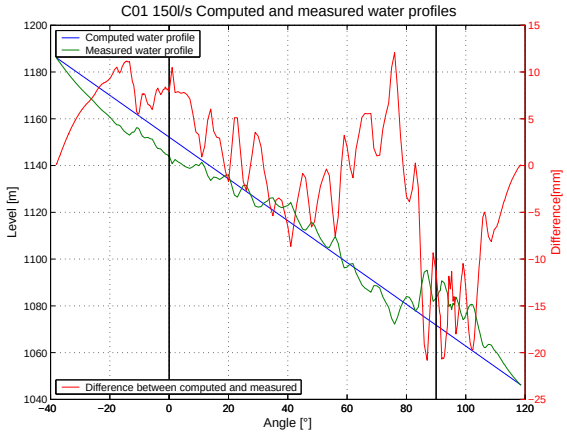	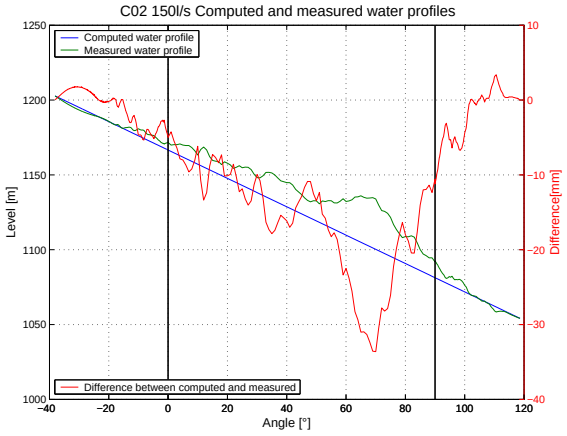
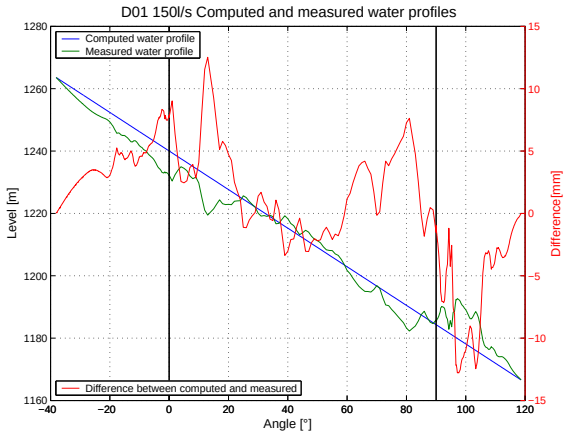	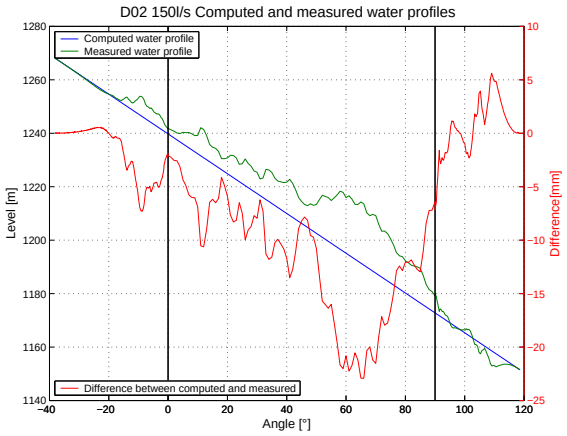

Smooth wall (Hersberger)	Undulated wall
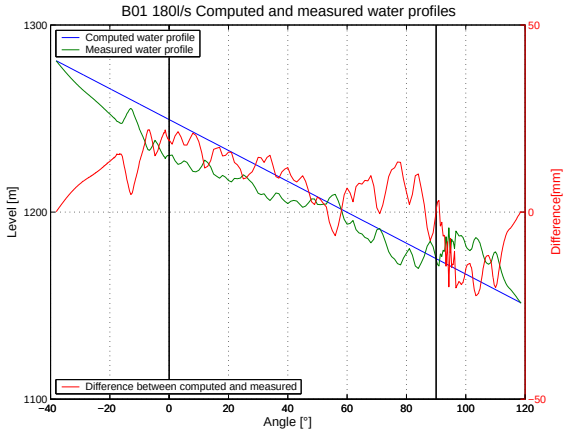	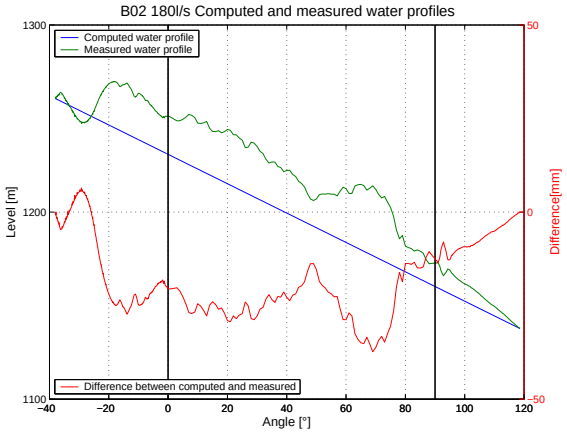
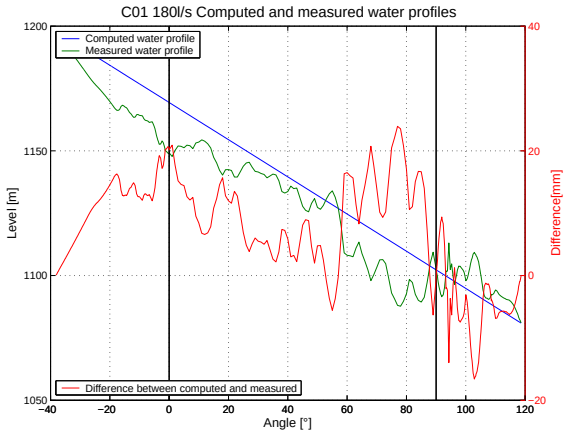	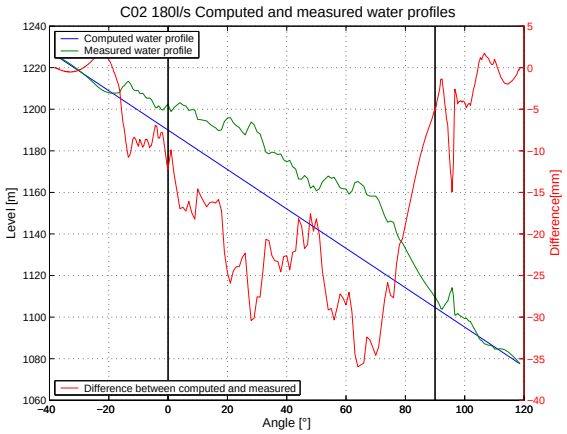
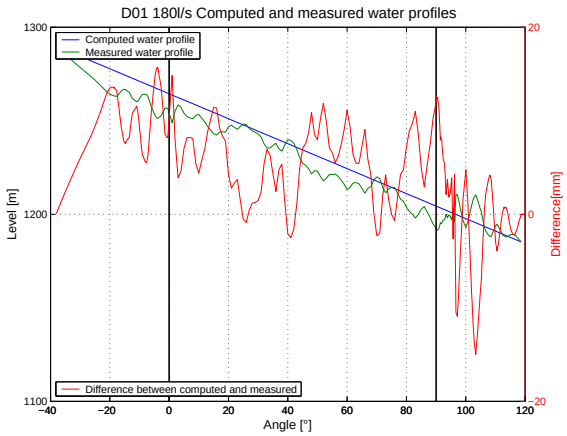	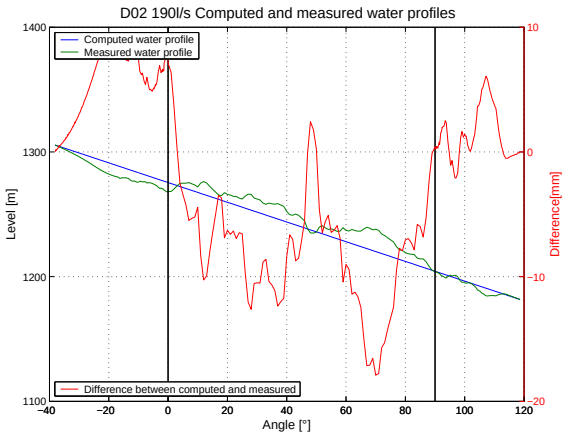

Smooth wall (Hersberger)	Undulated wall
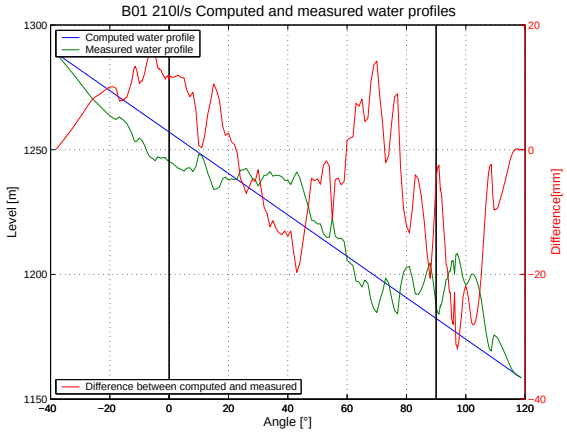	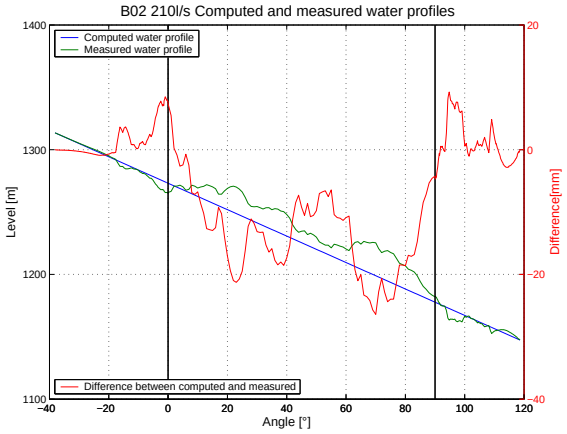
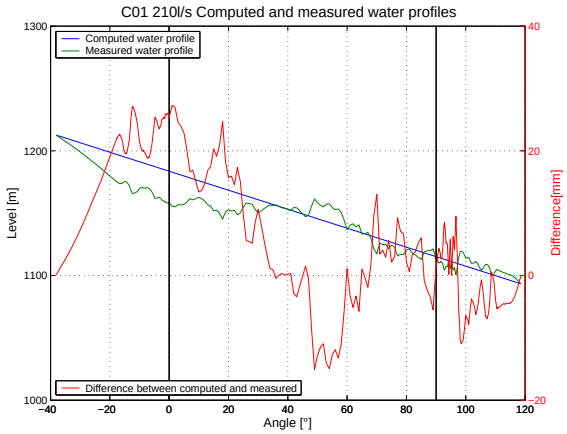	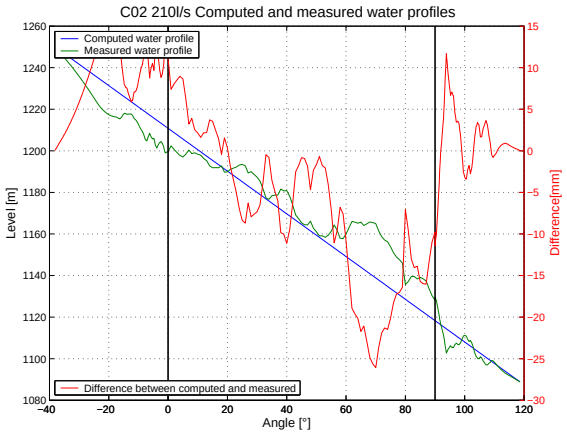
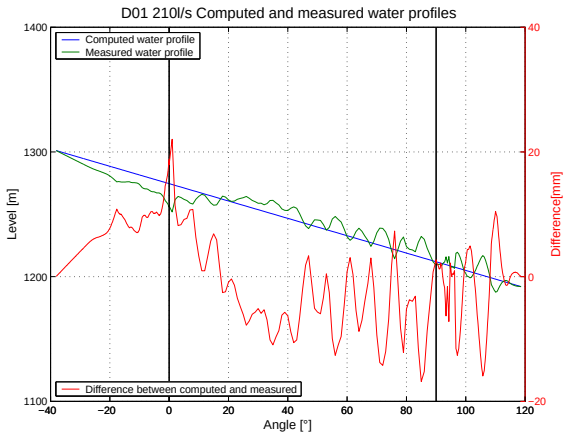	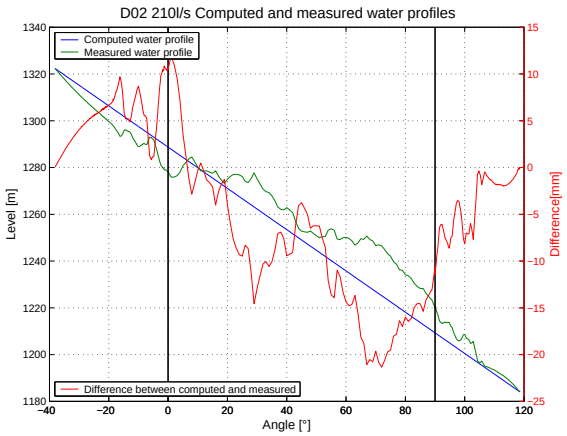

F.2 Water reference level R2

Smooth wall (Hersberger)	Undulated wall
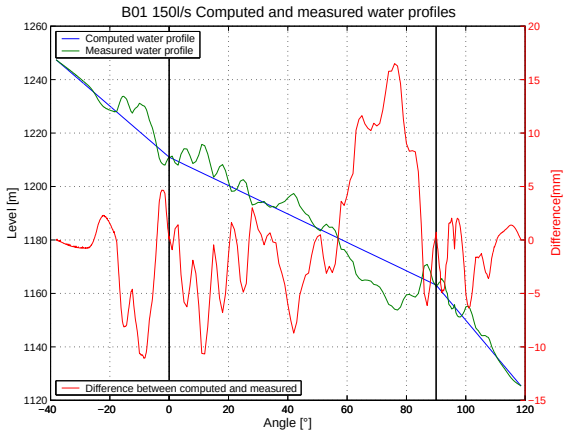	Data non available
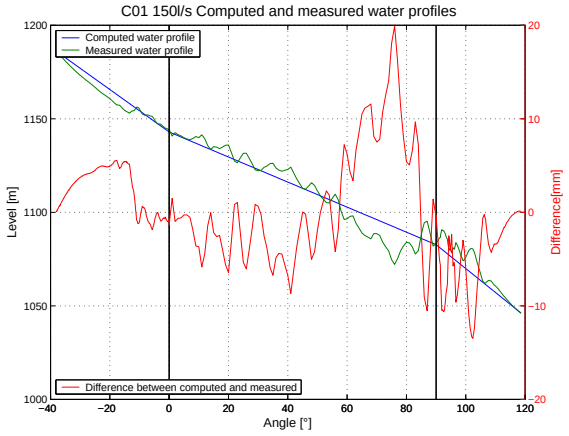	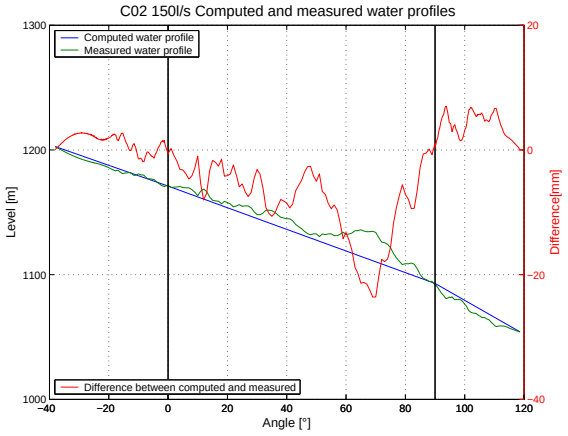
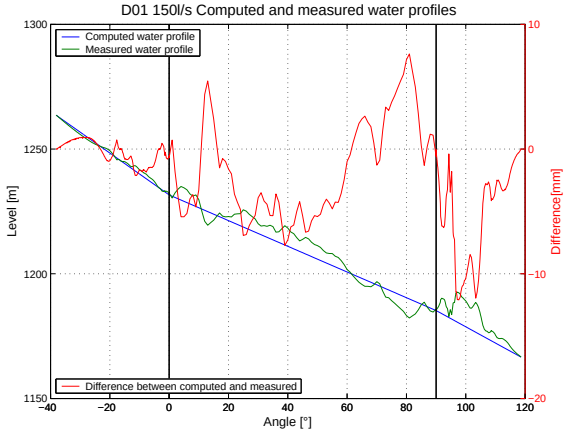	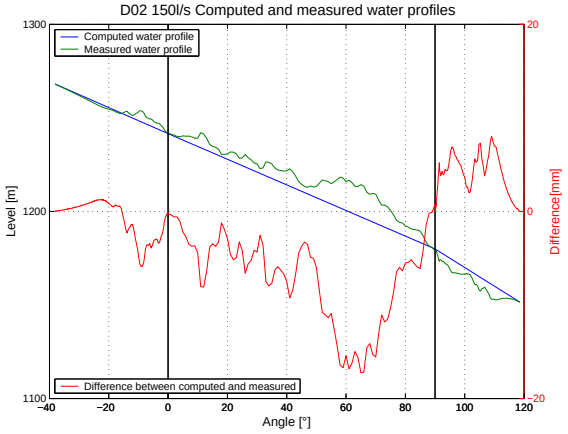

Smooth wall (Hersberger)	Undulated wall
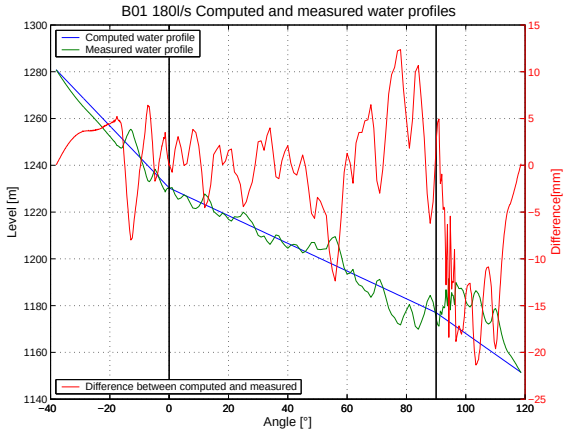	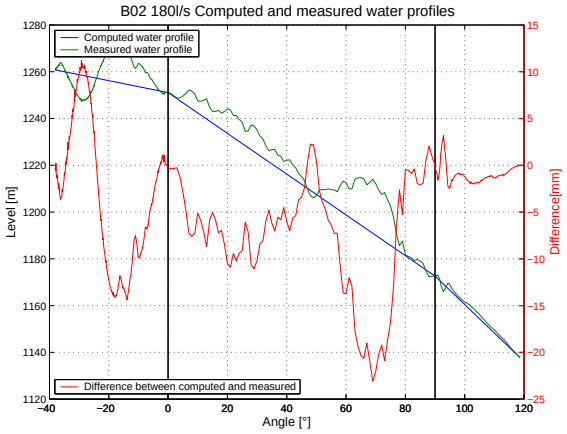
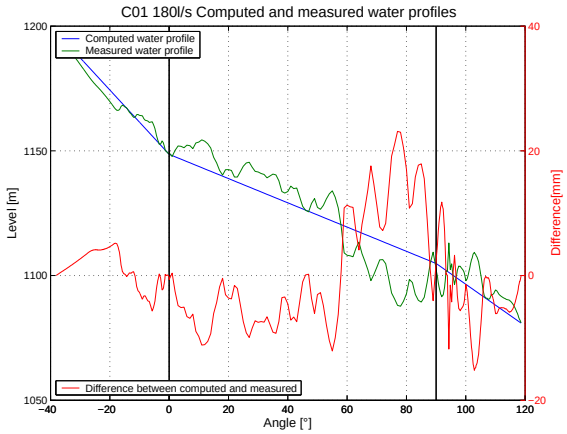	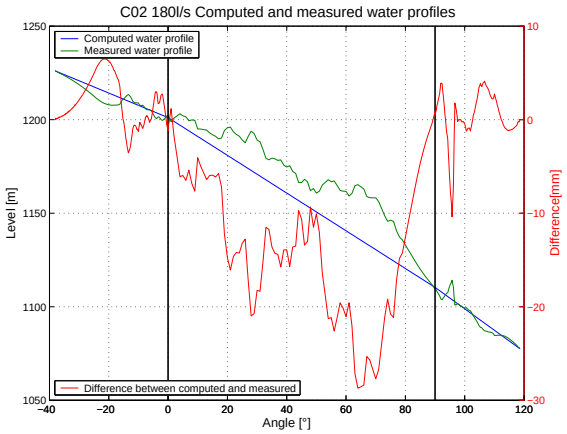
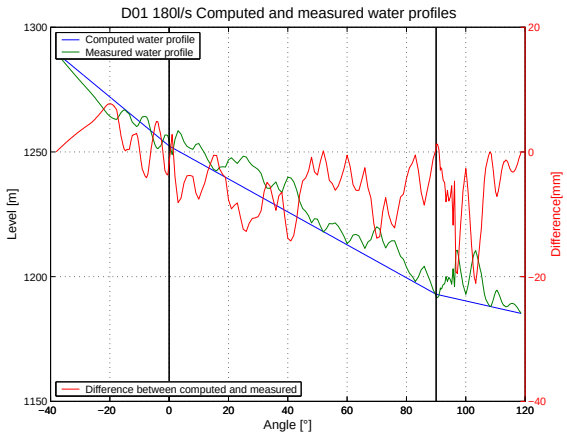	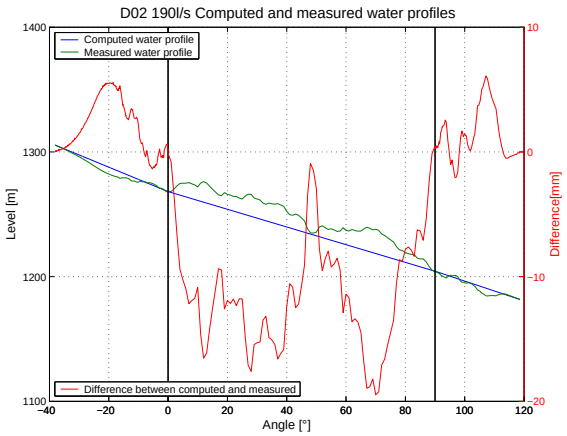

Smooth wall (Hersberger)	Undulated wall
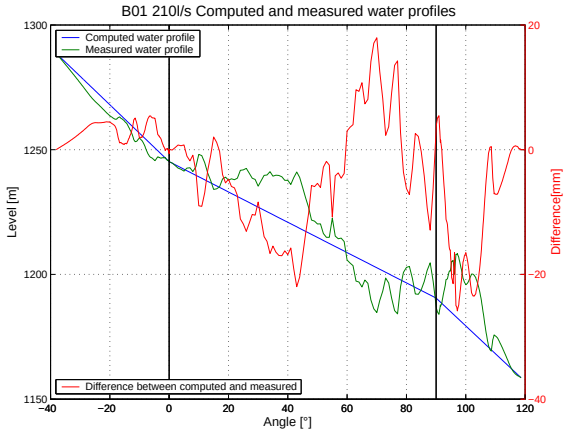	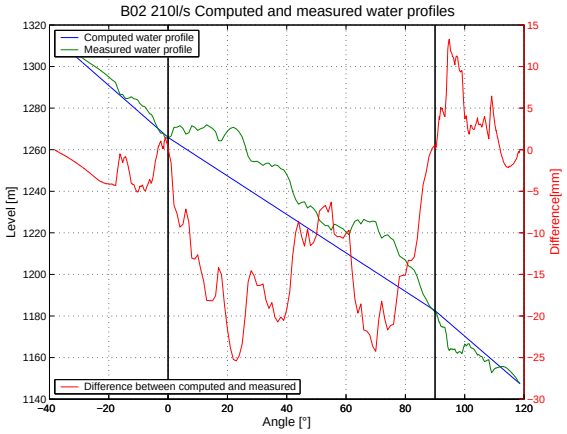
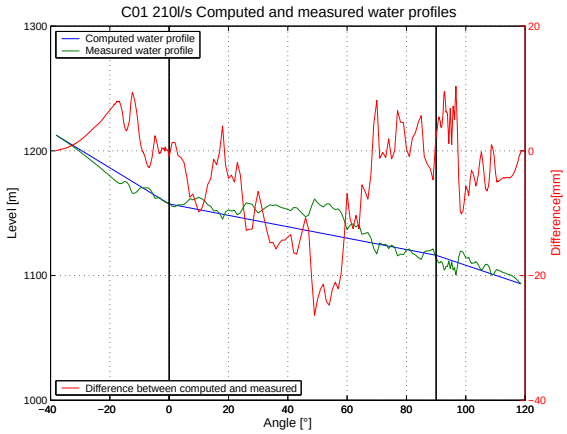	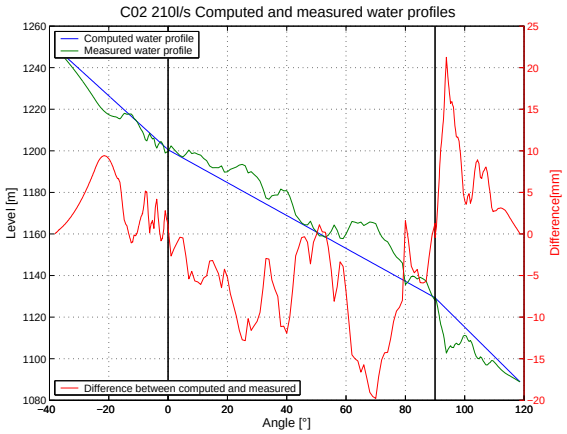
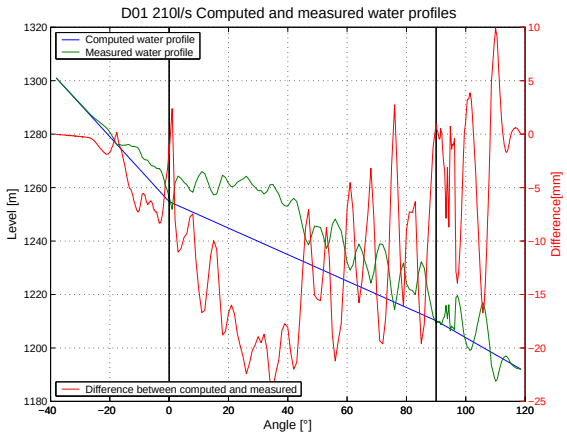	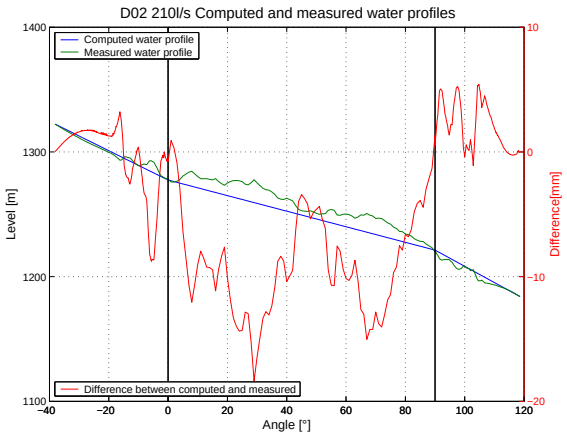

F.3 Water reference level R4

Smooth wall (Hersberger)	Undulated wall
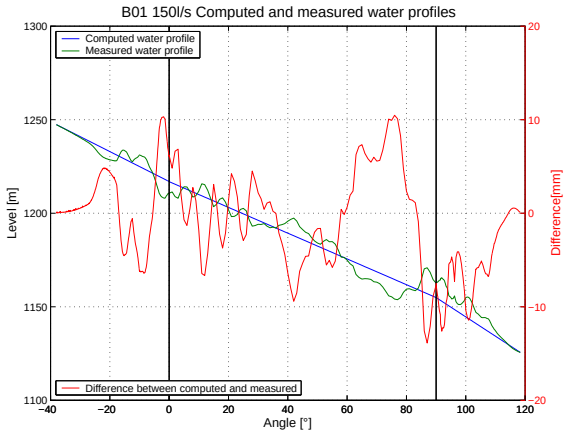	Data non available
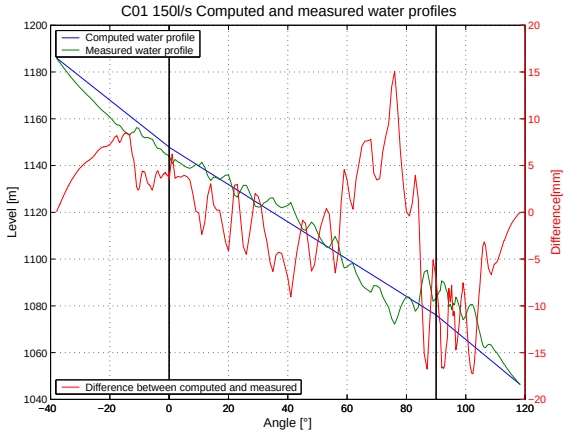	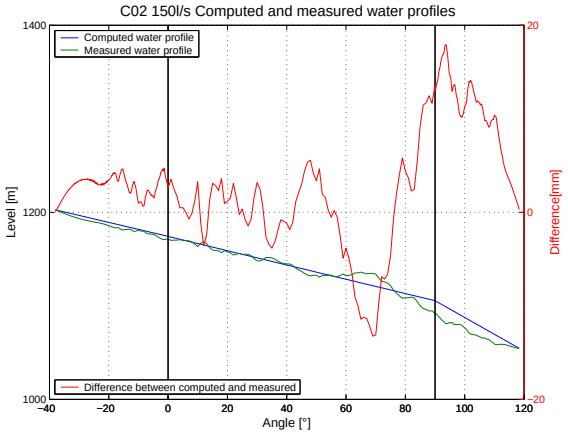
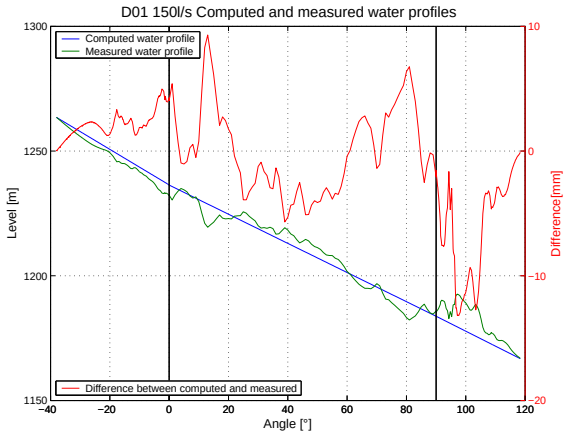	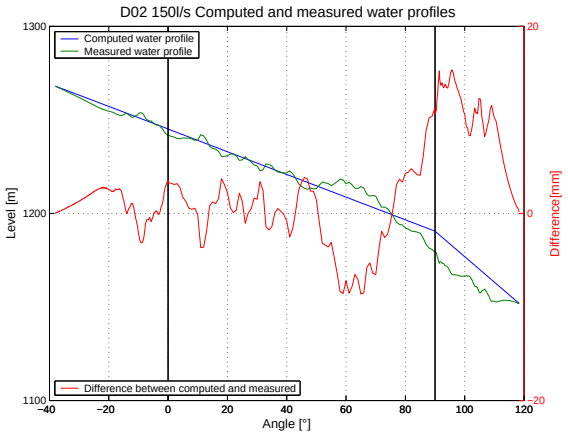

Smooth wall (Hersberger)	Undulated wall
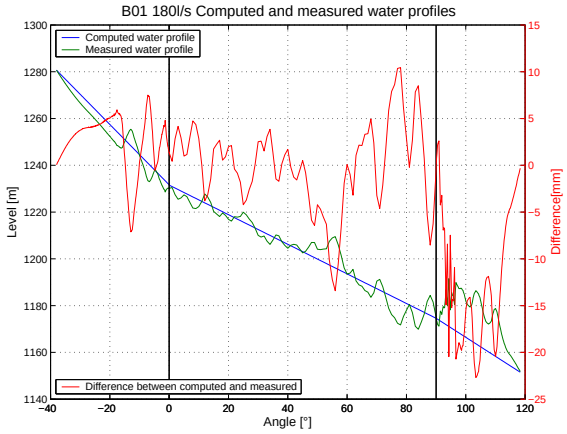	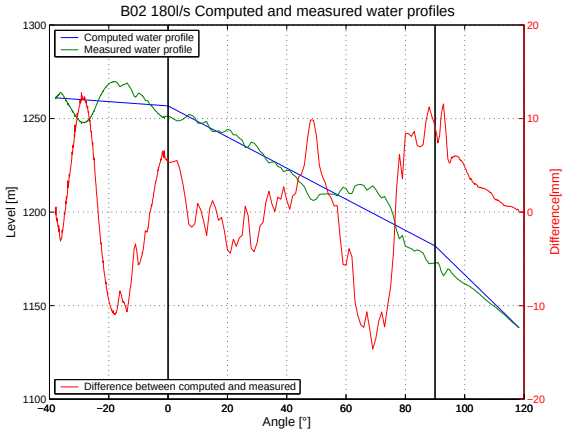
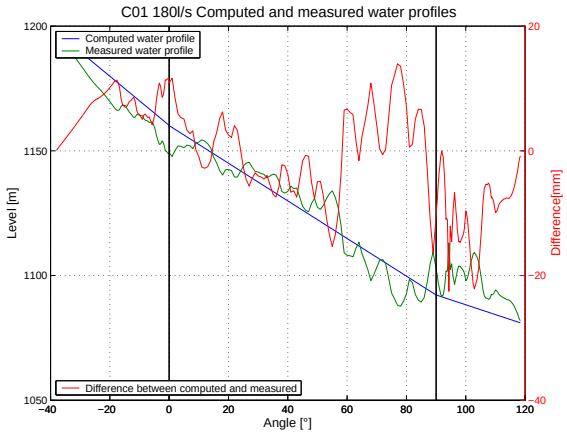	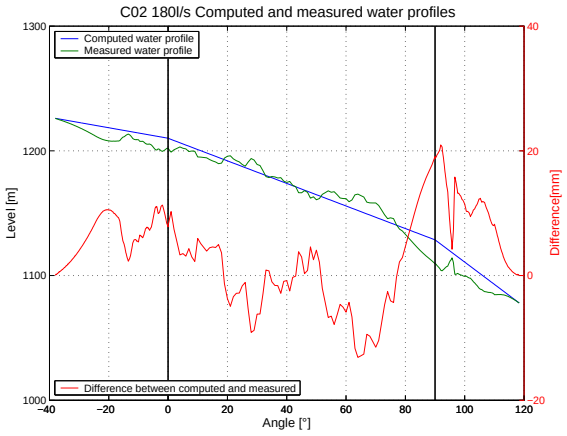
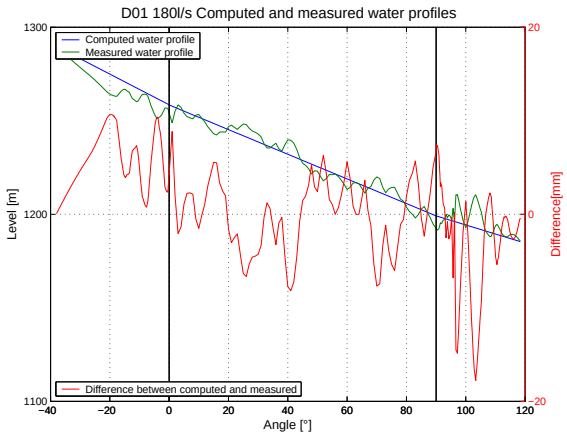	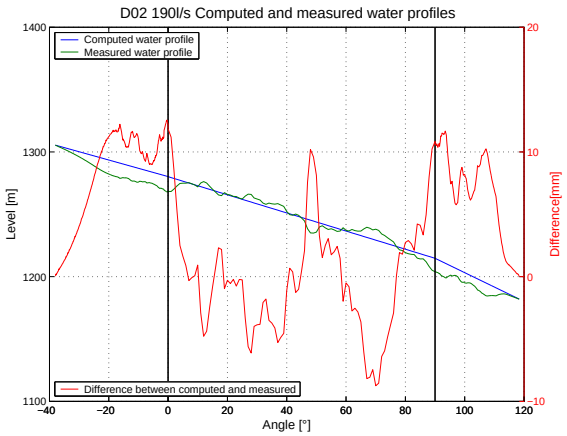

Smooth wall (Hersberger)	Undulated wall
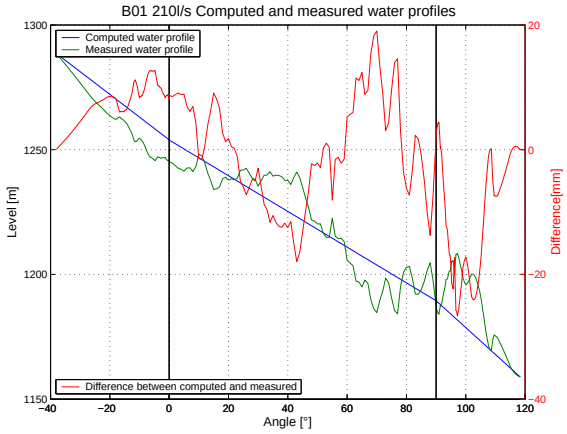	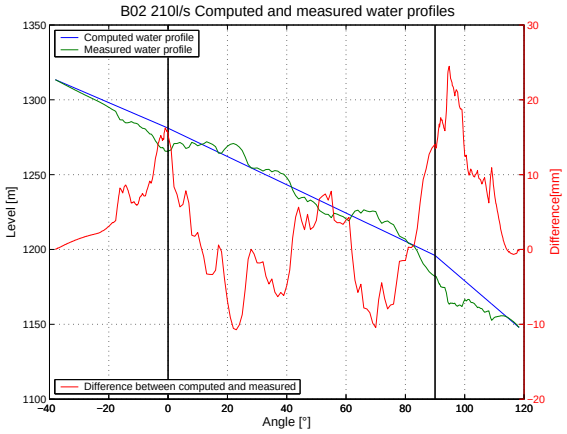
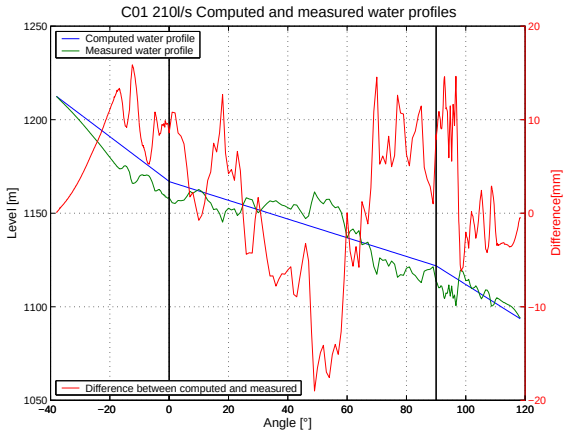	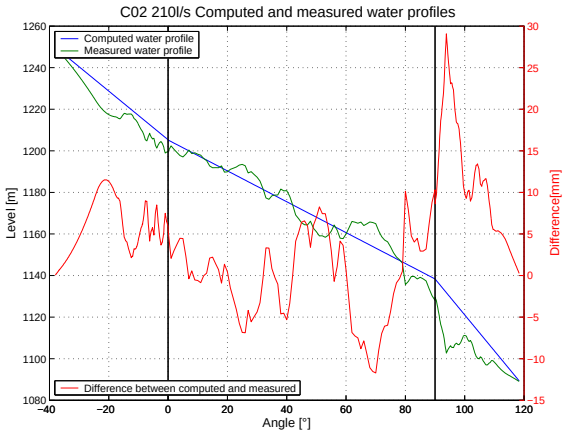
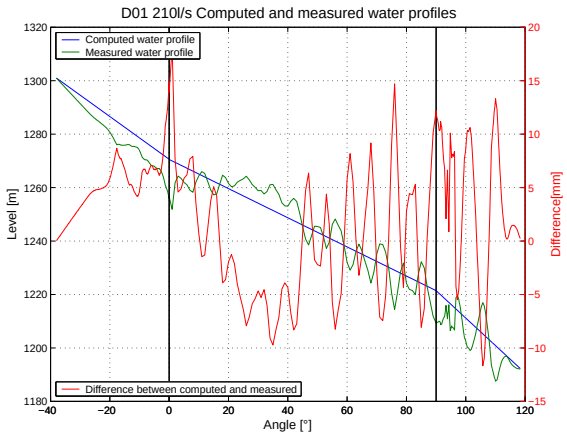	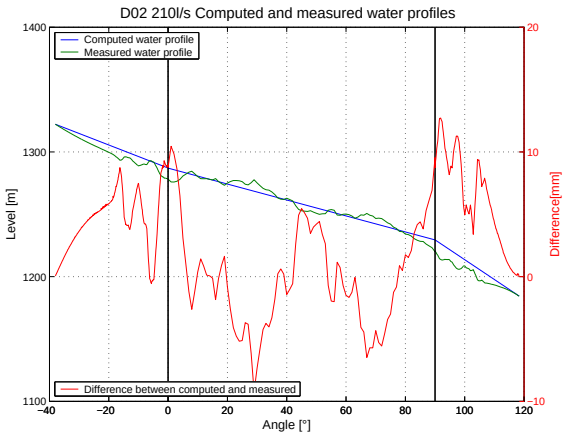

Appendix G

Water surface pictures

This Appendix gives pictures of the water surface of all the tests. More information can be found at the section 4.5.

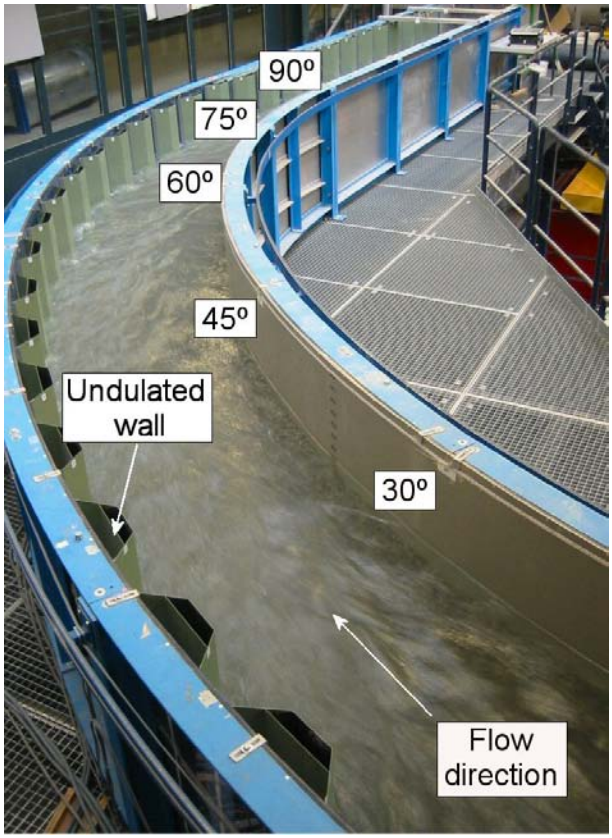

Slope	Q=150l/s	Q=180l/s [1]	Q=210l/s
$0,5\%$	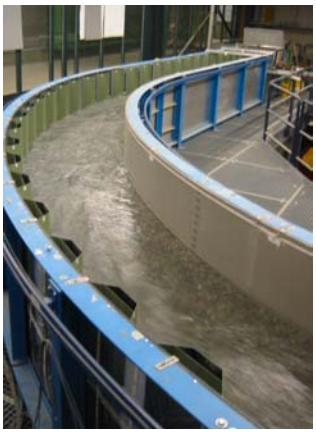	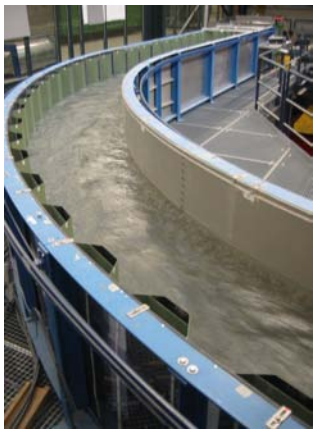	
$0,7\%$	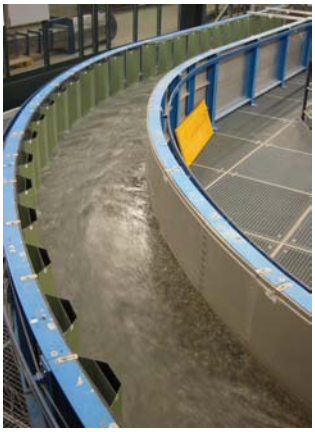	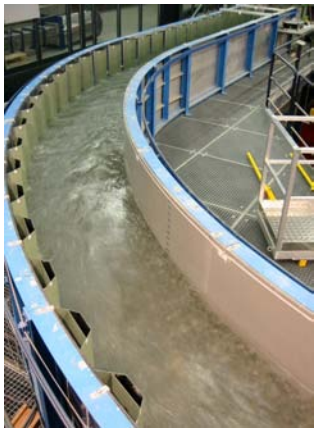	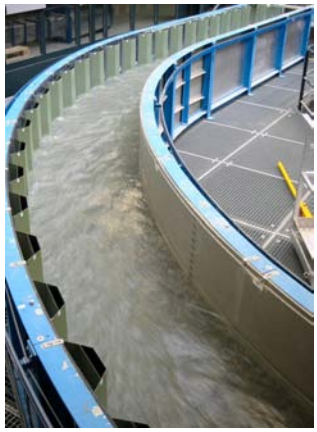
$0,35\%$	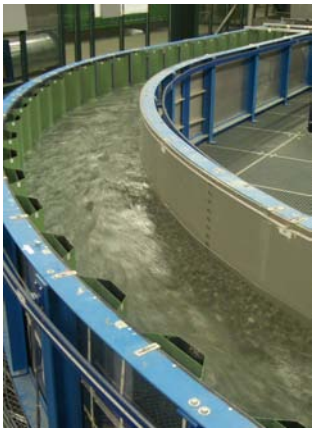	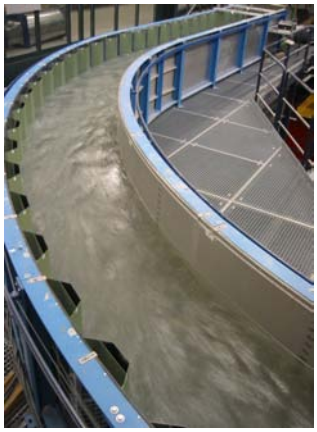	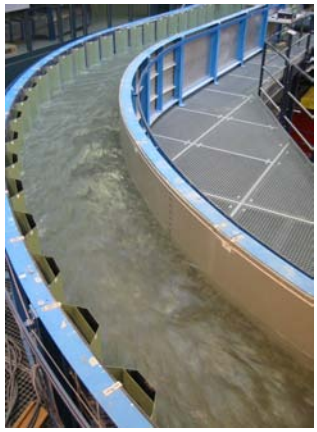

[1]The test with a bed slope of 0,35% has a discharge of 190 l/s

Appendix H

Pictures of the grain size distribution of the bed material

This Appendix gives the pictures of the bed granulometry at the end of the test. The pictures were systematically taken from 0° to 90° every 15° . More information can be found at the Section 4.4.

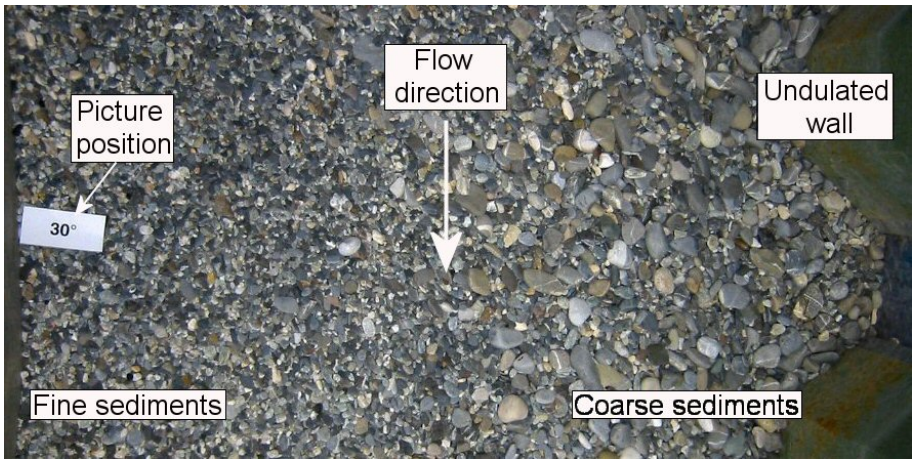

H.1 Channel slope $S_0 = 0.5\%$

Pos.	Q=150l/s	Q=180l/s	Q=210l/s
0°			
15°			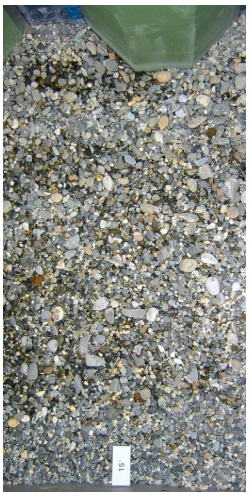
30°			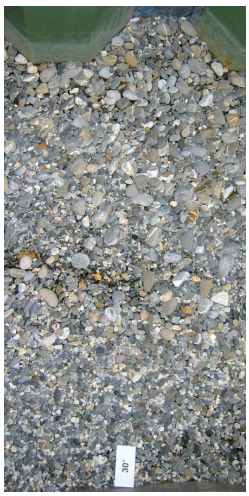
45°			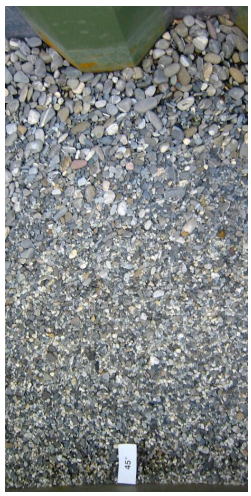

Pos.	Q=150l/s	Q=180l/s	Q=210l/s
60°			
75°			
90°			

H.2 Channel slope $S_0 = 0.7\%$

Pos.	Q=150l/s	Q=180l/s	Q=210l/s
0°		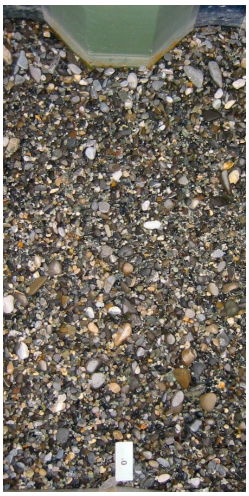	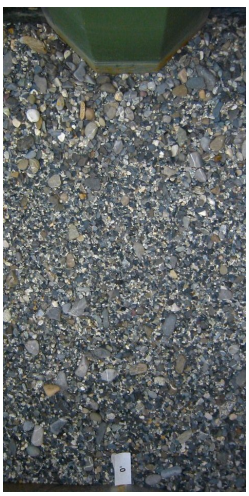
15°			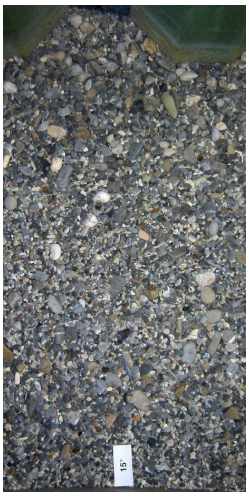
30°		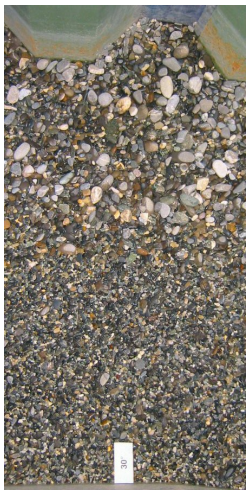	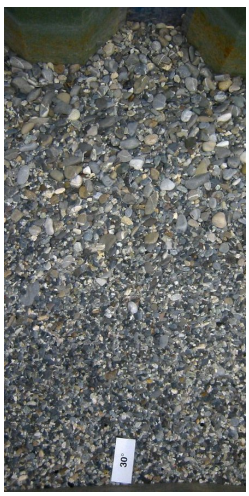
45°	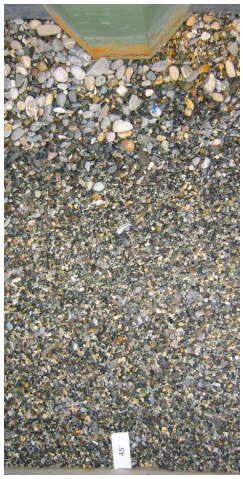	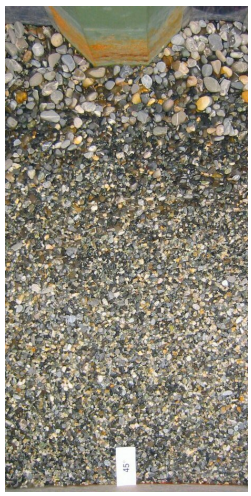	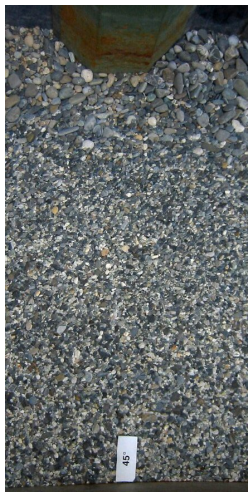

Pos.	Q=150l/s	Q=180l/s	Q=210l/s
60 °			
75 °			
90 °			

H.3 Channel slope $S_0 = 0.35\%$

Pos.	Q=150l/s	Q=190l/s	Q=210l/s
0°		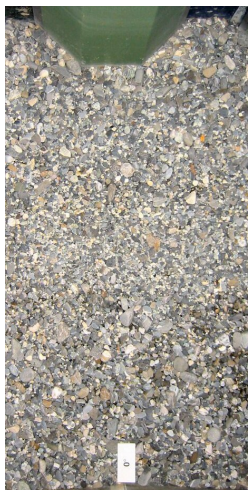	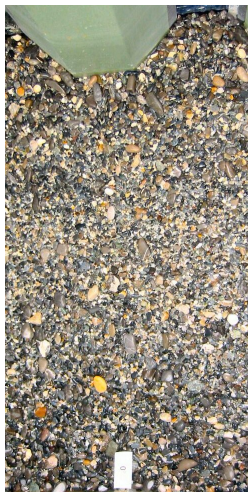
15°		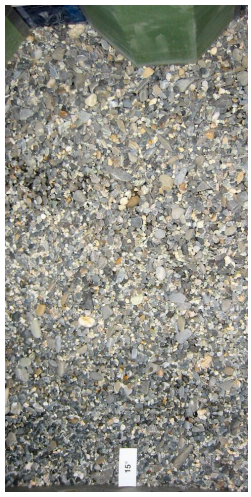	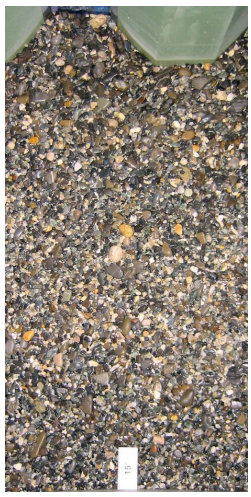
30°		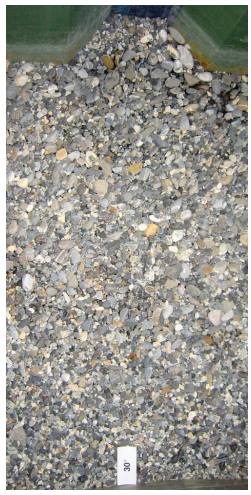	
45°	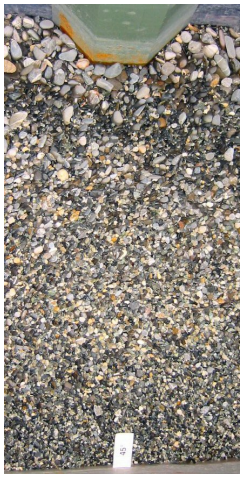		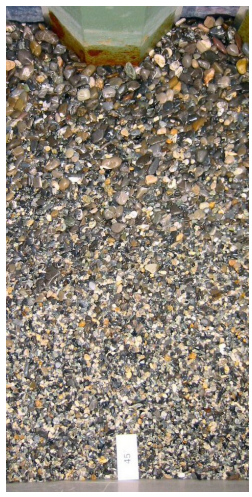

Pos.	Q=150l/s	Q=190l/s	Q=210l/s
60 °			
75 °		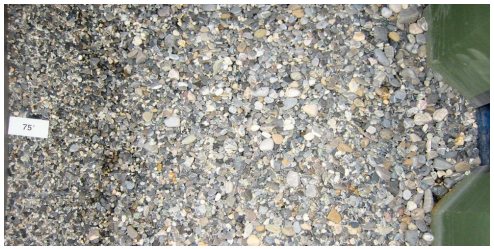	
90 °			

Appendix I

Grain size distribution of the armoring layer

This Appendix gives the grain size distribution of the armoring layer after the test. The samples were taken at 45° and 90° near the inner and the outer side of the bend.

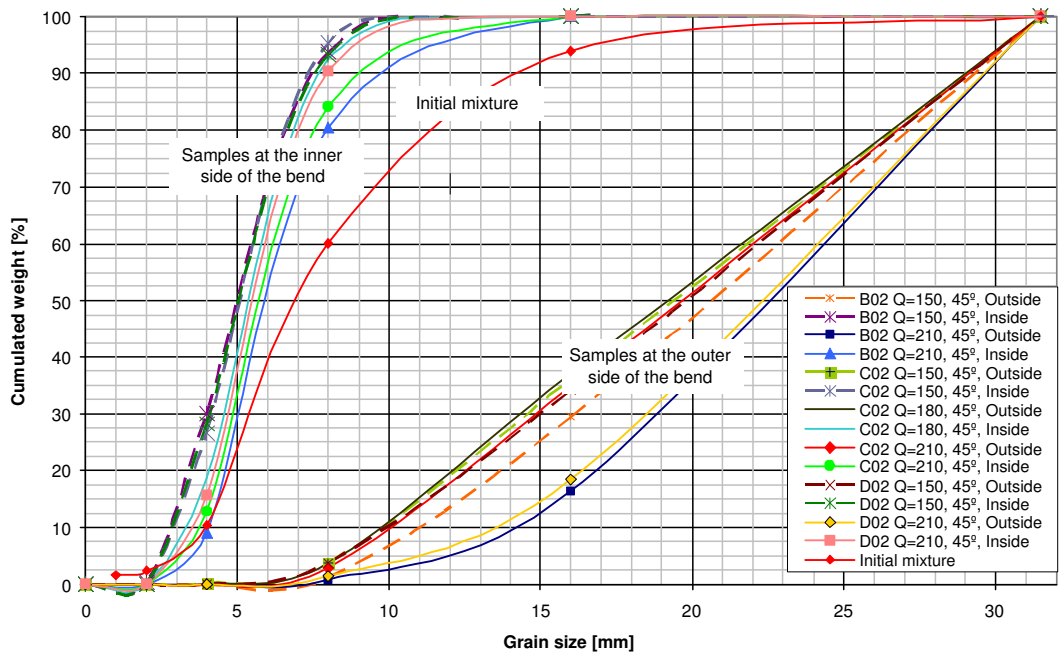

I.1 45° with the undulated wall

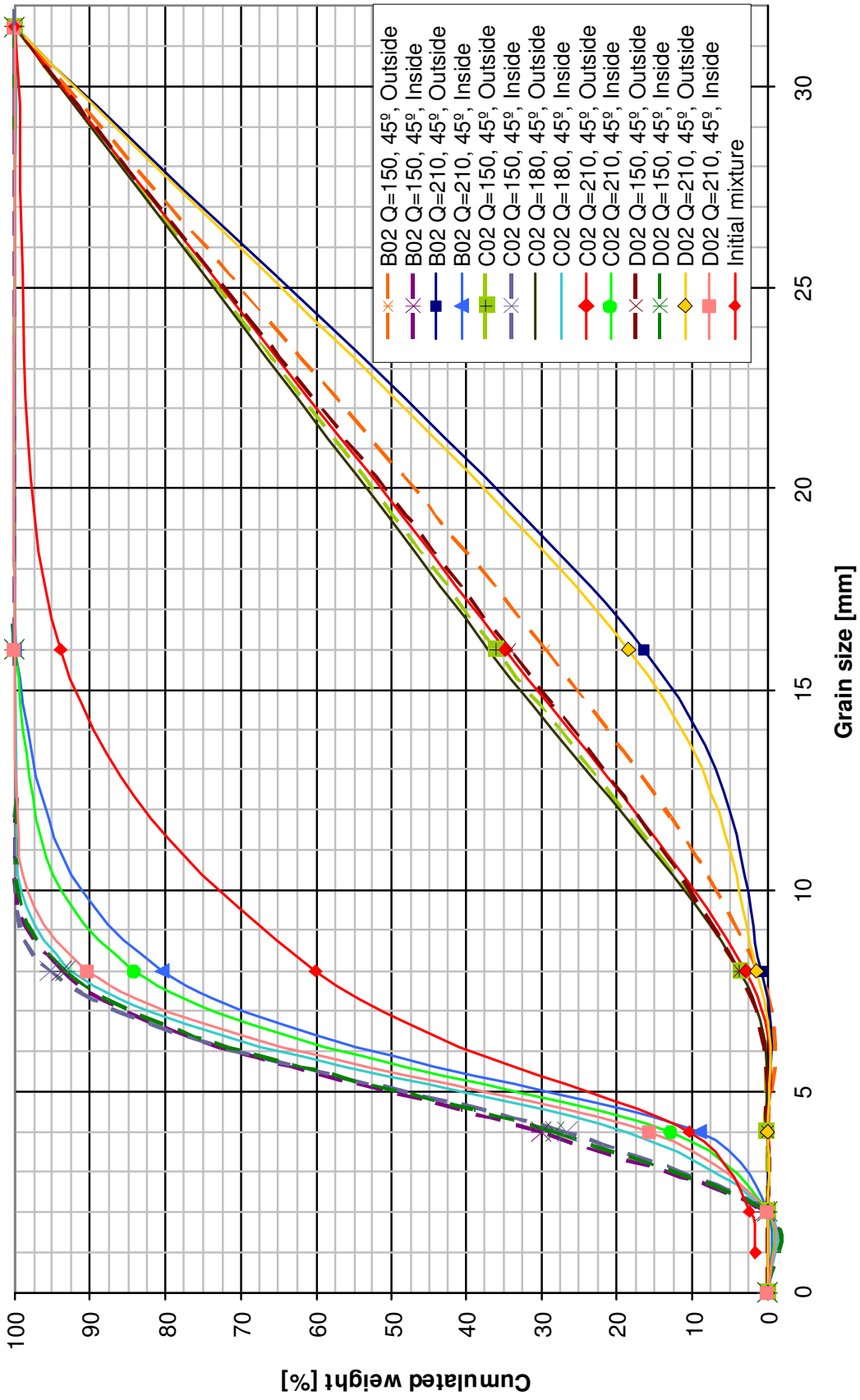

I.2 90° with the undulated wall

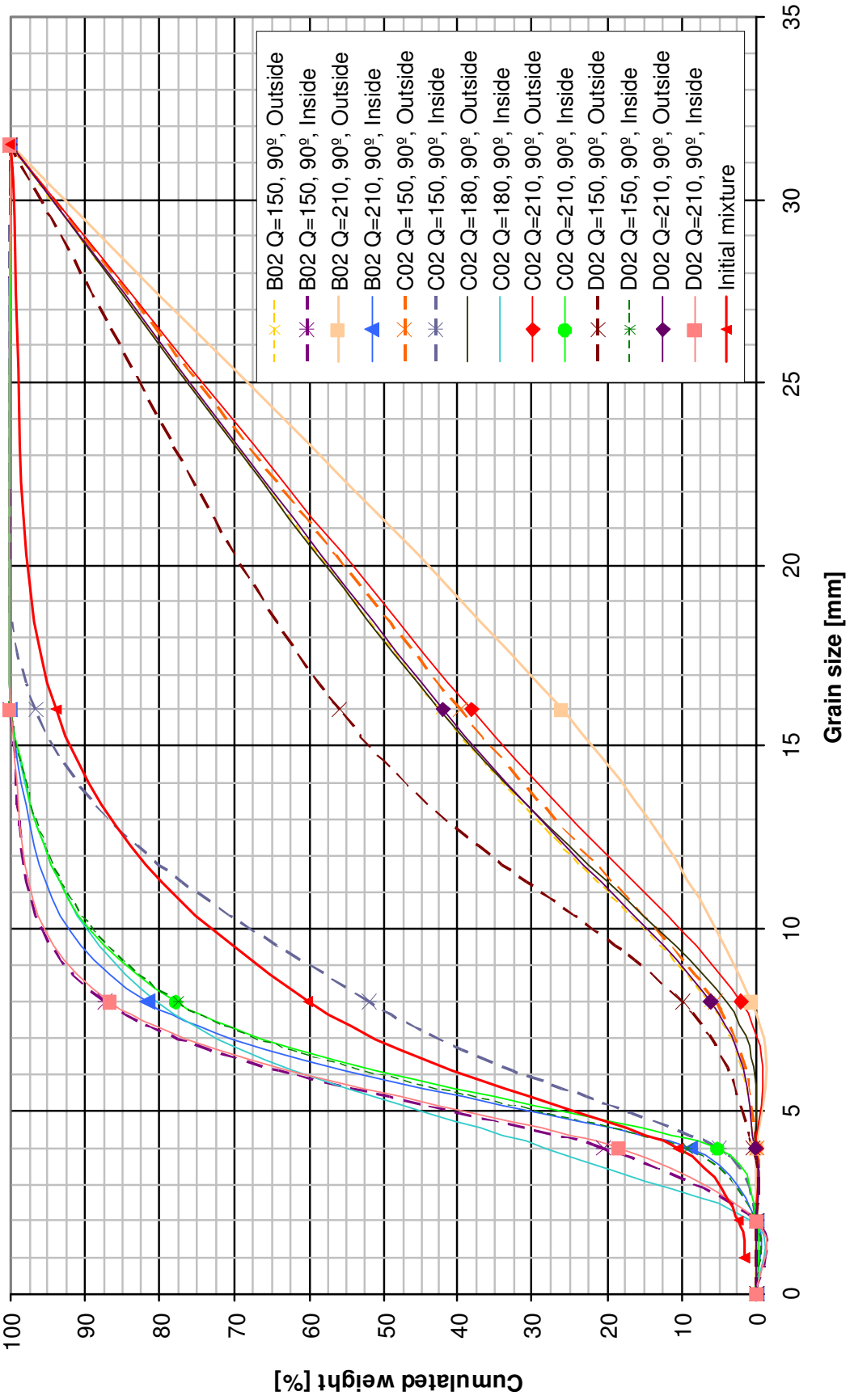

Appendix J

Longitudinal energy profiles

This Appendix gives the kinetic energy profile and the energy profile along the channel of all the tests. More information can be found at the Section 4.6.1.

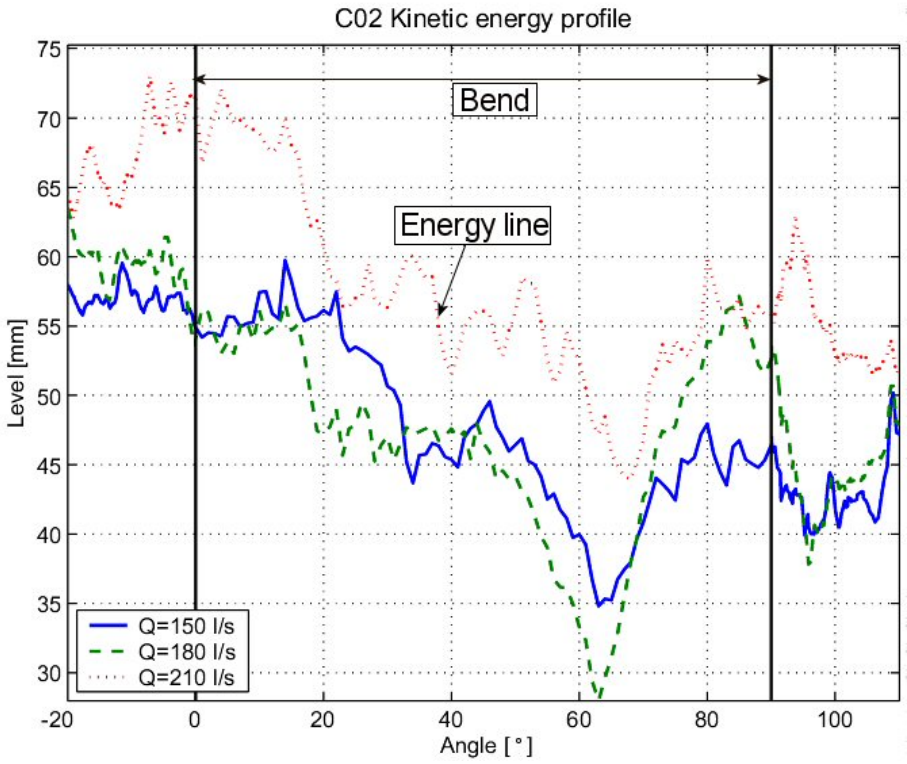

J.1 Kinetic energy

Smooth wall (Hersberger)	Undulated wall[1]

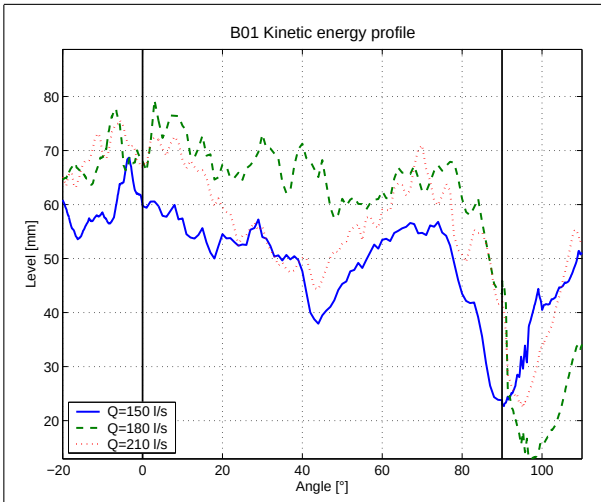

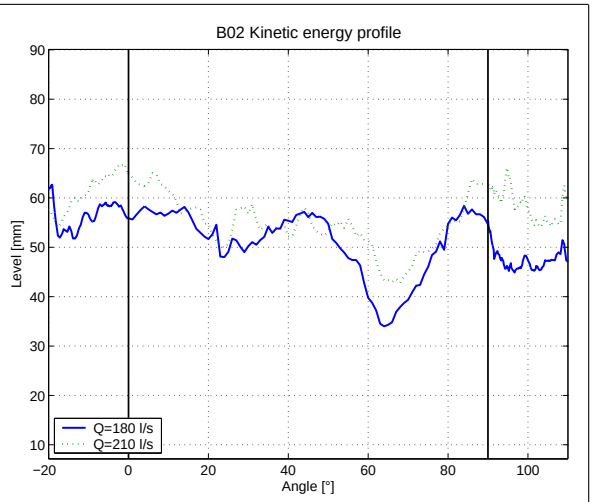

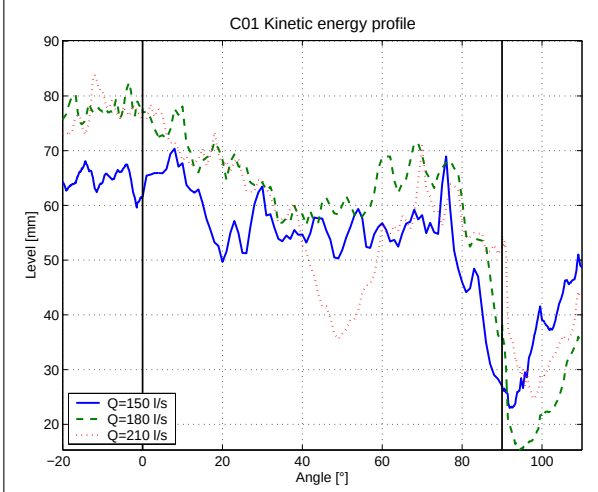

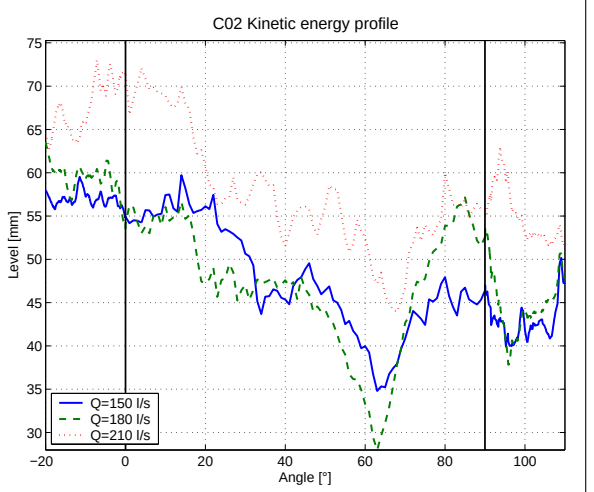

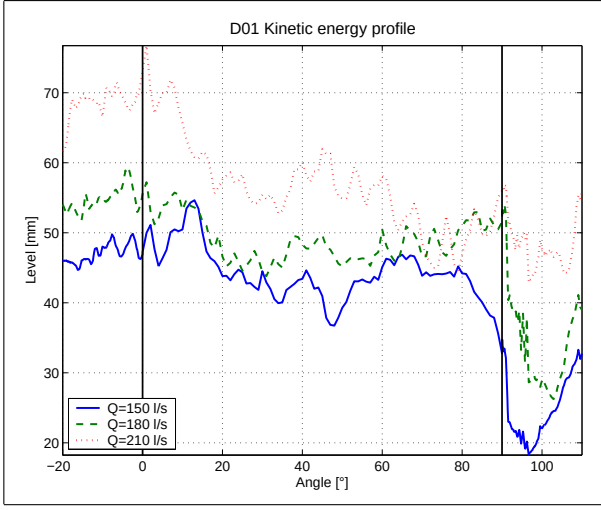

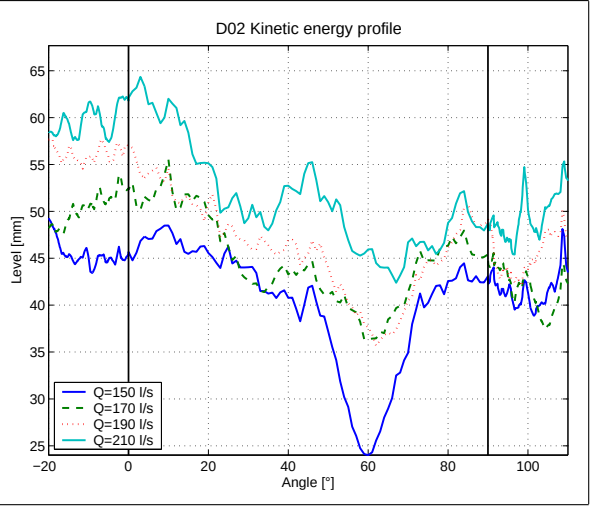

[1]For the test B02 with 150 l/s the energy level is not available

J.2 Energy

Smooth wall (Hersberger)	Undulated wall[1]

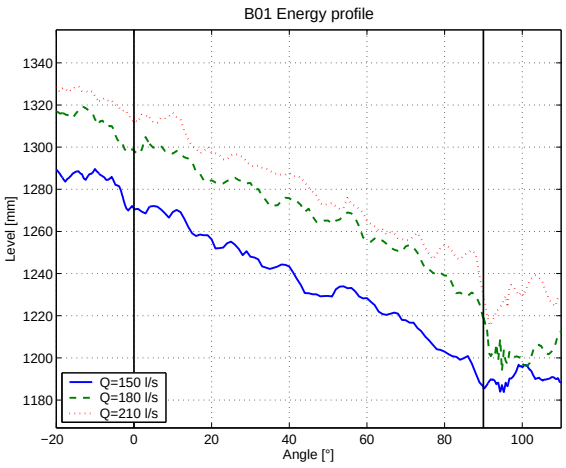

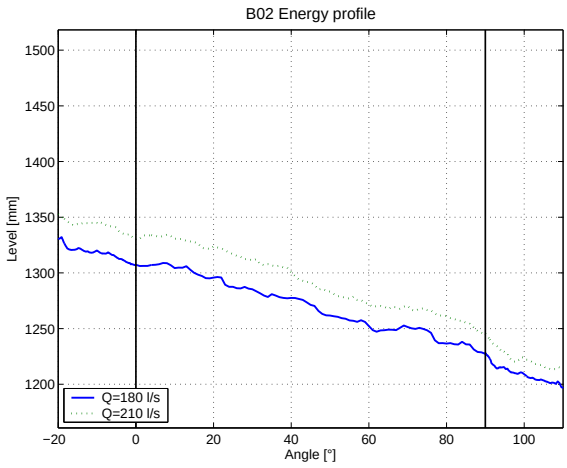

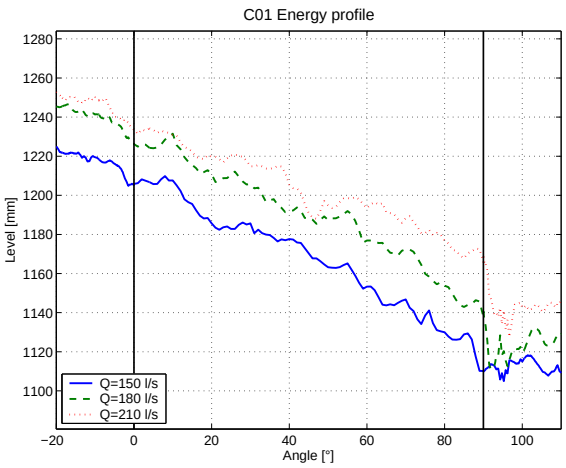

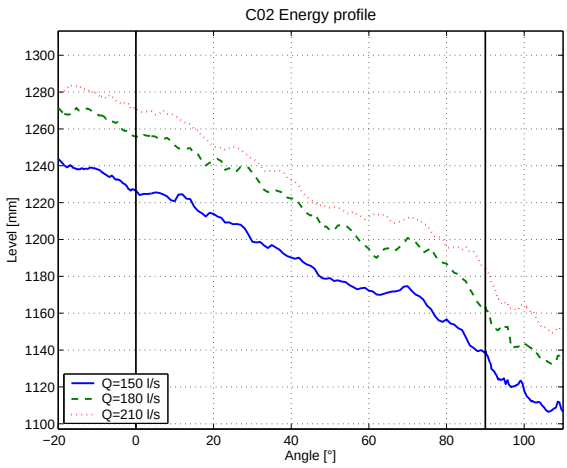

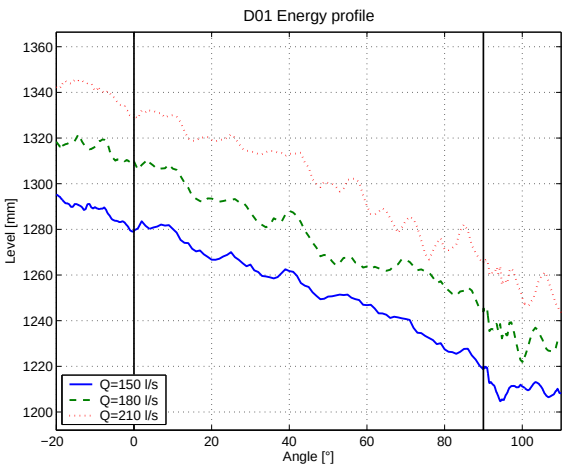

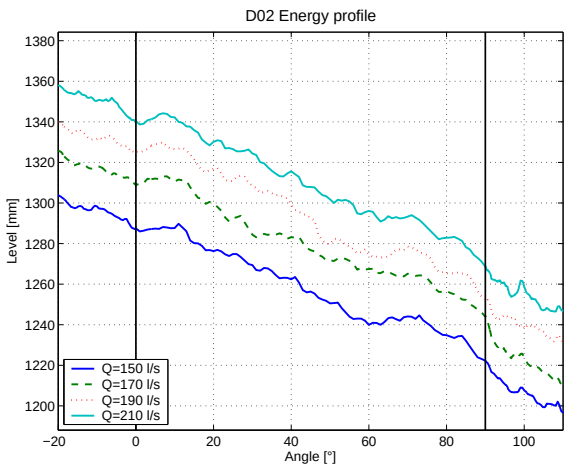

[1]For the test B02 with 150 l/s the energy level is not available

Appendix K

Longitudinal velocities

This Appendix gives the longitudinal velocities measured with a electromagnetic flow sensor in six cross sections along the channel. More information can be found at the section 4.7.

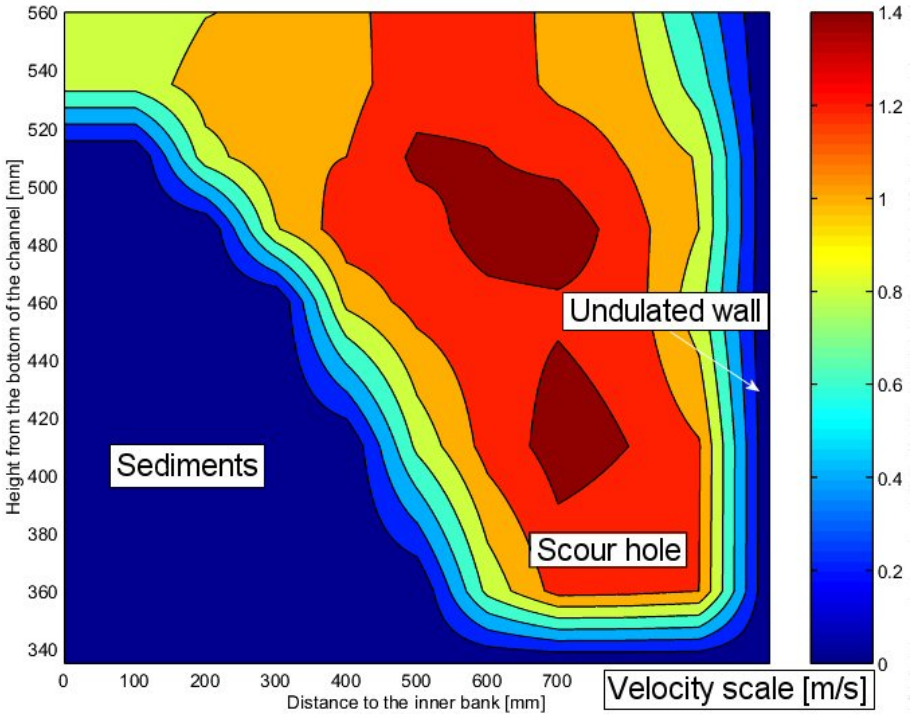

K.1 Longitudinal velocities at $S_0 = 0.5\%$ and $Q = 150l/s$

ENTRY REACH	-2,85m	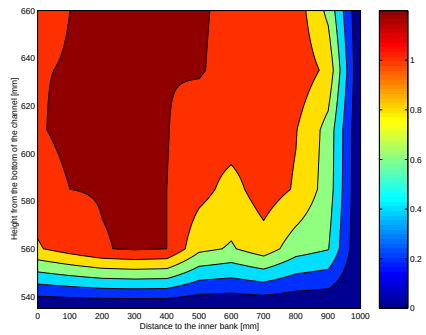	-2m	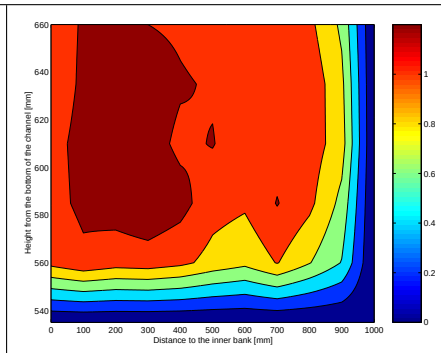
BEND	46 °	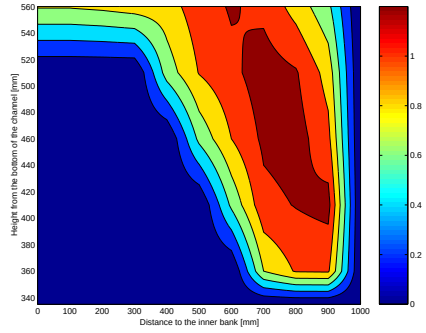	72 °	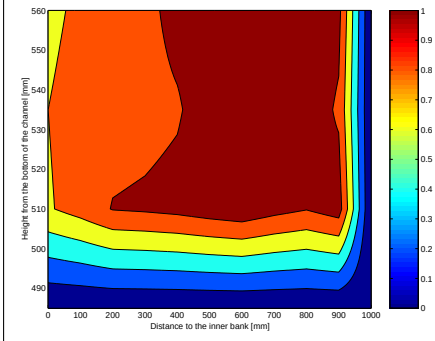
OUTLET REACH	1m	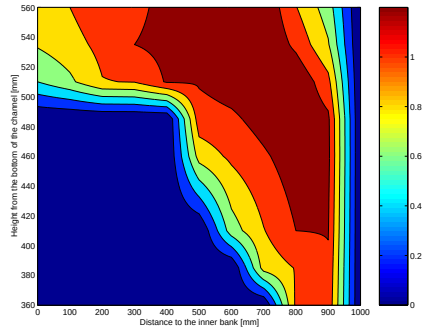	2,4m	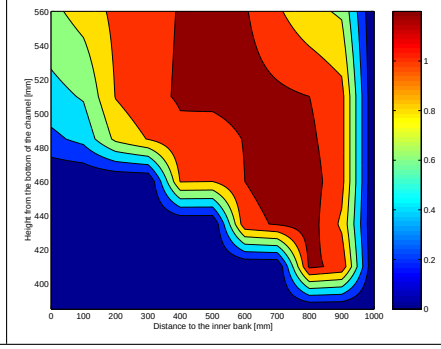

K.2 Longitudinal velocities at $S_0 = 0.5\%$ and $Q = 180l/s$

ENTRY REACH	-2,85m	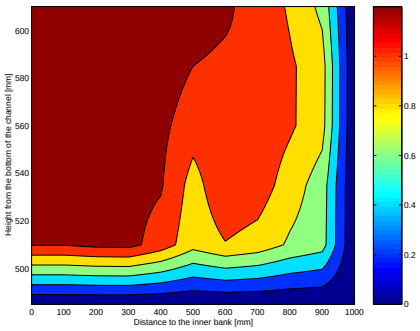	-2m	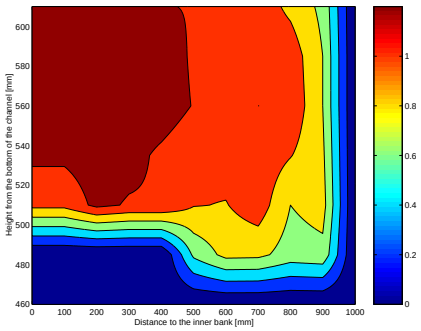
BEND	46 °	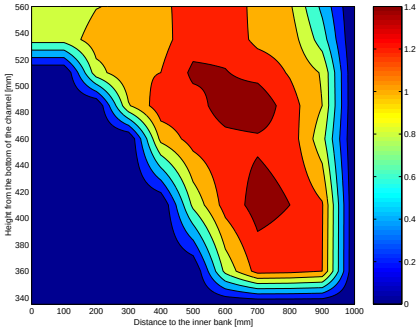	72 °	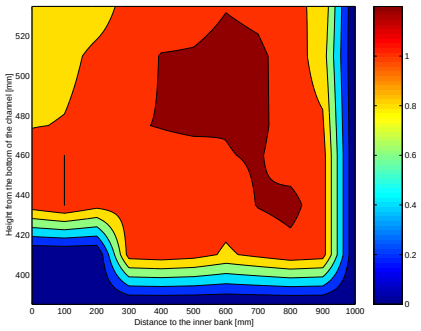
OUTLET REACH	1m	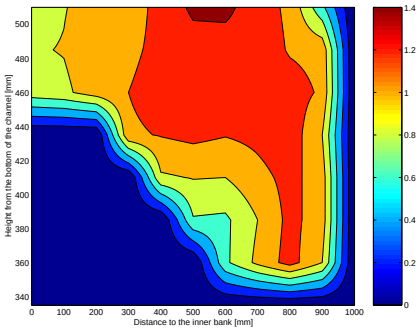	2,4m	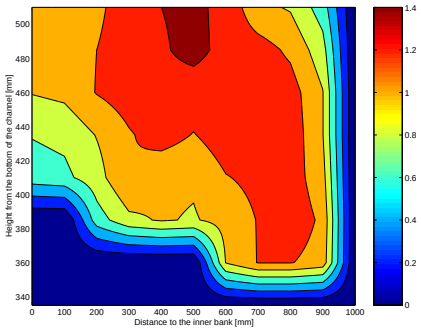

K.3 Longitudinal velocities at $S_0 = 0.5\%$ and $Q = 210l/s$

ENTRY REACH	-2,85m	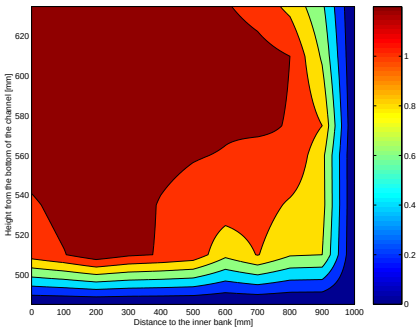	-2m	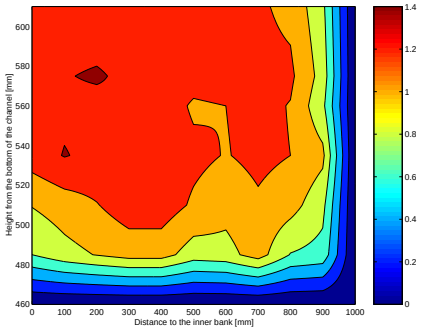
BEND	46 °	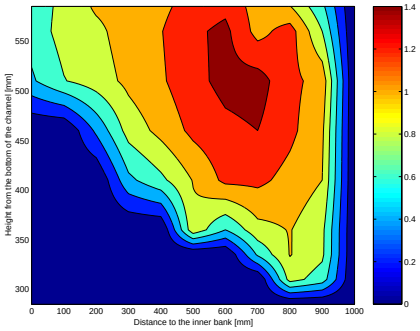	72 °	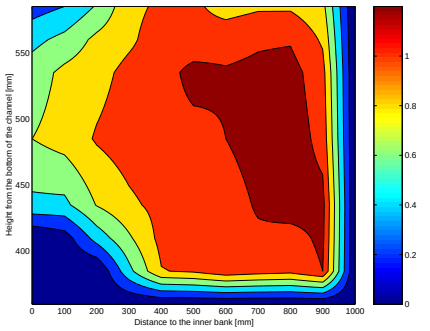
OUTLET REACH	1m	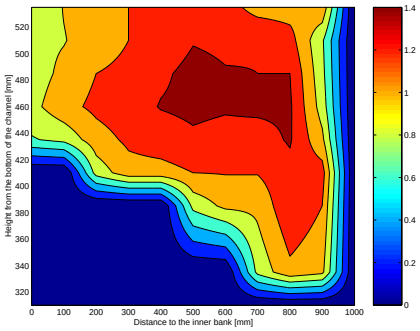	2,4m	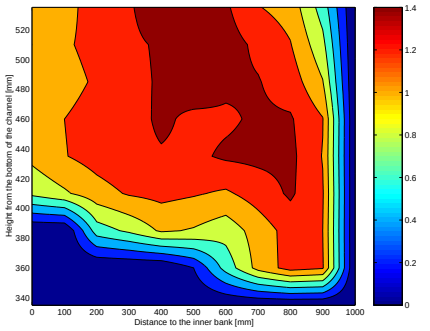

K.4 Tangential velocities at $S_0 = 0.7\%$ and $Q = 150l/s$

ENTRY REACH	-2,85m	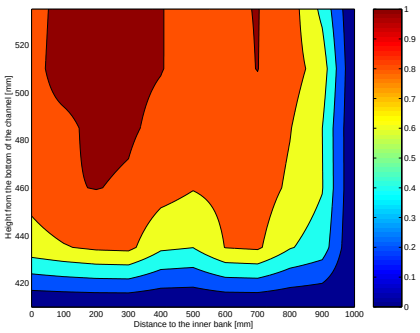	-2m	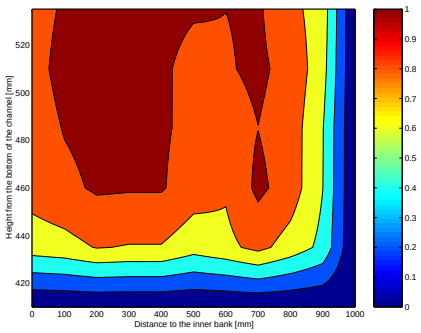
BEND	46 °	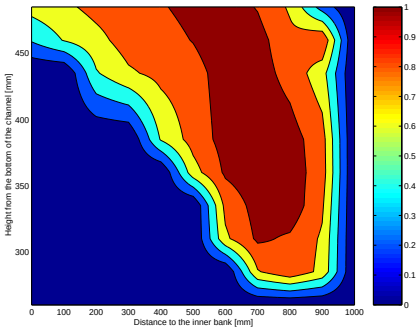	72 °	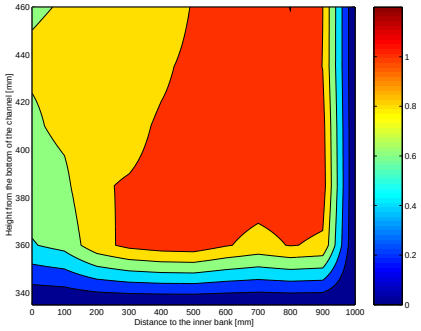
OUTLET REACH	1m	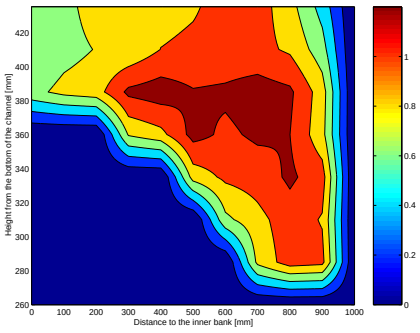	2,4m	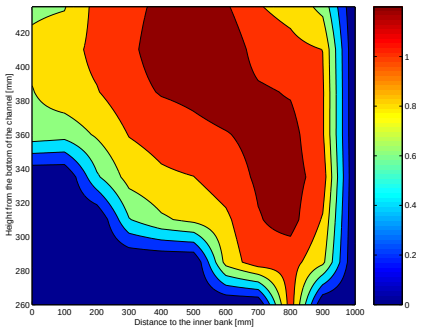

K.5 Longitudinal velocities at $S_0 = 0.7\%$ and $Q = 180l/s$

ENTRY REACH	-2,85m	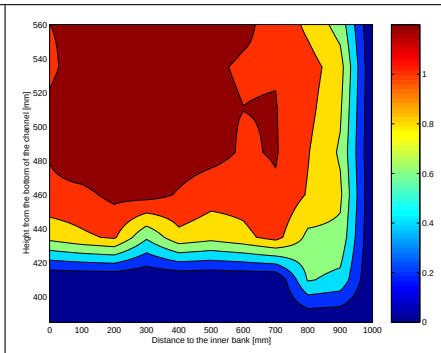	-2m	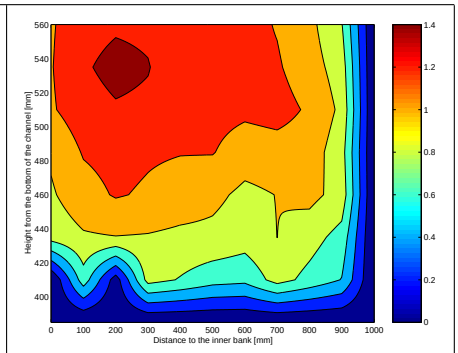
BEND	46 °	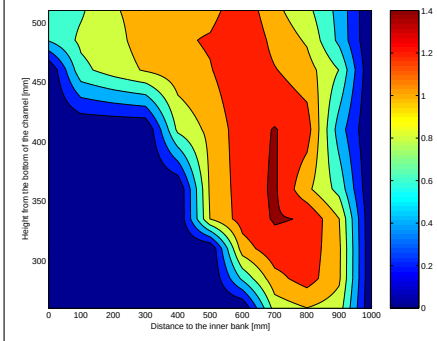	72 °	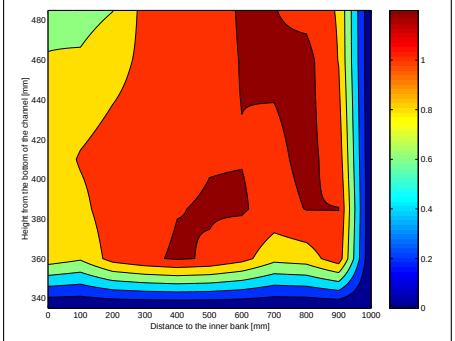
OUTLET REACH	1m	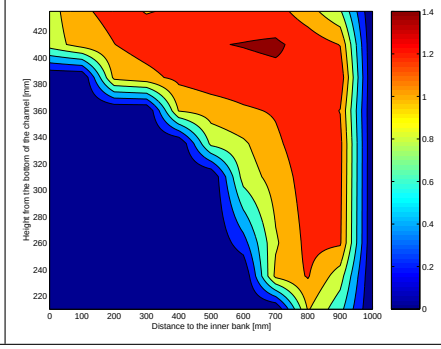	2,4m	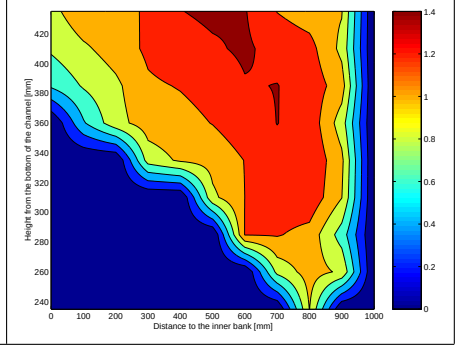

K.6 Longitudinal velocities at $S_0 = 0.7\%$ and $Q = 210l/s$

ENTRY REACH	-2,85m	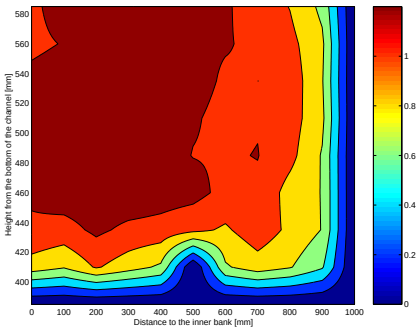	-2m	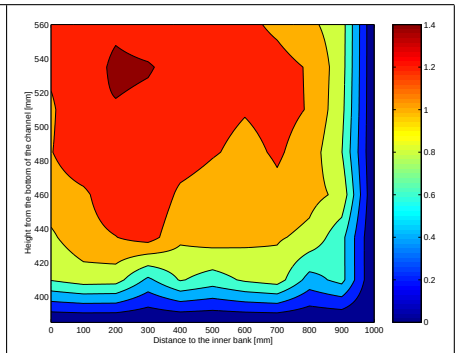
BEND	46 °	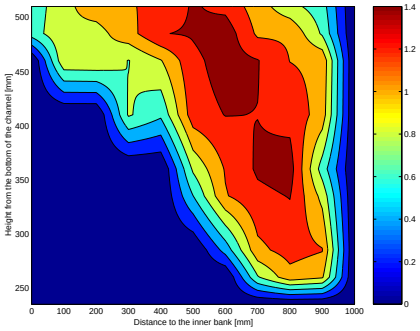	72 °	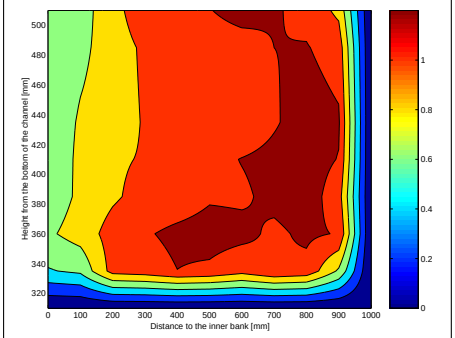
OUTLET REACH	1m	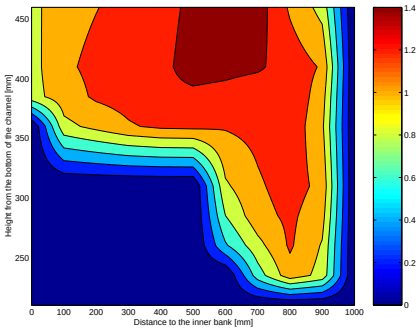	2,4m	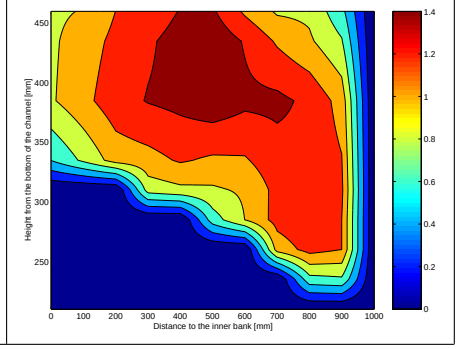

K.7 Longitudinal velocities at $S_0 = 0.35\%$ and $Q = 150l/s$

ENTRY REACH	-2,85m	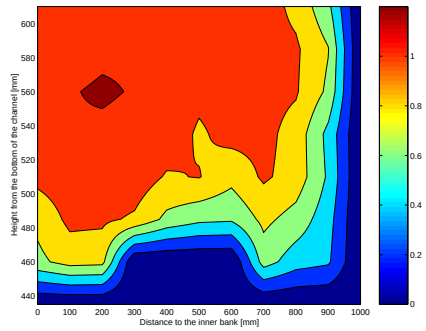	-2m	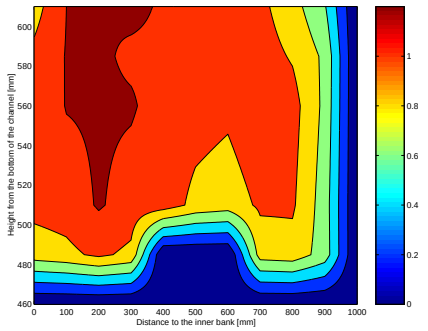
BEND	46 °	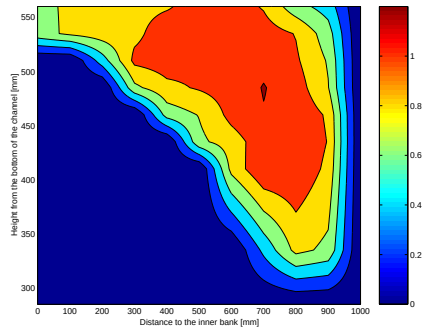	72 °	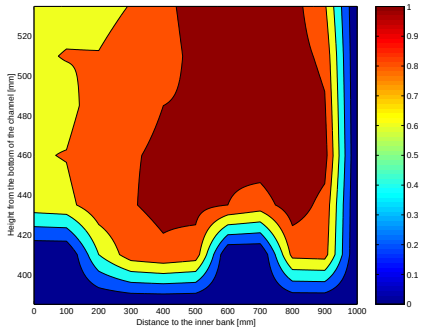
OUTLET REACH	1m	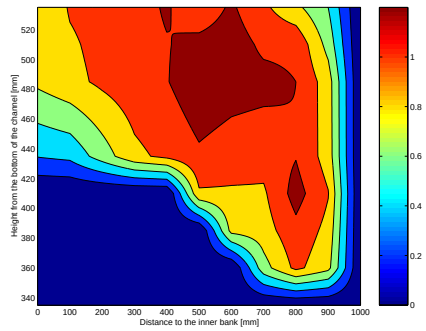	2,4m	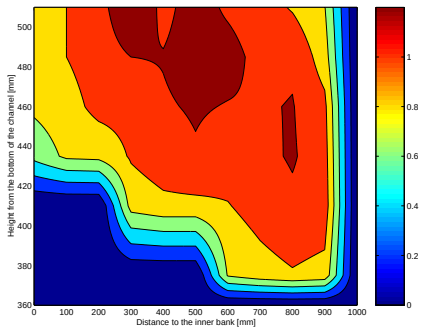

K.8 Longitudinal velocities at $S_0 = 0.35\%$ and $Q = 170l/s$

ENTRY REACH	-2,85m	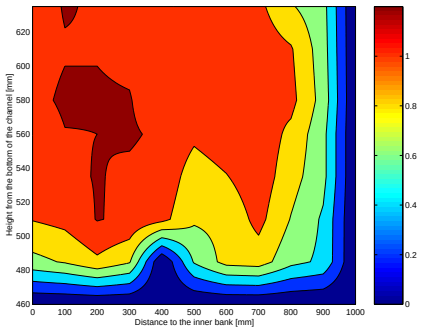	-2m	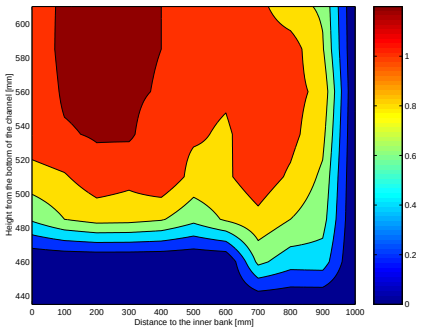
BEND	46 °	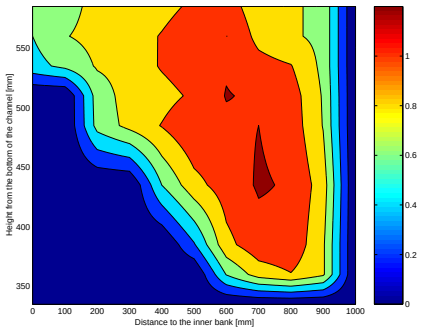	72 °	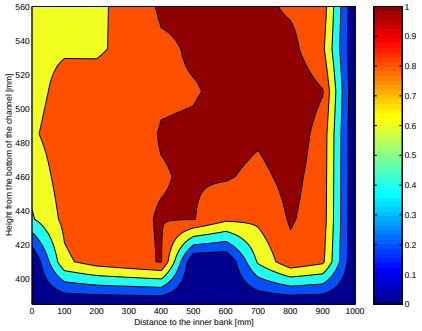
OUTLET REACH	1m	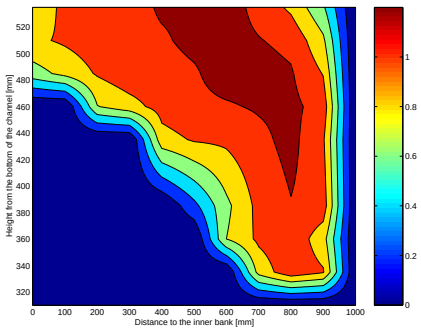	2,4m	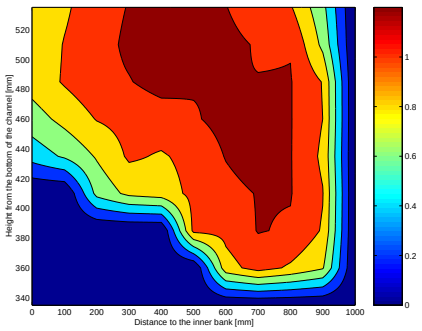

K.9 Longitudinal velocities at $S_0 = 0.35\%$ and $Q = 190l/s$

ENTRY REACH	-2,85m	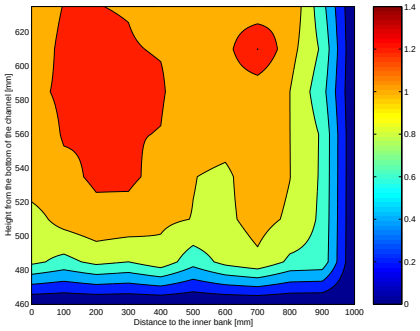	-2m	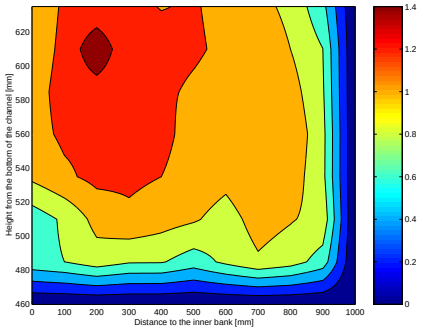
BEND	46 °	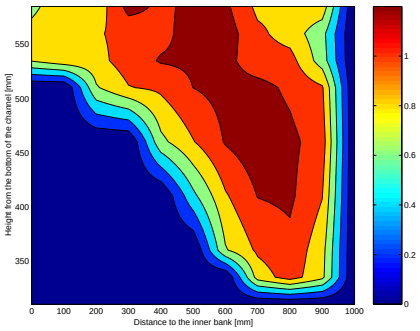	72 °	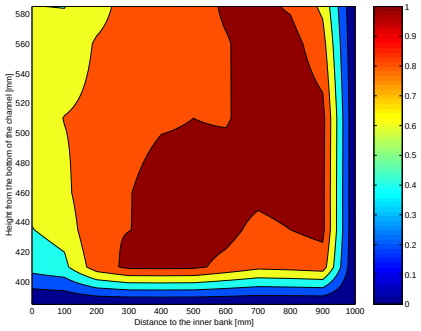
OUTLET REACH	1m	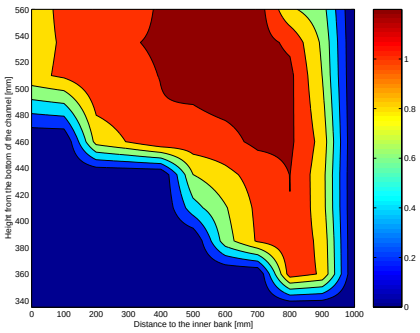	2,4m	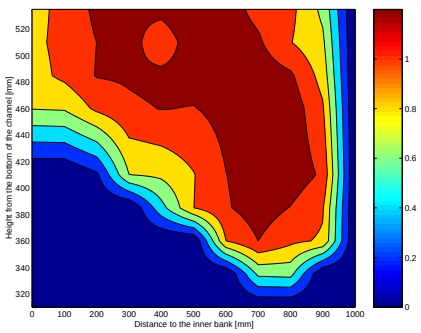

K.10 Longitudinal velocities at $S_0 = 0.35\%$ and $Q = 210l/s$

ENTRY REACH	-2,85m	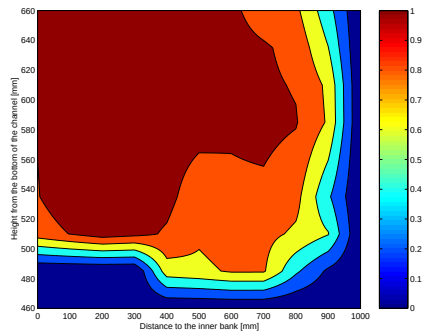	-2m	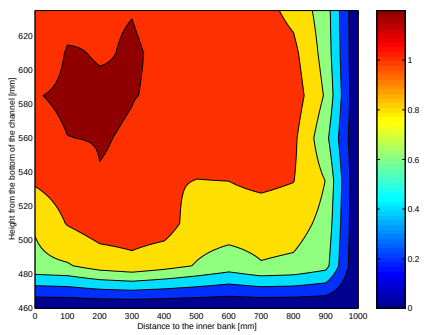
BEND	46 °	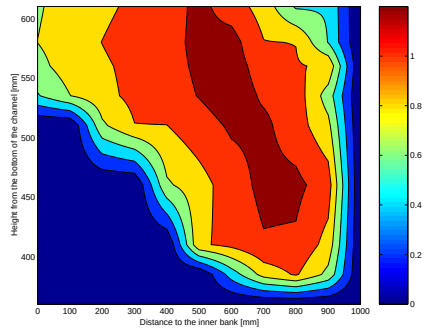	72 °	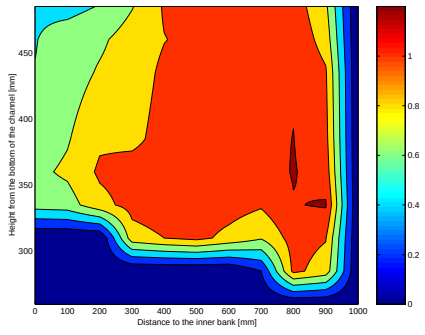
OUTLET REACH	1m	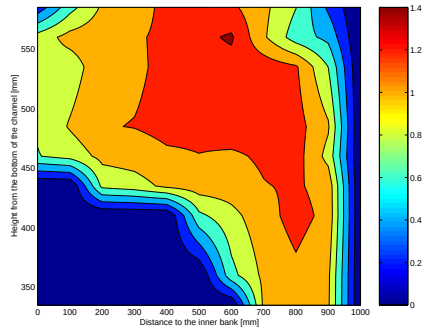	2,4m	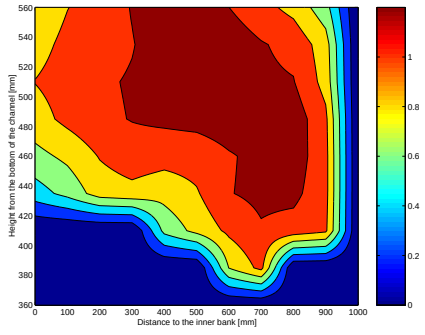

Appendix L

Required minimum thickness of undulated wall

This Appendix gives the required minimum thickness of the undulated wall as a function of the wall hight, wall width, water height and friction angle of the soil. Two load cases: during a flood and after a flood have been considered. More information can be found at the section 5.

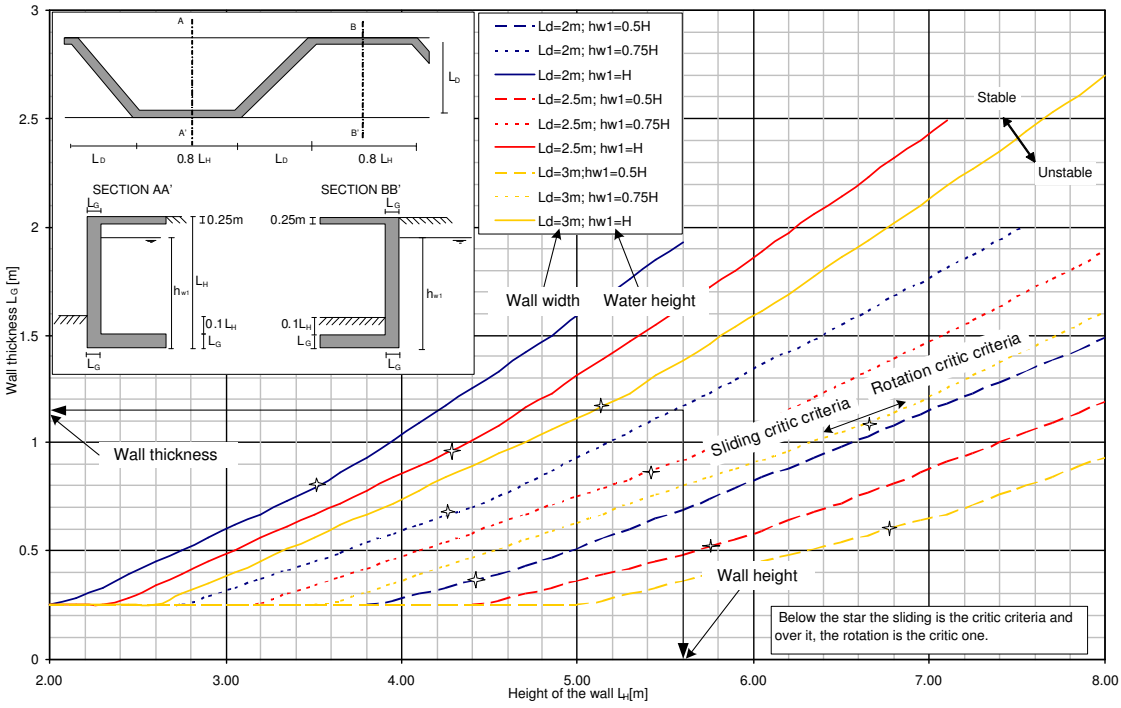

Example: The load case is after a flood and h_{w1}=0.75 H, $\psi = 35°$, L_D=2 m, and wall height H=5.6 m. The minimum required wall thickness is 1.15 m.

L.1 Loads during a flood

L.1.1 $\varphi = 30°$

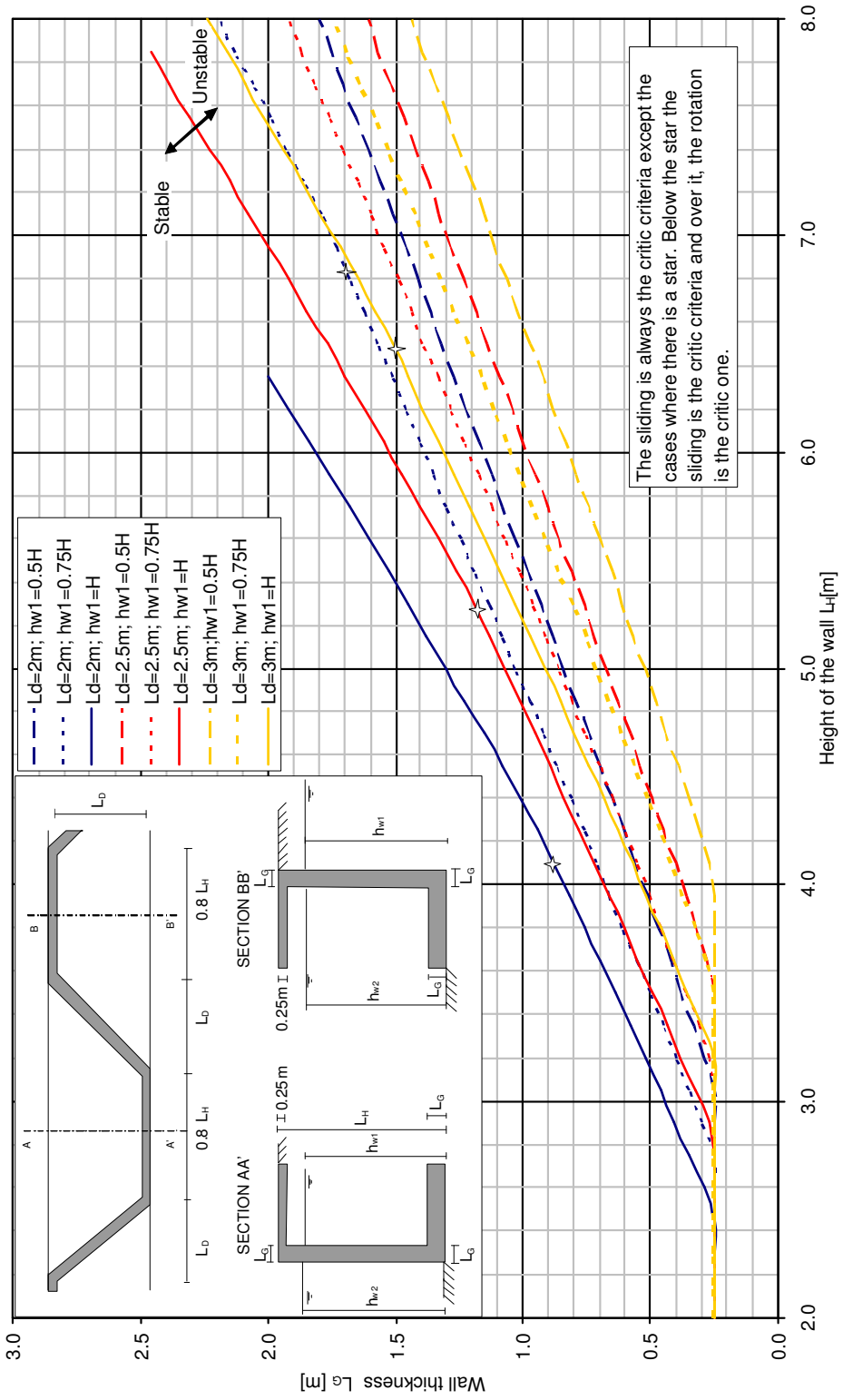

L.1.2 $\varphi = 35°$

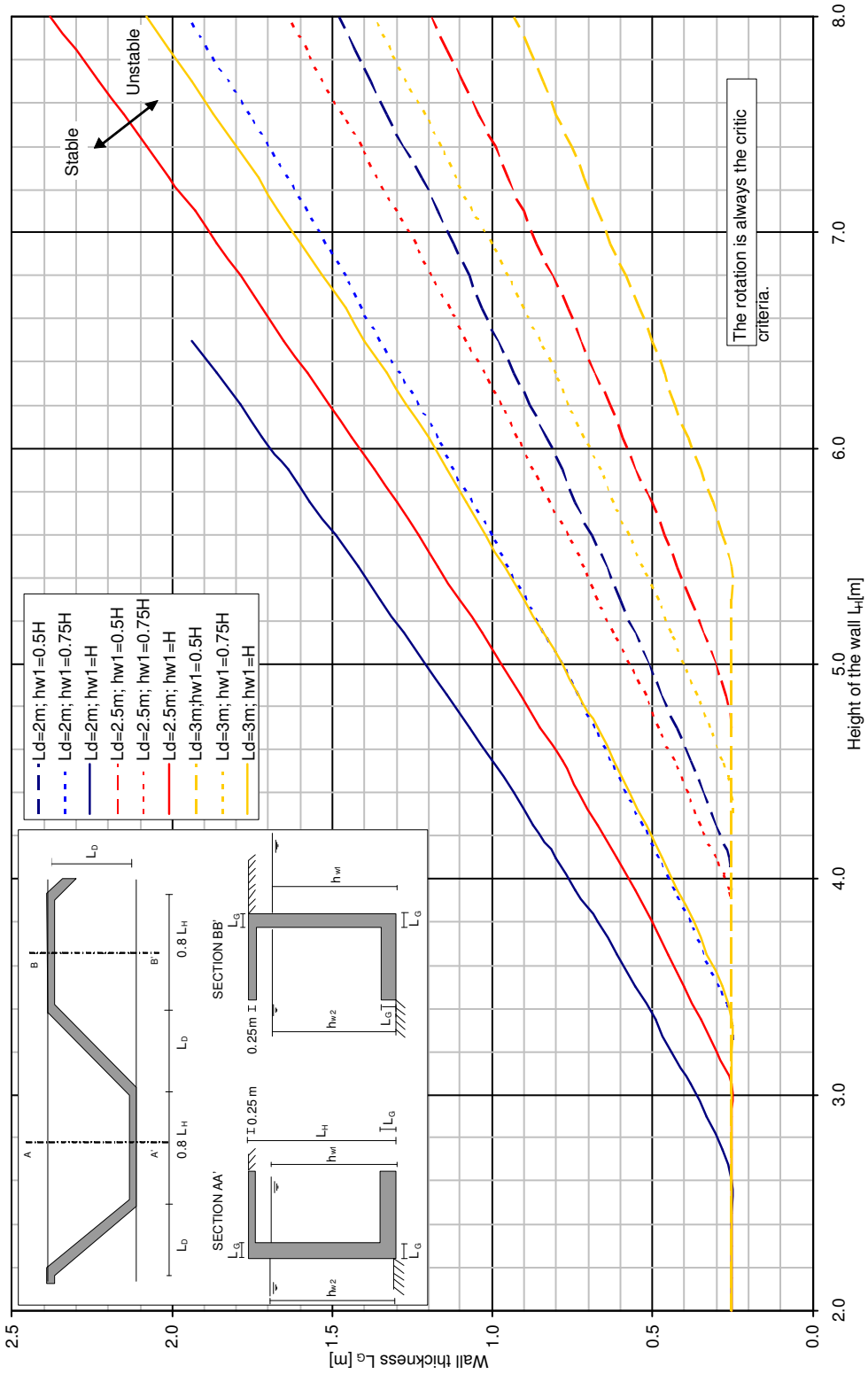

L.1.3 $\varphi = 40°$

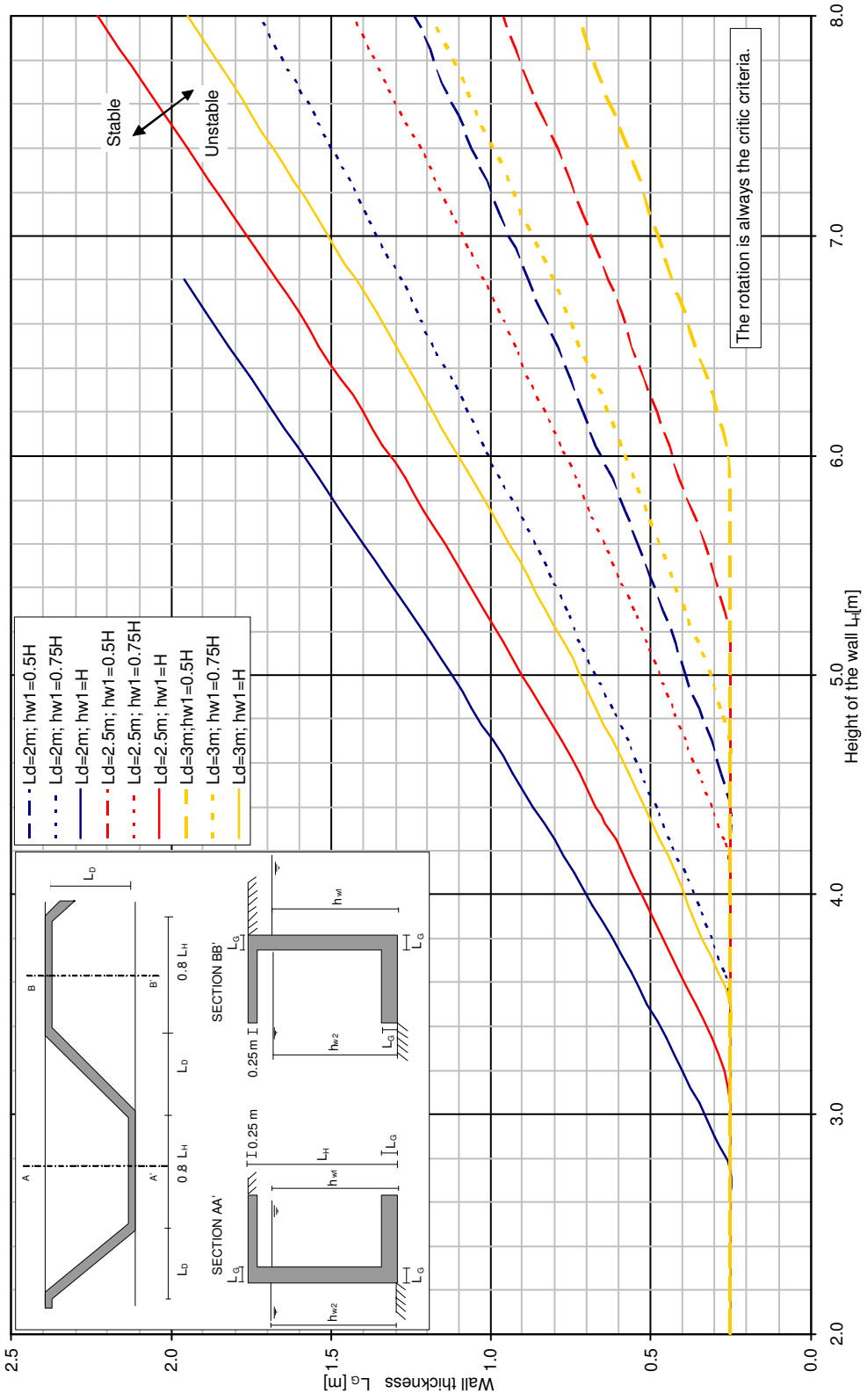

L.2 Loads after a flood

L.2.1 $\varphi = 30°$

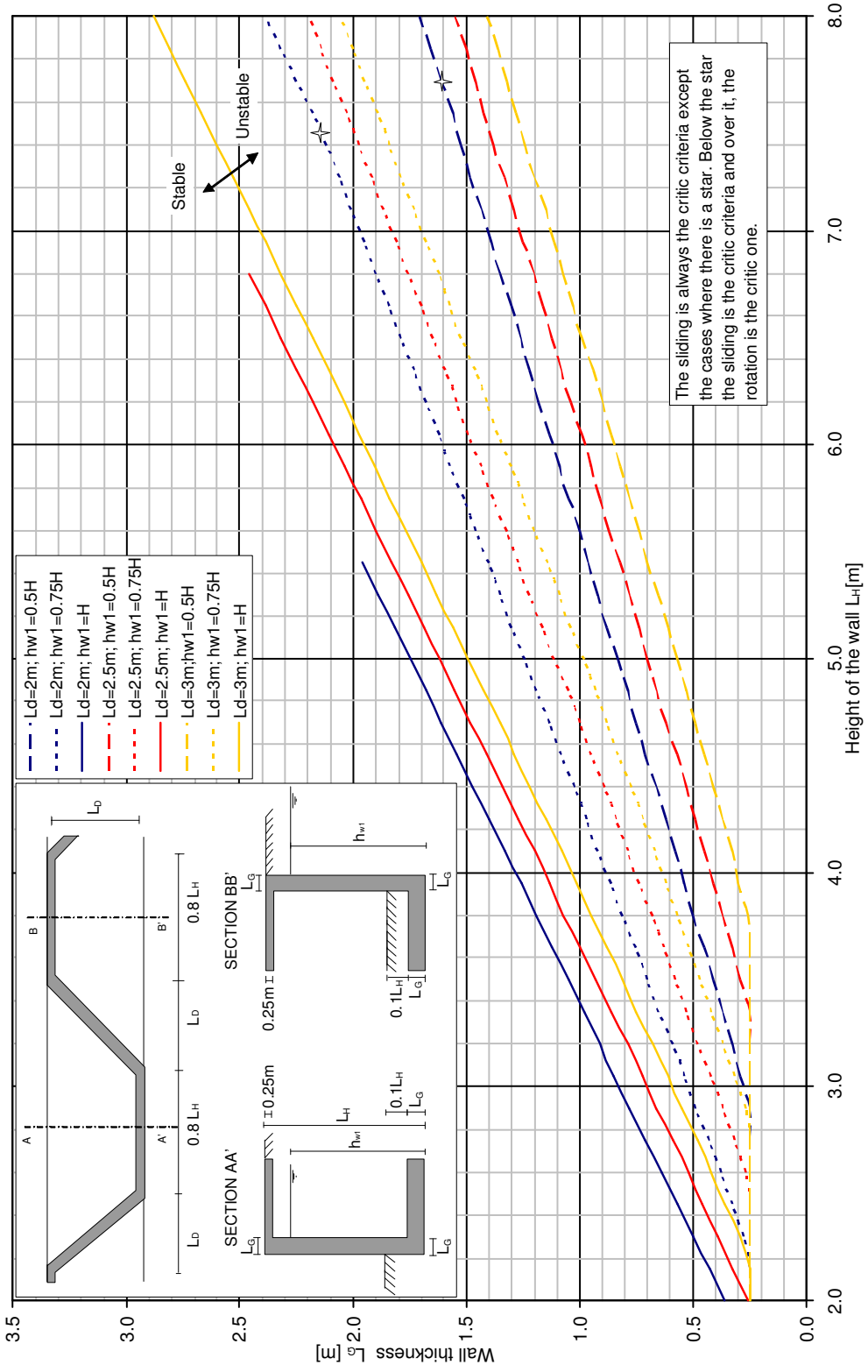

L.2.2 $\varphi = 35°$

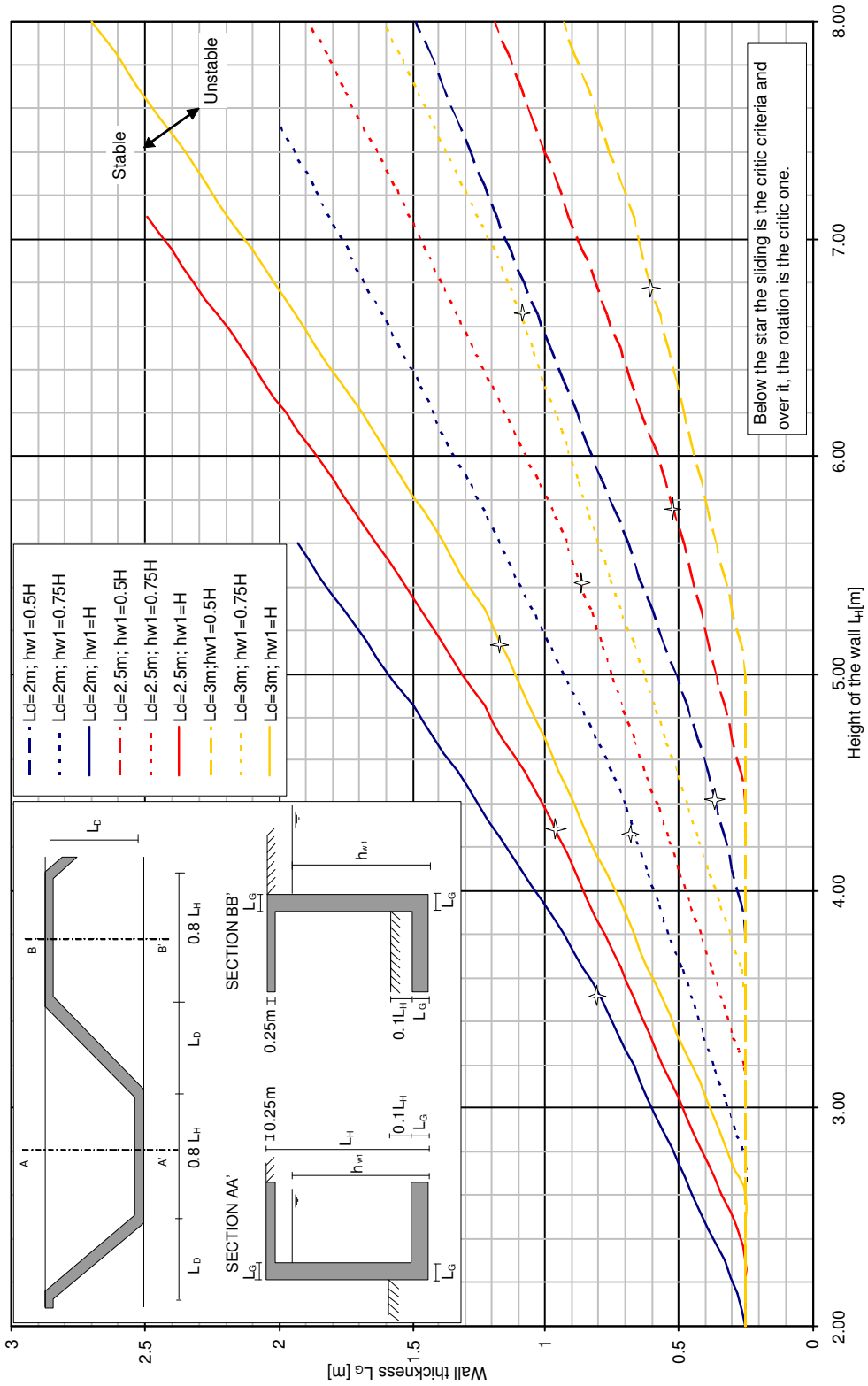

L.2.3 $\varphi = 40°$

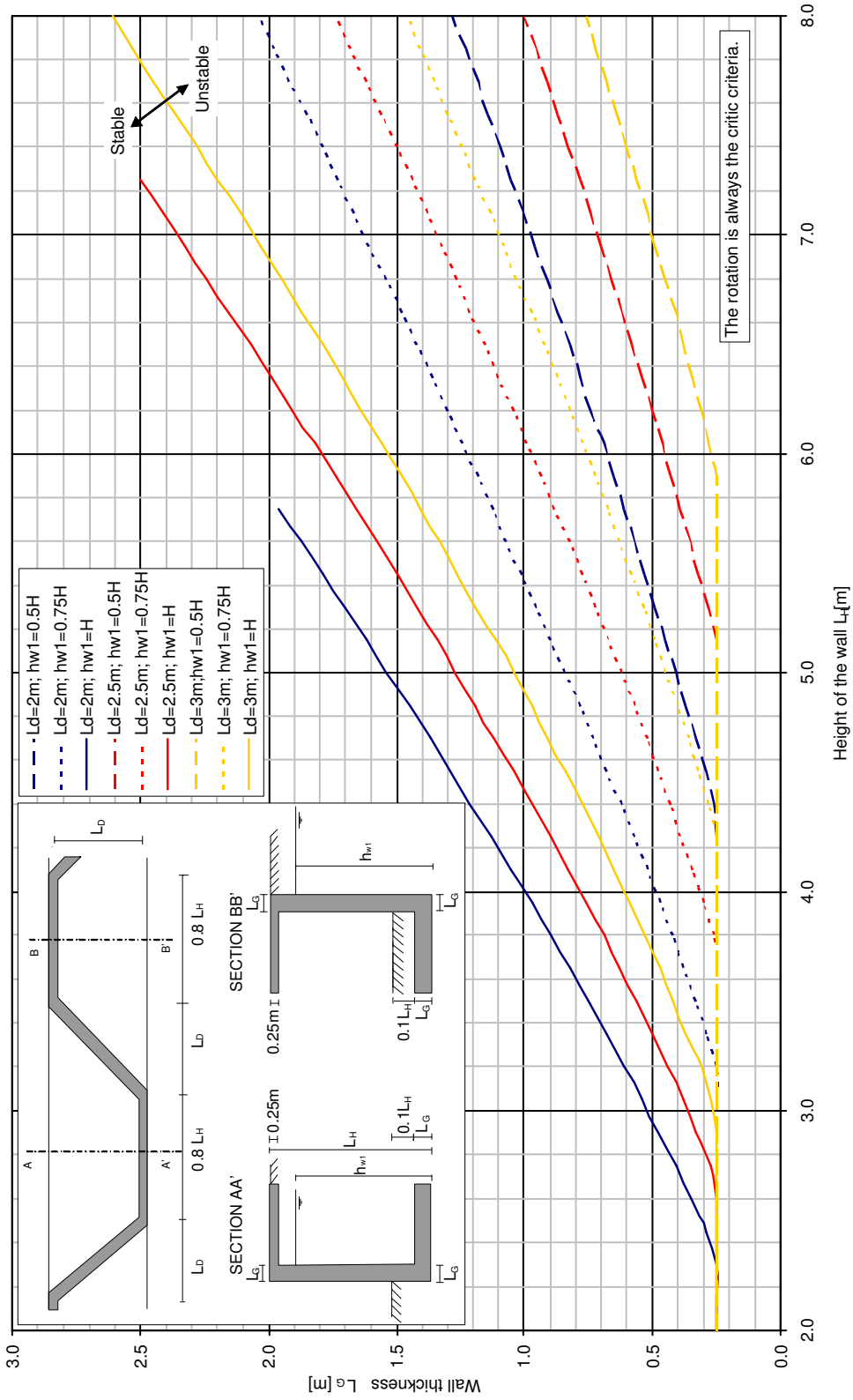

Communications du Laboratoire de Constructions Hydrauliques ISSN 1661-1179
Ecole Polytechnique Fédérale de Lausanne
Editeur: Prof. Dr A. Schleiss

N°	21	2005	Conférence sur la recherche appliquée en relation avec la troisième correction du Rhône - Nouveaux développements dans la gestion des crues
N°	22	2005	INTERREG IIIB - Projet ALPRESERV. Conférence sur la problématique de la sédimentation dans les réservoirs - Gestion durable des sédiments dans les réservoirs alpins
N°	23	2005	Master of Advanced Studies (MAS) in hydraulic schemes Collection des articles des travaux de diplôme
N°	24	2006	S. Sayah Efficiency of brushwood fences in shore protection against wind-wave induced erosion
N°	25	2006	P. Manso The influence of pool geometry and induced flow patterns in rock scour by high-velocity plunging jets
N°	26	2006	M. Andaroodi Standardization of civil engineering works of small high-head hydropower plants and development of an optimization tool
N°	27	2006	Symposium érosion et protection des rives lacustres Bases de dimensionnement des mesures de protection des rives lacustres
N°	28	2007	A. Vela Giró Bank protection at the outer side of curved channels by an undulated concrete wall

ISSN 1661-1179

Prof. Dr A. Schleiss
Laboratoire de constructions hydrauliques - LCH
EPFL, Bât. GC, Station 18, CH-1015 Lausanne
http://lchwww.epfl.ch
e-mail: secretariat.lch@epfl.ch